



UNIVERSITÀ DEGLI STUDI DELL'AQUILA

Department of Civil, Construction-Architectural and
Environmental Engineering

Doctoral Thesis

**The development of the short supply timber chain:
classification, mechanical characterization and
application of local wood.**

Ph.D. Course in Civil, Construction-Architectural
and Environmental Engineering

XXXVI cycle

Candidate
Luca Spera

SSD
ICAR/09

Course Coordinator
Prof. Marcello Di Risio

Thesis Tutor
Prof. Massimo Fragiaco

Co-Tutor
Ph.D. Martina Sciomenta



The development of the short supply timber chain:
classification, mechanical characterization and
application of local wood.

Candidate: **Luca Spera**

Thesis Tutor: **Prof. Massimo Fragiaco**

Co-Tutor: **Ph.D. Martina Sciomenta**

The development of the short supply timber chain: classification, mechanical characterization and application of local wood.

Luca Spera

275116

Department of Civil, Construction-Architectural and Environmental Engineering-

DICEAA

University of L'Aquila

Copyright ©2024, Luca Spera. All rights reserved.

Material for which the author is the copyright owner cannot be used without the written permission of the author. The permission to reproduce copyright protected material does not extend to any material that is copyright of a third party; authorization to reproduce such material must be obtained from the copyright owners concerned.

Website: <http://diceaa.univaq.it/>

Acknowledgements

I would like to express my sincere gratitude to the thesis tutor Prof. Massimo Fragiaco and the co-tutor Eng. Ph.D. Martina Sciomenta for their assistance at every stage of the research project, for their insightful comments and suggestions, and for helping me finalize the project.

I would like to thank Prof. Manuela Romagnoli, Prof. Chiara Bedon, Prof. Angelo Di Egidio, Prof. Giuseppe Scarascia Mugnozza, Eng. Ph.D. Cristiano Fabrizio, Eng. Ph.D. Yuri De Santis, Dr. Ph.D. Michela Nocetti and Dr. Ph.D. Michele Brunetti for contributions and for sharing their experience. I would like to thank B.Eng. Fabio Santavicca, mayor of the Santo Stefano di Sessanio municipality, and Dr. Francesco Contu, head of the Coordination and Planning Office in the Dept. of Agriculture (Forests and Parks) of the Abruzzo Region offices in L'Aquila, for their availability and contributions, and Eng. Ph.D. Matteo Izzi, Assolegno Regulatory Office of FederlegnoArredo, for support and suggestions.

The contribution of all the companies Xlam Dolomiti, in the person of Eng. Albino Angeli, Pagano, in the person of Mr. Andrea Pagano, Lamel Legno, in the person of Eng. Giuseppe Sammartino, Akzonobel, in the person of Dr. Enzo Mattaini, Rothoblaas, in the persons of Mr. Peter Lang, Eng. Luca Sestigiani, Eng. Andrés Reyes, and Design SAM, in the person of Mr. Felice Mastrangeli, was fundamental for the production of the engineered wood products and for the realization of the specimens. The assistance for the experimental tests, provided by Mr. Alfredo Peditto, Mr. Edoardo Ciuffetelli, and Eng. Pasqualino Gualtieri of the materials and structures testing laboratory (LPMS) of the University of L'Aquila, was greatly appreciated.

Lastly, I am deeply grateful to my family and to the most important person in my life, Alessia, without whom this thesis would have not been possible.

Abstract

Short supply chain wood achieved by means of a sustainable forest management can produce several benefits such as: the increase in value of the forested areas due to the alternative use of wood in modern structural components; the environmental advantages as CO₂ emissions reduction, landscaping improvement and landslide hazard reduction; the economic recovery of areas usually underdeveloped and abandoned. Abruzzo Region, in the central-southern area of the Italian peninsula, offers extensive wooded areas of about 400.000 ha with different timber species. The most abundant softwood species is pine with about 19.000 ha out of a total of about 25.000 ha of covered area. The most abundant hardwood species is beech with about 122.000 ha out of a total of about 360.000 ha of forested areas. The aim of this work is to study possible applications of local wood in the construction sector, with particular regard to the aforementioned species, in order to encourage its use also in high technological content products such as glue-laminated timber (glulam) beams and cross-laminated timber (X-lam or CLT) panels.

Experimental tests along with analytical models and numerical simulations were considered and performed to compare novel engineered wood products, made of Italian beech and Corsican pine wood, with commercial components made of softwood. The mechanical characterization of these products was achieved as well as the study of interesting topics such as the in-plane behaviour, with the in-depth analysis of the buckling phenomenon, and the out-of-plane behaviour, for the reinforcement of existing timber floors, of CLT panels.

Furthermore, the application of glulam joists and timber planks made of Italian beech wood for the realization of new wooden floors was studied, with insights about flexible timber-to-timber connections.

Beech results a timber species with a great potential, thanks to its high mechanical properties; on the other hand, Corsican pine offers light weight and more workability. Therefore, these two timber species are compatible to each other to produce laminated wood, with a noteworthy possibility to optimize the material depending on the future state of stress of the single lamellas, and they result to be important resources for structural purposes.

Sommario

La filiera corta del legno, attraverso una gestione sostenibile delle foreste, è in grado di produrre nel corso degli anni diversi benefici tra i quali: valorizzazione delle aree boschive per mezzo di un utilizzo alternativo del legno in componenti strutturali innovativi; vantaggi ambientali legati alla riduzione delle emissioni di CO₂, al miglioramento del paesaggio e alla riduzione del rischio frana; ripresa economica di aree rurali solitamente abbandonate e sottosviluppate. La Regione Abruzzo, situata nella zona centro-meridionale della penisola italiana, presenta estese aree boschive caratterizzate da diverse specie legnose, per un totale di quasi 400.000 Ha di superficie. La conifera più abbondante è il pino con circa 19.000 Ha su un totale di circa 25.000 Ha di superficie coperta. Per quanto riguarda le latifoglie, il faggio è la specie preponderante con circa 122.000 Ha su un totale di circa 360.000 Ha di superficie boschiva. Lo scopo del lavoro in oggetto è quello di studiare le possibili applicazioni del legno locale nel settore delle costruzioni, al fine di incentivarne l'utilizzo anche in prodotti ad alto contenuto tecnologico quali travi in legno lamellare incollato (glulam) e pannelli in legno lamellare incrociato (X-Lam o CLT). A tal fine sono stati effettuati test sperimentali che, insieme allo sviluppo di modelli analitici e a simulazioni numeriche, hanno permesso di confrontare nuovi prodotti a base di legno, realizzati in legno di origine italiana di faggio e pino laricio, con prodotti commerciali in legno di conifera. Dopo aver caratterizzato dal punto di vista meccanico i suddetti prodotti mediante prove di laboratorio, sono state affrontate tematiche quali il comportamento nel piano e fuori piano di pannelli X-Lam, approfondendo nel primo caso il fenomeno di instabilità a carico di punta e nel secondo caso il rinforzo di solai lignei esistenti. Inoltre, è stata analizzata la possibile applicazione di travetti in legno lamellare incollato e tavole di legno da filiera corta, in particolare faggio di origine italiana, per la realizzazione di nuovi solai in legno, con approfondimenti sul tema delle connessioni flessibili legno-legno. Dall'analisi delle due specie legnose individuate, il faggio presenta grandi potenzialità grazie alle sue elevate proprietà meccaniche, mentre il pino laricio offre leggerezza e maggiore lavorabilità. Pertanto, queste due specie legnose sono idonee per produrre legno lamellare, con la possibilità di ottimizzare il materiale in funzione del futuro stato di sollecitazione delle singole lamelle, e risultano essere risorse importanti per fini strutturali.

Contents

Thesis organization	1
Introduction	2
Research objectives	3
1. The short wood supply chain	6
1.1. State of the art.....	7
1.2. Solid wood and wood-based composites.....	8
1.3. The research case in Abruzzo.....	12
2. Timber grading	18
2.1. Visual strength grading.....	19
2.2. Machine strength grading	21
3. Cross-laminated timber panels	24
3.1. Homogeneous beech and hybrid beech-Corsican pine CLT panels	25
3.1.1. Introduction	26
3.1.2. Experimental investigation.....	27
3.1.2.1. Characterization of materials.....	27
3.1.2.2. CLT specimens.....	27
3.1.3. Test methods.....	29
3.1.3.1. Bending and shear test perpendicular to the plane	29
3.1.3.2. In-plane bending and shear test.....	30
3.1.3.3. Test methods and instruments	30
3.1.4. Test results.....	31
3.1.4.1. Bending	31
3.1.4.1.1. Perpendicular-to-plane bending tests	31
3.1.4.1.2. In-plane bending tests	32
3.1.4.2. Shear.....	32
3.1.4.2.1. Perpendicular-to-plane shear tests.....	32
3.1.4.2.2. In-plane shear tests.....	33
3.1.5. Numerical investigation	33
3.1.5.1. Methods.....	33

3.1.5.2. Experimental comparisons	34
3.1.5.3. Comparison with C24 Spruce panels	35
3.1.6. Conclusions	35
References	36
3.2. Buckling behaviour of short supply chain CLT panels	39
3.2.1. Introduction	40
3.2.2. Materials and methods.....	42
3.2.2.1. Specimens description.....	42
3.2.2.2. Central axial compressive test.....	42
3.2.2.3. Experimental results.....	44
3.2.3. Analytical model	44
3.2.3.1. General glued multilayer beam model	44
3.2.3.1.1 Kinematics	46
3.2.3.1.2 Statics.....	47
3.2.3.1.3 Constitutive laws.....	48
3.2.3.2. Three-layer CLT beam model	49
3.2.3.2.1 Coupling parameters	50
3.2.3.2.2 Euler’s buckling load and the elastic solution for the imperfect three-layer CLT beam	51
3.2.3.2.3 Stability verification.....	53
3.2.4. Comparison between analytical and experimental results.....	55
3.2.5. Conclusion.....	56
Appendix	57
References	58
3.3. Timber in existing buildings.....	61
3.4. Out-of-plane strengthening of existing timber floors with Cross Laminated Timber panels made of short supply chain beech.....	61
3.4.1. Introduction	62
3.4.2. Reinforcing interventions	64
3.4.3. Comparison of selected intervention techniques	65
3.4.3.1 Calculation approach.....	65
3.4.3.2 Slip moduli and performance	66
3.4.3.3 Bending stiffness	67
3.4.3.4 Weight.....	71
3.4.4. Bending moment and normal stresses	73

3.4.5. Conclusions	75
3.4.6. References	76
4. Glue-laminated timber beams	78
4.1. Homogeneous beech and hybrid beech-Corsican pine glue-laminated timber beams.....	79
4.1.1. Introduction	80
4.1.2. Materials & methods	81
4.1.2.1 Characterization of the raw material	81
4.1.2.2 Glue-laminated beam specimens.....	81
4.1.3. Test methods.....	82
4.1.3.1 Bending and shear tests	82
4.1.3.2 Test methods and instruments	82
4.1.4. Test results.....	83
4.1.4.1 Bending	83
4.1.4.2 Shear.....	83
4.1.5. Standard comparison	83
4.1.5.1 Beam grading	84
4.1.5.1.1 Homogeneous beams	84
4.1.5.1.2 Hybrid beams	85
4.1.6. Finite elements modelling	87
4.1.6.1 Main purpose.....	87
4.1.6.2 Model description.....	87
4.1.7. Conclusions	88
References	90
4.2. Timber-timber composite (TTC) joints made of short-supply chain beech: Push-out tests of inclined screw connectors	92
4.2.1. Introduction	92
4.2.2. State of the art.....	94
4.2.3. Materials and methods.....	96
4.2.3.1 Glulam production.....	97
4.2.3.2 Timber characterization.....	98
4.2.3.3 Specimens description.....	99
4.2.3.4 Test setup and instrumentations	100
4.2.3.5 Calculation methods of the mechanical parameters of connections.....	101

4.2.4. Results	102
4.2.5. Deflection limits	105
4.2.5.1 Short-term deflection.....	105
4.2.5.2 Long-term deflection.....	107
4.2.6. Ultimate limit states.....	109
4.2.7. Conclusions	115
4.2.8. References	116
Concluding remarks	120
Subjects for further research.....	127
Appendix	129
References	132
List of publications	136

List of figures

1.2	Fig. 1 Examples of laminations for glued solid timber (UNI EN 14080:2013).	9
1.2.	Fig. 2 Glued solid timber with two and three laminations (©2024, dataholz.eu).	10
1.2.	Fig. 3 Glued laminated timber (UNI EN 14080:2013).	10
1.2.	Fig. 4 Glued laminated timber (©2024, dataholz.eu).	11
1.2.	Fig. 5 Cross-laminated timber (©2024, XLAM DOLOMITI).	11
1.3.	Fig. 6 Spread of species in Abruzzo Region.	13
1.3.	Fig. 7 Beech forests in the Province of L'Aquila.	15
1.3.	Fig. 8 Cutting of trees in logs and boards.	17
2.1.	Fig. 9 Visual grading: top) based on size and position of defects (knots, grain deviation) on the surface of the timber structural element; middle) isolated or grouped knots; bottom) grain deviation (UNI 11035:2022).	20
2.2.	Fig. 10 ViSCAN of Microtec (Rosewood, 2021).	23
3.1.	Fig. 1. Master Panels: left) Assembly phase; right) After pressing.	28
3.1.	Fig. 2. Test set-up for bending perpendicular to the plane ($a = b = 6H$) and rolling shear test ($a = b = 3H$) []. adapted from [17].	28
3.1.	Fig. 3. Test set-up for in-plane bending ($a = b = 6H$) and shear test ($a = b = 3H$) []. adapted from [17].	28
3.1.	Fig. 4. Set-up left) Equipment details; right) Upper view.	29
3.1.	Fig. 5. Collapse patterns of Beech panels in perpendicular-to-plane bending test: A) HB with polyurethane adhesive collapsed for rolling shear and delamination; B) Homogeneous HB panels with polyurethane adhesive collapsed for delamination; C) BP configuration panels collapsed for rolling shear and delamination. D) HB panels with melamine adhesive collapsed for rolling shear.	30
3.1.	Fig. 6. Collapse patterns of HP panels in perpendicular-to-plane bending test: E) Collapse for bending and knot influence of panels made in by classified boards (Series 5). F) Collapse due to knots cluster influence of panels realized with non-classified boards (Series 5bis).	30
3.1.	Fig. 7. Typical in-plane bending collapse.	31

3.1.	Fig. 8. Comparison between specimens from Master Panels 2B, 4B, 6 and 7 (in-plane shear tests).	32
3.1.	Fig. 9. Comparison of FE models with experimental in-plane shear test.	33
3.1.	Fig. 10. Comparison of FE models with experimental perpendicular-to-plane shear test.	33
3.1.	Fig. 11. Comparison of FE models with experimental bending test in-plane (left) and perpendicular-to-plane (right).	34
3.1.	Fig. 12. Comparison of C24 Red Spruce with test materials in-plane shear test. (For interpretation of the references to colour in this figure legend, the reader is referred to the web version of this article.)	34
3.1.	Fig. 13. Comparison of C24 Red Spruce with test materials in-perpendicular-to-plane shear test. (For interpretation of the references to colour in this figure legend, the reader is referred to the web version of this article.)	35
3.1.	Fig. 14. Comparison of C24 Red Spruce with test materials in-perpendicular-to-plane bending test. (For interpretation of the references to colour in this figure legend, the reader is referred to the web version of this article.)	35
3.2.	Fig. 1 Setup description: a machine test; b displacement transducers position and knives; c setup design detail.	43
3.2.	Fig. 2 Failure modes: a–c bending–buckling; d–f rolling shear;g, h delamination.	45
3.2.	Fig. 3 Axial displacement versus compressive load F: a homogeneous HB specimens; b hybrid HB specimens.	46
3.2.	Fig. 4 Midspan displacement versus compressive load F: a and, top b recorded curves for the homogeneous and hybrid specimens, respectively; c and, bottom d re-elaborated curves for the homogeneous and hybrid specimens, respectively	46
3.2.	Fig. 5 Reference system: imperfect beam under a concentrated compression load.	46
3.2.	Fig. 6 Kinematic quantities: a undeformed shape; b deformed shape.	47
3.2.	Fig. 7 Detail (in the deformed shape) of the kinematic and static quantities of the glue line between i-th and i + 1-th layers	47
3.2.	Fig. 8 Static quantities in the deformed configuration and global resultants.	47
3.2.	Fig. 9 Static equilibrium for the i-th layer.	48
3.2.	Fig. 10 Kinematics of the generic section in the CLT panel.	49
3.2.	Fig. 11 Limit configurations for the single section.	50
3.2.	Fig. 12 Diagrams of the coupling parameters and varying with g and G2 within their ranges of interest for CLT panels.	52

3.2.	Fig. 13 Buckling load efficiency varying with g and $G2$ within their ranges of interest for CLT panels.	52
3.2.	Fig. 14 Experimental (thin line) and analytical (thick line) mid-span displacement versus compressive load F .	52
3.2.	Fig. 15 Elastic response of the imperfect HO-CLT panel under a tip load expressed by functions of the abscissa x ($F = 0,5 F_{cr} - e_0 = 0.25$ mm).	54
3.2.	Fig. 16 Rigid displacement and deformation displacement components.	57
3.4	Fig. 1 Three-dimensional view and cross-section details of the case-study floor object of intervention (dimensions in mm).	65
3.4	Fig. 2 Cross-section of the examined composite system (dimensions in mm).	66
3.4	Fig. 3 Example of bending stiffness variation (8 mm diameter screws): ULS (a); SLS (b).	69
3.4	Fig. 4 3D graphs of bending stiffness variation (10 mm diameter screws): ULS (a); SLS (b).	69
3.4	Fig. 5 3D graphs of bending stiffness variation (12 mm diameter screws): ULS (a); SLS (b).	70
3.4	Fig. 6 Comparison between limit cases and flexible cases, in terms of ULS bending stiffness for 12 mm diameter screws.	70
3.4	Fig. 7 Typical trend of η parameter for 12 mm diameter screws K2 case.	71
3.4	Fig. 8 Percentage weight variation of reinforcement, compared to the total permanent weight of timber floor with reinforcing intervention.	72
3.4	Fig. 9 Quantitative comparison of selected reinforcement techniques in terms of $(EI)_{eff}$ (ULS).	72
3.4	Fig. 10 ULS bending stiffness-to-weight increase for K3 case.	73
3.4	Fig. 11 Bending moment distributions along the span for $K= 0$, $K2$, and $K= \infty$ cases, and maximum normal stresses distributions along the cross-section height for each reinforcement.	74
4.1.	Fig. 1. Glue-laminated timber beams: left) Gluing phase; right) Assembly prior to pressing.	82
4.1.	Fig. 2. Test set-up for bending perpendicular to the plane ($a = b = 6H$) and rolling shear test ($a = b = 3H$) [adapted from [22]].	82
4.1.	Fig. 3. Set-up left) Equipment details; right) Front view.	83
4.1.	Fig. 4. Details of failure modes of the bending tests: 1), 2), and 3) bending failure modes; 2) and 6) delamination failure modes; 3) and 5) influence of defects.	84
4.1.	Fig. 5. Load-displacement curves: left) homogeneous beech specimens; right) beech/Corsican pine specimens.	85
4.1.	Fig. 6. Load-displacement curves: left) homogeneous beech specimens; right) beech/Corsican pine specimens.	86
4.1.	Fig. 7. Chart of characterization and grading procedure of laminations and beams.	86

4.1.	Fig. 8. Comparison of load–deflection curve from experimental tests vs hypothetical beam classified as DT24 DT38 and DT46.	87
4.1.	Fig. 9. Beam cross section for γ -method calculations.	87
4.1.	Fig. 10. Comparison of load–deflection curves from experimental tests vs hypothetical beam classified as GL44hyb and analytical evidences from γ -method calculations.	88
4.1.	Fig. 11. a) Four-point bending experimental setup, b) FE model beam with ending support and load plates details c) Setup carriage, d) Setup hinge.	89
4.1.	Fig. 12. Vertical deflection (w) for glulam beam GL 44 hyb.	89
4.2.	Fig. 1 Glue-laminated timber beams: a) Manufacturing of finger joints and bonding; b) Face gluing.	98
4.2.	Fig. 2 Push-out specimens and related floor scheme: a) Series 1: single layer of planking with floor joists; b) Series 2: double layer of cross planking.	100
4.2.	Fig. 3 Tests: a) Testing instruments and loading machine; b) Single-layer planking: laser transducers position; c) Double-layer crossed planking: laser transducers position.	101
4.2.	Fig. 4 Test results: a) single planking; b) double-crossed planking.	102
App.	Fig. 1 Example of 3D FE model.	129
App.	Fig. 2 Boundary conditions named BC-2.	129
App.	Fig. 3 Boundary conditions named BC-3.	130
App.	Fig. 4 Flow chart for the procedure followed for CLT panels.	130

List of tables

1.3.	Table 1 Softwood and hardwood forested area in Abruzzo.	13
3.1.	Table 1 Mean properties of timber species, derived from the VISCAN procedure.	27
3.1.	Table 2 Mean properties of the examined CLT specimens.	28
3.1.	Table 3 Perpendicular-to-plane bending test.	29
3.1.	Table 4 In-plane bending test results.	30
3.1.	Table 5 Perpendicular-to-plane shear test results.	31
3.1.	Table 6 In-plane shear test results.	32
3.2.	Table 1 Mean properties of timber species, derived from the non-destructive measurements.	42
3.2.	Table 2 Axial compression test campaign evidence.	44
3.2.	Table 3 Mechanical properties of the wood species used for the CLT specimens.	51
3.2.	Table 4 Critical and limit loads from the analytical model.	55
3.2.	Table 5 Comparison between analytical and experimental results.	55
3.2.	Table 6 Comparison between analytical and updated experimental results.	56
3.4	Table 1 Slip moduli for different reinforcements.	66
3.4	Table 2 Limit cases of calculated bending stiffness: $(EI)_0$ for $K=0$ and $(EI)_\infty$.	68
3.4	Table 3 γ_1 coefficients for different reinforcements (K2).	68
3.4	Table 4 Flexible connections (ULS): calculated $(EI)_{\text{eff}}$ for K1, K2, and K3.	68
3.4	Table 5 Flexible connections (SLS): calculated $(EI)_{\text{eff}}$ for K1, K2, and K3.	68
3.4	Table 6 η values for different reinforcement (K2).	71
4.1.	Table 1 Mean values of the density (ρ), dynamic modulus of elasticity (E_{dyn}), measured during strength grading and mean values of bending strength (f_m)...	81
4.1.	Table 2 Size (B = base; L = length; H = height), configuration and test type of the examined glue-laminated timber specimens.	82

4.1.	Table 3 Bending test results.	83
4.1.	Table 4 Shear test results.	85
4.1.	Table 5 Homogeneous beech beam features evaluated assuming a board class DT 24.	86
4.1.	Table 6 Homogeneous beech beam features evaluated assuming a board class DT 46.	86
4.1.	Table 7 Homogeneous beech beam features evaluated assuming a board class DT 38.	87
4.1.	Table 8 Bending stiffness evaluation applying γ -method formulation and EN 338 modulus of elasticity.	88
4.1.	Table 9 Bending stiffness evaluation applying γ -method formulation and experimental modulus of elasticity.	88
4.1.	Table 10 Numerical evidences and comparison for homogeneous beams.	89
4.1.	Table 11 Numerical evidences and comparison for hybrid beams.	89
4.1.	Table 12 Numerical evidences and comparison with commercial GL 24 h beam.	90
4.2.	Table 1 Mechanical properties of planks and glulam beams.	98
4.2.	Table 2 Test configurations.	99
4.2.	Table 3 Screw configuration 1a ($F_{est} = 60$ kN).	103
4.2.	Table 4 Screw configuration 2a ($F_{est} = 100$ kN).	103
4.2.	Table 5 Screw configuration 1b ($F_{est} = 45$ kN).	104
4.2.	Table 6 Screw configuration 2b ($F_{est} = 60$ kN).	104
4.2.	Table 7 Experimental slip moduli for the single fastener.	105
4.2.	Table 8 Shor-term deflections values [mm] varying geometry for $Q_k = 2$ kN/m ² .	106
4.2.	Table 9 Shor-term deflections values [mm] varying geometry for $Q_k = 4$ kN/m ² .	106
4.2.	Table 10 Long-term deflections values [mm] ($G_{k2} = 1$ kN/m ² and $Q_k = 2$ kN/m ²).	107
4.2.	Table 11 Long-term deflections values [mm] ($G_{k2} = 2$ kN/m ² and $Q_k = 2$ kN/m ²).	107
4.2.	Table 12 Long-term deflections values [mm] ($G_{k2} = 1$ kN/m ² and $Q_k = 4$ kN/m ²).	108
4.2.	Table 13 Long-term deflections values [mm] ($G_{k2} = 2$ kN/m ² and $Q_k = 4$ kN/m ²).	108
4.2.	Table 14 Slip moduli at ULS for the single fastener.	109

4.2.	Table 15 ULS for coupled tensile-bending ($G_{k2} = 1 \text{ kN/m}^2$ and $Q_k = 2 \text{ kN/m}^2$).	110
4.2.	Table 16 ULS for coupled tensile-bending ($G_{k2} = 2 \text{ kN/m}^2$ and $Q_k = 2 \text{ kN/m}^2$).	111
4.2.	Table 17 ULS for coupled tensile-bending ($G_{k2} = 1 \text{ kN/m}^2$ and $Q_k = 4 \text{ kN/m}^2$).	111
4.2.	Table 18 ULS for coupled tensile-bending ($G_{k2} = 2 \text{ kN/m}^2$ and $Q_k = 4 \text{ kN/m}^2$).	112
4.2.	Table 19 Design compression stresses $\sigma_{c,0,d}$ for the planking.	112
4.2.	Table 20 Load on a fastener $F_{i,d}$ ($G_{k2} = 1 \text{ kN/m}^2$ and $Q_k = 2 \text{ kN/m}^2$).	113
4.2.	Table 21 Load on a fastener $F_{i,d}$ ($G_{k2} = 2 \text{ kN/m}^2$ and $Q_k = 2 \text{ kN/m}^2$).	113
4.2.	Table 22 Load on a fastener $F_{i,d}$ ($G_{k2} = 1 \text{ kN/m}^2$ and $Q_k = 4 \text{ kN/m}^2$).	114
4.2.	Table 23 Load on a fastener $F_{i,d}$ ($G_{k2} = 2 \text{ kN/m}^2$ and $Q_k = 4 \text{ kN/m}^2$).	114

Thesis organization

A brief description of the thesis structure is given below. The thesis is presented as a compendium of scientific articles which includes a general introduction, four main chapters, concluding remarks and subjects for further research.

The background in which the studies are carried on and the objectives pursued by the research are described in the “Introduction” and “Research objectives” paragraphs, respectively.

The first chapter “The short wood supply chain” reports the state of the art referring to international and national projects of similar nature, explores the main applications of timber as structural component, and defines the Abruzzo Region context focusing on its forest heritage.

The second chapter “Timber grading” regards the visually and by machine timber strength grading with insights about standards and procedures usually applied in Italy.

The third chapter “Cross-laminated timber panels”, as indicated in the title, is focused on this kind of engineered wood product and it exposes three different works published in international journals regarding the mechanical characterization, the buckling behaviour, and the possible application as retrofitting material of thin novel CLT panels, respectively.

The last chapter “Glue-laminated timber beams” studies another kind of engineered wood product: it presents a published paper concerning the mechanical characterization of homogeneous and hybrid glulam beams and a work related to flexible timber-to-timber connections topic.

Although each paper has a stand-alone structure, there is a common thread that links and makes them complementary to each other in order to progressively delve into various topics of interest. The “Concluding remarks” section sums up the main achievements and points out the outcomes of all the research papers and works.

For the sake of clarity, the contribution of the PhD candidate to each paper is stated in the following: formal analysis, investigation, writing, review and editing for the paper published in Construction and Building Materials journal; formal analysis, writing, review and editing for the paper published in Engineering Structures journal; experimental investigation and writing for the paper published in Archives of Civil and Mechanical Engineering journal; methodology, formal analysis, data curation, writing, review and editing for the paper published in buildings journal; formal analysis, investigation and writing for the last ongoing work.

Introduction

In recent times, wood as construction material has spread in Italy both in the realization of new structures and in the strengthening of ancient buildings. The sixth report about the wood building sector by FederlegnoArredo, a study centre which develop accurate market analysis of the wooden construction chain in Italy, pointed out that a total turnover of 1.39 billion euro was achieved by this sector in 2020, confirming Italy as the fourth European country for the construction of wooden buildings (Centro Studi FederlegnoArredo, 2021).

Until 2000, wood was principally used for refurbishment and retrofit of historical timber floors and roofs, and for construction of roofs in new residential buildings, with only few cases of single-storey sportive centres such as swimming pools and halls. The principal used elements were made of sawn, glued solid or glued laminated timber, connected with metal fasteners like screws, nails, dowels, and bolts, exclusively.

Moreover, in that period important research on timber-concrete composite floors was carried out, in order to stiffen existing timber floors (van der Linden & Blass, 1996), and also on different strengthening techniques of degraded timber elements and joints (Parisi & Piazza, 2000; Tampone, 1996). After 2000, up-to-date wood building systems, such as light-frame, moment-resisting frames, and solid panel construction, were promoted and used for the erection of houses, multi-storey buildings, and large malls. In addition to sawn timber, engineered wood products

were introduced to overcome some limits of the raw material (Fridley, 2002; Lam, 2001). There was also an advancement in the seismic design of multi-storey timber buildings, thanks to the competitiveness of new structural products. For instance, cross-laminated timber (CLT or X-Lam) panels, which consists of layers of timber planks glued together at a right angle to each other, allow to obtain massive panels to realize walls and floors of multi-storey timber buildings (Ceccotti et al., 2013). Due to the fragile behaviour of timber members, the structures ductility has to be ensured by the connections. For this reason, another important result was the progress of the connection systems, leading to high performance self-drilling screws (Hossain et al., 2018) and two-dimensional and three-dimensional nailing plates (Izzi et al., 2018).

Due to its advantages as construction material, timber has proved to be competitive with other common materials such as reinforced concrete and steel for multi-storey buildings, both in terms of structural behaviour (Reynolds et al., 2016) and economically (Mallo & Espinoza, 2016), and it has earned more trust from designers, being a real alternative as compared to other materials.

On the other hand, wood has a more complex behaviour than concrete and steel, and unlike the latter ones it cannot be considered homogeneous and isotropic, but it is usually regarded as heterogeneous, due to its defects such as knots and grain deviation, and anisotropic, which means that it offers different mechanical properties depending on the angle to the grain.

Bearing in mind these characteristics, timber can be effectively used to build or retrofit in a sustainable and appropriate way.

Research objectives

The aim of this work is to promote the use of local wood for structural purposes in Italy, with particular regard to the Abruzzo Region, to the Province of L'Aquila, and to several municipalities such as Santo Stefano di Sessanio, Calascio, Castel del Monte, Castelvechio Calvisio, and Carapelle Calvisio.

Italy is an historically importer country of wood, although its area is covered for thirty percent by unused forests, and the amount of imported timber is about the eighty percent of the overall usage. Therefore, the use of locally grown timber could be beneficial in order to economically enhance the value of local forested areas and to reduce the carbon dioxide emissions due to the importations, starting from manufacturing simple structural components up to building zero-kilometer

constructions as an ideal final goal. The nature of the project requires a multidisciplinary approach with the collaboration of institutions and local authorities, such as Ente Gran Sasso e Monti della Laga National Park, Abruzzo Region offices, National Research Council of Italy (CNR), universities, forestry consortia, cooperatives and forest companies, providing at first preliminary steps such as the identification of suitable areas, the procurement, cutting and classification, and then the choice of the best technology to produce wood-based structural components and the study of possible applications of these products in local constructions and buildings. Furthermore, such an approach, in the context of a sustainable forest management, could produce environmental, economic, and social advantages, thanks to the possibility to increase the forested areas, to the economic recovery of these areas usually underdeveloped, and to the use of wood in structural components rather than only as firewood.

In addition, the production waste such as bark, branches, and sawdust, could be used as biomass for the production of energy, while fully respecting the European principles of bioeconomy (European Commission, 2018).

The importance of using timber in building is evident especially in term of sustainability because of the long-term storing of carbon dioxide in the wooden members and the reduced embodied energy with respect to other construction materials. Added to this, exploiting native forests could lead to relevant benefits such as the reductions of importations, the increase of job opportunities, the consequent reduction of depopulation of rural areas, the economic and environmental enhancement of local woods in accordance with national regulations. The aforementioned territories, characterized by unexploited forest resources and shared development strategies, possess the necessary factors and know-how to extend localized artisanal productions to a greater production context both locally and nationally, since, in the last decades, the growing demand for wood-based products for structural purposes is on the rise. Wooden constructions represent the future, not only for the economic recovery and the enhancement of internal mountain areas but also for the ecological turning point of the construction sector, essential for reducing carbon emissions and to achieve the goals set by 2030 Agenda (United Nations General Assembly, 2015).

The innovative aspects of this project lie in the real knowledge of the territory, of its problems and its potential. All these topics have to be highlighted through constructive discussions with institutions. The strongest innovative connotation is that the proposal of current interest aims at enhancing woodland resources with the cooperation of Local Administrations, such as union of municipalities headed by the

Municipality of Santo Stefano di Sessanio, the Abruzzo Region, the Campo Imperatore and the Subequano Forestry Consortia, CO.LAFOR. Consortium of Agro-Forestry Works, as well as artisanal realities and universities.

Given the territorial context, the aim of the research is the assessment of all possible applications of locally grown timber, both in poorly industrialized products, such as boards and sawn timber, and in highly engineered products, such as glue-laminated timber members and cross-laminated timber panels.

To synthesize, the main research objectives can be indicated as the following:

1. To identify the most abundant locally grown wood species or in any case of Italian origin on which the research must be conducted.
2. To produce engineered wood products (EWP) such as glue-laminated timber beams and cross-laminated timber panels after a suitable classification procedure.
3. To mechanically characterize the EWP of the previous objective by means of experimental tests according to national and European standards.
4. To analyse possible applications of the previously characterized EWP in the local building context.

1. The short wood supply chain

The issues of sustainability and eco-efficiency of buildings have become the focus of the building policies of most administrations and public organizations at the local, national, and international level.

In this context, the choice of wood as renewable construction material appears to be a logical consequence in consideration of the property of wood to fix carbon through the process of chlorophyll photosynthesis and of lower consumption in terms of energy and climate-altering emissions in the production and transformation processes compared to other materials used in construction such as concrete, steel, and masonry. In addition to these benefits, the processing waste during the transformation phases and the material itself at the end of its life cycle can be used for waste-to-energy. Therefore, it is evident that there are several environmental advantages that can be achieved from a suitable and smart use of this material both as an energy source and as a building material (Ramage et al., 2017).

The development of a short supply chain of timber could be a valid mean to provide an increased value to native forests and to foster sustainable practices (Romagnoli et al., 2019). The idea of using the best parts of locally grown trees to manufacture solid wood members and wood-based composites, while the remaining parts could be employed as biomass for energy production, is fundamental and is expected to play a significant role to reduce the carbon footprint and to cater for the increasing wood demand for structural and non-structural uses. Besides the economic enhancement of the woodland, environmental and social advantages can be obtained

through a sustainable forest management, including landscaping improvement, carbon dioxide reduction, possible touristic development, and recovery of usually underdeveloped areas offering jobs in the forestry and construction sectors and preventing depopulation.

The investigation of locally grown wood species can be an incentive to use local resources in different applications and at the same time to strengthen forestry policies aimed at preserving and managing the forest heritage in a sustainable way. The knowledge of the current restrictive legislation and consistency of the woods is the first step to take so as to identify suitable areas and choose the best species to produce structural components and more. An innovative and rational use of forest products coming from a short supply chain, or in any case from national origin, requires a sharing of objectives and a considerable degree of interdisciplinarity.

A reconsideration of the traditional role of wood in construction can contribute to the achievement of a modern and optimized use of timber and concretely encourage the well-known principle of "cascading use of wood". The general purpose of the research project concerns the enhancement of short wood supply chains, promoting good practices and developing technological solutions both for structural and non-structural functions for a more environmentally friendly building sector. Consequently, this project is of great interest for the Abruzzo Region, especially for the very high content of innovation it could bring to the regional forest-wood supply chain. Indeed, there are no other research projects in progress in this Region aimed at evaluating uses of the wood raw material other than those aimed at the production of thermal energy. Despite the great forest heritage of the Region and the potential it could develop, it is not yet possible to look beyond the more common uses as firewood. Hence the benefits in terms of growth of the regional forest sector this research could promote.

1.1. State of the art

Over the last few years, a significant research case was developed in Sardinia in order to assess the goodness of locally grown timber, namely maritime pine, to produce cross-laminated timber panels (Fragiacomo et al., 2015). Even though maritime pine has generally low mechanical properties, it proved to be suitable to manufacture medium quality CLT panels because of the features of this technology (Concu et al., 2018). Indeed, the different layers are glued together at a right angle and this layout improves the overall behaviour reducing the influence of defects.

However, the preliminary tests were needful to estimate the mechanical properties of the maritime pine, which results as a low-grade material with large knots and significant grain deviation. From this evaluation the most suitable technology to exploit the raw material was chosen. The principal aim was to present the short procurement chain of timber as a real mean to improve forest management, to extend forested areas and to enhance native species of Mediterranean forests.

The current extension of conifers in these areas is the result of artificial introduction over the course of time due to different historical, social, and environmental motivations. Among the Mediterranean pines, the maritime pine is considered relatively fast growing and quite common, therefore it was selected to be investigated in that project. Another goal of the research work is to be a positive example of forestry good practice and enhancement in the national context, since in Italy wood is mainly used as energy source. As a matter of fact, wood used as firewood produces two negative effects because it has a low added value, and it ends the carbon stocking process. Hence the importance of exploiting locally grown timber to produce high added value products for structural purposes.

The huge hardwood forests extension in Europe has recently focused the attention on the possible application of these species to produce engineered wood products (Aicher et al., 2014; Brunetti, Nocetti, Pizzo, Aminti, et al., 2020; Ehrhart et al., 2020; Frese & Blaß, 2007), such as cross-laminated timber (CLT) and glue-laminated timber (glulam). These structural components are usually manufactured from softwood species, therefore experimental investigations are required in order to assess the goodness of hardwood species members. In particular, there are some issues to be faced in order to use effectively hardwood in engineered wood products, such as structural bonding. For instance, beech wood is known to be difficult to be bonded due to its high density. Some interesting results have been achieved even for hybrid configurations, in which both softwood and hardwood species are considered, as described in the following.

1.2.Solid wood and wood-based composites

Timber as building material offers many advantages: first of all, the environmental benefit, since wood is the only material which requires solar energy, water and air to grow, resulting in a regeneration over 25 to 50 years rotation cycles and in a reduced embodied energy, and which absorb the carbon dioxide from the surrounding environment, reducing the climate-altering gasses until its combustion;

secondly, timber can be used alone due to the high tensile and compression strength, unlike other materials such as concrete and masonry, and it also presents a high strength-to-weight ratio; lastly, there are other benefits over other materials such as aesthetical appearance, pleasant smell, hygroscopicity, thermal insulation, speed of erection and more.

In contrast, sawn timber presents critical disadvantages like great anisotropy, influence of defects, influence of the moisture content, reduced modulus of elasticity and creep behaviour, combustibility, durability problems if in contact with water, and reduced ductility. However, some of these problems can be solved using engineered wood products like glued solid timber, glued laminated timber, and cross-laminated timber. As a matter of fact, the size of structural components made of sawn timber is limited by the size of the tree and only straight members can be produced. In addition, there is an evident anisotropic behaviour with significant strength reduction and reduced reliability due to defects. All these limits can be overcome by means of wood-based composites which reduce the scatter of results because of the controlled manufacturing process, improve the timber behaviour, and allow to produce larger dimension and possibly curved members.

Glued solid timber consists of lamellae with thicknesses from 45 to 85 mm which are bonded together up to a total number of five according to EN 14080 (UNI Ente nazionale italiano di unificazione, 2013).

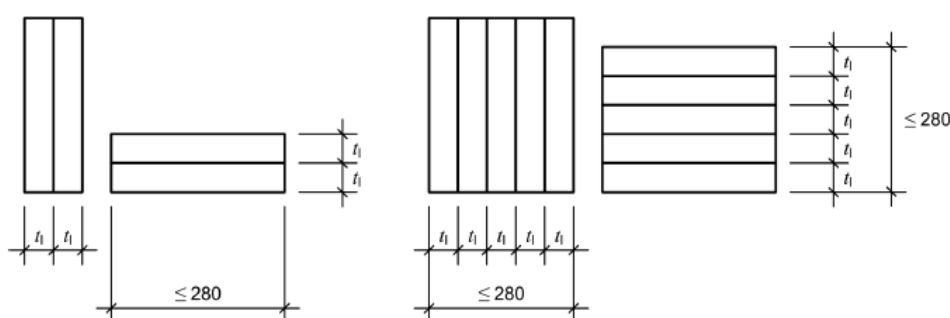


Fig. 1 Examples of laminations for glued solid timber (UNI EN 14080:2013).

The lamellae present a grain direction parallel to each other and the total cross-section shall not exceed 280 x 280 mm. Glued solid timber members are predominantly bending stressed and are employed as beams and columns in new buildings but also for renovation of ancient buildings.

This kind of technology represents the least industrialized level of engineered wood products taken into account in this paragraph, as it mainly consists of small and straight components.



Fig. 2 Glued solid timber with two and three laminations (©2024, dataholz.eu).

Another important wood-based composite is glue-laminated timber (glulam) which is one of the first wood composite for structural employments. The first use of glulam dates to the early 1890s and, despite the long period since its introduction, it is still a modern material due to the possibility of manufacturing straight or curved long sized members, with great aesthetical appearance, high mechanical properties, and good optimisation of the starting lamellae. It consists of wood members manufactured by gluing planks together so as to have the same grain direction. The lamellae, unlike glued solid timber, are thinner with a range from 40 to 50 mm thick and a length from 1500 to 5000 mm. The laminations are joined lengthwise with finger joints for long sized members up to 40 m and are also glued together up to 2 m height. The final product offers several advantages in terms of geometrical shape, aesthetic appearance, and improved strength and stiffness properties.

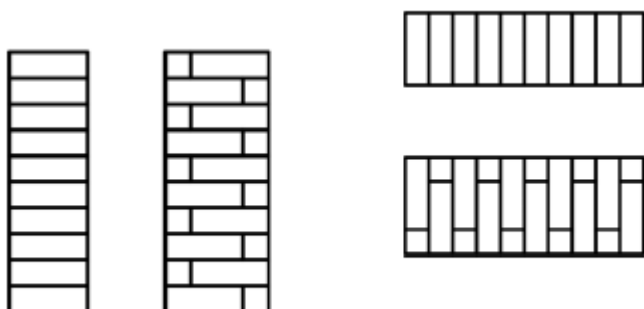


Fig. 3 Glued laminated timber (UNI EN 14080:2013).

Indeed, the defects such as knots are smaller and spread throughout the member volume, leading to a more homogeneous material, and the overall mechanical properties are increased also because of the controlled manufacturing process, which

requires drying, grading and stiffness testing phases.

Conifers are the most currently used wood species to produce glulam due to the lower density and a better shape of the logs, and they have played a fundamental role to promote and increase trusting in the glulam technology.



Fig. 4 Glued laminated timber (©2024, dataholz.eu).

However, the use of hardwoods in building, already examined in the past (Egner & Kolb, 1966; Gehri, 1980), has proved to be a valid option especially in those territories where there is a prevalence of these species. In the last few years, several studies were addressed to the investigation of novel glulam components made of hardwood and they present positive results in term of material optimisation and mechanical properties.

Lastly, cross-laminated timber (CLT or X-Lam) has gained in popularity in the mass timber construction sector in the last twenty years. It consists in prefabricated solid slabs obtained by gluing together lumber layers at a right angle, in order to manufacture two-dimensional components with a more in-plane isotropic strength and greater in-plane stability.



Fig. 5 Cross-laminated timber (©2024, XLAM DOLOMITI).

CLT panels are usually used to build walls, floors, and roofs of multi-storey timber buildings up to ten storeys. Some examples of high-rise timber building are the 9-storey Stadthaus Building at Murray Grove in London, and the 10-storey Fortè Building in Melbourne, but there is also a new challenge addressed to design timber skyscrapers, represented by the 24-storey Hoho Tower in Vienna and the 34-storey residential tower in Stockholm. Among the advantages of this technology, there are also the possibility of using low-grade timber to produce medium quality panels, the reduced splitting tendency in connection regions thanks to the contribution of the orthogonal layers, and the easy and quick assembling on site which allows to reduce hazard and construction time. In contrast, the main disadvantages are the large volume of timber needed, which could determine a high total cost, and the reduced strength in the main direction because only the layers parallel to the grain carry the load. Despite these drawbacks, cross-laminated timber is a valid option to build multi-storey building due to the excellent seismic performance of this solid panel construction system, as investigated in the SOFIE Project in 2007 by means of shaking table tests with a seismic input equal to Kobe earthquake of 1995 (Ceccotti et al., 2013).

Further investigations were developed to manufacture CLT panels with short supply chain timber and the outcomes were encouraging both for homogeneous configurations and for hybrid ones (Brunetti, Nocetti, Pizzo, Negro, et al., 2020).

1.3. The research case in Abruzzo

The main aim of the present thesis is to promote the use of short supply chain timber in the Abruzzo Region, central-southern Italy. Although this area has a great abundance of forests, local wood is hardly used and only for energy production.

The first step is the identification of suitable areas in the Province of L'Aquila, see Fig. 6, from which wood of local species, such as downy oak, beech, or chestnut, could be supplied and transported to local sawmills. As a subsequent step, poorly industrialized products made of local timber such as boards and sawn woods could be manufactured by local plants, see Fig.7. In this way there is an incentive to use native wood as higher value components in building rather than as firewood. The fundamental principle of the supply chain is the circular economy, which consists in the sequential use of wood for different purposes, according to the so-called "cascading use". The principal purpose is the manufacture of structural members, using the best parts of trees, and the secondary one is the energy production, using

in this case only the low-quality parts of trees such as bark, sawdust, and branches. Timber as construction material favours a long-term accumulation of carbon dioxide, providing the satisfaction of some environmentally friendly principles of the current European and National policy.

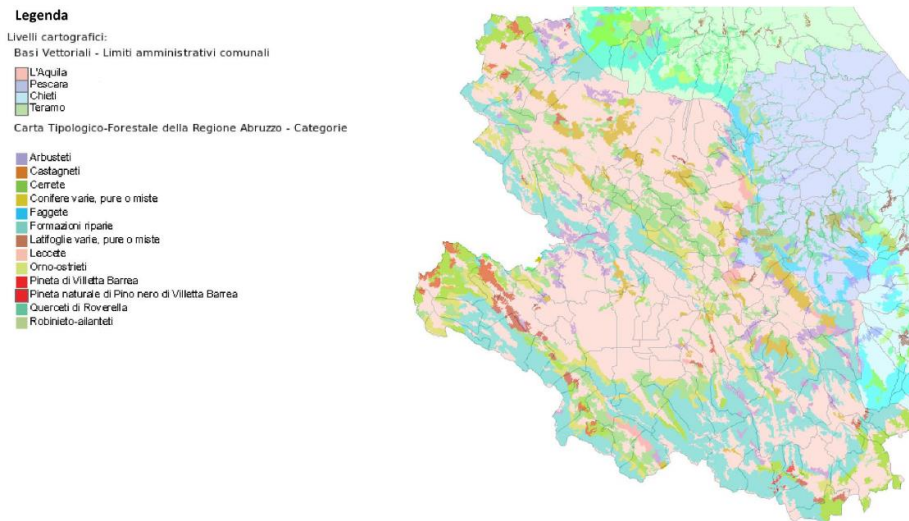


Fig. 6 Spread of species in Abruzzo Region.

Table 1 Softwood and hardwood forested area in Abruzzo.

Softwoods	Area [Ha]
Spruce forests	362
Silver fir forests	724
Scots and mountain pine forests	1.086
Black pine and larch pine forests	19.158
Mediterranean pinewoods	2.534
Other coniferous forests	1.448
Total	25.312
Hardwoods	Area [Ha]
Beech forests	122.402
Oak and downy oak forests	81.779
Cerrete and Farnetto woods	30.741
Chestnut groves	5.068
Hornbeam forests	46.145
Hygrophilous forests	20.270
Other deciduous forests	48.760

Holm oak forests	8.687
Total	363.852
Total regional forested area	389.164

The territory of the lands of the “Baronia di Carapelle”, called in this way to remember the belonging of all the villages to a single political and administrative unit for several centuries, includes the municipalities of “Santo Stefano di Sessanio”, “Carapelle Calvisio”, “Castelvecchio Calvisio”, “Calascio”, “Castel del Monte”, and “Villa Santa Lucia degli Abruzzi”, each located in the Province of L'Aquila (Abruzzo, Italy).

All the municipalities of this area are marked by a strong historical identity, which had its greatest splendour in the late Middle Ages and the early Renaissance, and by a territorial, cultural, and social identity which unfortunately becomes increasingly weaker due to the important demographic decrease.

Indeed, such rural areas are characterized by an evident depopulation which started between the two world wars, and which still cannot be stopped today. The decrease in population and the high rate of aging have caused the consequent reduction of economic activities, especially agricultural ones. The progressive abandonment of agricultural practices involves an important, often irreversible, modification of the agricultural landscape with a consequent decrease in the levels of biodiversity. The loss of cultural identity also began in the last century and continues today even if the various local associations are trying to preserve the memory of these places.

The heterogeneity of the territory, from hilly landscapes with Mediterranean climate to mountain-alpine environments with continental climate, manifests itself in very small spaces, giving the area unique characteristics in its kind. In these places, the man-environment relationship is still close, and little changed for centuries, influenced by the use of the Earth's resources, sheep breeding and agriculture. The enormous landscape and naturalistic value given by the variety of ecosystems, by the geo-morphological, vegetational and zoological complexity is enriched by the clearly visible signs that a compatible interaction between man and the environment has left over the centuries. Since the middle of the last century, especially in the most difficult environments, these values have undergone a strong impoverishment mainly due to abandonment but also to an exploitation of the soils often in contrast with the principles of eco-compatibility and environmental sustainability.

From a geographical and geological point of view, the territory of the "Baronia di Carapelle" is dominated by the “Gran Sasso d'Italia”, the mountain massif with the highest peak of the Apennines (Corno Grande 2912 m), which has alpine

characteristics with steep walls, basins, valleys, glacial moraines, and alpine landscapes.



Fig. 7 Beech forests in the Province of L'Aquila.

The highest peaks delimit to the north, in the central southern sector of the massif, the vast tectonic depression of “Campo Imperatore”, extended for about 40 km with a NW-SE direction at an average altitude of about 1600 meters, and constitute an orographic barrier that strongly influences the climate of the area. As a matter of

fact, unlike the north-eastern side, rainfall is low and the continental climate, together with the characteristics of the limestone substrate, leads to slopes without woods and vast arid meadows used for the summer grazing of sheep. Another evident feature is the presence of numerous dejection fans such as the large "Canala" of Monte Prena. The area occupied by the "Gran Sasso" according to the geobotanical subdivision of Italy (Pedrotti, 1996) is included in the Euro-Siberian Region (Apennine Province, Umbrian - Marchigiano - Abruzzese Apennine Sector). The geographical location and the altitude contribute significantly to increase the flora and vegetation diversity of the area and for this reason, in a relatively small area, there is the coexistence of Mediterranean-type plant communities with species from the subalpine and alpine ranges.

In the "Baronia" area, in a very small space of about 14 km, the landscape varies from the hills of "Villa Santa Lucia degli Abruzzi" and "Castelvecchio Calvisio" with a mild climate (Mediterranean), to the mountain-alpine zone with a continental climate. The orography, the very different conformation of the territory, and the climatic characteristics contribute to the progressive transformation of the landscape. Considering the distinctive elements, it is useful to delimit areas that have one or more aspects in common by describing the "altitudinal zones", each characterized by specific vegetation. For instance, there is the Sub-Mediterranean hilly area which has an altitude between 400 and 600 meters above sea level with expansion up to 800 m. It is characterized by the cultivation of the olive tree and by the presence of holm oak, downy oak and in general by species of Mediterranean vegetation. This area is in the southernmost part of the territories of "Castelvecchio Calvisio" and minimally of "Villa Santa Lucia degli Abruzzi". Moreover, the hilly area represented by the territories of "Castelvecchio Calvisio", "Villa Santa Lucia degli Abruzzi" and "Santo Stefano di Sessanio" is characterized by the coppice of oak. Instead, the Oro-Mediterranean Mountain zone, which reaches up to 1800 m a.s.l., is present in all the municipalities and is characterized by extensive grasslands and, only in some areas, by beech forests, typical trees of the latitudinal zone. In the territories of "Castel del Monte" and "Villa Santa Lucia degli Abruzzi" there is a type of beech forest that occupies the range between 1000 and 1300 m.

In the zone of arid hilly and submontane pastures, which has an altitude of 800 m up to 1100-1400 m and substantially affects all the municipalities, at lower altitudes the pastures can be interrupted by oak bushes such as in the surroundings of "Castelvecchio" or by reforestation pine forests such as in "Santo Stefano di Sessanio" or by areas of cultivated lands such as in "Villa Santa Lucia degli Abruzzi" and "Castel del Monte".

Therefore, the prevalent wood species are hardwood ones such as downy oak (*Quercus pubescens*), holm oak (*Quercus ilex*), beech (*Fagus sylvatica*), and chestnut (*Castanea sativa*), with only few exceptions of softwood species due to reforestation of pine forests. Further information about beech forests in Abruzzo Region are addressed in the 4.2 section, where timber-timber composite joints, made from logs of diameter ranging from 300 mm to 400 mm and from planks with 130 mm width and 45 mm thickness (see Fig. 8), are examined.



Fig. 8 Cutting of trees in logs and planks.

2. Timber grading

The term “timber” indicates wood used for building or other engineering aims. This natural material has been exploited as construction material since pre-historic ages thanks to its excellent properties. There are two main categories of trees: exogenous and endogenous. The first category includes trees that grow outwards by the addition of concentric annual rings, and the second one includes trees that grow inwards in a longitudinal fibrous mass. The exogenous trees are the most commonly used for engineering purposes, and they are further classified in two groups: conifer or evergreen and deciduous or broad-leaf trees. From the first group, the so-called softwood is obtained, which is resinous and splits easily. This kind of wood is generally light in colour and weight and presents low mechanical properties. From the second group, the so-called hardwood is obtained, which presents a non-resinous and close-grained structure. This second kind of wood presents greater mechanical properties than softwood and it is generally dark in colour and heavy in weight.

Regarding wood microstructure, the material is anisotropic which means that the strength depends on the direction of the stress. Considering wood macrostructure, timber is heterogeneous which means that the strength depends on the size of the element. The larger the volume of the member, the larger the probability of finding a defect, and the lower the strength of the member. Due to defects in wood, strength

grading of timber is fundamental in order to assess the mechanical properties of a single element. There are several defects which affect the macrostructure of wood such as defects due to natural forces, defective seasoning, and conversion. Therefore, a suitable strength grading, visual or by machine, is necessary for structural purposes.

2.1. Visual strength grading

Wood is a biological material and presents a high intrinsic variability of properties, such as strength and stiffness, and for this reason a phase of material grading is required in order to produce structural components. This variability is mainly due to the influence of defects (knots, grain deviation, and more), unlike other building materials such as concrete and steel which can be approximately considered homogeneous. The classification can be of two types, visual or by machine, and must be performed by qualified personnel and by certified machines according to rigorous experimental protocols, respectively. The Italian Technical Standards for Construction currently in force (Ministero delle Infrastrutture e dei Trasporti, 2018) indicate the strength grading as a mandatory requirement for the structural use of wood. This requirement must be guaranteed for both solid wood and wood-based products, including glued solid timber, glue-laminated timber, and cross-laminated timber. The strength grading process requires that each single wood element, like planks or sawn timber, is assigned at a strength class, according to UNI EN 338 (UNI Ente nazionale italiano di unificazione, 2016), so as to attribute reliable strength and stiffness values. The rules and criteria to be followed must be objective and repeatable in order to standardize the grading, which must be applied by all producers responsible for transforming wood into a building material.

Visual strength grading is usually performed by a wood technologist and consists in identifying all those defects that can reduce the mechanical performance of the wooden element. In particular, the size and number of nodes, the presence of lesions and cracks, the inclination of the grain and the width of the growth rings are assessed. The main current standards are the UNI 11035-1 (UNI Ente nazionale italiano di unificazione, 2022a), UNI 11035-2 (UNI Ente nazionale italiano di unificazione, 2022b), UNI 11035-3 (UNI Ente nazionale italiano di unificazione, 2010), UNI EN 1912 (UNI Ente nazionale italiano di unificazione, 2012b), and the aforementioned UNI EN 338.

The grain direction is determined with reference to a minimum length of 1000 mm,

from the ratio between two perpendicular dimensions (x and y). This ratio is expressed as a percentage according to the following expression: $F = (x / y) 100$. It can be determined by identification of any shrinkage cracks present on the element or using a specific carpenter tool.

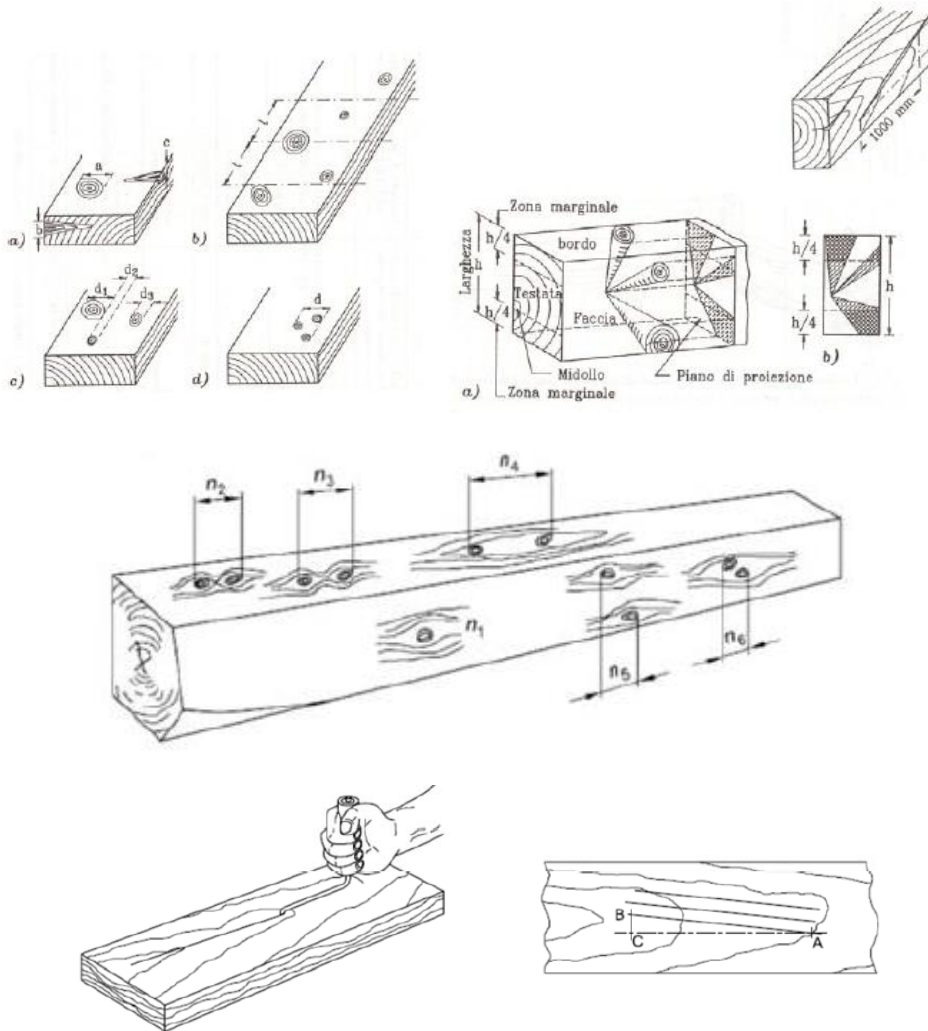


Fig. 9 Visual grading: top) based on size and position of defects (knots, grain deviation) on the surface of the timber structural element; middle) isolated or grouped knots; bottom) grain deviation (UNI 11035:2022).

Regarding knots, those having a diameter not greater than 5 mm are not taken into consideration. Furthermore, all types of knots are admissible (adherent, falling, healthy, black, etc.). There are specific rules to distinguish the various types of nodes, which are indicated with different names, such as n_1 for the isolated nodes, n_2 for the groups of nodes aligned less than 150 mm apart, n_3 for the isolated nodes aligned more than 150 mm apart, n_4 for the groups of nodes more than 150 mm away

with inclined grain, n_5 for the isolated nodes not aligned less than 150 mm away and with the original grain direction between them, and n_6 for the groups of nodes with grain that does not recover the original direction.

The width of the growth rings, where required, must be measured at a head of the sawn timber, and is equal to the average width, expressed in millimetres, of the rings themselves. The measurement is carried out on the longest line perpendicular to the growth rings, starting from a distance equal to 25 mm from the pith when it is present. The width of the rings (ω) is given by the ratio between the length z on which the measurement is made (at least equal to 75 mm when possible) and the number of rings (N) included in z .

This type of grading has the advantage of being less expensive than machine grading, as it can be performed without the aid of special tools by suitably trained and expert operators, adding to the fact that the strength grading rules for the classification are already available for most of the wood species, including the Italian ones. Among the disadvantages, there are the limited number of strength classes that can be identified, and the lower efficiency intended as a greater amount of waste.

2.2. Machine strength grading

The machine grading consists in the instrumental measurement of one or more properties of a structural wood element, in order to assign it to a strength class (Bacher, 2008). In the most common machines, deformation is measured under the application of a known load or there is the measurement of the speed of ultrasound or the induction of vibrations in bending or compression, the scanning with X rays, the laser scanning, or the image analysis. The detected properties, by applying one or a combination of the previously indicated methods, are generally the static bending or tensile modulus, the dynamic bending modulus, the density, and the factor relating to the knots. For example, it is possible to evaluate the modulus of elasticity MOE by evaluating the deflection of a specimen subjected to a non-destructive bending test. In this way, an indirect strength measurement can be obtained by exploiting the correlation between the bending strength (MOR = modulus of rupture) and the modulus of elasticity (MOE). In Italy, the strength grading of wood for structural use was initially performed with visual methods exclusively. However, in the last few decades investigations have been carried out to develop machine classification systems for some local wood species (Nocetti et

al., 2010), so as to introduce also in Italy this methodology already widespread in many European and extra-European countries. Parameters that can be used by different machines have been identified to classify wood effectively, guaranteeing the statistical reliability standards required by European legislation. In addition, to help small and medium-sized Italian companies, portable equipment was introduced, which could be shared by multiple production plants, so as to reduce initial investments for tools and instruments.

Machine grading presents several advantages over visual grading, including:

- high classification efficiency with consistent reduction of waste;
- possibility of assigning timber in a greater number of strength classes;
- high speed of execution of the grading process;
- high repeatability of measurements and of the assignment to strength classes.

In this way it is possible both to enhance the best part of the material and to make the medium-low quality part suitable for structural uses, directing it towards the creation of wood-based products. However, the procedure that allows to set up a machine for the grading of structural timber is quite complex and expensive and requires compliance with codified procedures within the European legislation.

For each wood species and geographical origin, it is necessary to carry out a representative sampling of wood, which must be subjected to destructive tests in certified laboratories after the measurements with the grading machines.

Among the most used systems for machine grading, there is the Viscan by MiCROTEC, which allows to determinate the MOE of wood. By means of a laser interferometer, the frequency of the vibrations induced in the wooden planks or elements by a longitudinal percussion is measured.

Subsequently, through the software of the machine that uses statistical equations, the frequency spectrum (in Hz) is processed, from which the first maximum peak is obtained.

From this value it is possible to obtain, through successive mathematical elaborations, the dynamic modulus of elasticity, which can be expressed with the following equation: $E_{dyn} = MV \cdot (2lf)^2$ [N/mm²]; where l is the length of the board, f is the natural frequency of the vibration, and MV is the density (given by the ratio between the weight of the board and its volume).

The dynamic modulus of elasticity is the parameter (Indicating Property, IP) through which the machine can classify the material. In fact, the IP of the instrument must be related to a mechanical property of the material (grade determining property) and this correlation must be verified through specific tests on the material.

In Italy, many forested areas are covered by hardwood species and, since there is an increasing interest in their use as structural material, it could be valuable to enhance this natural resource. One of the most abundant species is beech (*Fagus sylvatica*) and important research has been carried out for the strength grading of beech boards both by visual and machine methods as described in the following works.



Fig. 10 ViSCAN of Microtec (Rosewood, 2021).

3. Cross-laminated timber panels

Cross-laminated timber (X-lam or CLT) is an engineered wood product obtained by gluing together timber planks layers at a right angle to each other, so that every layer presents grain direction orthogonal with respect to that of the adjacent layer.

In this way, the final product is a massive panel with two main orthogonal load-bearing directions. The number of layers is usually an odd number in order to have the outer layers with the same grain direction.

The main advantages of this engineered wood product are the more in-plane isotropic strength and stiffness compared to glulam (for this reason it can be used for slabs and walls), the greater in-plane stability with similar shrinkage and swelling in the strong directions, the possibility of using low-grade timber thanks to the system effect, and the reduced splitting tendency in connection regions thanks to the reinforcing effect of the orthogonal layers.

On the other hand, larger volume of timber is needed, and the strength is reduced in the main directions as only the boards loaded parallel to the grain carry the load.

In the current Italian technical standards for construction, NTC2018, CLT panels were officially added in the partial safety coefficient table and their structural use must be subject to the conferral of technical suitability by the central technical service of the Superior Council of Public Works. This certification procedure, i.e. Common Understanding of Assessment Procedure, is aimed at suitably characterizing the product and at defining an adequate control of factory production.

3.1. Homogeneous beech and hybrid beech-Corsican pine CLT panels

As first experimental investigation about the possible application of local wood in engineered wood products, the mechanical characterization of novel homogeneous beech (*Fagus sylvatica*) and hybrid beech (*Fagus sylvatica*) - Corsican pine (*Pinus nigra subsp. Laricio (Poir.) Maire*) CLT panels was performed.

Three-layered CLT panels made up with short procurement chain beech-Corsican pine timber and melamine-based adhesive were produced, both in homogeneous and hybrid configuration. This latter one was characterized by the outer layers made of beech wood and the inner layer made of Corsican pine wood.

Some panels were realized with polyurethane glue, usually employed for softwood by the production plant, in order to compare the mechanical behaviour of the products and the failure mechanisms showed.

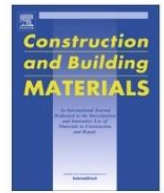
Four-point bending tests, both for the in-plane and perpendicular to-plane directions of the CLT panels, were performed according to EN 408 (UNI Ente nazionale italiano di unificazione, 2012a) with a span length of 18 times the thickness in the case of bending tests and of 9 times the thickness in the case of shear tests.

The test-setup was the same both for the bending and shear tests, with the specimens simply supported and the application of the load in two different points.

The load was applied by means of a hydraulic jack and it was divided via a rigid element in two symmetric loading points. Steel plates were interposed between the timber specimens and the steel supports and elements to prevent local indentations. Inductive displacement transducers, LVDT, were placed on both the faces of each specimen to evaluate vertical displacements as mean values.

Moreover, the local and global mechanical performance of these novel CLT panels was assessed by means of finite element numerical simulations, in order to compare the wood species beech (*Fagus Sylvatica L.*) and Corsican pine (*Pinus nigra subsp.laricio (Poir.) Maire*) with a widely diffused wood species, spruce, usually employed to produce CLT panels.

The experimental and numerical outcomes pointed out an excellent behaviour of homogeneous hardwood panels and a good performance of hybrid softwood-hardwood configuration with respect to C24 spruce CLT panels, introducing great possibilities of optimisation of the wood material as detailed in the following work by (Sciomenta et al., 2021).



Mechanical characterization of novel Homogeneous Beech and hybrid Beech-Corsican Pine thin Cross-Laminated timber panels

Martina Sciomenta^{a,*}, Luca Spera^a, Chiara Bedon^b, Vincenzo Rinaldi^a, Massimo Fragiaco^a, Manuela Romagnoli^c

^a Department of Civil, Architecture and Building and Environmental Engineering, University of L'Aquila, Via Giovanni Gronchi 18, 67100 L'Aquila, Italy

^b Department of Engineering and Architecture, University of Trieste, Via Alfonso Valerio, 6/1, 34127 Trieste, Italy

^c Department of Innovation of Biological, Food and Forestry Systems (DIBAF), University of Tuscia, Via S. Camillo de Lellis, 01100 Viterbo, Italy

HIGHLIGHTS

- Beech and Corsican Pine short chain supply boards were tested to realize CLT panels.
- Bending and shear test were performed in-plane and perpendicular-to-plane direction.
- Hybrid Beech-Corsican Pine CLT panels show high flexural and shear mechanical performances.
- Finite Elements analyses were carried out to compare C24 Spruce CLT panel with tested panels.

ARTICLE INFO

Article history:

Received 23 July 2020

Received in revised form 19 October 2020

Accepted 1 November 2020

Available online 20 November 2020

Keywords:

Cross-Laminated Timber (CLT)

Beech wood (*Fagus Sylvatica L.*)

Corsican Pine wood (*Pinus nigra* subsp.

laricio (Poir.) Maire)

Mechanical characterization

Hybrid configuration

Four-points-bending tests

Finite Element (FE) numerical analysis

Short supply chain

ABSTRACT

The great Beech forests extension in Europe has recently led to investigate the possible application of this hardwood species for the production of Cross-Laminated Timber (CLT) panels. In order to define the goodness of Beech CLT panels for structural applications, an extensive experimental study on novel, three-layered CLT panels made up with short procurement chain, Beech-Corsican Pine timber and melamine based adhesive was performed. The main aim is to define and summarize the mechanical performances of CLT panels both in the homogeneous and hybrid configurations. Major support is derived from bending and shear experimental investigations, both for the in-plane and perpendicular to-plan directions. Moreover, based also on Finite Element (FE) numerical simulations, the local and global mechanical performance of these novel panels is further assessed, towards a widely diffused market product (C24 Spruce CLT panels). The collected experimental and numerical results reveal an overall good behavior of homogeneous hardwood panels, and an excellent performance of hybrid softwood-hardwood configuration, with great opportunity on construction applications.

© 2020 Elsevier Ltd. All rights reserved.

1. Introduction

Cross Laminated Timber (CLT) is a widespread type of prefabricated multi-layered timber panel. The constitutive layers, made up of adjacent boards, are tied together with glue under pressure and are characterized by an alternated grain direction orientation. CLT is typically manufactured from softwood, mainly Norway spruce and fir that commonly belong to C24, C18 or C16 strength classes [1]. In the last years many efforts have been addressed to exploit tree species of short supply chain to obtain wood products also

suitable for structural building [2], according to the principles of the European and Italian Bioeconomy strategy [3] launched at 2012 which sustain the low carbon economy.

From this point of view, many locally grown timber species have been investigated to find new opportunities in their exploitation [4] for the production of CLT worldwide. Samples of this good practice are Sikora et al. [5] which analyzed the influence of the thickness on mechanical performance in bending and shear of Irish Sitka spruce CLT panels, Fortune and Quenneville [6] who analyzed the behavior of CLT panels realized by using locally grown Radiata Pine and Concu et al. [7] and Fragiaco et al. [8] respectively examined the behavior of Italian Marine Pine in Sardinia for the CLT short procurement chain in the Mediterranean area.

* Corresponding author.

E-mail address: martina.sciomenta@univaq.it (M. Sciomenta).

In the recent times, the employment of hardwood has become a central topic due its abundance and a fine ratio between density and mechanical properties.

The most widespread hardwood species in Central Europe are Beech (*Fagus sylvatica*) and deciduous Oak (*Quercus robur*, *Quercus petraea*) [9]; Franke [10] and Aicher [9] successfully investigated respectively the mechanical properties of Beech and hybrid Beech/Spruce in CLT. In the recent times Beech of Italian provenance has been also classified according to European standard 14081-2 [11]. In this paper the mechanical characterization of three layered CLT panel made of homogeneous Beech, Corsican Pine and hybrid Beech/Corsican Pine was performed experimentally as in bending as in shear tests with loads' application in the in-plane and perpendicular-to-plane direction. Moreover, in this work, the mechanical performance of the aforementioned panels were compared with those of samples made of C24 Spruce, usually manufactured for the marked production, by carrying on finite elements simulations. The idea is to investigate the perspectives of Beech hardwood use, alone or in hybrid configuration with low graded softwood timber, in the manufacturing of thin CLT panels due to their wide potential applications in structural field such as reinforcement of ancient building slabs [12] or in new CLT ribbed slab [13]. The obtained results are restricted to thin CLT panels, further future potential investigation could deal with the mechanical characterization of thicker panels which are usually used for slabs and wall elements.

2. Experimental investigation

2.1. Characterization of materials

The three-layered CLT panels object of study were produced by using softwood: Corsican Pine (*Pinus nigra* subsp. *laricio*) and hardwood: Beech (*Fagus sylvatica* L.) originated from a Southern Italy (Calabrian) forest. Raw material was cut into boards having a nominal section of 120 mm width and 20 mm thick. Beech boards had an average length of 3.10 m while the Corsican Pine ones of 4.00 m. A batch of 597 Beech boards and 220 Corsican Pine boards with different sawn pattern to boards and kiln-dried to a moisture content of 10%, in order to satisfy the manufacturers requirement for gluing process. The visual grading was carried out at National Council for Research - Institute for Bio-Economy of Sesto Fiorentino (CNR-IBE) on Corsican Pine which could be already classified according to the technical standards UNI 11,035 1-2 [14] and EN 1912 [15] provisions. In the present study machine strength method was carried out according to EN 14081-2 rules [11].

Each board was first weighted to estimate the density ρ . Later, for each board, the natural frequency of vibration f_1 was measured by using a laser interferometer MICROTEC Viscan-FMMF. The dynamic elastic modulus $E_{0,dyn}$ was thus calculated as:

$$E_{0,dyn} = \rho \cdot (2 \cdot l \cdot f_1)^2 \quad (1)$$

where l is the board's length and f_1 is the frequency.

The 95% of Beech boards was classified as D40, in accordance with EN 338 [16], while 5% of the samples was discarded because of defects (presence of fiber deviations and not uniform planing) [11]. In the case of Corsican Pine boards, the 73% of them was classified as C20 (EN 338 [16]), while the remaining 27% was classified less than C20, but no class was attributed.

Table 1
Mean properties of timber species, derived from the VISCAN procedure.

Timber species	ρ [kg/m ³]	M.C[%]	f_1 [Hz]	MOE_{dyn} [N/mm ²]	MOR [N/mm ²]	MOE_{local} [N/mm ²]	MOE_{global} [N/mm ²]
Beech	755.79	9.58	748.83	16076.51	80.07	16153.52	15537.93
Corsican Pine	511.63	13	529.88	9650.18	38.19	9748.14	8497.38

A total amount of 365 Beech boards and 90 Corsican Pine boards was hence used for manufacturing a series of CLT panels. Regression expressions were calculated based on 119 specimens of Calabrian Beech and 80 Corsican Pine specimens coming from different sites upon which was based the certification of settings for the machine VISCAN classifications in accordance with [11].

The regressions used for the estimation of Modulus of Rupture (MOR), as well as the global and local values of Modulus of Elasticity (MOE_{global} and MOE_{local} respectively).

The mean properties obtained by the grading procedure and the evaluated MOR and $MOEs$ are summarized in Table 1.

For the research study herein discussed, two different types of adhesives were used, namely a melamine Urea Formaldehyde (MUF) adhesive (GripPro™ Design – AkzoNobel, that was obtained by mixing a two component hardener (H002) and a liquid flexible resin (A002)), and a one-component Polyurethane adhesive (Loctite® HBS 049- Purbond). The choice of employing the melamine adhesive was due to the usage of Beech hardwood boards in panel's homogeneous and hybrid configurations with Corsican Pine's boards. The GripPro™ adhesive is specifically designed for softwood, as well as for hardwood timber, such as Beech, Birch, Oak and Chestnut.

Prior to the panel production, a total amount of 21 Corsican Pine boards were mechanically characterized according to EN 408 [17], and the bending strength $f_{m,l}$ was calculated. Based on EN 14,358 [18], a statistical evaluation of the so-derived bending strength was carried out. The characteristic (5% quantile) bending strength according to normal distribution, that is more accurate for timber samples, was thus calculated in 34.2 MPa, with a mean value of 41.4 MPa and a standard deviation of 3.8.

2.2. CLT specimens

An extended experimental campaign was performed to assess the mechanical properties of three-layered CLT specimens of Beech and Corsican Pine in homogeneous and hybrid configurations, prior to the industrial production. The hybrid configuration herein discussed is composed by two Beech outer layers and a Corsican Pine inner layer. A total of 11 three-layered CLT plates, hereafter called "Master Panels", were manufactured at the XLam Dolomiti factory (Castelnuovo – TN – Italy), see (Fig. 1 right). Each Master Panel was suitably cut, so as to obtain a total of 102 specimens with different geometry, layout configuration and adhesive type. The main properties of the tested panels are summarized in Table 2.

The realization of Master Panels was preferred in order to minimize the waste of materials and the number of pressings. Moreover, such a choice also ensured the presence of uniform pressure conditions for all the specimens. Prior to the Master Panels' assembly, the boards were cut to the required length and planed to a thickness of 18 mm. This resulted in a cross-sectional depth of 54 mm for all the specimens. The layering of the boards and the gluing process were performed manually (Fig. 1 left). The narrow board edges were not bonded. The adhesive amount was 190 g/m² and 150 g/m² respectively for melamine and polyurethane. Both the adhesives were applied in a factory condition of 17°C, with an environmental moisture of 50%. The whole assembly time was of half-hour for the Master Panels glued with melamine adhesive, and 15 min for the Master Panels realized with the polyurethane glue. The Master Panel glued with MUF

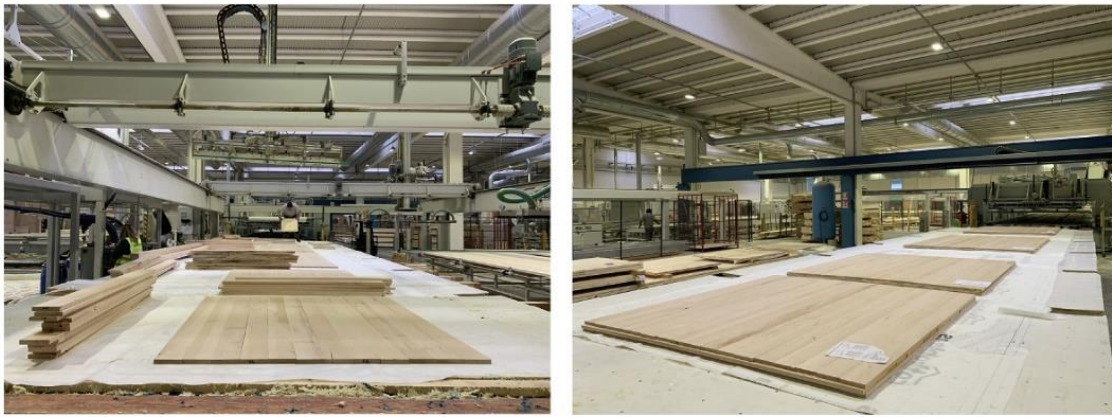


Fig. 1. Master Panels: left) Assembly phase; right) After pressing.

Table 2
Mean properties of the examined CLT specimens.

Master Panel ^o	Configuration/Timber	Adhesive type	Specimen			Test type	Loading condition	
			n ^o	W[mm]	L[mm]			H[mm]
1	Homogeneous/Beech	Melamine	7	240	1180	54	Bending	Perpendicular to plane
			7	240	600	54	Shear	Perpendicular to plane
2A	Homogeneous/Beech	Melamine	7	54	2760	144	Bending	In-plane
2B	Homogeneous/Beech	Melamine	7	54	1440	144	Shear	In-plane
3	Hybrid	Melamine	7	240	1180	54	Bending	Perpendicular to plane
			7	240	600	54	Shear	Perpendicular to plane
4A	Hybrid	Melamine	7	54	2760	144	Bending	In-plane
4B	Hybrid	Melamine	7	54	1440	144	Shear	In-plane
5	Homogeneous/Corsican Pine	Polyurethane	7	240	1180	54	Bending	Perpendicular to plane
			7	240	600	54	Shear	Perpendicular to plane
5bis	Homogeneous/Corsican Pine*	Polyurethane	7	240	1180	54	Bending	Perpendicular to plane
			7	240	600	54	Shear	Perpendicular to plane
6	Homogeneous/Beech	Melamine	7	54	2400	240	Shear	In-plane
7	Hybrid	Melamine	7	54	2400	240	Shear	In-plane
8	Homogeneous/Beech	Polyurethane	2	240	1180	54	Bending	Perpendicular to plane
			2	240	600	54	Shear	Perpendicular to plane

*Corsican Pine classified less than C20 in accordance with EN 338 [16].

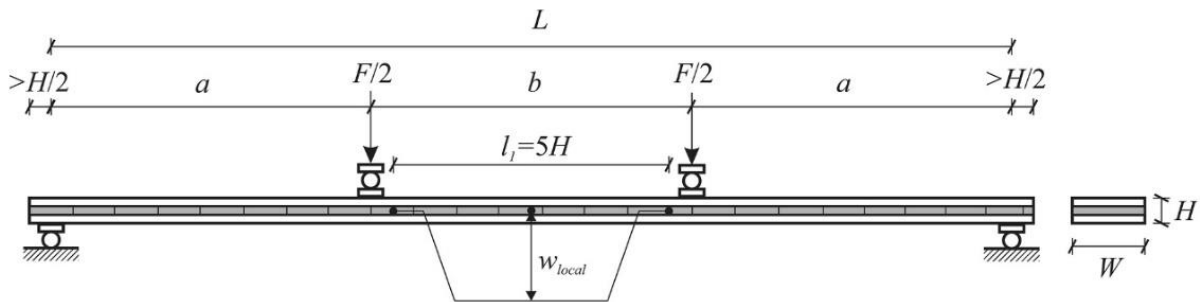


Fig. 2. Test set-up for bending perpendicular to the plane ($a = b = 6H$) and rolling shear test ($a = b = 3H$) [1]. adapted from [17]

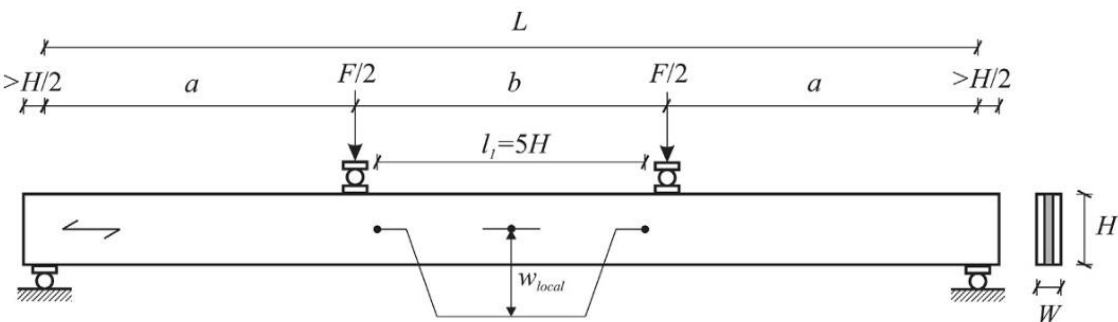


Fig. 3. Test set-up for in-plane bending ($a = b = 6H$) and shear test ($a = b = 3H$) [1]. adapted from [17]

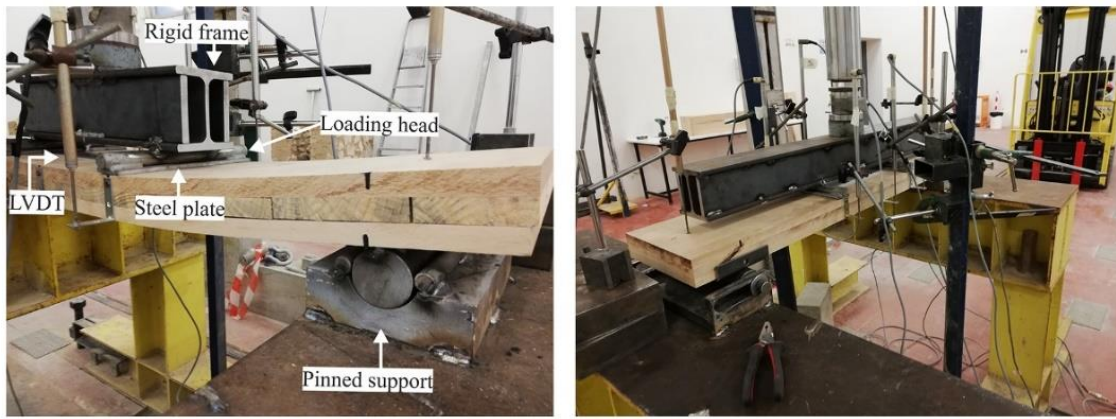


Fig. 4. Set-up left) Equipment details; right) Upper view.

were then cold-pressed for 3 h, with a pressure of 1.4 N/mm² for two hours.

3. Test methods

In accordance with EN 16351 [19], the bending and shear stiffness parameters (both in-plane and perpendicular to plane) were evaluated from a four-point bending test setup. A short span beam

was taken into account, as an alternative to the rolling shear test (EN 789:2005 [20]).

3.1. Bending and shear test perpendicular to the plane

The bending test perpendicular to the plane of CLT elements is a four point bending test over a span length of 24 to 36 times the thickness (*H*). Based on EN 16351 [19], if the ratio of width (*W*)

Table 3
Perpendicular-to-plane bending test.

Master Panel-Specimen n°	Configuration/Timber	<i>E</i> ₀ [N/mm ²]	<i>E</i> _{m,gl} [kNm ²]	<i>F</i> _{max} [kN]	<i>f</i> _m [N/mm ²]	Failure mode
1-1	Homogeneous/Beech	13,872	42,18	42,38	58,86	d
1-2		13,137	39,94	61,28	85,11	r + d
1-3		–	–	57,37	79,68	r + d
1-4		12,897	39,22	58,06	80,64	r + d
1-5		12,085	36,75	60,36	83,83	r + d
1-6		14,960	45,49	64,30	89,30	d
1-7		18,470	56,16	85,05	118,13	r + d + b
Average		14,237	43,29	61,26	85,08	
<i>S</i> _y		0,15	0,15	0,20	0,20	
3-1	Hybrid	15,329	46,53	49,61	68,90	r + d
3-2		10,696	32,47	45,07	62,60	r + d
3-3		–	–	30,27	42,04	d
3-4		16,924	51,38	53,88	74,83	r + d
3-5		16,386	49,74	46,77	64,96	r + d
3-6		15,421	46,81	38,90	54,03	d
3-7		16,663	50,58	43,36	60,22	r + d
Average		15,237	46,25	43,98	61,08	
<i>S</i> _y		0,17	0,17	0,19	0,19	
8-1	Homogeneous/Beech	13,376	40,67	68,70	95,42	d
8-2		12,632	38,41	66,57	92,46	r + d
Average		13,004	39,54	67,64	93,94	
<i>S</i> _y		0,05	0,05	0,05	0,05	
5-1	Homogeneous/Corsican Pine	9660	29,33	31,78	44,14	b + k
5-2		6513	19,78	29,85	41,46	b + k
5-3		11,762	35,72	39,22	54,47	b + k
5-4		10,068	30,57	39,53	54,90	b + k
5-5		8332	25,30	21,27	29,54	r + k
5-6		14,943	45,38	26,89	37,35	b + k
5-7		8791	26,70	38,18	53,03	b + k
Average		10,010	30,40	32,39	44,98	
<i>S</i> _y		0,26	0,26	0,23	0,23	
5bis-1	Homogeneous/Corsican Pine*	4175	12,68	19,03	26,43	b + k
5bis-2		5242	15,92	20,50	28,47	b + k
5bis-3		4106	12,47	18,15	25,21	b + k
5bis-4		6128	18,61	25,79	35,82	b + k
5bis-5		6704	20,36	16,99	23,60	b + k
5bis-6		4902	14,89	14,20	19,72	b + k
5bis-7		4719	14,33	21,03	29,21	b + k
Average		5140	15,61	19,38	26,92	
<i>S</i> _y		0,18	0,18	0,19	0,19	

b: bending failure, d: delamination, k: knots influence, r: rolling shear, s: shear.



Fig. 5. Collapse patterns of Beech panels in perpendicular-to-plane bending test: A) HB with polyurethane adhesive collapsed for rolling shear and delamination; B) Homogeneous HB panels with polyurethane adhesive collapsed for delamination; C) BP configuration panels collapsed for rolling shear and delamination. D) HB panels with melamine adhesive collapsed for rolling shear.

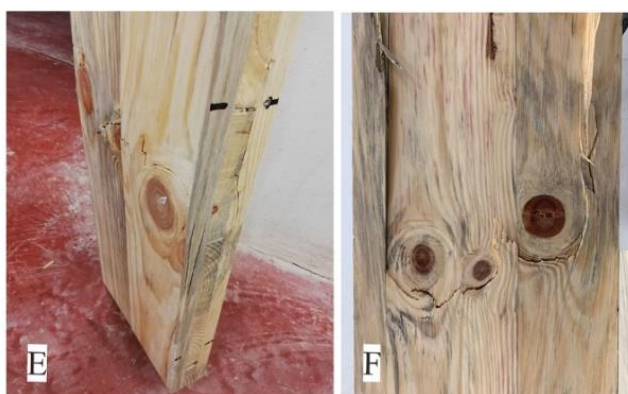


Fig. 6. Collapse patterns of HP panels in perpendicular-to-plane bending test: E) Collapse for bending and knot influence of panels made in by classified boards (Series 5). F) Collapse due to knots cluster influence of panels realized with non-classified boards (Series 5bis).

to thickness: $W/H \geq 4$, the test configuration can be taken from EN 16351 [19] or from EN 408 [17]. In our case the ratio W/H was 4.44 so, the configuration of four point bending test over a span length

of 18 times H was assumed, coherently with EN 408 [17] (Fig. 2). Rolling shear test perpendicular to the plane was performed with the same test-setup (Fig. 2), over a span length of $9H$.

3.2. In-plane bending and shear test

The in-plane bending test of CLT elements is a four point bending test over a span length of 18 times the thickness (H) (Fig. 3). In-plane shear test was performed with the same test-setup (Fig. 3), over a span length of $9H$. Lateral restraints were adopted in order to prevent buckling; their shape and position was suitably chosen in order to allow the specimen's deflection without frictional phenomenon.

3.3. Test methods and instruments

The load was applied through an hydraulic jack, and distributed via a rigid beam fixed under the piston, on two symmetric loading heads (Fig. 4 right). The loading rate was kept fix that was set in $0.003H$ mm/s, so as to reach the failure configuration after 300 ± 120 s. All the specimens were simply supported at the ends. Moreover, small steel plates (no larger than one-half the test piece's thickness) were interposed between the supports and the bottom surface of the specimens, in order to minimize the risk of possible local indentations. For this latter reason, additional steel plates were placed between the loading heads and the top face of the specimens (Fig. 4 left). The deformations w were taken as the average of measurements detected by inductive displacement transducers (LVDT) that were placed on both the faces of each specimen. All the tests were performed in a heated and air-conditioned environment, with about 20° .

The experimental measures of forces and deflections were thus accounted to evaluate the local and global stiffness parameters (EN 408 [17]):

$$EI_{m,gl} = \frac{a l_1 (F_2 - F_1)}{16 (w_2 - w_1)} \quad (4)$$

with l_1 the gauge length (equal to five times the thickness), F_1 and F_2 the 10% and 40% of the ultimate force F_{max} respectively, and w_1 and w_2 the related recorded deflections.

Table 4
In-plane bending test results.

Master Panel-Specimen n°	Configuration/Timber	E_0 [N/mm ²]	$EI_{m,gl}$ [kNm ²]	F_{max} [kN]	f_m [N/mm ²]	Failure mode
2A-1	Homogeneous/Beech	-	-	30,16	69,82	b
2A-2		11,688	157,06	35,00	81,02	b
2A-3		11,977	160,95	26,96	62,40	b
2A-4		12,433	167,06	23,66	54,77	b + d
2A-5		9533	128,10	30,60	70,83	b
2A-6		12,668	170,23	34,06	78,84	b + d
2A-7		10,138	136,24	27,36	63,34	b
Average		11,406	153,27	29,69	68,72	
s_y		0,12	0,12	0,14	0,14	
4A-1	Hybrid	8269	111,12	32,49	75,21	b + d
4A-2		8868	119,16	31,93	73,91	b
4A-3		11,910	160,03	19,82	45,87	b
4A-4		10,301	138,42	30,78	71,24	b + d
4A-5		7795	104,75	35,55	82,29	b
4A-6		13,108	176,14	33,08	76,57	b
4A-7		9997	134,33	32,29	74,74	b + d
Average		10,035	134,85	30,85	71,40	
s_y		0,19	0,19	0,19	0,19	

b: bending failure, d: delamination, k: knots influence, r: rolling shear, s: shear.



Fig. 7. Typical in-plane bending collapse.

4. Test results

4.1. Bending

4.1.1. Perpendicular-to-plane bending tests

The results of perpendicular-to-plane bending tests are summarized in Table 3.

For each specimen, the flexural stiffness, the bending strength and the failure mode are proposed. Moreover, for each groups of panels, the average values and the standard deviation s_y is also estimated by logarithmically normal distribution (EN 14358:2016 [18]).

Table 5
Perpendicular-to-plane shear test results.

Master Panel-Specimen n°	Configuration/Timber	E_0 [N/mm ²]	$EI_{m,gl}$ [kNm ²]	F_{max} [kN]	f_v [N/mm ²]	Failure mode
1-1	Homogeneous/Beech	5007	15,23	84,80	4,91	r + d
1-2		13,983	42,52	56,07	3,24	d
1-3		–	–	71,25	4,12	d
1-4		–	–	97,75	5,66	r + d
1-5		14,050	42,72	62,23	3,60	d
1-6		16,903	51,40	37,44	2,17	d
1-7		17,449	53,05	103,55	5,99	d
Average		13,479	40,98	73,30	4,24	
s_y		0,52	0,52	0,36	0,36	
3-1	Hybrid	5458	16,57	55,98	3,24	r + d
3-2		–	–	66,48	3,85	r + d
3-3		10,803	32,80	58,47	3,38	r + d
3-4		15,373	46,67	68,93	3,99	r
3-5		16,503	50,10	70,55	4,08	r + d
3-6		8695	26,39	78,19	4,52	r
3-7		11,819	35,88	62,35	3,61	r
Average		11,442	34,73	65,85	3,81	
s_y		0,41	0,41	0,12	0,12	
8-1	Homogeneous/Beech	9102	27,68	102,12	5,91	d
8-2		14,652	44,55	74,41	4,31	r + d
Average		11,877	36,11	88,27	5,11	
s_y		0,34	0,34	0,09	0,09	
5-1	Homogeneous/Corsican Pine	12,617	38,31	56,70	3,28	r + d
5-2		14,859	45,12	44,54	2,58	s + d
5-3		13,140	39,90	69,43	4,02	s
5-4		–	–	69,07	4,00	r
5-5		6349	19,28	71,60	4,14	s
5-6		8984	27,28	57,60	3,33	d
5-7		–	–	54,50	3,15	s
Average		11,190	33,98	60,49	3,50	
s_y		0,35	0,35	0,17	0,17	
5bis-1	Homogeneous/Corsican Pine*	3868	11,75	32,50	1,88	b + k
5bis-2		5304	16,11	39,40	2,28	k
5bis-3		3950	12,00	36,36	2,10	b + s
5bis-4		6858	20,83	44,44	2,57	r + d
5bis-5		16,854	51,18	55,33	3,20	r
5bis-6		5194	15,77	43,73	2,53	b + k
5bis-7		3767	11,44	46,65	2,70	r + d
Average		6542	19,87	42,63	2,47	
s_y		0,53	0,53	0,17	0,17	

b: bending failure, d: delamination, k: knots influence, r: rolling shear, s: shear.

Table 6
In-plane shear test results.

Master Panel-Specimen n°	Configuration/Timber	E_0 [N/mm ²]	$EI_{m,gl}$ [kNm ²]	F_{max} [kN]	f_v [N/mm ²]	Failure mode
2B-1	Homogeneous/Beech	4266	57,33	56,14	5,41	b
2B-2		8794	118,17	57,76	5,57	b
2B-3		11,609	156,00	67,54	6,51	b
2B-4		15,817	212,54	73,81	7,12	b
2B-5		9405	126,38	69,73	6,73	b
2B-6		8161	109,67	67,19	6,48	b
2B-7		15,627	209,98	54,15	5,22	b
Average		10,526	141,44	63,76	6,15	
S_y		0,45	0,45	0,12	0,12	
4B-1	Hybrid	-	-	54,81	5,29	b
4B-2		-	-	53,46	5,16	b
4B-3		-	-	60,05	5,79	b
4B-4		9361	125,79	72,70	7,01	b
4B-5		-	-	60,19	5,81	b + d
4B-6		-	-	67,71	6,53	b
4B-7		8784	118,04	60,43	5,83	b + d
Average		9073	121,91	61,33	5,92	
S_y		0,05	0,05	0,11	0,11	
6-1	Homogeneous/Beech	-	-	91,87	5,32	s + d
6-2		9928	617,64	105,51	6,11	b
6-3		7140	444,18	87,63	5,07	s + b
6-4		6029	375,05	119,32	6,91	b
6-5		12,358	768,83	105,77	6,12	b
6-6		-	-	92,20	5,34	b
6-7		10,629	661,24	98,39	5,69	s + d
Average		9217	573,39	100,10	5,79	
S_y		0,30	0,30	0,11	0,11	
7-1	Hybrid	15,280	950,55	92,65	5,36	b + d
7-2		-	-	78,27	4,53	s + d
7-3		5846	363,73	96,48	5,58	s + b
7-4		8635	537,21	90,05	5,21	s + b
7-5		6951	432,45	86,16	4,99	s + d
7-6		-	-	72,36	4,19	s + b
7-7		2478	154,16	82,32	4,76	b
Average		7838	487,62	85,47	4,95	
S_y		0,66	0,66	0,10	0,10	

b: bending failure, d: delamination, k: knots influence, r: rolling shear, s: shear.

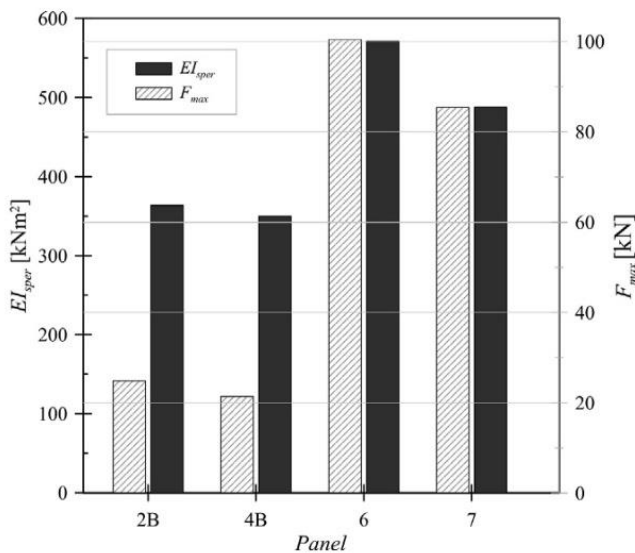


Fig. 8. Comparison between specimens from Master Panels 2B, 4B, 6 and 7 (in-plane shear tests).

additional tests would be advisable to confirm such a flexibility increment.

The specimens of Master panel 5 and 5bis (HP) proved to offer a similar failure mechanism, in particular due to the presence of knots. The calculated flexural stiffness was in fact substantially affected by defects, with a reduction of 40% from Corsican Pine

classified as C20 (Master panel 5) and for the not classified timber (Master panel 5bis). Such a finding highlights the need to have a good classification, avoiding node clusters (which in most of the cases led to premature collapse).

By comparing the results for the specimens from Master Panel 3 and 5, it can be confirmed that the hybrid configuration is an excellent solution for the employment of low graded timber in CLT panel with high mechanical performances.

4.1.2. In-plane bending tests

Regarding the in-plane bending tests, the obtained results are summarized in Table 4. Also in this case, the failure mechanisms that occurred in the experiments were found to be still related to bending and local delamination of the external boards. These failure mechanisms affected the portion of the panels between the load introduction and the end supports (Fig. 7).

By comparing the results obtained from Master Panel 2A (HB) with those coming from Master Panel 4A (BP), it is possible notice a good correlation in terms of ultimate force (4% of difference), but a scatter up to 12% in terms of flexural stiffness. These experimental outcomes further highlight the lower influence of the Corsican Pine inner layer on the mechanical in-plane bending performance assessment of the examined CLT panels.

4.2. Shear

4.2.1. Perpendicular-to-plane shear tests

The results of perpendicular-to-plane shear tests are summarized in Table 5. For each specimen, the flexural stiffness, the bend-

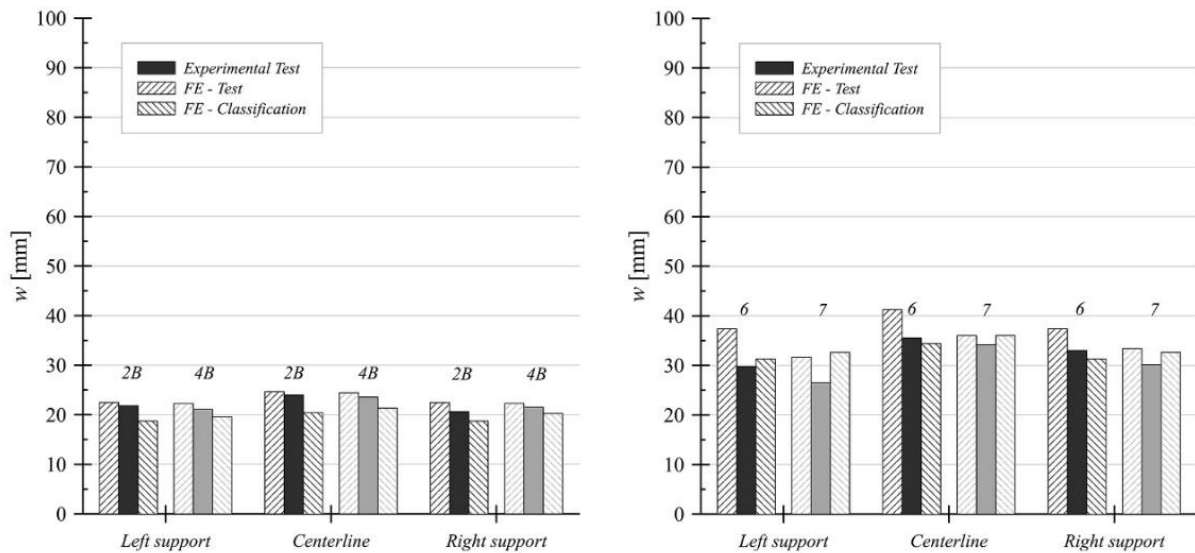


Fig. 9. Comparison of FE models with experimental in-plane shear test.

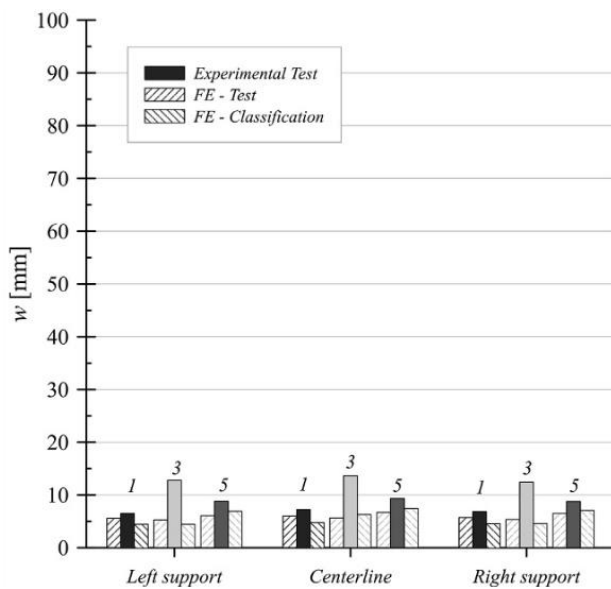


Fig. 10. Comparison of FE models with experimental perpendicular-to-plane shear test.

ing strength and the failure mode is reported. Moreover, for each groups of panel, the average values are also collected. For all of them, the prevailing failure pattern was rolling shear.

As also previously highlighted for the perpendicular-to-plane bending tests, most of the experimental trends were also confirmed for shear.

More in detail, by comparing the specimens obtained from Master Panel 1 (HB with melamine glue) with aster Panel 3 (BP), it is evident that the specimens have a scattered flexural stiffness (15%), and the maximum achieved force differs of 10%. The comparison of specimens form Master Panel 8 (HB with polyurethane glue) with those glued with melamine adhesive confirms the increment of flexibility, with consequent increment of ultimate failure force (20%). Also in this case, however, additional tests would be beneficial.

By comparing the results for samples from Master Panel 3 with Master Panel 5 (HP), it is possible conclude that the perpendicular-to-plane shear behavior is mostly stable, both in terms of stiffness

(2% of scatter) and in terms of ultimate force (8%). The specimens from Master Panel 5bis (HP not graded) recorded a marked reduction of flexural stiffness (41%) and ultimate force (30%), compared to the same configuration of graded timber (Master panel 5).

4.2.2. In-plane shear tests

In conclusion, the experimental results of in-plane shear are summarized in Table 6. Is necessary highlight that the prevailing failure mode is for bending and just a few specimens are characterized by a mixed bending and shear failure mode.

The specimens for in-plane shear tests were characterized by an identical length-to-width ratio (10), but different global dimensions. The CLT panels obtained from Master Panels 2B and 6, moreover, were characterized by an hybrid configuration, while those from Master Panels 4B and 7 had an homogenous Beech configuration. Accordingly, some further considerations can be derived in terms of the effect of size and layout configuration for the in-plane shear performance assessment (Fig. 8).

By comparing the results of samples from Master Panel 2B with 4B, and from 6 with 7, the influence of the panel configuration and size on the in-plane shear is investigated in Fig. 7. A light scatter in terms of elastic stiffness (14%) and ultimate force (4%) on shorter specimens (2B and 4B series) can be observed. This means that the usage of Corsican Pine in the inner layer doesn't involve marked reductions of mechanical shear performances. From the analysis of test results on wider specimens (from Master Panel 6 and 7), the influence of the inner softwood layer is more evident in terms of ultimate force (15%), while the scatter in terms of elastic stiffness is the same of shorter specimens.

5. Numerical investigation

Numerical Finite Elements (FE) simulations represent a useful tool to expand the results obtained from experimental test to CLT panels made by with different timber or with further layer configurations; foregoing the FE models need to be suitably calibrated on experimental evidences.

5.1. Methods

A series of Finite Element numerical simulations were performed by using the ABAQUS/Explicit software package [21], in

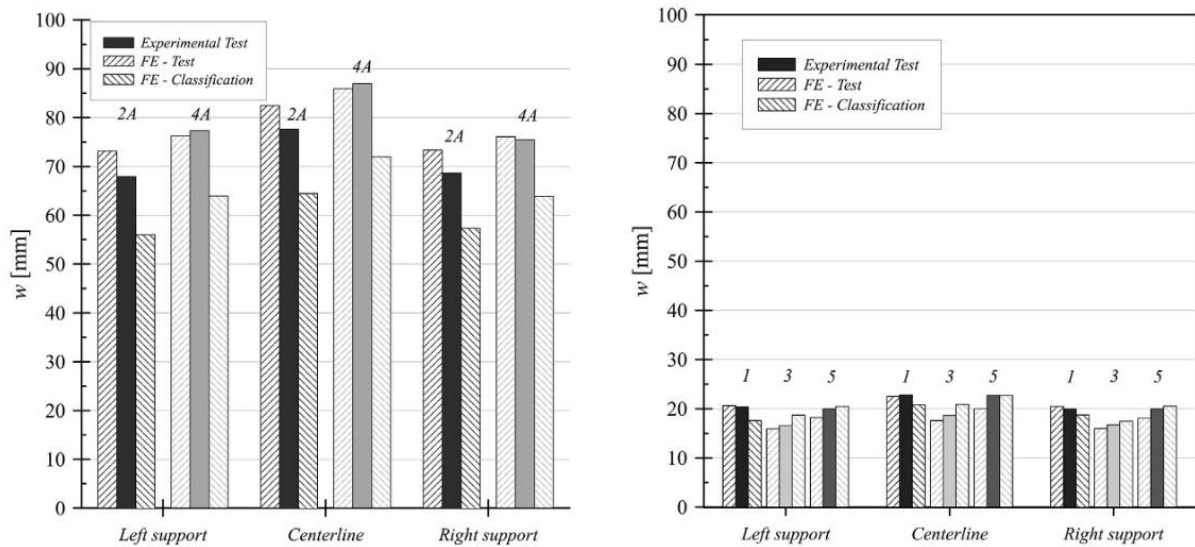


Fig. 11. Comparison of FE models with experimental bending test in-plane (left) and perpendicular-to-plane (right).

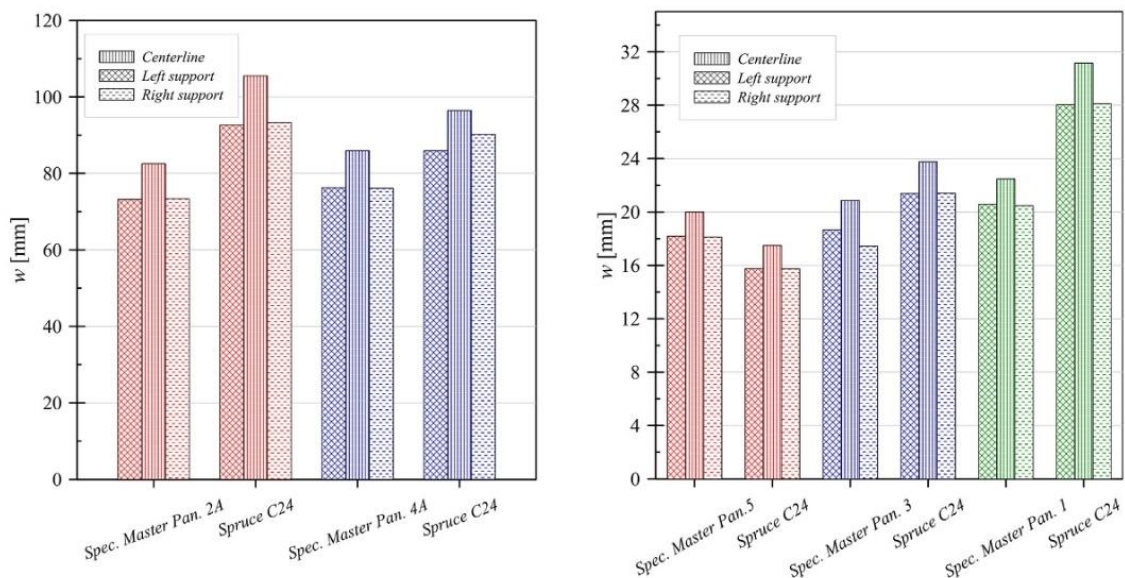


Fig. 12. Comparison of C24 Red Spruce with test materials in-plane shear test. (For interpretation of the references to colour in this figure legend, the reader is referred to the web version of this article.)

the form of quasi-static imposed force history for the examined CLT panels. Solid 8-node 3D elements were used (C3D8R-type stress-strain bricks with reduced integration) to describe the nominal geometry of the specimens. A rigid base support was also described via C3D8R-type, 3D solid elements, to schematically reproduce the testing machine (loading region and end supports) and the related effects (i.e., contact between the base surface and the circular section representative of the hinge support). At this stage of the study, the glue lines between the layers were accounted in the form of rigid “tie” constraints. At the same time, the interaction between the panels and the machine components was accounted as surface-to-surface contacts, including both the tangential ‘penalty’ and the normal ‘hard’ options. The static friction coefficient was set in $\mu = 0.3$ for steel-to-timber contact [22] and 0.2 for steel-to-steel contact between the machinery components [23].

Timber was modeled as orthotropic elastic material. The elastic and shear modulus were accounted in two different ways: first, in

accordance with the EN 338 board’s classification (D40 for Beech and C20 for Corsican Pine), and then, coherently with Table 1. The elastic modulus perpendicular to the grain was thus calculated as $E_{0,mean}/15$ (EN 384:2016 [24]), while the shear modulus was defined as $E_{0,mean}/16$ (EN 338 [16]). Steel was modelled by an isotropic, elastic Von Mises constitutive law by accounting for $E = 210\text{GPa}$ and $\nu = 0.3$ as nominal MOE and Poisson’ ratio.

5.2. Experimental comparisons

Figures 9, 10 and 11 show the comparison in terms of deflection obtained by performing FE analyses and experimental tests. The aim is to fit the experimental test with good accuracy in order to validate the numerical model; the same model will be adopted for further simulation (i.e. Section 4.3. Comparison with C24 Spruce panels)

From the previous comparisons, it is clear that FE models are able to capture the behavior of the examined specimens. In partic-

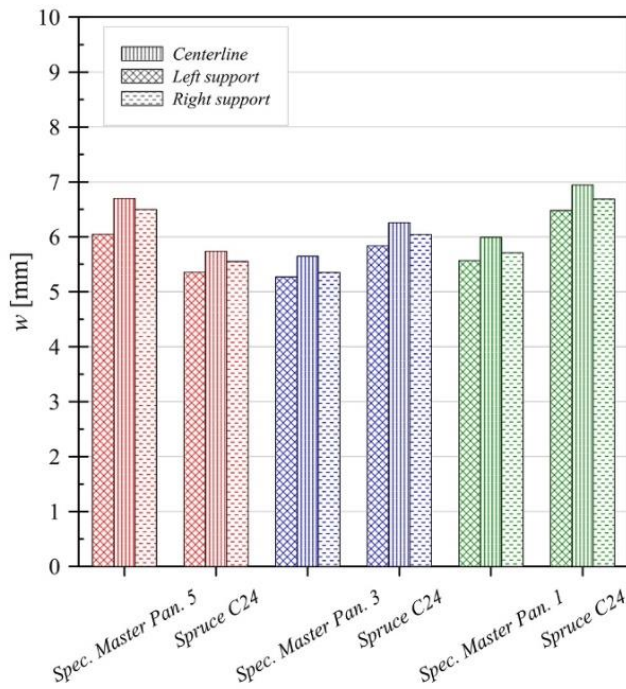


Fig. 13. Comparison of C24 Red Spruce with test materials in-perpendicular-to-plane shear test. (For interpretation of the references to colour in this figure legend, the reader is referred to the web version of this article.)

ular, the experimental deflections are close to the numerical predictions, as considering both the sets of elastic and shear modulus defined in the previous section.

The overall scatter was found in less than 10%, with the exception of samples from Master Panels 2A and 4A, for which minor accuracy was obtained by using the classification's elastic modulus. In those cases, the difference from test values was in fact calculated in 17%. Even larger scatter can be noticed, for the same

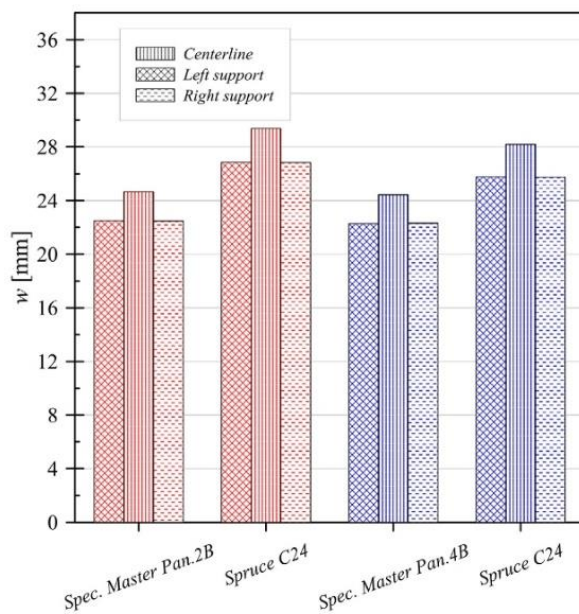


Fig. 14. Comparison of C24 Red Spruce with test materials in-perpendicular-to-plane bending test. (For interpretation of the references to colour in this figure legend, the reader is referred to the web version of this article.)

specimens, for perpendicular-to-plane shear, where the percentage scatter was found in about 35–40%.

5.3. Comparison with C24 Spruce panels

The FE models, as known, are useful to investigate the influence of various input parameters for a given structural system. In this research paper, in following Section 4.3 the potential of FE models was focused on the analysis of the effects due to timber's species and grading on mechanical response of CLT panels in shear and bending. In particular, a further set of analyses was carried out by adopting the previous test configurations, but a C24 Red Spruce section (with $E_{0,mean} = 11000$ MPa $E_{90,mean} = 370$ MPa $G = 690$ MPa the timber properties), which is commonly used for the production of CLT products.

In Figs. 12, 13 and 14 the so-collected results are proposed. Compared to traditional C24 Spruce panels, the overall good performance of panels with hybrid configuration can be appreciated, due to their limited deformability both in bending and shear. In particular, is clear that, for the same force level, the deflection is overall lower as for in-plane as for perpendicular-to-plane configurations, excepted in the case of comparison of Master Panel 5 with C24 Spruce panel, due to the different strength class of softwoods.

6. Conclusions

The present investigation was dedicated to the analysis of novel three-layered homogeneous Beech and hybrid Beech/Corsican Pine CLT panels bonded with melamine and polyurethane glue. Four point bending and shear tests were fulfilled, by applying loads as in the direction perpendicular-to-plane as in plane.

- From the bending test in the direction perpendicular-to-plane, rolling shear collapse modes were prevalent due to the reduced panel length.
- Knot influence was found to be a relevant parameter in the definition of mechanical performances and collapse mode of homogeneous Corsican Pine panels.

- Moreover, a limited number of in-plane bending and perpendicular-to-plane shear tests on polyurethane bonded panels, highlighted an increasing deformability and ultimate force related to the same panels bonded with melamine adhesive. However, such a finding should be deeply investigated with the support of additional tests.
- The size effect was also investigated, by comparing hybrid and homogeneous Beech configurations under in-plane shear tests. It was observed, by changing the panel dimensions, that the scatter of elastic stiffness between hybrid and homogeneous specimens was mostly constant. On the other side, the scatter of ultimate force increases from 4% to 15%.
- Overall, in any case, the mechanical performance assessment of the examined hybrid specimens revealed an excellent behavior, both in bending and in shear.
- Moreover, with the support of numerical simulation, the experimental outcomes were further assessed and compared with traditional C24 Spruce samples, that are representative of a widely used market product. The good performance of panels with hybrid configuration was further confirmed, giving evidence of a less pronounced deformability than the C24 Spruce panels, in both the bending and shear loading conditions.

The collected results revealed a good behavior of homogeneous hardwood panels and an excellent performance of the hybrid softwood-hardwood configuration. In this sense, the hybrid hardwood/low graded softwood panels could represent a great opportunity for the employment of locally grown timber species for mechanically efficient CLT panels.

Funding

This work was funded by Italian Ministry of University and Research - PRIN 2015, grant number 2015YW8JWA_002.

CRedit authorship contribution statement

Martina Sciomenta: Formal analysis, Investigation, Writing - original draft.

Declaration of Competing Interest

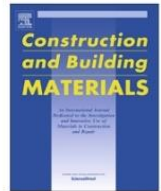
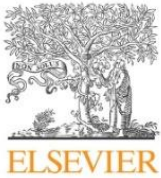
The authors declare that they have no known competing financial interests or personal relationships that could have appeared to influence the work reported in this paper.

Acknowledgements

The authors would like to thank the Pagano Srl, Xlam Dolomiti Srl for the manufacturing of CLT panel and the LPMS laboratory staff: Mr Edoardo Ciuffetelli and Mr.Alfredo Peditto.

References

- [1] R. Brandner, *Production and Technology of Cross Laminated Timber (CLT): A State-of-the-Art Report, Proceedings of the European Conference on Cross Laminated Timber (CLT)*, 2013.
- [2] M. Romagnoli, M. Fragiaco, A. Brunori, M. Follesa, G. Scarascia Mugnozza, Solid wood and wood based composites: The challenge of sustainability looking for a short and smart supply chain, *Lect. Notes Civ. Eng.* 24 (2019) 783–807, https://doi.org/10.1007/978-3-030-03676-8_31.
- [3] Commissione europea, "Bioeconomy policy," *Bioeconomy Policy*, 2017. <https://ec.europa.eu/research/bioeconomy/index.cfm?pg=policy>.
- [4] M. Romagnoli, D. Cavalli, R. Pernarella, R. Zanuttini, M. Togni, "Physical and mechanical characteristics of poor-quality wood after heat treatment," *IForest*, vol. 8, no. Dec2015, pp. 884–891, 2015, doi: 10.3832/ifer1229-007.
- [5] K.S. Sikora, D.O. McPolin, A.M. Harte, Effects of thickness of cross-laminated timber (CLT) panels made from Sitka spruce on mechanical performance in bending and shear, *Constr. Build. Mater.* 116 (2016) 141–150.
- [6] A.L. Fortune, P. Quenneville, A feasibility study of New Zealand Radiata Pine crosslam, S. Setunge. 2011.
- [7] G. Concu, B. De Nicolò, M. Fragiaco, N. Trulli, M. Valdes, Grading of maritime pine from Sardinia (Italy) for use in cross-laminated timber, *Proc. Inst. Civ. Eng. Constr. Mater.* 171 (1) (2018) 11–21, <https://doi.org/10.1680/jcoma.16.00043>.
- [8] M. Fragiaco, R. Riu, R. Scotti, Can structural timber foster short procurement chains within Mediterranean Forests? A research case in Sardinia, South-east Eur. For. 6 (1) (2015) 107–117, <https://doi.org/10.15177/seeefor.15-09>.
- [9] S. Aicher, M. Hirsch, Z. Christian, Hybrid cross-laminated timber plates with beech wood cross-layers, *Constr. Build. Mater.* 124 (2016) 1007–1018, <https://doi.org/10.1016/j.conbuildmat.2016.08.051>.
- [10] S. Franke, "Mechanical properties of beech CLT," in *WCTE 2016 - World Conference on Timber Engineering*, 2016.
- [11] M. Brunetti et al., Structural products made of beech wood: quality assessment of the raw material, *Eur. J. Wood Wood Prod.* 78 (5) (2020) 961–970, <https://doi.org/10.1007/s00107-020-01542-9>.
- [12] F.M. Soriano, N.G. Pericot, E.M. Sierra, Comparative analysis of the reinforcement of a traditional wood floor in collective housing. In depth development with cross laminated timber and concrete, *Case Stud. Constr. Mater.* 4 (2016) 125–145, <https://doi.org/10.1016/j.cscm.2016.03.004>.
- [13] P. Papastavrou, S. Smith, T. Wallwork, A. McRobie, N. Niemi, "The design of cross-laminated timber slabs with cut-back glulam rib downstands - From research to live project," in *WCTE 2016 - World Conference on Timber Engineering*, 2016.
- [14] UNI (Ente nazionale italiano di unificazione), "Legno strutturale - Classificazione a vista dei legnami secondo la resistenza meccanica. [Structural wood - Visible classification of wood according to mechanical resistance]," UNI 11035, 2010.
- [15] B. Standard, "Structural timber D Strength classes D Assignment of visual," UNI EN 19122012, 1998.
- [16] CEN (European Committee for Standardization), "Structural timber - Strength classes," EN 338, 2016.
- [17] UNI (Ente nazionale italiano di unificazione), "EN 408:2010 - Timber structures - Structural timber and glued laminated timber: Determination of some physical and mechanical properties," 2010.
- [18] UNI (Ente nazionale italiano di unificazione), UNI EN 14358:2016 - Timber structures - Calculation and verification of characteristic values, 2016.
- [19] CEN (European Committee for Standardization), "Timber Structures - Cross laminated timber - Requirements," prEN 16351, 2018.
- [20] UNI (Ente nazionale italiano di unificazione), UNI EN 789:2005 - Timber structures - Test methods - Determination of mechanical properties of wood based panels, 2005.
- [21] Dassault Systèmes Simulia, "Abaqus F.E.A. v. 6.12 computer software," Provid. RI, USA, 2015.
- [22] C. Bedon, M. Fragiaco, Numerical analysis of timber-to-timber joints and composite beams with inclined self-tapping screws, *Compos. Struct.* (2019) 13–28, <https://doi.org/10.1016/j.compstruct.2018.09.008>.
- [23] P. Zhang, T. Nagae, J. McCormick, M. Ikenaga, M. Katsuo, M. Nakashima, Friction-based sliding between steel and steel, steel and concrete, and wood and stone, *Proc. 14th World Conf. Earthq. Eng.* (2008).
- [24] British Standard Institution, BS EN 384:2010, Structural timber — Determination of characteristic values of mechanical properties and density, vol. 3, 2010.



Corrigendum to “Mechanical characterization of novel Homogeneous Beech and hybrid Beech-Corsican Pine thin Cross-Laminated timber panels” [Constr. Build. Mater. 271 (2021) 121589]

Martina Sciomenta^{a,*}, Luca Spera^a, Chiara Bedon^b, Vincenzo Rinaldi^a, Massimo Fragiaco^a, Manuela Romagnoli^c

^a Department of Civil, Architecture and Building and Environmental Engineering, University of L'Aquila, Via Giovanni Gronchi 18, 67100 L'Aquila, Italy

^b Department of Engineering and Architecture, University of Trieste, Via Alfonso Valerio, 6/1, 34127 Trieste, Italy

^c Department of Innovation of Biological, Food and Forestry Systems (DIBAF), University of Tuscia, Via S. Camillo de Lellis, 01100 Viterbo, Italy

For a mistake in writing the last versions of the above papers, the article “Mechanical characterization of novel Homogeneous Beech and hybrid Beech-Corsican Pine thin Cross-Laminated timber panels”, two authors were missing who provided the machine grading of beech and corsican pine boards and the regression analysis for the estimation of the mechanical properties of the boards from the non-destructive tests. So the authors of the article are:

Authors: Martina Sciomenta^a, Luca Spera^a, Chiara Bedon^b, Vincenzo Rinaldi^a, Michela Nocetti^c, Michele Brunetti^c, Massimo Fragiaco^a, Manuela Romagnoli^d

^a Department of Civil, Architecture and Building and Environmental Engineering, University of L'Aquila, Via Giovanni Gronchi 18, 67100 L'Aquila, Italy

^b Department of Engineering and Architecture, University of Trieste, Via Alfonso Valerio, 6/1, 34127 Trieste, Italy

^c CNR-IBE, Institute of BioEconomy, Via Madonna del Piano 10, 50019 Sesto Fiorentino, FI, Italy

^d Department of Innovation of Biological, Food and Forestry Systems (DIBAF), University of Tuscia, Via S. Camillo de Lellis, 01100 Viterbo, Italy

Moreover, the authors regret that some parts of the paragraph 2.1 need small revisions and it should be replaced with the text below.

The three-layered CLT panels object of study were produced by using softwood: Corsican pine (*Pinus nigra* subsp. *laricio*) and hardwood: beech (*Fagus sylvatica* L.) originated from a Southern Italy (Calabria) forest. Raw material was cut into boards having a nominal section of 120 mm width and 20 mm thick. Beech boards had an average length of 3.10 m while the Corsican pine ones of 4.00 m. A batch of 597 beech and 220 Corsican pine boards was collected and kiln-dried to a moisture content of 10%, in order to satisfy the manufacturers requirement for gluing process.

The boards were strength graded according to EN 14081-2 rules [14] by the grading machine ViSCAN-Portable (MiCROTEC). Each board was first weighted and measured to determine its density ρ . Then, the natural frequency of vibration f_1 induced by a percussion was measured by using a laser interferometer. The dynamic modulus of elasticity $E_{0,dyn}$ was thus calculated as:

$$E_{0,dyn} = \rho \cdot (2 \cdot l \cdot f_1)^2 \quad (1)$$

where ρ is the density of the board, l is the length and f_1 is the frequency.

The machine settings used for the strength grading of the boards of both beech and pine were developed in previous studies [11],[15]. The strength class combinations used to qualify the raw material were D40 and rejects for beech and C20 and rejects for pine (EN 338 [16]).

The 95% of beech boards was classified as D40, while 5% of the samples was discarded because of defects (presence of fiber deviations and not uniform planing). In the case of Corsican pine boards, the 73% of them was graded as C20, while the remaining 27% was rejected.

A total amount of 365 beech boards and 90 Corsican pine boards was hence used for manufacturing a series of CLT panels. Regression analysis was performed based on destructive tests carried out on beech and pine raw material for the machine setting development [11],[15]. Linear regression were used for the estimation of the Modulus of Rupture (MOR), as well as the global and local Modulus of Elasticity (MOE_{global} and MOE_{local} respectively) from the dynamic modulus of elasticity measured during machine grading.

The mean properties obtained by the grading procedure and the evaluated MOR and MOEs are summarized in Table 1.

For the research study herein discussed, two different types of adhesives were used, namely a melamine Urea Formaldehyde (MUF) adhesive (GripPro™ Design – AkzoNobel, that was obtained by mixing a two component hardener (H002) and a liquid flexible resin (A002)), and a one-component Polyurethane adhesive (Loctite[®] HBS 049-Purbond). The choice of employing the melamine

DOI of original article: <https://doi.org/10.1016/j.conbuildmat.2020.121589>

* Corresponding author.

E-mail address: martina.sciomenta@univaq.it (M. Sciomenta).

Table 1

Mean properties of timber species, derived from the non-destructive measurements.

Timber species	ρ [kg/m ³]	MC [%]	f_1 [Hz]	MOE_{dyn} [N/mm ²]	MOR [N/mm ²]	MOE_{local} [N/mm ²] [N/mm ²]	MOE_{local}
Beech	756	9.6	749	16077	80.1	16154	15538
Corsican pine	512	13.0	530	9650	38.2	9748	8497

mine adhesive was due to the usage of beech hardwood boards in panel's homogeneous and hybrid configurations with Corsican pine's boards. The GripPro™ adhesive is specifically designed for softwood, as well as for hardwood timber, such as beech, birch, oak and chestnut.

Funding (in ADDITION)

The development of machine setting for black pine was performed in the frame of the A.Pro.Fo.Mo.project, financed by GAL-

Start, (Leader m. 124, PSR 2007-2013 Toscana Region). The financial support is gratefully acknowledged.

References

- [14] CEN (European Committee for Standardization), Timber Structures – Strength graded structural timber with rectangular cross section – Part 2: Machine grading; additional requirements for type testing, EN 14081-2, 2018.
- [15] M. Nocetti, M. Bacher, M. Brunetti, A. Crivellaro, J.W.G. van de Kuilen, Machine grading of Italian structural timber: preliminary results on different wood species, in: WCTE 2010 – World conference on timber engineering, 2010.

3.2. Buckling behavior of short supply chain CLT panels

The out of plane buckling behaviour of thin cross-laminated timber panels is an interesting topic to be deepened, especially for panels subjected to in-plane actions during their service life. Since wood is an orthotropic material, the variation of mechanical properties with respect to the inclination to the grain affects the performances of the single layer and of the overall panel.

In addition, the rolling-shear modulus of the orthogonal layers influences the Eulerian critical load along with the glue tangential stiffness.

Considering the thin short supply chain CLT panels described in the previous paragraph, experimental central axial compressive tests were carried out to obtain the failure limit load of the specimens, both for the homogeneous beech configuration and for the hybrid beech-Corsican pine configuration.

The specimens were positioned between two one-way knife hinges to reproduce a constraint condition as similar as possible to the theoretical one. During the tests, a loading cell and laser displacement transducers were used to detect load values and panels displacements respectively.

A general analytical model was developed for 5 layers CLT panels and then applied to the 3 layers configuration studied. This mechanical model schematizes the CLT panels as planar Timoshenko beams connected through glue lines represented as a continuous distribution of linear tangential and normal elastic springs.

Two non-dimensional parameters were introduced as coupling parameters, one to consider the interaction between layers due to the glue tangential stiffness and the other to consider the rolling shear stiffness of the inner layer.

Three different failure criteria were considered to assess the limit load value: the first one accounts for the bending–buckling failure; the second one refers to the rolling shear failure mechanism of the inner layer; the third one takes into account the delamination phenomena.

All these failures were observed during the experimental campaign, and, for this reason, they were considered to determine the theoretic compression limit load.

Considering the tests were conducted on a variable timber material, excellent agreement was achieved between experimental and theoretical values, as analysed in the following work by (Fabrizio et al., 2023).



Experimental investigation and beam-theory-based analytical model of cross-laminated timber panels buckling behavior

Cristiano Fabrizio¹ · Martina Sciomenta¹ · Luca Spera¹ · Yuri De Santis¹ · Stefano Pagliaro¹ · Angelo Di Egidio¹ · Massimo Fragiaco¹

Received: 8 February 2023 / Revised: 10 May 2023 / Accepted: 4 June 2023
© The Author(s) 2023

Abstract

This paper investigates the buckling behavior of three-layered cross-laminated timber (CLT) panels, from both the experimental and analytical standpoints. Two different series of specimens are considered: the homogeneous ones, which are entirely made of beech, and the hybrid ones, whose inner layers are made of Corsican pine. The experimental tests aim to evaluate the failure limit loads of the specimens, when loaded by an increasing compression tip force. The analytical formulation is first obtained for a panel with a generic number of layers and after it is specialized for a three-layered panel. Timber layers are modeled as internally constrained planar Timoshenko beams linked together by adhesive layers, which are modeled as a continuous distribution of normal and tangential elastic springs. A closed-form solution of the buckling problem is obtained. The achieved Eulerian critical load of CLT panels depends on two parameters, which account for (1) the interaction between timber layers (due to the glue tangential stiffness) and (2) the rolling shear stiffness of the inner layer. Three different failure criteria are introduced to estimate the limit load. Finally, the analytical limit loads and the experimental ones are compared.

Keywords Cross-laminated timber (CLT) · Beech wood (*Fagus sylvatica* L.) · Load-bearing capacity · Axial compression · Buckling analytical model · Ayrtton–Perry criterion

1 Introduction

Many types of timber structural elements (i.e., columns, trusses, and frame structures) undergo axial compression or combined axial compression and bending during their lifetime functions; the risk that they deflect laterally, under this load conditions, is called flexural buckling.

The load-bearing capacity of timber members is not easy to predict as it is influenced by several variables which can be gathered in two groups: the first one involves the geometrical features, the boundary conditions, the material and environmental properties (i.e., strength and service class) and the load duration; the second comprises the geometrical (i.e., initial curvature) and structural imperfections (i.e., knots, growth deviations, amount of moisture content). The effect of these latter variables was deeply investigated in Refs. [1–5] while the influence of the material properties on the load-bearing capacity was analyzed by Blaß [6–8].

Furthermore, two key aspects should be considered: (i) a geometric effect called P-delta which describes the non-linear increasing of deformations due to the increasing eccentricity of the axial load, as well as (ii) the non-linear

✉ Martina Sciomenta
martina.sciomenta@univaq.it

Cristiano Fabrizio
cristianomichele.fabrizio@gmail.com

Luca Spera
luca.spera@graduate.univaq.it

Yuri De Santis
yuri.desantis@univaq.it

Stefano Pagliaro
stefano.pagliaro@univaq.it

Angelo Di Egidio
angelo.diegidio@univaq.it

Massimo Fragiaco
massimo.fragiaco@univaq.it

¹ Department of Civil, Architecture and Building and Environmental Engineering, University of L'Aquila, Via Giovanni Gronchi 18, 67100 L'Aquila, AQ, Italy

behavior of timber material under compression actions parallel to the grain. A large investigation on the P-delta effect on axially compressed timber elements was carried out by Tetmajer [9] and confirmed by test campaign by Larsen and Pedersen [10], the influence of non-linearity of timber on the interaction between moment and axial force was numerically defined by Buchanan [11, 12].

The current National codes and Standards (i.e., Eurocode 5 [13]) provide two methods for the calculation of the load-bearing capacity of axially compressed columns with and without eccentricity; the most simple one is based on the effective length method (ELM), while, the other accounts for a second-order analysis of the structure. This latter method, by the way, considers timber as an elastic material so it is not able to take into account its material non-linearity.

The ELM considers a simple equivalent column hinged at both ends; the P-delta effect is taken implicitly into account through a buckling factor, k_c . The buckling factor is used here to reduce the compressive strength of the timber column in the direction parallel to the grain and depends on the effective length of the structural element which can be expressed by the slenderness ratio λ .

Several experimental tests have been performed to define the influence of slenderness ratios on failure modes strain and ultimate bearing capacity of glulam columns made of different timber species: bamboo [14], larch [15], European beech [16]. Moreover, the effect of imperfections such as knots [17] and cracks [18], was also investigated as experimentally as performing FEM fittings and parametric analyses.

A novel strain-based model to analyze the load-bearing capacity with and without eccentricity is proposed in Ref. [19] for solid elements; in this work, it is highlighted how the non-linear behavior of timber when subjected to compression parallel to the grain considerably influences the load-bearing capacity. Based on this latter model and accounting for the Glos' stress-strain relation [20], in Ref. [21], Monte Carlo simulations were performed with the aim of investigating the influence of the varying material properties and slenderness.

Among the aforementioned solid and engineered wood products, an in-depth study of cross-laminated timber (CLT) column components has not yet been carried out. These latter structural elements result from the cut of prefabricated solid slabs made of adjacent planks layers glued together at a right angle.

In the last few decades, CLT has become popular in the mass timber construction field [22], especially for mid- and high-rise buildings, due to the numerous advantages [23] such as the high dimensional stability, elevated in-plane isotropic strength and stiffness with respect to sawn timber, high speed of installation [24], and the environmental

benefits compared to other construction materials like steel, concrete, and masonry.

The growing interest on CLT for design purposes and its great mechanical properties has led several authors to analyze deepen its mechanical characteristics as bending, tensile, shear, and compressive strength [25–31]. Although, as previously highlighted, many studies have been conducted to clarify the in-plane and out-of-plane mechanical behavior of CLT panels, up to now, just limited research has been carried out to investigate the stability bearing capacity of CLT members under axial compression loads. In Ref. [32], the different axial compression behaviors of cross-laminated timber columns (CLTCs) and control glued-laminated timber columns (GLTCs) were investigated. The GLT column specimens had a greater compressive loading capacity than CLT column specimens but the latter highlighted a better ductility and energy absorption than GLT. In Ref. [33], the main aims were to define the stability bearing capacity of the CLT members in axial compression and to propose a CLT stability coefficient calculation method by suitably modifying that implemented for GLT in the Chinese Standard. In Ref. [34], Ye et al. accounted for the CLT rolling shear sensitivity arising from the out-of-plane bending and compression load combination; an analytical model which takes rolling shear effects into account to predict the load-carry capacity of CLT compression-bending members was provided.

Stability issues have to be addressed in view of challenging aims such as those analyzed in [35–38]. In the case of timber engineering, it is to realize increasingly high-rise timber buildings. Because of the low modulus of elasticity parallel to the grain of timber in general and of the even lower shear modulus which affects the orthogonal layers [39], CLT is more prone to undergo instability phenomena. Timber exhibits about one third of the modulus of elasticity of concrete in parallel to the grain, and the radial-tangential shear stiffness is roughly two order of magnitude lower than the longitudinal one [40], and as a consequence, timber structures may suffer from buckling.

Considering the technology of cross-laminated timber, the orthogonal layers are influenced by the radial-tangential shear stiffness, usually called rolling shear stiffness [41], and, therefore, it is expected that shear effects are important in this type of wood-based composite.

Some researches pointed out how the properties of the entire CLT panel are strongly influenced by the type of wood of which its layers are made [42, 43], their thickness [44], and the type of glue adopted [45, 46]. Other studies [47–50], have investigated panels made with wood species other than fir and spruce, which are currently the most used species for CLT industrial manufacturing. In this context, panels made of some native hardwoods species such as beech, yellow-poplar, and tropical hardwood (i.e., rubberwood, batak)

have shown an excellent behavior. This evidence is relevant considering the impact that the use of hardwood, especially local, would have on the production of CLT panels. The development of a short supply chain of wood is a possible mean to economically enhance the woodlands and to achieve environmental and social benefits [51]. Wood can be effectively used to manufacture products for structural purposes, but it is necessary to investigate the potential of each local species to identify the most suitable technology to employ. An interesting research case was carried out in Italy, where maritime pine from Sardinia was employed to produce cross-laminated timber panels. Preliminary tests were required to evaluate the physical and mechanical properties so as to demonstrate the suitability of this locally grown species to produce CLT panels [52]. In addition, the activation of a short supply chain of timber could lead to a sustainable forest management and to a better exploitation of the raw material [53]. Nowadays in Europe, the attention is focusing on hardwoods especially for manufacturing wood-based composite due to their great mechanical properties [54]. Despite the fact that softwood has played a central role in the market of glue-laminated timber and cross-laminated timber, the abundance of hardwoods in European forests has determined the need to analyze their performances [55].

The current work aims to deeply analyze the buckling and post-buckling behavior of CLT panels. The specimens' added value lies in (i) the short supply chain origin of both hardwood beech and softwood Corsican pine and in (ii) the homogeneous beech and hybrid beech–Corsican pine configuration, devised for defining a possible optimization of material. To reach the purposed aim, an experimental test campaign is first carried on. As a result, the ultimate load and the failure modes are accounted for. At a second stage, analytical models are formulated and fitted with the previous evidences and then discussed.

2 Materials and methods

2.1 Specimens description

To carry on this experimental campaign, two of the most interesting Italian hardwood and softwood timber species, beech and Corsican pine, were chosen. The raw material for both species came from Calabrian forests, South Italy. All the steps that led to obtaining the final product were carried out with short supply chain procedures. An amount of 365 beech boards and 90 Corsican pine boards were specifically classified as D40 and C20 [50] and planed to a thickness of $h = 18$ mm to guarantee the adequate planar surface necessary for the face gluing. Two different series of three-layered cross-laminated timber (CLT) panels, made, respectively, of beech and Corsican pine and only beech, were realized to

carry out an extended experimental campaign to assess their mechanical properties prior to the industrial production. The hybrid configuration is composed by two beech outer layers and one Corsican pine inner layer. The layering of the boards and the gluing process were performed by hand.

Timber boards were tiled, overlapped, and glued together by a melamine urea formaldehyde (MUF) adhesive [GripPro™ Design—AkzoNobel, that was obtained by mixing with the ratio 2–1 the two components: hardener (H002) and liquid flexible resin (A002)]. The narrow board edges were not bonded. The choice of employing the melamine adhesive was due to the usage of beech hardwood boards in both homogeneous and hybrid beam configurations with Corsican pine boards. In particular, the GripPro™ adhesive is specifically designed for softwood as well as for hardwood timber, such as beech, birch, oak, and chestnut. The average of glue grammage was 190 g/m^2 . The adhesive was applied in a factory condition of $17 \text{ }^\circ\text{C}$, with an environmental moisture of 50%. Formed beams were then cold-pressed for 2 h, with a pressure of 1.4 N/mm^2 . No finger joints were forecasted in cross-laminated panels of this experimental campaign.

From this production, an amount of seven specimens for each series was accounted for these tests, their features are summarized in Table 1.

2.2 Central axial compressive test

The experimental tests were performed at the Laboratory of Structures, Tests and Materials of the University of L'Aquila (Italy), Department of Civil, Architecture and Building and Environmental Engineering. The typical duration of buckling experiments was in the range of 30 min long and an appropriate setup was developed, to provide the desired loading and boundary conditions to the tested CLT panel. Each specimen was positioned between a couple of one-way knife hinges whose shape has been designed to ensure the right positioning in the underlying and overlying wedges (Fig. 1a, c). The distance between the axes of end hinges is $l = 1064$ mm. The wedges were connected to the machine test support devices by bolts.

During the test, a total of four laser displacement transducers were used. Their position (Fig. 1b) was on both sides of the span area of the specimen; the transducers 1 and 3

Table 1 Size (B =width; T =thickness; L =length), configuration, and test type of the examined CLT specimens

Panel series	Configuration timber	Specimen			
		No.	B (mm)	L (mm)	T (mm)
HO	Homogeneous beech	7	144	800	54
HB	Hybrid beech/Corsican pine	7	144	800	54

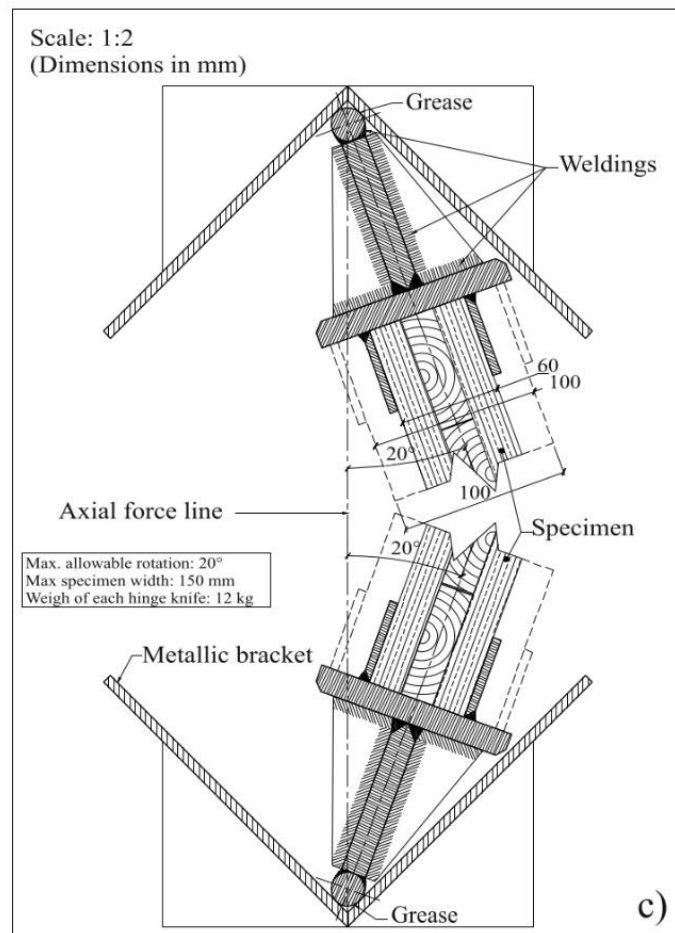
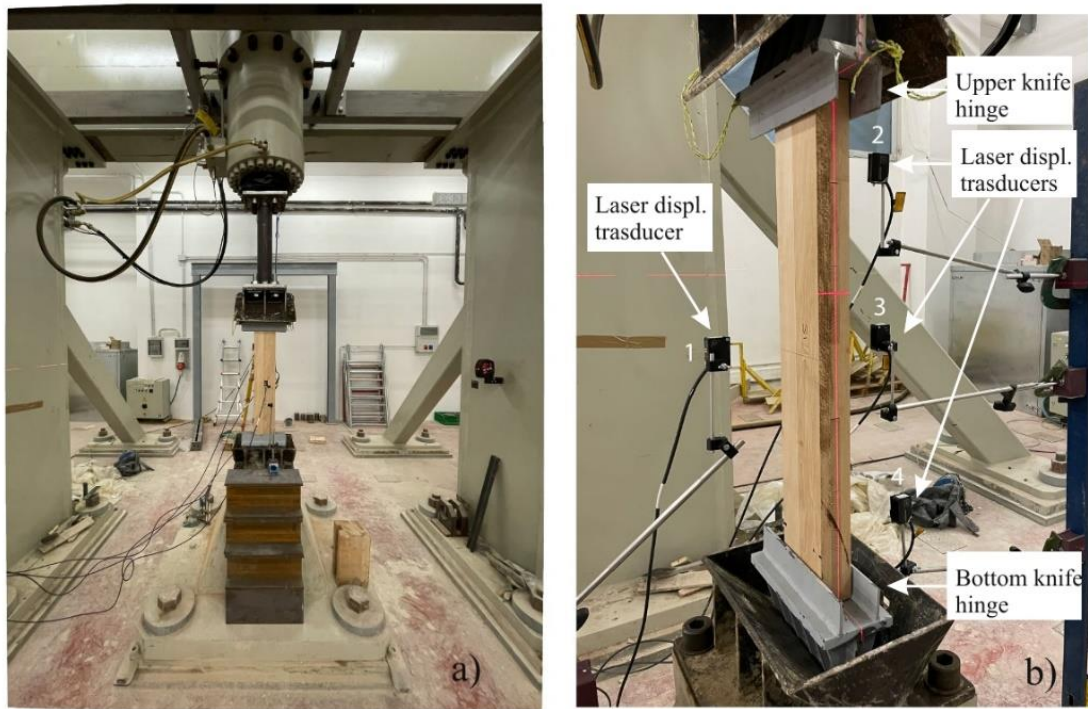


Fig. 1 Setup description: **a** machine test; **b** displacement transducers position and knives; **c** setup design detail

were used to measure the middle deflections of the specimen, while the transducers 2 and 4 could measure some torsional effects. The in-plane compressive load F , continuously monitored by means of a load cell, was applied by means of an Instron-Schenck hydraulic servo-controlled jack along the width B .

In the process of specimen loading, a preload F_0 was applied to the specimen to eliminate the gap between the ends of the specimen and the supports. In this experimental test, the preloaded load value F_0 was taken as 30% of the estimated ultimate load value of the specimen.

The tests were carried out under displacement control; in particular, a limit of 15 mm was fixed for the vertical lowering of the machine crossbeam. Two different speed rates have been set: the first, until the critical load was reached, was equal to 0.44 mm/s, and once the critical load was reached, the speed rate has been reduced to 0.33 mm/s.

2.3 Experimental results

The ultimate loads F_b and the failure modes are summarized in Table 2. Some examples of failure modes are defined in Fig. 2. Regardless of configuration, panels reached similar average limit load levels equal to 200 kN for the homogeneous configuration and 192 kN for the hybrid configuration. Panels having an homogeneous configuration were characterized by a bending due to buckling (tension and

compression) failure while the main failure mode of hybrid specimens was rolling shear. The standard deviation s_y and the 5th percentile m_k are given in Table 2.

The axial displacement versus compressive load F curves are shown in Fig. 3, both for the seven homogeneous specimens (Fig. 3a) and for the seven hybrid specimens (Fig. 3b). The curves of the homogeneous and hybrid specimens reach the final slope after an initial settlement of the specimens. It is worth observing that after such initial settlement, the slope of the linear increasing branches of the curve is almost the same both for the homogeneous and hybrid panels.

The recorded mid-span displacement versus compressive load F curves are shown in Fig. 4, both for the homogeneous (Fig. 4a) and hybrid (Fig. 4b) specimens. They all show the existence of some problems of the experimental apparatus. Specifically, due to the unavoidable imperfections of the experimental setup, it was necessary to re-elaborate the acquired data to extract the displacement component linked to the deformation of the specimen only. The imperfections of the setup that cannot be fully eliminated include: the misalignment of the two hinges with respect to the longitudinal axis of the specimen, the imperfect contact of the end sections of the specimen with base and top steel plates, and the presence of a gap between the lateral steel plates of the end restraints and the specimen. The accurate procedure to clean up the experimental curves from the imperfections is described in the Appendix. Finally, the re-elaborated mid-span displacement versus compressive load F curves are shown in Fig. 4c, d for the homogeneous and hybrid specimens, respectively.

Table 2 Axial compression test campaign evidence

Specimen no.	F_b (kN)	Failure mode
HO-1	211	b
HO-2	183	b
HO-3	165	b
HO-4	203	b
HO-5	205	b
HO-6	218	d
HO-7	217	b
Average	200	
s_y	19	
m_k	157	
HB-1	234	b
HB-2	187	r
HB-3	134	r
HB-4	241	r+d
HB-5	204	r+d
HB-6	204	d
HB-7	141	d+b
Average	192	
s_y	41	
m_k	99	

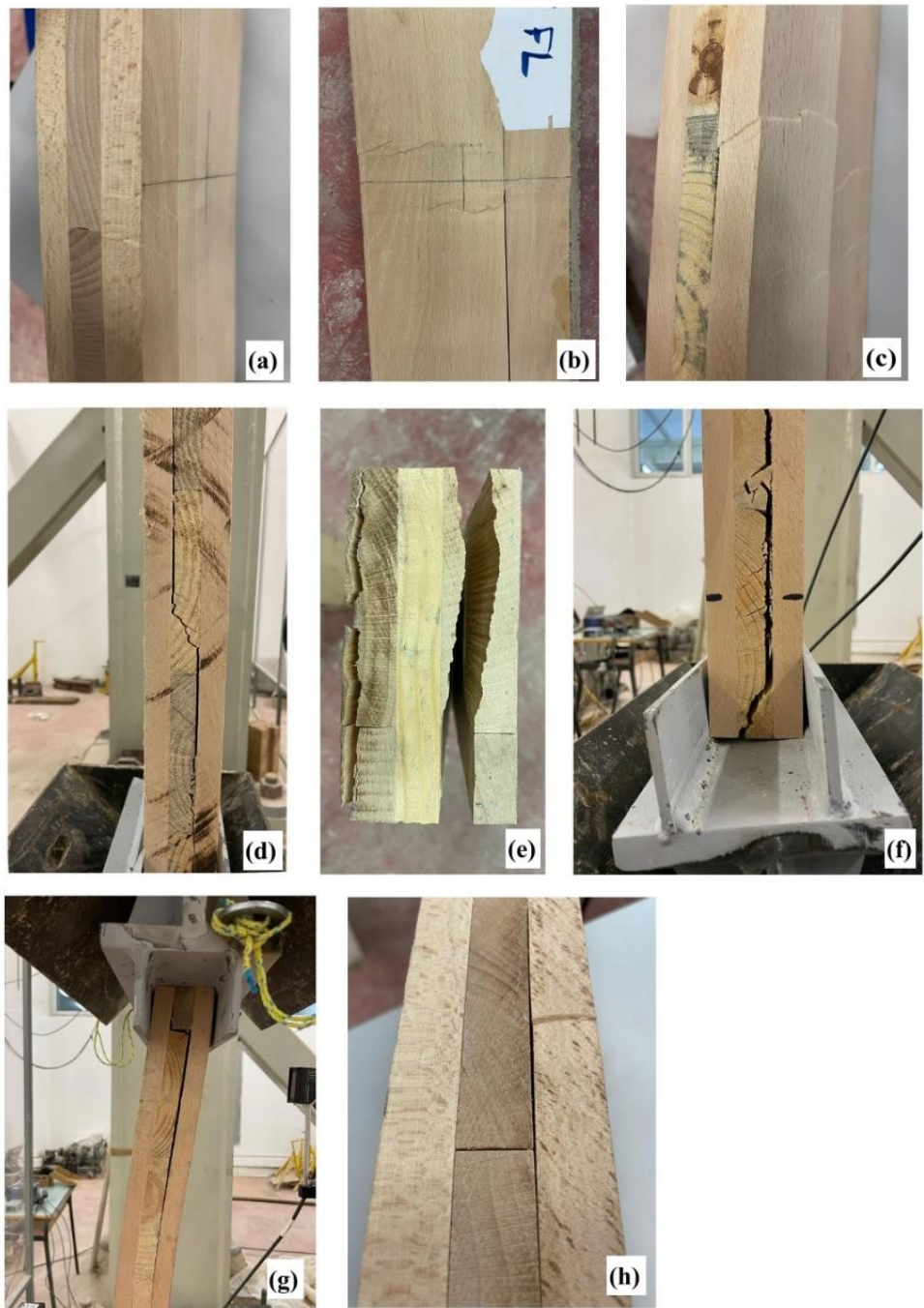
b bending–buckling failure, d delamination, r rolling shear

3 Analytical model

3.1 General glued multilayer beam model

To understand the results of the experimental campaign and in the attempt to extend such results for practical use, an analytical model is here developed. A general model is first introduced with the aim to approach the buckling of a glued multilayer beam subject to a concentrated compression load, after which it will be adapted to the three layers CLT panel object of the present paper. As the model is intended to interpret the experimental results described before, it will be made reference to an initial imperfection of the panels as in Fig. 5. It is worth observing that the length l is taken equal to the distance between the two end hinges of the experimental apparatus ($l = 1064$ mm), even though the panel length is of 800 mm (see Table 1), since it is assumed that the entire system between the hinges undergoes bending–buckling deformation.

Fig. 2 Failure modes: **a–c** bending–buckling; **d–f** rolling shear; **g, h** delamination



The general mechanical model is made of N overlapped planar Timoshenko beams, with rectangular cross-sections of different height h_i ($i = 1 \dots, N$) and unique width b ; the beams are connected through $N - 1$ glue lines, represented by a continuous distribution of linear elastic springs that work along the tangential and normal directions, as in Refs. [56, 57]. Since the model aims to analyze its buckling behavior, it is developed according to the classical linearized

theory approach, which consider the hypothesis of small displacements and small strains, though imposing the equilibrium in a deformed shape adjacent to the reference equilibrium configuration (trivial solution).

The mathematical model is defined by three sets of three equations (kinematic, static, and constitutive) for each layer, which involve kinematic and static quantities related to the glue lines.

Fig. 3 Axial displacement versus compressive load F : **a** homogeneous HB specimens; **b** hybrid HB specimens

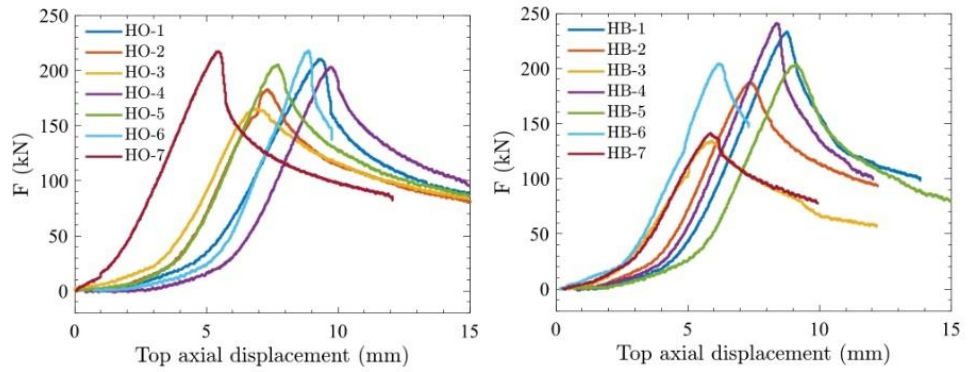


Fig. 4 Midspan displacement versus compressive load F : **a** and **b** recorded curves for the homogeneous and hybrid specimens, respectively; **c** and **d** re-elaborated curves for the homogeneous and hybrid specimens, respectively

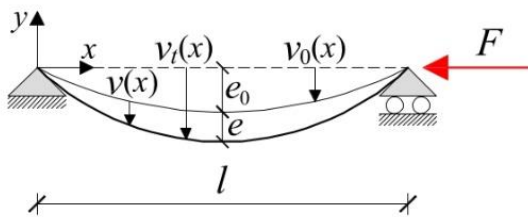
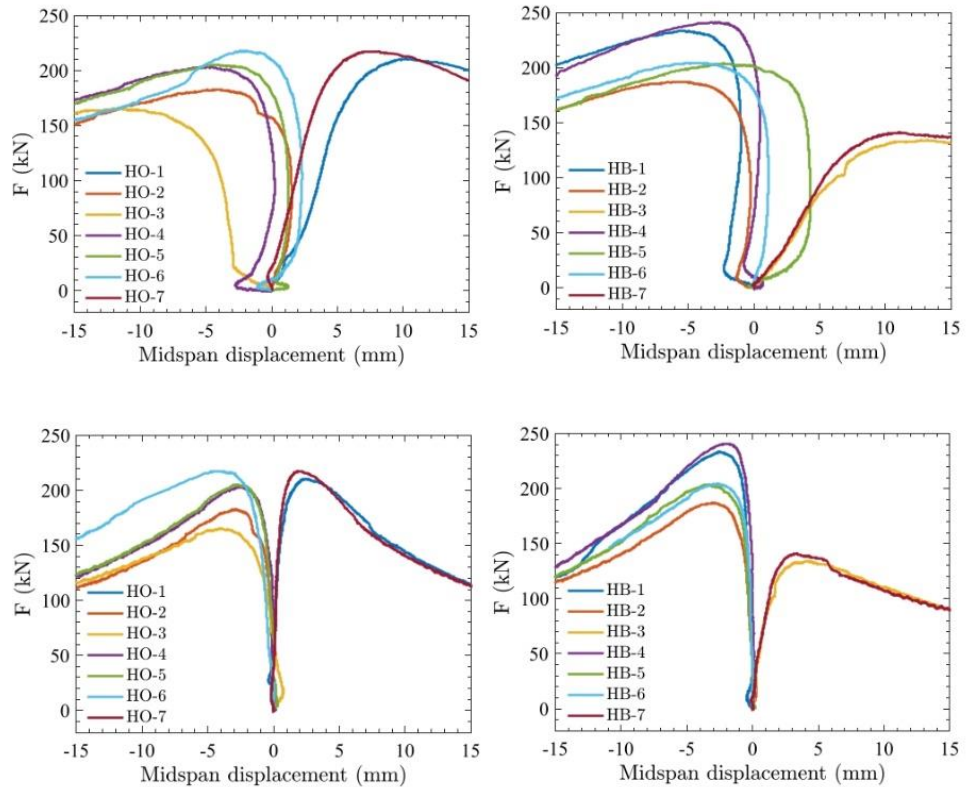


Fig. 5 Reference system: imperfect beam under a concentrated compression load

3.1.1 Kinematics

With reference to Fig. 6a, b, the kinematics on the entire system is described by a $3N$ displacement components vector $\mathbf{u}(x) = \{\mathbf{u}_1(x), \dots, \mathbf{u}_i(x), \dots, \mathbf{u}_N(x)\}^T$, expressed as a function on a unique variable x , lying along the beam length, in which $\mathbf{u}_i(x) = \{u_i(x), v_i(x), \varphi_i(x)\}^T$ encompasses the displacements of the i -th layer.

By neglecting the dependence on the variable x for simplicity, a generalized $5N - 2$ strain vector follows as $\boldsymbol{\varepsilon} = \{\boldsymbol{\varepsilon}_1, \boldsymbol{\varepsilon}_{g1,2}, \dots, \boldsymbol{\varepsilon}_{g(i-1),i}, \boldsymbol{\varepsilon}_i, \boldsymbol{\varepsilon}_{g(i,i+1)}, \dots, \boldsymbol{\varepsilon}_N\}^T$ in which the classical beam strains for the i -th layer are defined, adopting from now on the Lagrangian notation, as $\boldsymbol{\varepsilon}_i = \{\varepsilon_i, \gamma_i, \kappa_i\} = \{u'_i, v'_i - \varphi_i, \varphi'_i\}$, while for the $i, i + 1$ -th

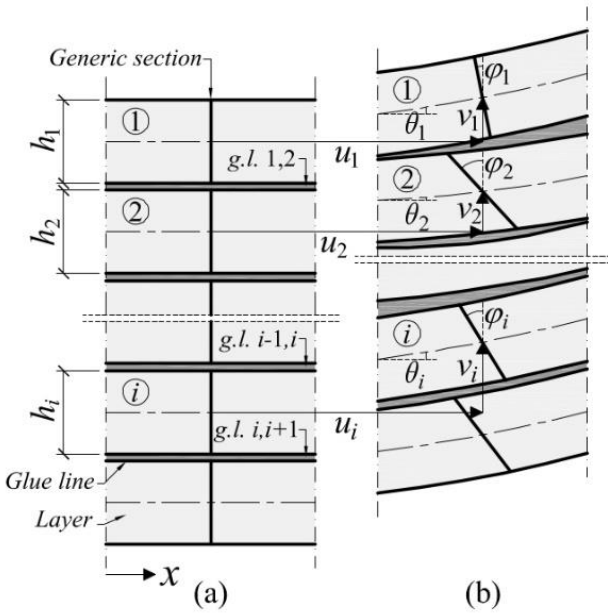


Fig. 6 Kinematic quantities: **a** undeformed shape; **b** deformed shape

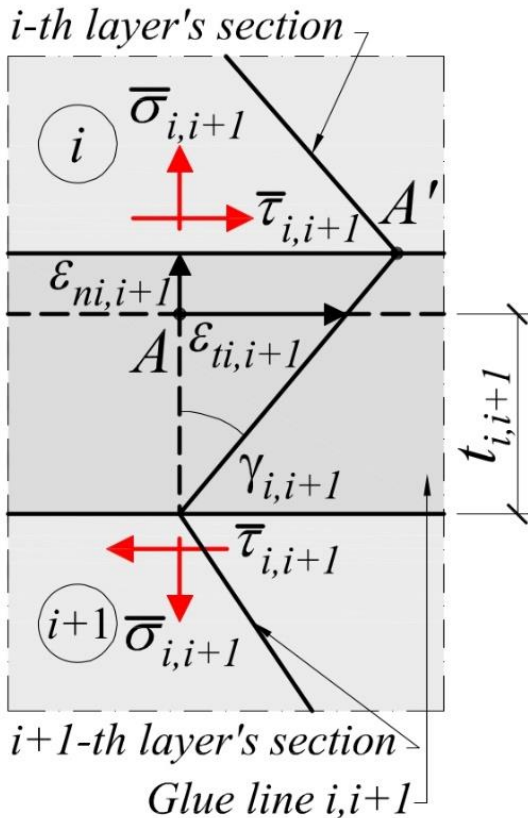


Fig. 7 Detail (in the deformed shape) of the kinematic and static quantities of the glue line between i -th and $i + 1$ -th layers

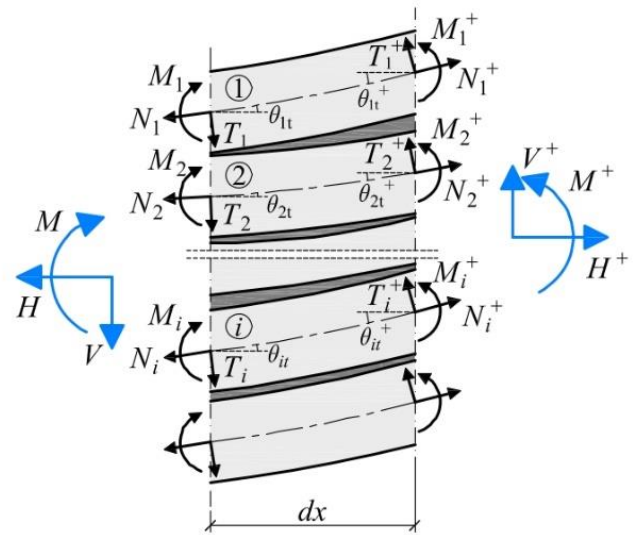


Fig. 8 Static quantities in the deformed configuration and global resultants

glue line (to be intended as: between layers i and $i + 1$) (Fig. 7):

$$\mathbf{e}_{gi,i+1} = \begin{Bmatrix} \epsilon_{ni,i+1} \\ \epsilon_{ti,i+1} \end{Bmatrix} = \begin{Bmatrix} v_i - v_{i+1} \\ \left(u_i + \frac{h_i}{2}\varphi_i\right) - \left(u_{i+1} - \frac{h_{i+1}}{2}\varphi_{i+1}\right) \end{Bmatrix} \quad (1)$$

It should be observed that, since the thickness of a real glue line may be of difficult estimation or control, it is worthy to express the components of $\mathbf{e}_{gi,i+1}$ independently from the thickness $t_{i,i+1}$; therefore, such components represent displacements, and thus they are dimensionally equal to a length.

3.1.2 Statics

The static quantities of the general model, (represented in Figs. 7, 8 as positive), are the generalized internal forces $N_i(x)$, $T_i(x)$ and $M_i(x)$ ($i = 1, \dots, N$), which represent the axial force, the shear force, and the bending moment, respectively, acting on the i -th layer, whereas quantities $\bar{\sigma}_{i,i+1}(x)$ and $\bar{\tau}_{i,i+1}(x)$ are, respectively, the normal and tangential stresses (per unit of length) acting along the contact interface between layers i and $i + 1$. These can be collected into a $(5N - 2) \times 1$ force vector $\mathbf{t}(x) = \{\mathbf{t}_1(x), \mathbf{t}_{g1,2}(x), \dots, \mathbf{t}_{gi-1,i}(x), \mathbf{t}_i(x), \mathbf{t}_{gi,i+1}(x), \dots, \mathbf{t}_N(x)\}^T$ with (neglecting again the dependence on the variable x for simplicity) $\mathbf{t}_i = \{N_i \ T_i \ M_i\}^T$ and $\mathbf{t}_{gi,i+1} = \{\bar{\sigma}_{i,i+1} \ \bar{\tau}_{i,i+1}\}^T$.

With reference to Fig. 8, the equilibrium equations, for each layer, should be written with respect to the adjacent deformed configuration defined by the angles $\theta_i = v'_i$

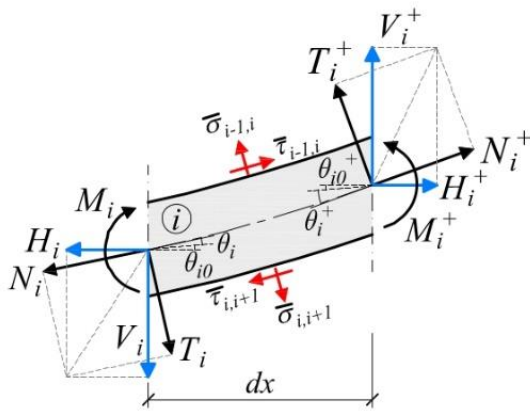


Fig. 9 Static equilibrium for the i -th layer

($i = 1, \dots, N$), which may include some initial imperfection and, in general, should be different for each layer as the glue lines are allowed to deform out of their plane. Since the forces N_i and T_i ($i = 1, \dots, N$) are not parallel and the sections stepwise, it may be convenient to express the equilibrium condition with reference to an infinitesimal portion of the deformed beam, cut by two vertical sections, spaced dx , and projecting the forces N_i and T_i in the horizontal and vertical direction.

In Fig. 9, the forces involved in the equilibrium of the single layer are portrayed and the apex $(\cdot)^+$ indicates the small increment derived by a series expansion up to the first order, so that $\alpha(x)^+ = \alpha(x) + \alpha'(x)dx$, $\alpha(x)$ being one of the kinematic or static entities shown in Fig. 9.

In the same figure, the rotations of the axis line are split in two parts, having distinguished the initial rotation $\theta_{i0} = v'_{0i}$, which may be present in the unloaded imperfect beam (Fig. 5), from the relative rotation $\theta_i = v'_i$, which rise from the initial imperfect shape, as an effect of the applied loads. It should be recalled that while the bending response of the layer is related to the (relative) rotation θ_i , the bending effect induced by the horizontal force H_i^+ depends on the (total) rotation $\theta_{it} = \theta_{i0} + \theta_i$.

With reference to Fig. 9, it should be also observed that strictly the glue stress $\bar{\sigma}$ and $\bar{\tau}$ vary in an unknown way along the layer's border; however, for simplicity, they are supposed uniform in dx and acting under the rotation θ_{it} .

For the i -th layer, it can be then demonstrated that the equilibrium equations read:

$$\begin{aligned} N'_i - (T_i \theta_{it})' - \bar{\sigma}_{i-1,i} \theta_{it} + \bar{\sigma}_{i,i+1} \theta_{it} + \bar{\tau}_{i-1,i} - \bar{\tau}_{i,i+1} &= 0 \\ T'_i + (N_i \theta_{it})' + \bar{\sigma}_{i-1,i} - \bar{\sigma}_{i,i+1} + \bar{\tau}_{i-1,i} \theta_{it} - \bar{\tau}_{i,i+1} \theta_{it} &= 0 \\ M'_i + T_i - (h_i/2)(\bar{\tau}_{i-1,i} + \bar{\tau}_{i,i+1} - \bar{\sigma}_{i-1,i} \theta_{it} - \bar{\sigma}_{i,i+1} \theta_{it}) &= 0. \end{aligned} \tag{2}$$

However, recalling that $H = \sum_i H_i = -F$ for the reference system (Fig. 5), the equilibrium equations can be simplified supposing that θ_{it} is small enough for each layer, such as $N_i \approx H_i$, and hence $N = \sum_i N_i \approx -F$, which implies that $N' = \sum_i N'_i \approx 0$; similarly the terms $\bar{\sigma} \theta_i$ and $\bar{\tau} \theta_i$ can be overlooked, thus determining the equilibrium equations in the form:

$$\begin{aligned} N'_i + \bar{\tau}_{i-1,i} - \bar{\tau}_{i,i+1} &= 0 \\ T'_i + (N_i \theta_{it})' + \bar{\sigma}_{i-1,i} - \bar{\sigma}_{i,i+1} &= 0 \\ M'_i + T_i - (h_i/2)(\bar{\tau}_{i-1,i} + \bar{\tau}_{i,i+1}) &= 0. \end{aligned} \tag{3}$$

3.1.3 Constitutive laws

Finally, the constitutive laws are introduced, based on a linear elastic uncoupled behavior for all the materials, according to the following expressions: $\mathbf{t}_i = [C_i] \mathbf{e}_i$ with $[C_i] = \text{diag}\{E_i A_i, G_i A_{it}, E_i I_i\}$, for the i -th layer, and $\mathbf{t}_{gi,i+1} = [C_{gi,i+1}] \mathbf{e}_{gi,i+1}$ with $[C_{gi,i+1}] = \text{diag}\{k_{i,i+1}, g_{i,i+1}\}$, for the $i, i+1$ -th glue line. Specifically, A_i , $A_{it} = 5/6 A_i$ (as the layers present a rectangular section), I_i , E_i , and G_i are, respectively, the cross-section area, the shear area, the moment of inertia, the Young modulus, and the shear modulus of the i -th layer. For the glue line between layers i and $i+1$, the stiffness of the two continuous bed of springs in the normal and tangential direction is defined, respectively (Fig. 7):

$$k_{i,i+1} = \frac{E_{gi,i+1} b}{t_{i,i+1}} \quad g_{i,i+1} = \frac{G_{gi,i+1} b}{t_{i,i+1}} \tag{4}$$

having considered the glue as an elastic continuum with Young modulus $E_{gi,i+1}$ and shear modulus $G_{gi,i+1}$. In the next numerical calculations, it is always assumed $t_{i,i+1} = 0.1$ mm.

It can be noted that globally, the general mechanical model is defined by $13N - 4$ kinematic and static unknowns against $13N - 4$ equations; therefore, the algebraic-differential problem associated to the proposed model is balanced.

3.2 Three-layer CLT beam model

The base mechanical system described above can be adapted to fit the specific three-layer CLT panels ($N=3$) used in the experimental campaign described in the previous sections, resulting in a global simplification of the mathematical formulation. Since the three layers of the specimens have the same thickness h and the same width b , a unique cross-section area $A_i = A = bh$, shear (rectangular) area $A_{it} = A_t = (5/6)bh$, and moment of inertia $I_i = I = bh^3/12$ is considered for each layer ($\forall i = 1, 2, 3$).

Due to the mechanical symmetry of the section of the CLT panels, as the outer layers are made of the same kind of wood, a single value for the elastic modulus $E_1 = E_3$ and for the shear modulus $G_1 = G_3$ are taken into account for the external layers.

Finally, for both the two glue lines, the same thickness t , Young modulus E_g , and shear modulus G_g are supposed; therefore, a single normal stiffness $k = k_{1,2} = k_{2,3}$ as well as a single shear stiffness $g = g_{1,2} = g_{2,3}$ are considered.

Equilibrium Eq. (3) now became:

$$\begin{array}{l}
 N'_1 - \bar{\tau}_{1,2} = 0 \\
 N'_2 + \bar{\tau}_{1,2} - \bar{\tau}_{2,3} = 0 \\
 N'_3 + \bar{\tau}_{2,3} = 0
 \end{array}
 \left|
 \begin{array}{l}
 T'_1 + (N_1\theta_{1t})' - \bar{\sigma}_{1,2} = 0 \\
 T'_2 + (N_2\theta_{2t})' + \bar{\sigma}_{1,2} - \bar{\sigma}_{2,3} = 0 \\
 T'_3 + (N_3\theta_{3t})' + \bar{\sigma}_{2,3} = 0
 \end{array}
 \right.
 \begin{array}{l}
 M'_1 + T_1 - \frac{h}{2}\bar{\tau}_{1,2} = 0 \\
 M'_2 + T_2 - \frac{h}{2}(\bar{\tau}_{1,2} + \bar{\tau}_{2,3}) = 0 \\
 M'_3 + T_3 - \frac{h}{2}\bar{\tau}_{2,3} = 0
 \end{array}
 \tag{5}$$

The CLT beam model can be further simplified by introducing some internal constraints, based on suitable assumptions on the mechanical behavior of the system. These constraints are expressed as follows:

$$\begin{aligned}
 \epsilon_{n12} = 0 &\rightarrow v_1 = v_2 = v \\
 \epsilon_{n23} = 0 &\rightarrow v_3 = v_2 = v \\
 \gamma_1 = 0 &\rightarrow \varphi_1 = v' = \theta_1 = \varphi \\
 \gamma_3 = 0 &\rightarrow \varphi_3 = v' = \theta_3 = \varphi \\
 N_2 &= 0.
 \end{aligned}
 \tag{6}$$

By means of Eq. (6)_{1,2}, the impossibility of the layers to detach from each other in the normal direction is introduced, thus resulting in a single displacement component $v_1 = v_2 = v_3 = v$ orthogonal to the layers' axes. Likewise it is supposed that the initial imperfection v_{i0} is equal for each layer, thus assuming $v_{i0} = v_0 \forall i = 1, 2, 3$ (Fig. 5). Based on the low thickness to length ratio of each layer, Eq. (6)_{3,4} enforces the shear non-deformability of the external timber layers (Euler–Bernoulli beam theory); such a constraint makes the rotation angles φ_1 and φ_3 slave quantities of the orthogonal displacement v , thus assuming the same value φ . Finally, Eq. (6)₅ is based on the fact that often in CLT panels, as in the case of the ones tested experimentally, the cross layers are made

of planks whose narrow borders are not glued or not even in contact; it is then supposed that the central layer is unable to bear any axial force. Nevertheless, as the inner planks hold some cross bending stiffness, which can be involved by the deflection of the outer layers, it is supposed that the central layer is able to bear some bending moment ($M_2 \neq 0$).

From Eqs. (6)₅ and (5)₂, it can now be written $\bar{\tau}_{1,2} = \bar{\tau}_{2,3} = \bar{\tau}$, which means that the two glue lines are subject to the same shear stress $\bar{\tau}$ and the same shear strain $\bar{\tau}/g = \epsilon_t = \epsilon_{t1,2} = \epsilon_{t2,3}$ while the global compressive force acting on the panels (Fig. 5) reads: $N = N_1 + N_3 = -F$ keeping itself constant along the panel.

Due to the internal constraints, some internal forces ($T_1, T_3, \bar{\sigma}_{1,2}, \bar{\sigma}_{2,3}$) become reactive quantities, as they cannot be expressed by the constitutive laws. Such reactive quantities can be then obtained by solving Eq. (5)_{7,9} with respect to T_1 and T_3 , and Eq. (5)_{4,6} with respect to $\bar{\sigma}_{1,2}$ and $\bar{\sigma}_{2,3}$. Together with Eq. (5)_{1,3}, the condensed equilibrium equations are, hence, obtained by substituting the relationships that provide the reactive forces $\bar{\sigma}_{1,2}$ and $\bar{\sigma}_{2,3}$ into Eq. (5)₅, and finally substituting, in the same equation, the derivatives of T_1, T_2 , and T_3 expressed

from Eq. (5)_{4,5,6}. The condensed equilibrium equations, thus, read:

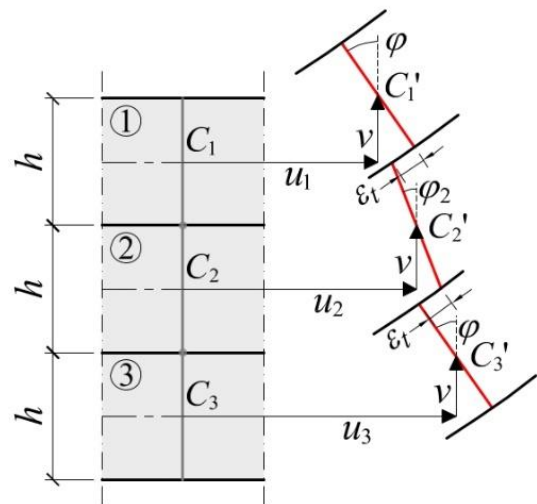


Fig. 10 Kinematics of the generic section in the CLT panel

$$\begin{aligned}
 N'_1 - \bar{\tau} &= 0 \\
 N'_3 + \bar{\tau} &= 0 \\
 (M_1 + M_2 + M_3)'' - 2N''_1 h + F(v + v_0)'' &= 0 \\
 M'_2 + T_2 - \bar{\tau}h &= 0
 \end{aligned} \tag{7}$$

in which it has been considered, from Eq. (6)_{3,4}, that $\sum_i (N_i \theta_{it})' = \sum_i N_i \theta'_{it} = -F(v'' + v_0'')$.

By substituting the constitutive laws (Sect. 3.1.3), and the kinematics equations (Sect. 3.1.1) (modified according to Eq. (6)) into Eq. (7), the field equations are obtained as:

$$\begin{aligned}
 E_1 A u''_1 - g \varepsilon_t &= 0 \\
 E_1 A u''_3 + g \varepsilon_t &= 0 \\
 2E_1 I \varphi''' + E_2 I \varphi_2''' - 2E_1 A u''_1 h + F(v + v_0)'' &= 0 \\
 E_2 I \varphi_2'' + G_2 A_t (\varphi - \varphi_2) - g \varepsilon_t h &= 0
 \end{aligned} \tag{8}$$

which represent a system of four coupled linear differential equations facing five kinematic unknowns ($u_1, u_3, \varepsilon_t, v, \varphi_2$); therefore, since the system is indeterminate, a new constraint is needed. However, before doing this, further considerations have to be made.

It should be now taken into account the relationships that exist among the various displacement components (Fig. 10), according to Eq. (1), from which the two axial displacements for the external layers are obtained in the form:

$$\begin{aligned}
 u_1 &= u_2 - \frac{h}{2} \left(\varphi + \varphi_2 - \frac{2}{h} \varepsilon_t \right) \\
 u_3 &= u_2 + \frac{h}{2} \left(\varphi + \varphi_2 - \frac{2}{h} \varepsilon_t \right).
 \end{aligned} \tag{9}$$

Summing both sides of Eq. (9) and deriving it, it follows: $\varepsilon_1 + \varepsilon_3 = 2\varepsilon_2$ which means that the axial displacement and strain of the central layer identify, respectively, the mean displacement and strain of the outer layers. Therefore, it can be written $-F = E_1 A \varepsilon_1 + E_1 A \varepsilon_3 = E_1 A (\varepsilon_1 + \varepsilon_3) = 2E_1 A \varepsilon_2$ and then $\varepsilon_2 = -F / (2E_1 A)$ which implies that the central layer axial strain is constant along the panel. This means that deriving twice Eq. (9) and substituting them into the field equations, Eq. (8)_{1,2} become equals, thus resulting in a differential system twice indeterminate (three independent equations against five unknowns). Therefore, two more constraints are needed.

3.2.1 Coupling parameters

To eliminate the indetermination of the problem, a simple but consistent attempt, from a mechanic standpoint, is to introduce the following two non-dimensional parameters:

$$\eta = \frac{\varphi_2}{\varphi} \quad \psi = \frac{2}{h} \frac{\varepsilon_t}{\varphi} \tag{10}$$

Although η as well as ψ should be, generally, functions of x , it is now supposed that they are both constant showing later the conditions under which such a hypothesis turns to be true. Then introducing Eq. (10) into Eq. (9), after derivation, the outer layers axial strains become:

$$\begin{aligned}
 \varepsilon_1 = u'_1 &= -\frac{F}{2E_1 A} - \frac{h}{2} (1 + \eta - \psi) \varphi' \\
 \varepsilon_3 = u'_3 &= -\frac{F}{2E_1 A} + \frac{h}{2} (1 + \eta - \psi) \varphi'.
 \end{aligned} \tag{11}$$

From Eqs. (10) and (11)₁, the field Eqs. (8), which have now become an algebraic-differential system of three equations facing three unknowns (v, η, ψ), read:

$$\begin{aligned}
 E_1 A (1 + \eta - \psi) \varphi'' + g \psi \varphi &= 0 \\
 E_1 [I(2 + \rho_E \eta) + Ah^2(1 + \eta - \psi)] v^{IV} + F(v + v_0)'' &= 0 \\
 2E_2 I \eta \varphi'' + 2G_2 A_t \varphi (1 - \eta) - gh^2 \psi \varphi &= 0
 \end{aligned} \tag{12}$$

in which the elastic modulus ratio $\rho_E = E_2 / E_1$ has been introduced. Equation (12)₂ can be then written in a compact form:

$$E_1 I_{eq} v^{IV} + F(v + v_0)'' = 0 \tag{13}$$

which, in absence of an initial imperfection (i.e. $v_0 = 0$), clearly recalls the classic elastic curve equation for the buckling of a Euler–Bernoulli’s beam, having introduced the equivalent moment of inertia:

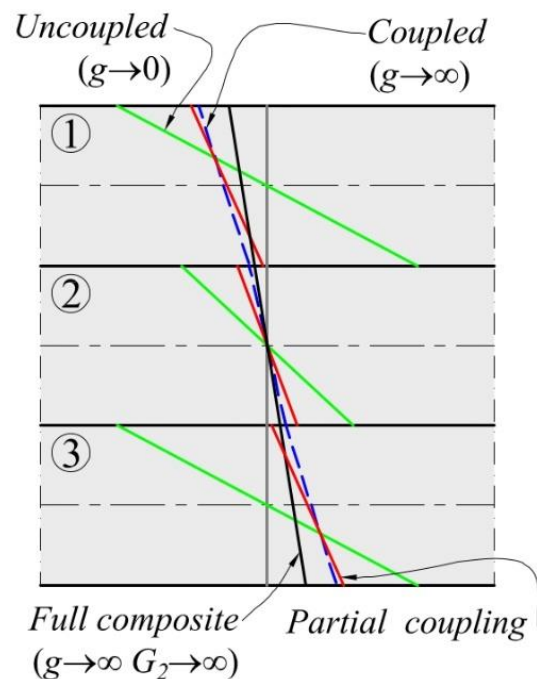


Fig. 11 Limit configurations for the single section

$$I_{eq} = I(2 + \rho_E \eta) + Ah^2(1 + \eta - \psi). \tag{14}$$

The two parameters η and ψ can now be determined from Eq. (12)_{1,3}, thus obtaining:

$$\begin{aligned} \psi &= \frac{E_1 A (1 + \eta) \varphi''}{E_1 A \varphi'' - g \varphi} \\ \eta &= -\frac{2G_2 A_t \varphi + E_1 A h^2 (1 - \psi) \varphi}{(2E_2 I + E_1 A h^2) \varphi'' - 2G_2 A_t \varphi}. \end{aligned} \tag{15}$$

These last equations effectively express two constant quantities provided that the differential Eq. (13) admits a solution v in the form $v(x) = -e \sin(\pi x/l)$. As known, such a circumstance may stem out assuming $v_0(x) = -e_0 \sin(\pi x/l)$ for the imperfect beam problem of Fig. 5, which, from now on, will be considered as the reference system for the analytical model, as it can be directly associated to the experimental set up.

From the abovementioned sine solution, it can be determined:

$$\begin{aligned} \psi &= \frac{2E_1 A \pi^2 (2G_2 A_t l^2 + E_2 I \pi^2)}{2G_2 A_t g l^4 + [E_1 A (2G_2 A_t + g h^2) + 2E_2 I g] l^2 \pi^2 + 2E_1 A E_2 I \pi^4} \\ \eta &= \frac{2G_2 A_t l^2 - E_1 A h^2 \pi^2 (1 - \psi)}{2G_2 A_t l^2 + E_1 A h^2 \pi^2 + 2E_2 I \pi^2} \end{aligned} \tag{16}$$

which, according to Eq. (14), determines the degree of coupling of the external layers. In this context, the parameter ψ represents the coupling flexibility of the glue lines whereas the parameter η represents the coupling efficiency of the central layer. Among all the parameters that appear in Eq. (16), those, which a specific attention is given to in this paper, are the glue line shear stiffness g and the shear modulus G_2 , the latter representing the rolling shear modulus of the central layer. With reference to Fig. 11, it is possible to define some limit conditions associated to the extreme values that g and G_2 may achieve.

Full composite beam

$$\left. \begin{aligned} g &\rightarrow \infty \\ G_2 &\rightarrow \infty \end{aligned} \right\} \Rightarrow \psi \rightarrow 0 \Rightarrow \eta \rightarrow 1 \tag{17}$$

$$\Rightarrow I_{eq} \rightarrow I_{FC} = I(2 + \rho_E \eta) + 2Ah^2$$

No slip in the glue lines, with the global section remaining plane while the quantity $Ah^2(1 + \eta - \psi)$ (Steiner's term) reaches its maximum value as $1 + \eta - \psi = 2$.

Coupled beam

$$\begin{aligned} g &\rightarrow \infty \Rightarrow \psi \rightarrow 0 \Rightarrow \eta \rightarrow \eta_C \\ &= \frac{2G_2 A_t l^2 - E_1 A h^2 \pi^2}{2G_2 A_t l^2 + E_1 A h^2 \pi^2 + 2E_2 I \pi^2} \\ \Rightarrow I_{eq} &\rightarrow I_C = I(2 + \rho_E \eta_C) + Ah^2(1 + \eta_C) \end{aligned} \tag{18}$$

No slip in the glue lines, with the global section that exhibits a broken line profile.

Uncoupled beam

$$\begin{aligned} g &\rightarrow 0 \Rightarrow \psi \rightarrow \psi_U = 1 + \frac{1}{1 + \frac{E_2 I \pi^2}{G_2 A_t l^2}} \\ \Rightarrow \eta &\rightarrow \eta_U = \frac{1}{1 + \frac{E_2 I \pi^2}{G_2 A_t l^2}} \\ \Rightarrow I_{eq} &\rightarrow I_U = I(2 + \rho_E \eta_U) \end{aligned} \tag{19}$$

With no tangential stress in the glue line, with a stepwise global section and with the Steiner's term that vanishes, the uncoupled panel behaves as if it was made of three stacked independent beams.

On the basis of the geometrical dimensions exposed in Table 1 and the mechanical properties shown in Table 3 (Sect. 4) for beech wood and glue, the variation of the coupling parameters η and ψ with g and G_2 is portrayed in Fig. 12. As can be observed especially from the right graphs of the figure, whatever value of the rolling shear stiffness G_2 , both the coupling parameters η and ψ depend very little on the stiffness of the glue g , since over a very small value of $g > 10,000 \text{ N/mm}^2$, the curve is substantially horizontal.

3.2.2 Euler's buckling load and the elastic solution for the imperfect three-layer CLT beam

Recalling Eq. (13), the Euler's critical load for the three-layer CLT panels follows the classical form:

$$F_{cr} = \frac{\pi^2}{l^2} E_1 I_{eq} \tag{20}$$

over which, according to Eq. (14), it is possible to evaluate the influence of g and G_2 . With reference to the geometrical (Table 1) and mechanical (Table 3, Sect. 4) values associated to the HO-CLT panel, in Fig. 13, the variation of F_{cr} with g

Table 3 Mechanical properties of the wood species used for the CLT specimens

			Beech	Corsican pine
Elastic modulus	E_1	N/mm ²	14.814	–
Elastic modulus	E_2	N/mm ²	991	364
Rolling shear modulus	G_2	N/mm ²	350	59
Compression strength	f_{cu}	N/mm ²	40	–
Rolling shear strength	f_{ru}	N/mm ²	6.0	2.0
Adhesive shear strength	τ_u	N/mm ²	12.25	12.25

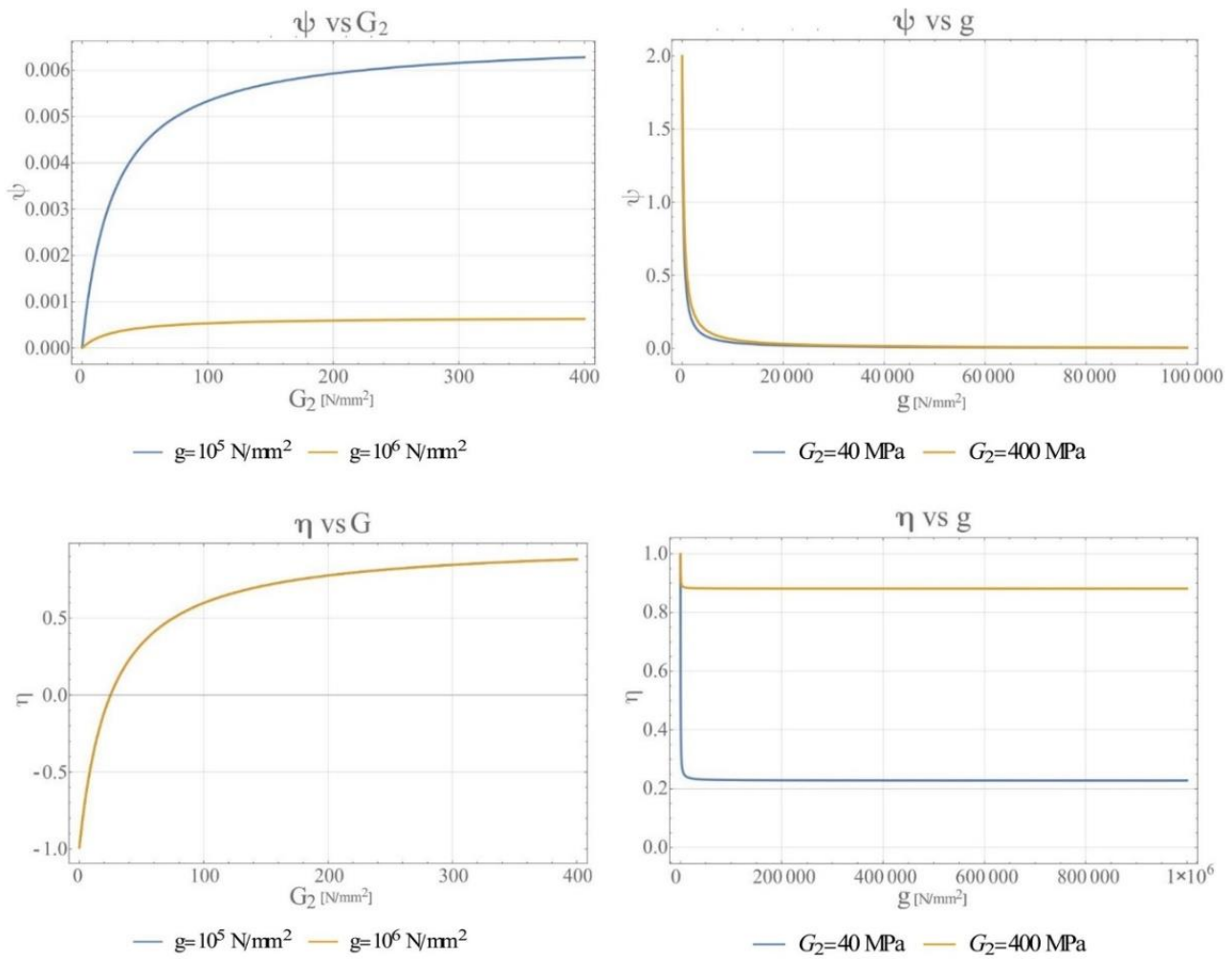


Fig. 12 Diagrams of the coupling parameters ψ and η varying with g and G_2 within their ranges of interest for CLT panels

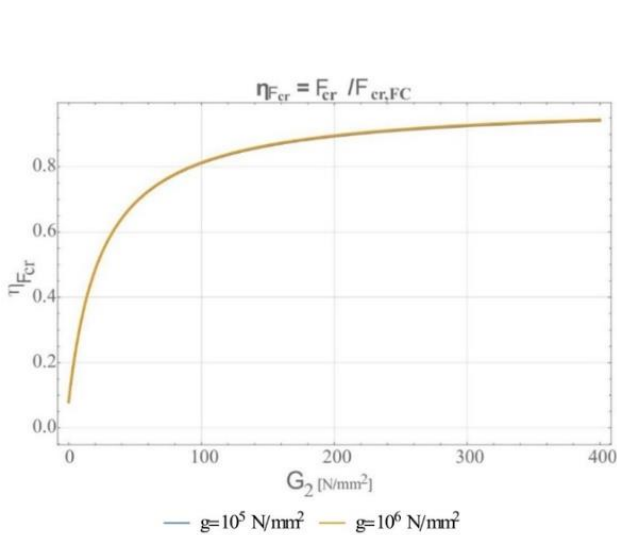


Fig. 13 Buckling load efficiency varying with g and G_2 within their ranges of interest for CLT panels

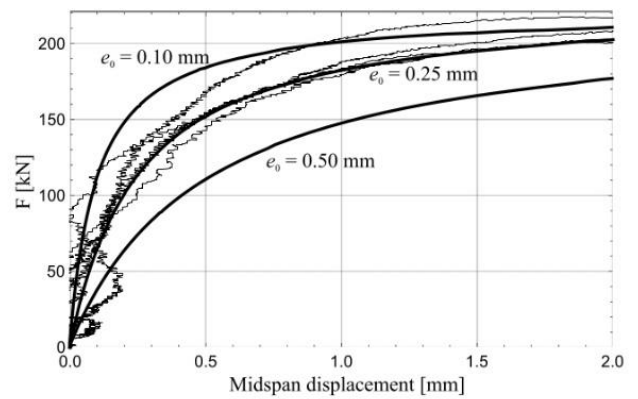


Fig. 14 Experimental (thin line) and analytical (thick line) mid-span displacement versus compressive load F

and G_2 is portrayed, by means of a buckling load efficiency $\eta_{F_{cr}} = F_{cr}/F_{cr,FC}$, being $F_{cr,FC}$ the critical load for the full composite beam.

Clearly, the influence of glue stiffness g is negligible whereas the rolling shear modulus plays a crucial role.

From the sine initial imperfection $v_0(x)$, the solution of Eq. (13), assuming the following boundary conditions $v(0) = v(l) = v''(0) = v''(l) = 0$ (Fig. 5), reads:

$$v(x) = -e \sin\left(\frac{\pi}{l}x\right) = -\frac{e_0 F}{F_{cr} - F} \sin\left(\frac{\pi}{l}x\right) \tag{21}$$

in which the applied force F and the initial eccentricity e_0 are assumed known. Specifically, the initial imperfection e_0 can be estimated by comparing the experimental mid-span displacement–compressive load F curves of Fig. 4c, d and the correspondent analytical ($v(l/2)$ versus F) curves obtained from the solution of Eq. (21). Figure 14 shows the experimental mid-span displacement–compressive load F of the homogeneous specimens HO-1, HO-4, HO-5, and HO-7, already shown in Fig. 4c (thin lines), and the analytical curves (thick lines) obtained for different initial imperfection e_0 . As can be observed, the best fitting among experimental and analytical curves occur for $e_0 = 0.25$ mm ($\approx L/4000$). As a final clarification, the curves in Fig. 14 are shown in a zoomed window with respect to those shown in Fig. 4c. Moreover, Fig. 14 shows the absolute value of the mid-span displacement. In the next section, the value of $e_0 = 0.25$ mm will be always used.

From Eq. (21), it is now possible to evaluate all the displacements, strains, and forces of the system. In particular, focusing on the static quantities, introducing the single i -th ($i = 1, 2, 3$) layer’s critical load as $F_{cri} = E_i I \pi^2 / l^2$ ($F_{cr1} = F_{cr3}$) and recalling the kinematic and constitutive equations of Sect. 0, it can be written from Eq. (11)₁:

$$N_1 = E_1 A u'_1 = -\frac{F}{2} - \frac{E_1 A h \pi^2 (1 + \eta - \psi)}{2 l^2} e \sin\left(\frac{\pi}{l}x\right) \tag{22}$$

$$M_1 = M_3 = E_1 I v'' = F_{cr1} e \sin\left(\frac{\pi}{l}x\right) \tag{23}$$

$$M_2 = E_2 I \eta v'' = F_{cr2} \eta e \sin\left(\frac{\pi}{l}x\right) \tag{24}$$

from Eq. (10)₂:

$$\bar{\tau} = g \varepsilon_t = -g \frac{\psi h \pi}{2 l} e \cos\left(\frac{\pi}{l}x\right) \tag{25}$$

from Eq. (5)_{7,9}:

$$T_1 = T_3 = -M'_1 + \frac{h}{2} \bar{\tau} = -\frac{\pi}{l} \left(F_{cr1} + \frac{g \psi h^2}{4} \right) e \cos\left(\frac{\pi}{l}x\right) \tag{26}$$

from Eq. (10)₁:

$$T_2 = G_2 A_t (1 - \eta) v' = -\frac{G_2 A_t \pi (1 - \eta)}{l} e \cos\left(\frac{\pi}{l}x\right) \tag{27}$$

eventually from Eq. (5)_{4,6}:

$$\bar{\sigma}_{1,2} = \frac{\pi^2 e}{4 l^4} \left\{ 2E_1 A h \pi^2 (1 + \eta - \psi) e \cos\left(\frac{2\pi x}{l}\right) + [4E_1 I \pi^2 + l^2 (gh^2 \psi - 2F)] \sin\left(\frac{\pi}{l}x\right) \right\} \tag{28}$$

$$\bar{\sigma}_{2,3} = \frac{\pi^2 e}{4 l^4} \left\{ 2E_1 A h \pi^2 (1 + \eta - \psi) e \cos\left(\frac{2\pi x}{l}\right) - [4E_1 I \pi^2 + l^2 (gh^2 \psi - 2F)] \sin\left(\frac{\pi}{l}x\right) \right\} \tag{29}$$

On the basis of the geometrical dimensions exposed in Table 1 and the mechanical properties shown in Table 3 (Sect. 4) for beech wood and glue, the elastic response of the homogeneous three-layer CLT panel is then described by the functions portrayed in Fig. 15.

3.2.3 Stability verification

Recalling the theoretical nature of the Euler’s buckling load and the fact that, in principle, it could never be reached, at least within the boundaries of the linearized theory, to interpret the results of the experimental campaign, it is now necessary to define some specific failure criteria, as in Ref. [58].

Basically, as it was described in Sect. 2.3, three failure modes have been observed in the tests: a bending–buckling mode, occurring in the middle of the panel, a rolling shear mode, detected at the ends, and a delamination mode, involving the glue at the extremities as well. To each of these modes, it is possible to associate an ultimate compression load which account for the achievement of the relevant failure stress in a specific part of the structural element. The ultimate load of the panel will be then the lowest of the three, for which an assessment is here presented.

Bending buckling mode

The flexural failure mode stems from the minimum (absolute maximum) compression stress reached in the middle of the panel at the very external surface of layer 1. Recalling the classical Navier’s formula, such a stress can be calculated as:

$$\sigma_{x,\min} = \frac{N_1(l/2)}{A} - \frac{M_1(l/2) h}{I} \frac{h}{2} \tag{30}$$

and therefore, from Eqs. (22) and (23)

$$\sigma_{x,\min} = -\frac{F}{2A} - \frac{E_1 h \pi^2 (2 + \eta - \psi)}{2 l^2} \frac{e_0 F}{F_{cr} - F} \tag{31}$$

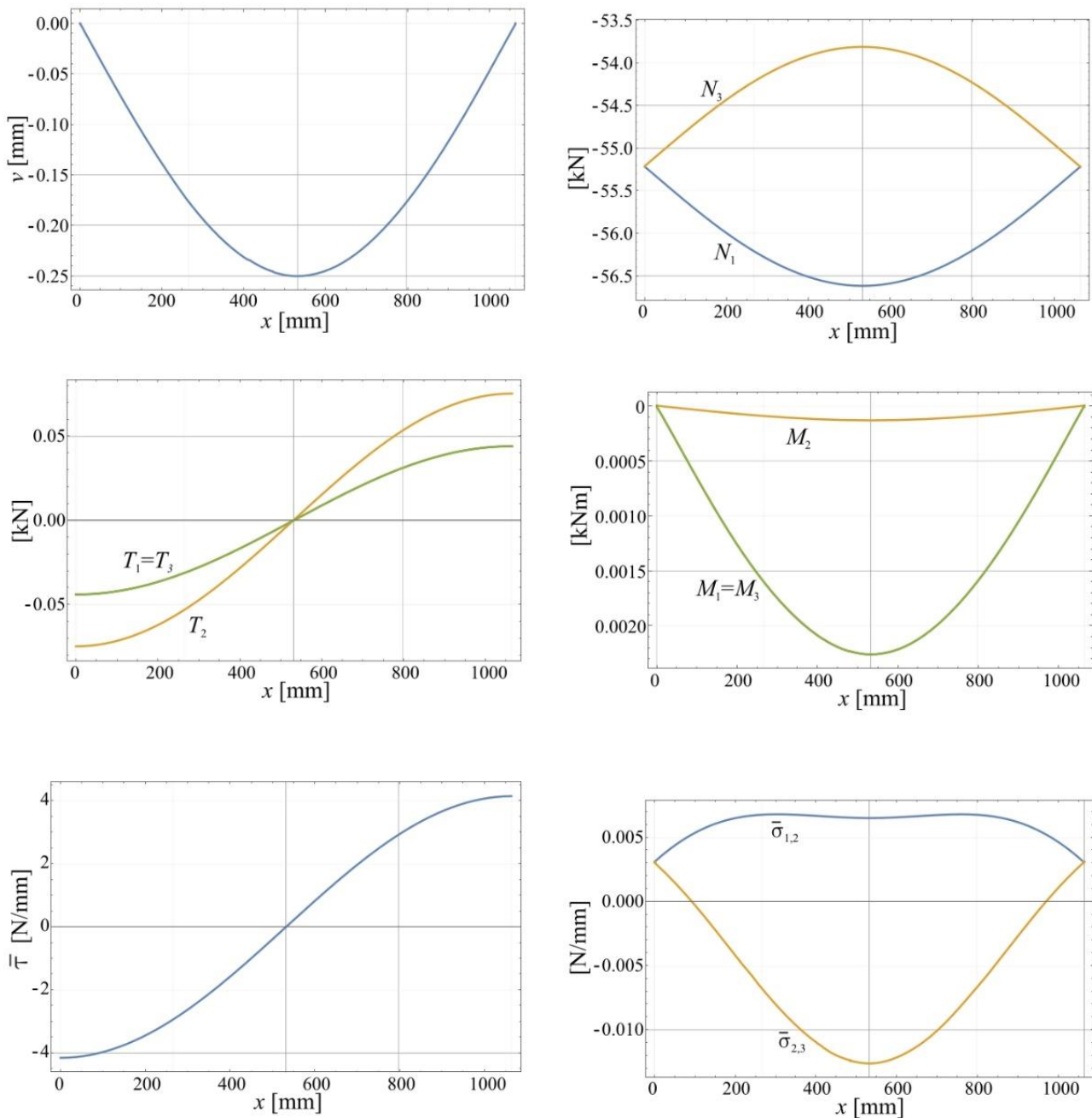


Fig. 15 Elastic response of the imperfect HO-CLT panel under a tip load expressed by functions of the abscissa x ($F=0,5 F_{cr} - e_0=0.25$ mm).

Given f_{cu} the compression failure stress of the layer's wood, it determines a limit compression load, for the straight panel, equal to $F_{cu} = 2 A f_{cu}$. The search for the ultimate load $F = F_{cb}$, which makes $\sigma_{x,min} = f_{cu}$ according to Eq. (31), follows the Ayrton–Perry criterion. After introducing the following non-dimensional parameter:

$$\beta_c = \frac{(2 + \eta - \psi) A h e_0}{I_{eq}} \tag{32}$$

from Eq. (31) it can be written:

$$\frac{F_{cb}}{F_{cu}} \left[1 + \beta_c \left(1 - \frac{F_{cb}}{F_{cr}} \right)^{-1} \right] = 1. \tag{33}$$

It is now introduced the relative slenderness in the form:

$$\bar{\lambda} = \sqrt{\frac{2f_{cu} A}{F_{cr}}} \tag{34}$$

from which, defining:

$$\phi = \frac{1}{2} \left(1 + \beta_c + \bar{\lambda}^2 \right) \tag{35}$$

and:

$$\chi = \frac{1}{\phi + \sqrt{\phi^2 - \bar{\lambda}^2}} \tag{36}$$

finally:

$$F_{cb} = \chi F_{cu} \tag{37}$$

Rolling shear mode

The rolling shear failure appears once the shear stress in the inner layer has reached the rolling shear strength f_{ru} . Such a circumstance may occur at the ends of the panel, where the shear force T_2 achieves its maximum (minimum) value. For simplicity it is considered a uniform distribution of the shear stress across the central layer section:

$$\tau_r = \tau_{xy,2} = T_2/A \tag{38}$$

from which, recalling Eq. (27):

$$\tau_{r,max} = \frac{T_2(x=l)}{A} = \frac{5}{6} \frac{G_2 \pi (1-\eta)}{l} \frac{e_0 F}{F_{cr} - F} \widehat{ABC}. \tag{39}$$

This can be modified introducing:

$$\beta_r = \frac{5}{6} \frac{G_2 \pi (1-\eta) e_0}{l} \tag{40}$$

and then writing:

$$\tau_{r,max} = f_{ru} = \beta_r \frac{F_{rb}}{F_{cr} - F_{rb}}, \tag{41}$$

where F_{rb} represents the limit compression load which determines the achievement of the rolling shear strength in the inner layer. This is, hence, defined as:

$$F_{rb} = \frac{f_{ru} F_{cr}}{\beta_r + f_{ru}}. \tag{42}$$

Delamination mode

The delamination of the glue at the ends of the panel should likely derive from the combined action of the shear stress $\bar{\tau}$ and the normal traction $\bar{\sigma}$ (Fig. 15); however, in this paper, for the sake of simplicity, it will be considered solely the first one.

Table 4 Critical and limit loads from the analytical model

			HO	HB
Critical load	F_{cr}	kN	220.8	170.2
Limit load—bending buckling mode	F_{cb}	kN	185.0	158.5
Limit load—rolling shear mode	F_{rb}	kN	219.8	168.4
Limit load—delamination mode	F_{gb}	kN	220.3	169.9
Limit compression load	F_b	kN	185.0	158.5

Table 5 Comparison between analytical and experimental results

			HO	HB
Analytical limit compression load	F_b	kN	185.0	158.5
Experimental failure load (mean)	F_{cb}	kN	200.0	192.0
Relative difference	–	%	7.4	17.4

The maximum shear stress (per unit of length) is evaluated from Eq. (25) for $x = l$, thus obtaining:

$$\bar{\tau}_{max} = g \frac{\psi h \pi}{2 l} \frac{e_0 F}{F_{cr} - F}. \tag{43}$$

Given the failure shear stress of the adhesive, which determines the delamination, its associated value $\bar{\tau}_u = \tau_u b$ stems from an ultimate load $F = F_{gb}$ which makes $\bar{\tau}_u = \bar{\tau}_{max}$ according to Eq. (43). Therefore, defining:

$$\beta_g = g \frac{\psi h \pi}{2 l} e_0 \tag{44}$$

it can be written:

$$\bar{\tau}_{max} = \bar{\tau}_u = \beta_g \frac{F_{gb}}{F_{cr} - F_{gb}} \tag{45}$$

and finally:

$$F_{gb} = \frac{\tau_u b F_{cr}}{\beta_g + \tau_u b} \tag{46}$$

Finally, the limit compression load for the CLT panel reads:

$$F_b = \text{Min}\{F_{cb}, F_{rb}, F_{gb}\} \tag{47}$$

4 Comparison between analytical and experimental results

The numerical value of the mechanical properties of the wood species considered in this analysis is reported in Table 3. The mean elastic moduli E_1 and E_2 were identified

in Ref. [59], where the same CLT panels were mechanically characterized from bending tests.

For beech wood, the rolling shear modulus and strength have been taken from [60], whereas the compression strength has been approximately defined from EN338, considering the mean experimental MOR shown in Ref. [59].

For Corsican pine wood, the rolling shear modulus has been calculated from EN338, as a fraction of 10% of the shear modulus normal to grain for a C20 graded soft wood, while the rolling shear strength derives from [50].

On the basis of a shear modulus of the glue $G_g = 642 \text{ N/mm}^2$, [59] and of an alleged glue line thickness $t = 0.1 \text{ mm}$, it can be calculated from Eq. (4), the shear stiffness of the glue: $g = 924.480 \text{ N/mm}^2$. However, regarding this last value, it should be considered the uncertainty related to the thickness of the glue line; therefore, it seems reasonable to consider g in the range $10^5 \div 10^6 \text{ N/mm}^2$.

The adhesive shear strength has been taken from [61].

The limit failure loads of the CLT panel are reported in Table 4. Specifically, the theoretical critical load for both the homogeneous and hybrid specimens is shown in the first line of Table 4. Such a critical load F_{cr} is obtained from Eq. (20). The limit loads that refer to the three different failure modes of the CLT panel are reported in the second, third, and fourth rows of Table 4. They are obtained from Eqs. (37), (42), and (46), respectively. Finally, the limit compression load F_b for the CLT panel, identified with the minimum value of the previous three limit loads, is reported in the last row of Table 4.

A comparison among the experimental and the analytical limit loads, here obtained, is finally performed. The analytical limit loads of the homogeneous and hybrid configuration of the CLT panels are displayed in the first row of Table 5. The mean experimental limit loads are reported in the second row of the same table. As can be observed, the percentage differences among analytical and experimental values are quite small. Specifically, the analytical model seems to evaluate better the limit failure behavior of the homogeneous CLT panels.

The minor ability of the analytical model to describe the failure limit behavior of the hybrid CLT panels seems to be related to the statistically scattered values provided by the experimental test. From a deeper observation of the numerical data in Table 2, the limit loads of the specimens HB-1

and HB-4 are higher than the highest limit load provided from the homogeneous CLT panels, which are supposed to be of higher resistance as the inner layer holds better mechanical properties. Since such a result appeared conceptually implausible, and thus to be traced back exclusively to the material uncertainty, it was deemed of interest to consider, beside the full range of test results for hybrid panels, also a reduced range in which the most unlikely results were excluded. This fact suggests to remove the results of the specimens HB-1 and HB-4 from the calculus of the experimental mean value of the limit load. The updated experimental limit load of the hybrid CLT panels, obtained from the HB-2, HB-3, HB-5, HB-6, and HB-7 specimens, is reported in the second row of Table 6. Considering this updated value, the relative difference between the analytical and experimental values decreases and becomes of the same order of magnitude of that of the homogeneous CLT panels.

Clearly, the comparison presented before relies on the specific value of the initial imperfection calibrated on the basis of the experimental results (Fig. 14). However, for designing purposes, the practical application of the analytical model would require the adoption of a general value of the initial imperfection e_0 , consistent with the standard production's tolerance. Obviously higher imperfections would result in lower limit compression loads for the CLT panel. For example, applying a value $e_0 = 1.00 \text{ mm}$ ($\approx L/1000$) to the reference system described before, it can be calculated a limit compression load $F_b = 161 \text{ kN}$ for HO specimens and $F_b = 140 \text{ kN}$ for HB specimens, with a relative reduction, with respect to the use of $e_0 = 0.25 \text{ mm}$, respectively, of almost 13% and 11%.

5 Conclusion

In this paper, the buckling behavior of three-layered CLT panels was investigated, first by means of 14 experimental tests and then by developing an analytical formulation calibrated on the specific test setup.

The experimental campaign was conducted on two different groups of seven specimens, each one related to a specific configuration characterized by the panels cross-section's arrangement. The first configuration (homogeneous, labeled HO) presented three layers made of the same timber specie (beech), whereas, in the second one (hybrid, labeled HB), the inner layer was made of a different timber specie (Corsican pine). The experimental tests aimed to evaluate the failure limit loads of the specimens, under an increasing tip compression force. The homogeneous panels showed almost exclusively a mid-span bending failure mode while for the hybrid panels, different failure mechanisms, such as rolling shear failure, as well as delamination failure, were observed at the ends, singularly or in conjunction. Such

Table 6 Comparison between analytical and updated experimental results

	HB		
Analytical limit compression load	F_b	kN	158.5
Experimental failure load (mean) ^a	F_{cb}	kN	174.0
Relative difference	–	%	8.9

^aHB-1, HB-4 tests removed

a circumstance is likely to follow from the lower rolling shear strength of the inner layer in the hybrid panels. Nevertheless, the two groups showed quite similar average limit loads; however, the hybrid specimens presented results with a higher standard deviation with respect to those related to the homogeneous ones.

An analytical model was then developed in the attempt to describe theoretically the system object of the experimentation. The moderately high length to width ratio of the specimens, the absence of side restraints in the test setup and, above all, the intent to develop a simplified approach to the problem at hand, led straight to a beam-based theoretical formulation. This was first introduced for a panel with a generic number of layers, modeled as a stack of planar Timoshenko beams connected each other by continuous distributions of normal and tangential elastic springs representing the glue lines. The general model was then adapted to a three-layer system, similar to the panels of the experimental campaign, by means of some internal constraints, and considering a side displacement field in the form of a sine, as a result of an initial sine shape for the imperfect panel's longitudinal axis line. From such a model, a closed-form solution for the elastic problem, together with the related Eulerian critical load, was determined; this was performed by introducing two non-dimensional parameters, ψ and η which express the interaction among the wooden layers due, respectively, to the tangential stiffness of the glue and the rolling shear tangential stiffness of the inner layer. It should be noted that the abovementioned closed-form solution stems from the hypothesis on the initial imperfect axis line's sine shape, which introduces some strict similarities with the γ -process [62]. Nevertheless, the proposed model includes the influence of the elastic response of the glue lines, which represents the novelty of the presented theoretical approach with respect to others [62] which generally overlook the presence of the adhesive layers. However, although it was recognized that the influence of the glue stiffness on the critical load is negligible, it should be highlighted that the modeling of the adhesive layers, beyond allowing a richer description of the response of the three-layer CLT panel, permitted the investigation of the delamination failure mode observed during the laboratory tests. Such a delamination mode enlarges the range of possible failure modes for a CLT panel, which includes the classical bending mode and the shear mode [58].

On the basis of the achieved closed-form solution and recalling the different failure mechanisms [63–65] detected during the experimental campaign, three different failure criteria were introduced, leading to a unique theoretic compression limit load. The first one accounts for the bending–buckling failure, the second refers to the rolling shear failure mechanism of the inner layer, and finally the last takes into account the delamination phenomena.

A comparison among the experimental and the theoretic limit loads was performed after the calibration of the analytical model on the basis of some of the experimental results as well as on some parameters derived from the literature. The comparison showed that the analytical formulation describes sufficiently well the real behavior of the CLT panels, both with a homogeneous or hybrid configuration, with relative differences on the limit loads lower than 20%.

As a beam-based formulation, the proposed model, besides being adopted for a comparison with the specific test described above, seems to configure a potential preliminary design tool for stability verification, since it considers one of the most demanding configuration for a three-layer panel wall, though substantially unusual in the construction practice, with no vertical sides' restraints and hinges on both the horizontal ends. However, it should be recognized that the model is clearly unable to describe the two-dimensional buckling behavior of a panel wall in the presence of restraints along its vertical border and/or of a width to height ratio higher than unity.

Appendix

As a result of the initial imperfections, the tested specimens are subjected to a rigid roto-translation motion. By referring to Fig. 16, naming u_B , u_M , and u_T the displacements in the vicinity of the upper hinge, the lower hinge, and the mid-span, respectively, and indicating with the subscripts r and d the rigid displacement and deformation components, the rigid motion component of the transverse mid-span displacement is:

$$\begin{aligned} u_{M,r} &= \frac{u_{T,r} + u_{B,r}}{2} = \frac{(u_T + u_{T,d}) + (u_B + u_{B,d})}{2} \\ &= \frac{u_T + u_B}{2} - \frac{u_{T,d} + u_{B,d}}{2}. \end{aligned} \quad (48)$$

Assuming the mean deformation displacement near the hinges to be negligible compared to the mean total

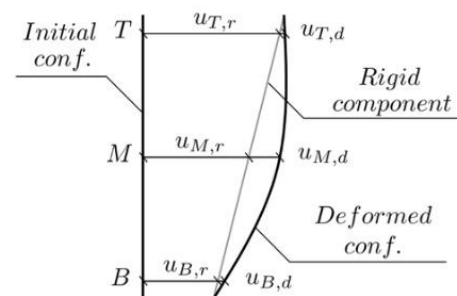


Fig. 16 Rigid displacement and deformation displacement components

displacement, the displacement component linked to the deformation of the specimen alone can be rewritten:

$$u_{M,d} = u_M - \frac{u_T + u_B}{2}. \quad (49)$$

Specifically, Fig. 16, in abscissa, shows the mid-span displacement evaluated by Eq. (48).

Funding Open access funding provided by Università degli Studi dell'Aquila within the CRUI-CARE Agreement. This study was funded by Italian Ministry of University and Research—PRIN 2015, Grant number 2015YW8JWA_002.

Declarations

Conflict of interest The authors declare no conflicts of interest.

Ethical approval All procedures performed in studies do not involve human/animal participants.

Open Access This article is licensed under a Creative Commons Attribution 4.0 International License, which permits use, sharing, adaptation, distribution and reproduction in any medium or format, as long as you give appropriate credit to the original author(s) and the source, provide a link to the Creative Commons licence, and indicate if changes were made. The images or other third party material in this article are included in the article's Creative Commons licence, unless indicated otherwise in a credit line to the material. If material is not included in the article's Creative Commons licence and your intended use is not permitted by statutory regulation or exceeds the permitted use, you will need to obtain permission directly from the copyright holder. To view a copy of this licence, visit <http://creativecommons.org/licenses/by/4.0/>.

References

- Kessel MH, Schönhoff T, Hörsting P. Zum Nachweis von druckbeanspruchten Bauteilen nach DIN 1052:2004–08, Teil 1. *Bauen mit Holz*. 2005;107(12):88–96.
- Kessel MH, Schönhoff T, Hörsting P. Zum Nachweis von druckbeanspruchten Bauteilen nach DIN 1052:2004–08, Teil 2. *Bauen mit Holz*. 2006;108(1):41–4.
- Möller G. Zur Traglastermittlung von Druckstäben im Holzbau. *Bautechnik*. 2007;84(5):329–34.
- Becker P, Rautenstrauch K. Time-dependent material behavior applied to timber columns under combined loading. Part II: creep-buckling. *Holz als Roh- und Werkstoff*. 2001;59(6):491–5.
- Hartnack R, Schober K-U, Rautenstrauch K. Computer simulations on the reliability of timber columns regarding hygrothermal effects. In: *Proceedings of CIB-W18 meeting 35: paper no. 35-2-1*, Kyoto, Japan (2002).
- Blaß HJ. Tragfähigkeit von Druckstäben aus Brettschichtholz unter Berücksichtigung streuender Einflussgrößen. Dissertation, Universität Fridericiana Karlsruhe, Karlsruhe (1987).
- Blaß HJ. Design of columns. In: *Proceedings of the 1991 international timber engineering conference*, vol. 1. London: TRADA; 1991. p. 1.75–1.81.
- Blaß HJ. Buckling length. In: *Timber engineering, STEP 1*. Almere, Netherlands: Centrum Hout; 1995.
- Tetmajer L. Die Gesetze der Knickungs- und der zusammengesetzten Druckfestigkeit der technisch wichtigsten Baustoffe. Materialprüfungs-Anstalt am Schweiz. Zurich: Polytechnikum Zurich; 1896.
- Larsen HJ, Pedersen SS. Tests with centrally loaded timber columns. In: *Proceedings of CIB-W18 meeting 4: paper no. 4-2-1*. Paris (1975).
- Buchanan AH. Strength model and design methods for bending and axial load interaction in timber members. Dissertation, University of British Columbia, Vancouver (1984).
- Buchanan AH, Johns KC, Madsen B. Column design methods for timber engineering. *Can J Civ Eng*. 1985;12(4):731–44.
- EN 1995 Eurocode 5 2003. Design of timber structures, part 1-1: general-common rules and rules for buildings. CEN/TC 250, European Committee for Standardisation, Brussels.
- Wei Y, Zhou M, Zhao K, Zhao K, Li G. Stress-strain relationship model of glulam bamboo under axial loading. *Adv Compos Lett*. 2020. <https://doi.org/10.1177/2633366X20958726>.
- Zhou X, Zeng D, Wang Z. Experimental study on mechanical properties of Larch Glulam columns under axial compression. *Appl Mech Mater*. 2016;847:38–45. <https://doi.org/10.4028/www.scientific.net/AMM.847.38>.
- Ehrhart T, Steiger R, Palma P, Gehri E, Frangi A. Glulam columns made of European beech timber: compressive strength and stiffness parallel to the grain, buckling resistance and adaptation of the effective-length method according to Eurocode 5. *Mater Struct*. 2020. <https://doi.org/10.1617/s11527-020-01524-6>.
- Guo Y, Zhou S, Cui J, Huang Z. Effect of knot on stability of glulam column under axial compressive loading. *J Civ Archit Environ Eng*. 2017;39:44–9. <https://doi.org/10.11835/j.issn.1674-4764.2017.03.006>.
- Zhang J, He M, Li Z. Compressive behavior of glulam columns with initial cracks under eccentric loads. *Inte J Adv Struct Eng*. 2018;10:1–9. <https://doi.org/10.1007/s40091-018-0181-5>.
- Theiler M, Frangi A, Steiger R. Strain-based calculation model for centrally and eccentrically loaded timber columns. *Eng Struct*. 2013;56:1103–16. <https://doi.org/10.1016/j.engstruct.2013.06.032>.
- Glos P. Zur Bestimmung des Festigkeitsverhaltens von Brettschichtholz bei Druckbeanspruchung aus Werkstoff- und Einwirkungskenngrößen, Dissertation, TU München. Munich (1978).
- Frangi A, Steiger R, Theiler M. Design of timber members subjected to axial compression or combined axial compression and bending based on 2nd order theory. In: *Conference: meeting 48 of the international network on timber engineering research INTER*, Sibenik, Croatia, vol 48; 2015.
- Brandner R, Flatscher G, Ringhofer A, Schickhofer G, Thiel A. Cross laminated timber (CLT): overview and development. *Eur J Wood Wood Products*. 2016. <https://doi.org/10.1007/s00107-015-0999-5>.
- Jeleč M, Varevac D, Rajčić V. Cross-laminated timber (CLT)—a state of the art report. *GRAĐEVINAR*. 2018;70(2):75–95. <https://doi.org/10.14256/JCE.2071.2017>.
- Van De Kuilen JWG, Ceccotti A, Xia Z, He M. Very tall wooden buildings with cross laminated timber. *Procedia Eng*. 2011;14:1621–8. <https://doi.org/10.1016/j.proeng.2011.07.204>. (ISSN 1877-7058).
- Pang S-J, Jeong GY. Effects of combinations of lamina grade and thickness, and span-to-depth ratios on bending properties of cross-laminated timber (CLT) floor. *Constr Build Mater*. 2019;222:142–51.
- Wang F, Wang X, Yang S, Jiang G, Que Z, Zhou H. Effect of different laminate thickness on mechanical properties of cross-laminated timber made from Chinese fir. *Sci Silvae Sin*. 2020;56:168–75.

27. Li Q, Wang Z, Liang Z, Li L, Gong M, Zhou J. Shear properties of hybrid CLT fabricated with lumber and OSB. *Constr Build Mater.* 2020;261: 120504.
28. Wang Z, Fu H, Gong M, Luo J, Dong W, Wang T, Chui YH. Planar shear and bending properties of hybrid CLT fabricated with lumber and LVL. *Constr Build Mater.* 2017;151:172–7.
29. Gong Y, Ye Q, Wu G, Ren H, Guan C. Effect of size on compressive strength parallel to the grain of cross-laminated timber made with domestic larch. *Chin J Wood Sci Technol.* 2020;35:42–6.
30. Gong Y, Ye Q, Wu G, Ren H, Guan C. Prediction of the compressive strength of cross-laminated timber (CLT) made by domestic *Larix Kaempferi*. *J Northwest For Univ.* 2020;35:234–7.
31. Rahman M, Ashraf M, Ghabraie K, Subhani M. Evaluating Timoshenko method for analyzing CLT under Out-of-plane loading. *Buildings.* 2020. <https://doi.org/10.3390/buildings10100184>.
32. Wei P, Wang B, Li H, Wang L, Peng Si, Zhang L. A comparative study of compression behaviors of cross-laminated timber and glued-laminated timber columns. *Constr Build Mater.* 2019;222:86–95. <https://doi.org/10.1016/j.conbuildmat.2019.06.139>.
33. Zirui H, Dongsheng H, Chui YH, Shen Y, Daneshvar H, Sheng B, Chen Z. Modeling of cross-laminated timber (CLT) panels loaded with combined out-of-plane bending and compression. *Eng Struct.* 2022. <https://doi.org/10.1016/j.engstruct.2021.113335>.
34. Ye Q, Gong Y, Ren H, Guan C, Wu G, Chen X. Analysis and calculation of stability coefficients of cross-laminated timber axial compression member. *Polymers (Basel).* 2021;13(23):4267. <https://doi.org/10.3390/polym13234267>.
35. Yang Z, Shaoyu Z, Jie Y, Liu A, Jiyang F. Thermomechanical in-plane dynamic instability of asymmetric restrained functionally graded graphene reinforced composite arches via machine learning-based models. *Compos Struct.* 2023;308:116709.
36. Yang Z, Liu A, Lai SK, Safaei B, Lv J, Yonghui H, Fu J. Thermally induced instability on asymmetric buckling analysis of pinned-fixed FG-GPLRC arches. *Eng Struct.* 2022;250: 113243.
37. Yang Z, Helong W, Yang J, Liu A, Babak S, Lv J, Fu J. Non-linear forced vibration and dynamic buckling of FG graphene-reinforced porous arches under impulsive loading. *Thin-Walled Struct.* 2022;1812022: 110059.
38. Yang Z, Liu A, Yang J, Lai SK, Lv J, Fu J. Analytical prediction for nonlinear buckling of elastically supported FG-GPLRC arches under a central point load. *Materials (Basel).* 2021;14(8):2026. <https://doi.org/10.3390/ma14082026>. (PMID: 33920651; PMCID: PMC8073894).
39. Pina JC, Flores EIS, Saavedra K. Numerical study on the elastic buckling of cross-laminated timber walls subject to compression. *Constr Build Mater.* 2019;199:82–91. <https://doi.org/10.1016/j.conbuildmat.2018.12.013>. (ISSN 0950-0618).
40. Blass HJ, Fellmoser P. Influence of rolling shear modulus on strength and stiffness of structural bonded timber elements. *CIB-W18 meet., Scotland.* (2004).
41. Sandoli A, Calderoni B. The rolling shear influence on the out-of-plane behavior of CLT panels: a comparative analysis. *Buildings.* 2020;10:42. <https://doi.org/10.3390/buildings10030042>.
42. Yusoh AS, Tahir PM, Uyup MKA, Lee SH, Husain H, Khaidzir M. Effect of wood species, clamping pressure and glue spread rate on the bonding properties of cross-laminated timber (CLT) manufactured from tropical hardwoods. *Constr Build Mater.* 2020. <https://doi.org/10.1016/j.conbuildmat.2020.121721>.
43. Azambuja RR, DeVallance D, McNeel J. Evaluation of low-grade Yellow-Poplar (*Liriodendron tulipifera*) as raw material for cross-laminated timber panel production. *For Products J.* 2022;72:1–10. <https://doi.org/10.1307/FPJ-D-21-00050>.
44. Sikora KS, McPolin DO, Harte AM. Effects of thickness of cross-laminated timber (CLT) panels made from Sitka spruce on mechanical performance in bending and shear. *Constr Build Mater.* 2016;116:141–50.
45. Adnan NA, Tahir PM, Husain H, Lee SH, Khairun Anwar Uyup M, Arip MNM, Ashaari Z. Effect of ACQ treatment on surface quality and bonding performance of four Malaysian hardwoods and cross laminated timber (CLT). *Eur J Wood Wood Products.* 2021;79:285–99.
46. Musah M, Wang X, Dickinson Y, Robert R, Rudnicki M, Xie X. Durability of the adhesive bond in cross-laminated northern hardwoods and softwoods. *Constr Build Mater.* 2021. <https://doi.org/10.1016/j.conbuildmat.2021.124267>.
47. Aicher S, Hirsch M, Christian Z. Hybrid cross-laminated timber plates with beech wood cross-layers. *Constr Build Mater.* 2016;124:1007–18. <https://doi.org/10.1016/j.conbuildmat.2016.08.051>.
48. Franke S. Mechanical properties of beech CLT. In: *WCTE 2016—World conference on timber engineering*; 2016.
49. Crovella P, Kurzinski S. Predicting the strength and serviceability performance of cross-laminated timber (CLT) panels fabricated with high-density hardwood. In: *WCTE 2020—World conference on timber engineering*; 2021.
50. Sciomenta M, Spera L, Bedon C, Rinaldi V, Nocetti M, Brunetti M, Fragiaco M, Romagnoli M. Mechanical characterization of novel homogeneous beech and hybrid Beech-Corsican Pine thin cross-laminated timber panels. *Constr Build Mater.* 2021. <https://doi.org/10.1016/j.conbuildmat.2020.121589>.
51. Romagnoli M, Fragiaco M, Brunori A, Follesa M, Scarascia Mugnozza G. Solid wood and wood based composites: the challenge of sustainability looking for a short and smart supply chain. *Lect Notes Civ Eng.* 2019;24:783–807. https://doi.org/10.1007/978-3-030-03676-8_31.
52. Concu G, De Nicolo B, Fragiaco M, Trulli N, Valdes M. Grading of maritime pine from Sardinia (Italy) for use in cross-laminated timber. *Proc Inst Civ Eng Constr Mater.* 2018;171(1):11–21. <https://doi.org/10.1680/jcoma.16.00043>.
53. Fragiaco M, Riu R, Scotti R. Can structural timber foster short procurement chains within Mediterranean Forests? A research case in Sardinia. *South-East Eur For.* 2015;6(1):107–17. <https://doi.org/10.15177/see-for.15-09>.
54. Aicher S, Christian Z, Dill-Langer G. Hardwood glulams—emerging timber products of superior mechanical properties. 2014. <https://doi.org/10.1314/2.1.5170.1120>.
55. Kovryga A, Peter S, van de Kuilen JWG. Mechanical properties and their interrelationships for medium-density European hardwoods, focusing on ash and beech. *Wood Mater Sci Eng.* 2019. <https://doi.org/10.1080/17480272.2019.1596158>.
56. Chirivi S, Ibell T, Contento A, Di Egidio A. Linear static behavior of curved beams coupled with strings representing also fiber-reinforced masonry arches. *Adv Struct Eng.* 2016;19(1):53–64.
57. Simoneschi G, Di Egidio A, de Leo AM, Contento A. On the use of reinforcing layers to improve the static behaviour of arches or shells with single curvature. *Adv Struct Eng.* 2016;19(8):1302–12.
58. Perret O, Douthe C, Lebé A, Sab K. A shear strength criterion for the buckling analysis of CLT walls. *Eng Struct.* 2020. <https://doi.org/10.1016/j.engstruct.2020.110344>.
59. Sciomenta M, Di Egidio A, Bedon C, Fragiaco M. Linear model to describe the working of a three layers CLT strip slab: experimental and numerical validation. *Adv Struct Eng.* 2021. <https://doi.org/10.1177/13694332211020403>.
60. Aicher S, Christian Z, Hirsch M. Rolling shear modulus and strength of beech wood laminations. *Holzforchung.* 2016;70(8):773–81. <https://doi.org/10.1515/hf-2015-0229>.
61. Samara Jadi Cruz de O, Ophelia B, Arrigoni M, Christian J. Plywood Experimental Investigation and Modeling Approach for Static and Dynamic Structural Applications. In: *Andreas Ö, Holm A (eds). Improved Performance of Materials : Design and*

- Experimental Approaches, vol. 72, Springer, pp.119–141, 2018, Advanced Structured Materials book series, 978-3-319-59589-4. https://doi.org/10.1007/978-3-319-59590-0_11.
62. Bogensperger T, Silly G, Schickhofer G. Comparison of methods of approximate verification procedures for cross laminated timber. Research report in Brandner R, et al., editor. Properties, testing and design of cross laminated timber. A state-of-the-art report by COST Action FP1402/WG 2. Aachen: Shaker Verlag. 2018.
63. Szalai J. Complete generalization of the Ayrton–Perry formula for beam-column buckling problems. *Eng Struct.* 2017;153:205–23. <https://doi.org/10.1016/j.engstruct.2017.10.031>.
64. Ehrhart T, Brandner R. Rolling shear: test configurations and properties of some European soft- and hardwood species. *Eng Struct.* 2018;172:554–72. <https://doi.org/10.1016/j.engstruct.2018.05.118>.
65. Clauß S, Joscak M, Niemz P. Thermal stability of glued wood joints measured by shear tests. *Eur J Wood Wood Products.* 2011;69:101–11. <https://doi.org/10.1007/s00107-010-0411-4>.

Publisher's Note Springer Nature remains neutral with regard to jurisdictional claims in published maps and institutional affiliations.

3.3. Timber in existing buildings

It is well known that wood has physical-mechanical properties such that it can be included among the most commonly used building materials: it is in fact light, with an excellent weight/strength ratio, durable if used with suitable precautions, and with sufficient fire resistance if well designed. In Italy, wood has been used since ancient times essentially for the construction of load-bearing members and structures, such as floors and roofs.

There are basically two types of wooden floors in historic buildings: floors with a main load-bearing frame of the same length as the span to be covered and floors with a main load-bearing frame whose length is shorter than the span to be covered. The first type is further subdivided into single-frame floors and compound-frame floors. The simple one-way floors, which are the most common types, are made with wooden elements of reduced and rectangular section, with a base less than the height, called joists. The spacing between the joists is variable from about 30 cm up to 50 cm, depending on the geographical area of construction of the floor and the type of floor used. The support in the wall is about 10-15 cm.





The elements are placed parallel to the smaller dimension of the room which generally does not exceed 4-5 meters. Above the joists there is the deck consisting of flat tiles or bricks, mostly found in Central Italy, or of wood planks, prevalent mainly in Northern Italy. The planks can be simply put together and equipped with joint cover to avoid the passage of dust and to hide any imperfections or provided with male-female joint. Above the deck there is a substrate, a bedding layer and finally the actual floor. The existing timber floors in historic buildings are usually bent and degraded due to fungi and insect attack, humidity, construction errors, and change of use. For these reasons, it is often necessary to stiffen floors or to substitute portions of wooden elements. Since large part of the existing masonry buildings in historical centres is subjected to superintendence of architectural heritage restrictions, some common interventions are not always applicable.

Hence the idea of using the aforementioned local wood thin CLT panels in reversible strengthening interventions for hypothetical floor with geometry included in the most common ranges, as detailed in the following work by Spera et al., 2024.

3.4. Out-of-plane strengthening of existing timber floors with Cross Laminated Timber panels made of short supply chain beech

Article

Out-of-Plane Strengthening of Existing Timber Floors with Cross Laminated Timber Panels Made of Short Supply Chain Beech

Luca Spera ¹, Martina Sciomenta ¹, Chiara Bedon ^{2,*} and Massimo Fragiaco ¹

¹ Construction-Architecture & Environmental Engineering, Department of Civil, University of L'Aquila, 67100 L'Aquila, Italy; luca.spera@graduate.univaq.it (L.S.); martina.sciomenta@univaq.it (M.S.); massimo.fragiacomo@univaq.it (M.F.)

² Department of Engineering and Architecture, University of Trieste, 34127 Trieste, Italy

* Correspondence: chiara.bedon@dia.units.it; Tel.: +39-040-558-3837

Abstract: Establishing short supply chains for timber has become important especially in Italy, which is an historically wood-importer country. Timber is an environmentally friendly construction material and a potential mean to reduce carbon footprint produced every year by the building sector. In addition to its sustainability benefits, reversible strengthening interventions can be attained for existing structures. As such, timber can be efficiently used to preserve and protect historical buildings which are, due to architectural and aesthetic values, fundamental components of the Italian cultural heritage. In this study, the use and potential of novel cross-laminated (X-Lam or CLT) timber panels made of Italian hardwood (i.e., beech) for strengthening of existing timber floors is investigated. A quantitative comparison between the mechanical performances of the proposed wood-based product and common retrofitting techniques, such as double-crossed timber planks and reinforced concrete slabs, is carried out in terms of bending stiffness (which is evaluated according to Eurocode 5), influence of weight and reversibility of intervention. It is shown that CLT panels represent a good compromise/alternative for the realisation of reversible and sustainable reinforcing interventions, with rather well promising performances.

Keywords: wooden floors; composite sections; strengthening interventions; out-of-plane stiffness; Cross Laminated Timber (CLT); beech (*Fagus sylvatica* L.)



Citation: Spera, L.; Sciomenta, M.; Bedon, C.; Fragiaco, M. Out-of-Plane Strengthening of Existing Timber Floors with Cross Laminated Timber Panels Made of Short Supply Chain Beech. *Buildings* **2024**, *14*, 749. <https://doi.org/10.3390/buildings14030749>

Academic Editors: João Gomes Ferreira and Ana Isabel Marques

Received: 11 February 2024

Revised: 5 March 2024

Accepted: 8 March 2024

Published: 11 March 2024



Copyright: © 2024 by the authors. Licensee MDPI, Basel, Switzerland. This article is an open access article distributed under the terms and conditions of the Creative Commons Attribution (CC BY) license (<https://creativecommons.org/licenses/by/4.0/>).

1. Introduction

In the Mediterranean countries, a considerable part of the ancient building stock is composed of masonry buildings with timber floor and roof systems. Being the floors susceptible both to in-plane and out-of-plane loads, it is crucial to define their behaviour under the combination of these actions as they play a key role in the definition of the building vulnerability and seismic response.

Floors in-plane stiffness both with the effectiveness of the connections with the shear-walls, ensure a lateral loads redistribution and an efficient holding of the load bearing walls, improving the seismic performance of the whole building (box-behaviour) [1]. Whereas, a high out-of-plane stiffness assures the compliance of deflections limits under the action of vertical loads, which mostly burden the structure for its entire life. Unfortunately, most of the traditional timber floors have low out-of-plane and/or in-plane stiffness; this condition both with the lack of connections to the main masonry walls which led to the vulnerability to seismic action of the ancient masonry buildings and represent a significant limitation [2]. In some cases, the existing floors could require additional strengthening and stiffening in the out-of-plane direction as they were designed to bear moderate loads and, in most cases, they suffer from excessive deflections with respect to current requirements. Permanent deflection due to creep can also reach critical values [3].

To face this latter condition several strengthening techniques have been developed to increase both the bending stiffness and load-bearing capacity of existing timber floors. One of the most widespread approaches consists in increasing the inertia of the floor joists by adding a reinforcement on its upper side; the results is a T-composite beam section having as web the original timber and as flange the new element, connected to the existing beam by the mechanical connections [4]. The aforementioned fasteners ensure the composite behaviour; while, their type and features are the main factors that govern the efficiency of the intervention. The solution of adding a top reinforced concrete slab of 40–50 mm height is one of the most widespread used for new floors and refurbishing and enhancing the performance of existing timber floors since it was developed in the 70 s.

Different mechanical connection systems have been applied in practice [5], such as for example dowel type fasteners, notches [6], studs [7], glued in rods [8], plates [9] or even the combination of various fastening systems [10]. Despite the observed advantages of hybrid timber-to-concrete (TTC) systems, like for example their increased load-bearing capacity, but also airborne sound transmission, structural fire rating, seismic performance and thermal mass, TCC solutions have also some significant drawbacks. Among others, there are differential deformations (namely those owing to shrinkage of concrete and moisture variation on timber [11], the lack of clear guidelines for their design (long term behaviour still remains a complex issue at the moment) and especially the significant increase in permanent loads, invasiveness, and low reversibility of intervention, which makes them unsuitable for use on valuable historic buildings [4].

To overcome all these disadvantages, the use of timber elements, instead of concrete slabs, has been proposed as an alternative, mechanical efficient option to strengthen existing timber floors [12]. Timber-to-timber (TTT) composite sections have undeniable advantages, compared to the aforementioned TTC sections. More precisely, these can be listed as the use of traditional materials and the 'dry' assembly methods, which promote the compatibility between materials as well the intervention reversibility and/or recoverability. Another relevant benefit concerns the characteristics of timber in terms of natural carbon sink and renewable material [13], which make this type of reinforcement technique rather efficient from an energetic/environmental viewpoint.

One of most awkward and discussed issues concerns the historical value preservation of building heritage, which has been often affected by invasive retrofit interventions aimed at reducing the carbon dioxide emissions or the seismic risk [14–16]. In particular, in the last decades, the indiscriminate demolition and replacement of timber floors and roofs with reinforced concrete (RC) slabs and steel beams appeared as really common strategy. It is thus clear that this practice has relevant negative consequences in terms of (i) increased seismic forces, given their inertial characteristics, (ii) low deformations and, consequently, low energy dissipation of RC member compared to timber elements [13], and (iii) additional weight on the existing wall/foundation system, which could not be able to provide sufficient low-bearing capacities [17]. The most widespread solutions adopted to realize TTT sections involve the use of different types of connectors [3,18–20] to join new timber planks or CLT panels to the existing floors. Both the TTC and TTT strengthening techniques are realized by minimizing the thickness of the reinforced floors, in order to preserve the existing floor level and internal room height. Nevertheless, despite the numerous advantages, the elastic moduli of timber products are relatively low compared to concrete and/or steel, hence TTT floors are characterized by very low bending stiffness, which makes them prone to excessive short- and long-term deflections, as well as sensitivity to human-induced vibrations [21,22]. Increasing the thickness of flat timber slabs is the easiest way to satisfy the deflection and vibration control requirements for long-span floors, but the application of excessively thick solid timber floors is not economically justifiable and minimally structurally efficient [22].

In this framework, the importance of CLT panels has become so relevant that several studies [23–27], have concerned panels made with different wood species compared to fir and spruce, which are currently the most used species for CLT industrial productions.

An interesting research case was carried out in Italy, where Sardinian maritime pine was employed to produce CLT panels. Preliminary tests carried out to evaluate the physical and mechanical properties, and thus to demonstrate the suitability of this locally grown species to produce CLT panels, can be found in [28]. To note that CLT panels made of some native hardwood species, such as beech, yellow-poplar and tropical hardwood (i.e., rubberwood, batai, etc.), were found as very performing. These literature evidences are particularly relevant, considering the impact that hardwood and new bonding techniques [29] could have on the production of CLT panels. In particular, it was highlighted in [26] the excellent out-of-plane and shear mechanical performance of the examined homogeneous beech or hybrid Corsican pine-beech CLT specimens. By comparing (via numerical simulations) the mechanical response of hardwood panels with those made of traditional C24 spruce, they proved to experience lower deflections and to be less deformable in both bending and shear loading conditions.

Therefore, in the context of retrofitting interventions of existing timber floors, the application of novel homogeneous Italian beech CLT panels, which were experimentally investigated by Sciomenta et al. [26], as reinforcing element, is further considered and addressed in present study. For quantitative comparative purposes, moreover, the predicted mechanical performances are assessed towards some common strengthening techniques of typical use for wooden floors.

2. Reinforcing Interventions

Since wood is light and workable, through centuries it has been largely used for the realization of floors for ordinary buildings, and even in those with monumental importance. In the framework of typical timber floors, two main parts (frame and slab) can be variably designed, as a function and class of use of the primary structure.

In Italy, the frame is generally made of one or two orders of beams. In the second case, the primary order is composed of beams, while the secondary order consists of joists. The function of the frame is to bear structural permanent, non-structural permanent, and accidental loads, acting at the floor intrados and extrados. The slab usually presents a different structure which locally varies with the Italian region: in some cases, it is constituted by one or more layers of timber planks, while in other cases it consists of tiles. The primary roles of slab are to distribute the different design loads among the frame components and to increase the lateral stiffness of the frame, thus contributing to the distribution of the horizontal actions towards the main structural vertical elements. In this paper, a one-way system for timber floors (made of sawn wood joists and planks) is taken into account.

Three different strengthening techniques are considered to improve the bending stiffness for a case-study, existing timber floor consisting of sawn timber joists (with cross section of 160 mm by 200 mm, and spacing of 350 mm), and an upper layer of boards (30 mm in thickness).

All the interventions include the use of a reinforcement above the existing floor, see Figure 1, which is connected by means of screws.

The difference lies in the nature of strengthening element, which is respectively:

- a double-crossed timber planking, made of hardwood, with a mean modulus of elasticity parallel to the grain $E_{mean,II} = 14,237$ MPa and a mean density $\rho_{mean} = 756$ kg/m³;
- a CLT panel made of hardwood, with $E_{mean,II} = 14,237$ MPa and $\rho_{mean} = 756$ kg/m³ [26];
- a RC slab with secant modulus of elasticity $E_c = 31,447$ MPa and $\rho_{mean} = 2500$ kg/m³.

To note that the first technique is fully reversible and commonly used in all practical situations, where a minimally invasive intervention—but mechanical efficiency—is required.

In contrast, the third system is clearly not reversible and can be used, where high floor stiffening is necessary, only in those buildings which are not protected by the Fine Art Monument. The second solution is halfway between (i) and (iii), as it constitutes a reversible intervention and anyway allows a quite significant floor strengthening.

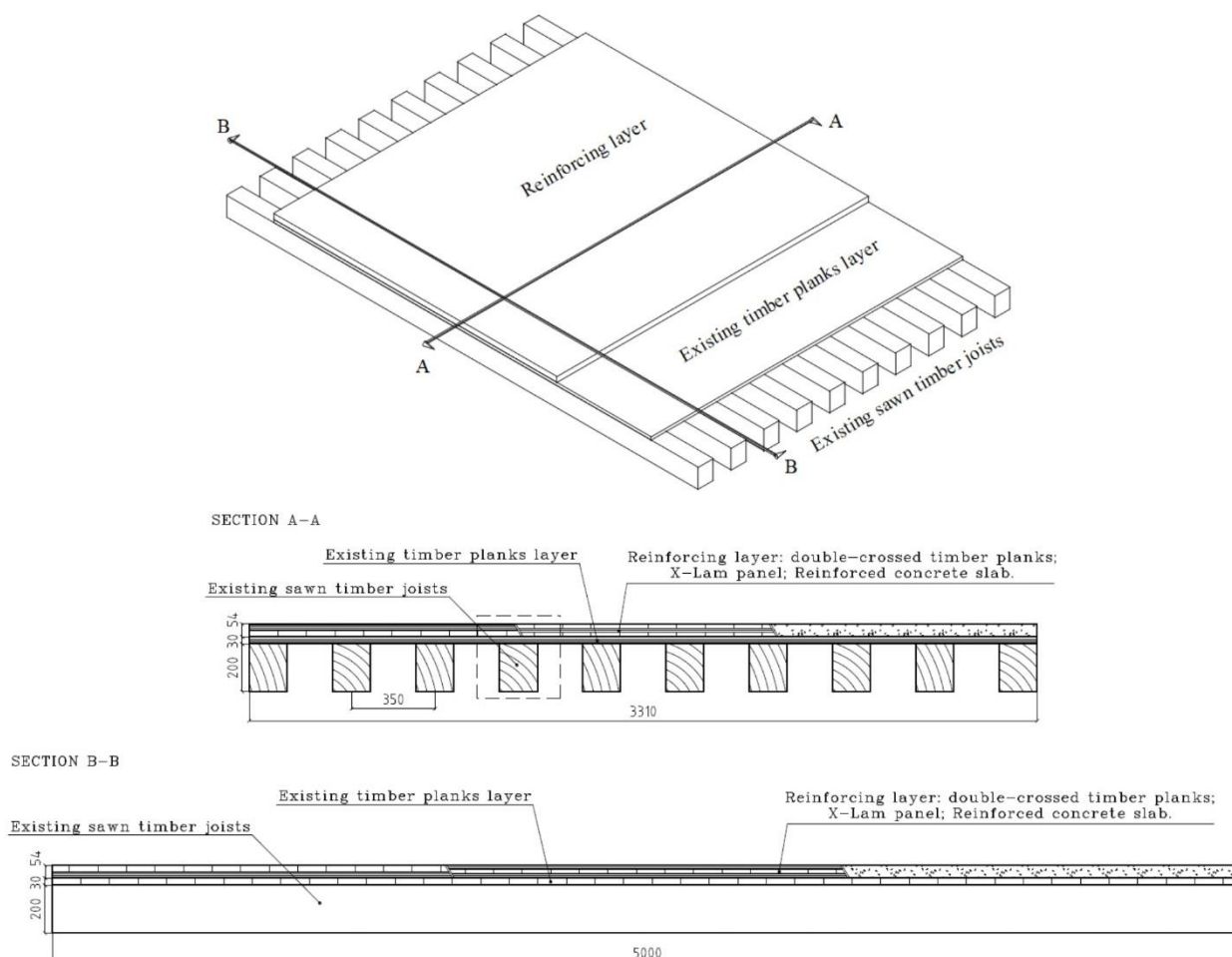


Figure 1. Three-dimensional view and cross-section details of the case-study floor object of intervention (dimensions in mm).

With the aim to mechanically compare the effect of three different reinforcing systems with the same dimensions, the thickness of herein proposed novel CLT panels, equal to 54 mm, is taken into account for the above options (i), (ii) and (iii). The connection between the existing timber floor and the reinforcement is assumed flexible, as it is realized by means of screws with variable diameter and spacing as described in the following paragraphs.

3. Comparison of Selected Intervention Techniques

3.1. Calculation Approach

The selected intervention techniques were applied to the case-study floor system schematized in Figure 1. Considering a single joist for the 5 m span floor, see Figure 2, the bending stiffness was first evaluated according to the mechanically jointed beams theory, as specified by Annex B of Eurocode 5 [30].

Such a linear elastic theory assumes (i) a simply supported boundary condition for the beam, (ii) a connection by mechanical fasteners with slip modulus K , between the individual parts of the composite section, (iii) a constant or uniformly varying spacing of fasteners, and (iv) a sinusoidal or parabolic distribution of bending moment.

In addition, the percentage weight increment was also calculated to underline the influence of reinforcing system on the permanent load acting on the floor, and thus to use it as a further influencing parameter for mechanical performance assessment.

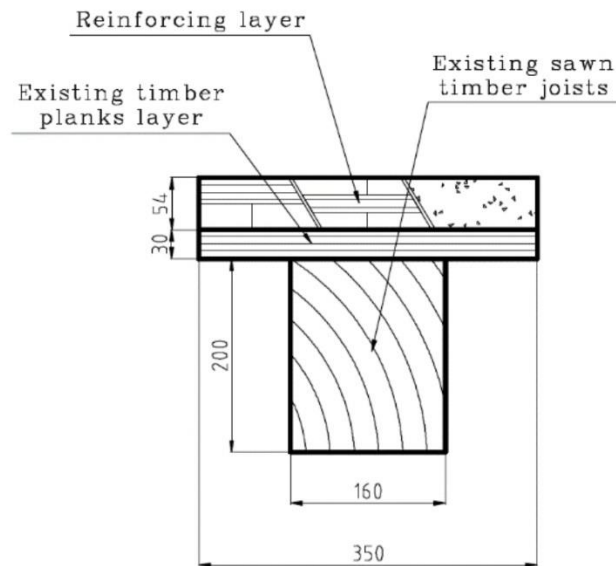


Figure 2. Cross-section of the examined composite system (dimensions in mm).

3.2. Slip Moduli and Performance

Considering the flexible connection between the existing timber floor and the reinforcing system, the slip modulus (both for ULS and SLS) increases progressively, going from the double-crossed planking to the RC slab.

For timber-to-timber connections, in particular, the mean density (ρ_{mean}) is calculated considering the mean densities of the two jointed timber members ($\rho_{m,1}$ and $\rho_{m,2}$), as in Equation (1):

$$\rho_{mean} = \sqrt{\rho_{m,1} \cdot \rho_{m,2}} \quad (1)$$

For concrete-to-timber connections, the mean density is based on the mean value of the timber element, and K_{ser} should be multiplied by 2. Assuming a mean density of the existing timber elements of 500 kg/m^3 , the resulting mean densities are 615 kg/m^3 in the cases of D40 strength class timber planks and novel beech CLT panel, and 1000 kg/m^3 in the case of the RC slab.

For screw diameters (d) equal to 8, 10, and 12 mm, the corresponding slip moduli K_{ser} (for SLS) and K_u (for ULS) were thus evaluated according to Eurocode 5 [11], see Equations (2) and (3):

$$K_{ser} = \rho_{mean}^{1.5} \frac{d}{23} \quad (2)$$

$$K_u = \frac{2}{3} K_{ser} \quad (3)$$

In doing so, a reduction coefficient for K_{ser} (equal to 0.7) was also taken into account, in order to include a stiffness reduction due to the presence of existing planking [31–33]. As shown in Table 1, the so calculated slip moduli change depending both on the density of reinforcement and on the screw diameter.

Table 1. Calculated slip moduli for different reinforcements.

Reinforcing System	$d = 8 \text{ mm}$		$d = 10 \text{ mm}$		$d = 12 \text{ mm}$	
	K_{ser} [N/mm]	K_u [N/mm]	K_{ser} [N/mm]	K_u [N/mm]	K_{ser} [N/mm]	K_u [N/mm]
(i) Timber / (ii) CLT	3712	2475	4640	3093	5568	3712
(iii) RC	5444	3630	6805	4537	8167	5444

Assuming the RC slab as reinforcing system, it can be seen that the K_{ser} slip modulus, and consequently the K_u slip modulus, increases of about 47%, compared to timber planks or CLT panels. A further comparison between the aforementioned formulation and the new one which has been recently developed in the draft of Eurocode 5, Annex K [34] was thus carried out. In particular, Equation (4) was used to evaluate the mean slip modulus per fastener in case of timber-to-timber connections:

$$K_{SLS} = 0.12 \left(\rho_{mean,1} t_{h,1}^{0,1} + \rho_{mean,i}^{1,1} + \rho_{mean,2} t_{h,2}^{0,1} \right) d^{1,1} \quad (4)$$

where:

- $\rho_{mean,1}$ and $\rho_{mean,2}$ is the mean density of member 1 or 2;
- $\rho_{mean,i}$ is mean density of the interlayer;
- $t_{h,1}$ and $t_{h,2}$ is the thickness of member 1 or 2;
- d is the fastener diameter.

The so calculated values were greater than those in Table 1 of about 10–12%, affecting the bending stiffness of the composite section with a minimal overestimation of about 1–2%. For this reason, the slip moduli in Table 1 were adopted in the following, as they are plausible by comparison with the values determined experimentally in the literature, as for example in the case of hardwood-softwood connection with interlayer [19].

3.3. Bending Stiffness

For the composite section in Figure 2, composed of a single joist with 160 mm by 200 mm cross-section, an upper layer of timber planks, and a strengthening system, comparative bending calculations were carried out in accordance with Equations (5) and (6):

$$(EI)_{eff} = \sum_{i=1}^2 (E_i I_i + \gamma_i E_i A_i a_i^2) \quad (5)$$

$$\gamma_i = \left[1 + \frac{\pi^2 E_i A_i s_i}{(K_i l^2)} \right]^{-1} \quad (6)$$

with:

- $(EI)_{eff}$ = effective bending stiffness of the composite section;
- E_i = modulus of elasticity of the i -th element;
- I_i = second moment of area of the i -th element;
- γ_i = gamma coefficient of the i -th element;
- A_i = cross-sectional area of the i -th element;
- a_i = distance between the geometric centre of the i -th element and the centre of the composite section;
- s_i = spacing of fasteners;
- $K_i = K_{ser}$ for the serviceability limit state and K_u for the ultimate limit state calculations;
- l = span of joist.

Since the joist as in Figure 1 are considered simply supported, the connection system is made of 8, 10, or 12 mm diameter screws with variable spacing, which is set equal to a minimum value (s_{min}) near the end-restraints and to a maximum value (s_{max}) at mid-span. The limit cases of absence of connection ($K = 0$) or fully rigid connection ($K = \infty$) are also presented in Table 2, in terms of limit bending stiffness capacities for the examined composite section.

Three cases of flexible connections (K_1 , K_2 , and K_3) with different values of s_{max} and s_{min} are analysed. K_1 , K_2 , and K_3 present a maximum spacing of 200 mm, 150 mm, and 100 mm, and a minimum spacing of 150 mm, 100 mm, and 50 mm, respectively.

As a major result, the calculated slip moduli affect the corresponding γ_1 coefficients according to Equation (6). In particular, the coefficient decreases with the increase of the slip modulus, as shown in Table 3 for the intermediate flexible case (K_2). The γ_1 values in the case of RC slab are indeed similar to those determined in earlier studies [11].

Table 2. Limit cases of calculated bending stiffness: $(EI)_0$ for $K = 0$ and $(EI)_\infty$ for $K = \infty$.

Reinforcing System	$(EI)_0$ [Nmm ²]	$(EI)_\infty$ [Nmm ²]
None	8.54×10^{11}	8.95×10^{11}
(i) Timber plank	8.62×10^{11}	2.60×10^{12}
(ii) CLT panel	9.19×10^{11}	3.03×10^{12}
(iii) RC slab	9.98×10^{11}	3.88×10^{12}

Table 3. Coefficients for different reinforcements (K_2).

Reinforcing System	$d = 8 \text{ mm}$		$d = 10 \text{ mm}$		$d = 12 \text{ mm}$	
	γ_1 (SLS) [-]	γ_1 (ULS) [-]	γ_1 (SLS) [-]	γ_1 (ULS) [-]	γ_1 (SLS) [-]	γ_1 (ULS) [-]
(i) Timber	0.38	0.29	0.44	0.34	0.48	0.38
(ii) CLT	0.24	0.17	0.28	0.21	0.32	0.24
(iii) RC	0.17	0.12	0.20	0.15	0.24	0.17

Therefore, K_3 is the stiffer option, and all the three flexible cases are included between the limit cases, leading to bending stiffnesses greater than the case without connection and lower than the case of rigid connection. Both the ultimate limit state (ULS) and the serviceability limit state (SLS) are considered, see Tables 4 and 5, using the slip moduli K_{sl} and K_{ser} , respectively, in the evaluation of the coefficients γ_i .

Table 4. Flexible connections (ULS): calculated $(EI)_{eff}$ for K_1 , K_2 , and K_3 .

Reinforcing System	$(EI)_{eff}$ [Nmm ²]								
	K_1			K_2			K_3		
	$d = 8 \text{ mm}$	$d = 10 \text{ mm}$	$d = 12 \text{ mm}$	$d = 8 \text{ mm}$	$d = 10 \text{ mm}$	$d = 12 \text{ mm}$	$d = 8 \text{ mm}$	$d = 10 \text{ mm}$	$d = 12 \text{ mm}$
None		8.93×10^{11}			8.93×10^{11}			8.94×10^{11}	
(i) Timber	1.42×10^{12}	1.45×10^{12}	1.48×10^{12}	1.47×10^{12}	1.51×10^{12}	1.54×10^{12}	1.57×10^{12}	1.61×10^{12}	1.65×10^{12}
(ii) CLT	2.13×10^{12}	2.16×10^{12}	2.19×10^{12}	2.18×10^{12}	2.22×10^{12}	2.25×10^{12}	2.28×10^{12}	2.33×10^{12}	2.37×10^{12}
(iii) RC	3.09×10^{12}	3.11×10^{12}	3.12×10^{12}	3.12×10^{12}	3.14×10^{12}	3.16×10^{12}	3.19×10^{12}	3.22×10^{12}	3.25×10^{12}

Table 5. Flexible connections (SLS): calculated $(EI)_{eff}$ for K_1 , K_2 , and K_3 .

Reinforcing System	$(EI)_{eff}$ [Nmm ²]								
	K_1			K_2			K_3		
	$d = 8 \text{ mm}$	$d = 10 \text{ mm}$	$d = 12 \text{ mm}$	$d = 8 \text{ mm}$	$d = 10 \text{ mm}$	$d = 12 \text{ mm}$	$d = 8 \text{ mm}$	$d = 10 \text{ mm}$	$d = 12 \text{ mm}$
None		8.93×10^{11}			8.93×10^{11}			8.94×10^{11}	
(i) Timber	1.48×10^{12}	1.51×10^{12}	1.54×10^{12}	1.54×10^{12}	1.58×10^{12}	1.61×10^{12}	1.65×10^{12}	1.69×10^{12}	1.72×10^{12}
(ii) CLT	2.19×10^{12}	2.22×10^{12}	2.25×10^{12}	2.25×10^{12}	2.29×10^{12}	2.33×10^{12}	2.37×10^{12}	2.43×10^{12}	2.47×10^{12}
(iii) RC	3.12×10^{12}	3.15×10^{12}	3.17×10^{12}	3.16×10^{12}	3.19×10^{12}	3.22×10^{12}	3.25×10^{12}	3.29×10^{12}	3.33×10^{12}

As shown in Table 4 and Figure 3a, the ULS bending stiffness of the composite section with 8 mm screws increases from 59% (K_1) to 76% (K_3) with the double-crossed timber planks system, from 139% (K_1) to 155% (K_3) with the homogeneous beech CLT panel, and from 246% (K_1) to 257% (K_3) with the RC slab.

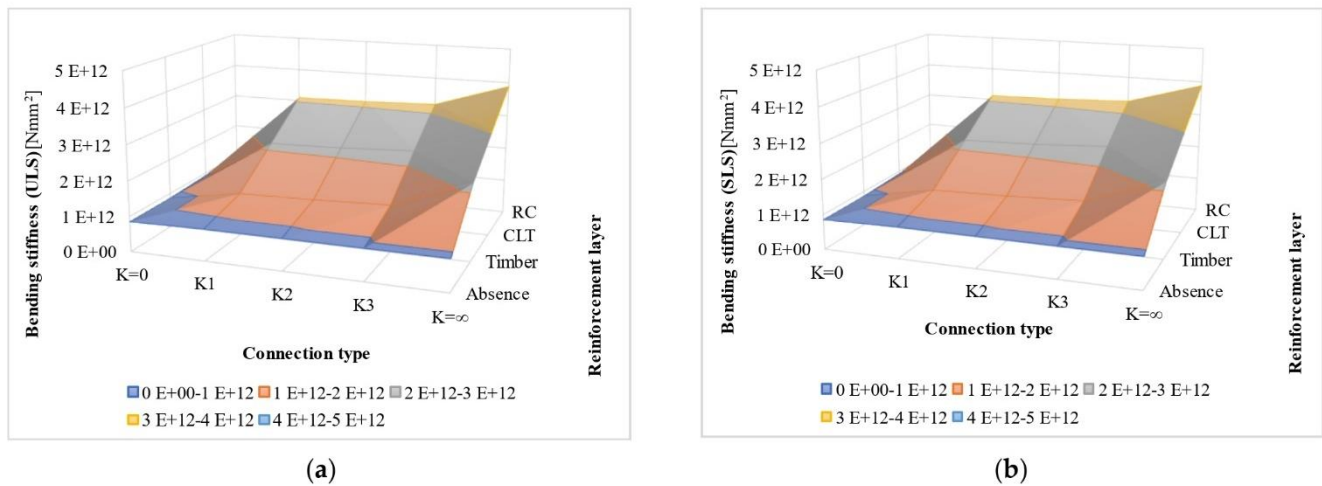


Figure 3. Example of bending stiffness variation (8 mm diameter screws): ULS (a); SLS (b).

The SLS bending stiffness, see Table 5 and Figure 3b, shows a greater increment, with a range from 66% (K_1) to 85% (K_3) in the case of crossed timber planking, from 145% (K_1) to 165% (K_3) in the case of X-Lam panel, and from 250% (K_1) to 264% (K_3) in case of RC slab.

The ULS bending stiffness for the composite section with 10 mm diameter screws, see Figure 4a, increases from 63% (K_1) to 81% (K_3) with the double-crossed timber planks system, from 142% (K_1) to 161% (K_3) with the homogeneous beech CLT panel, and from 248% (K_1) to 260% (K_3) with the RC slab.

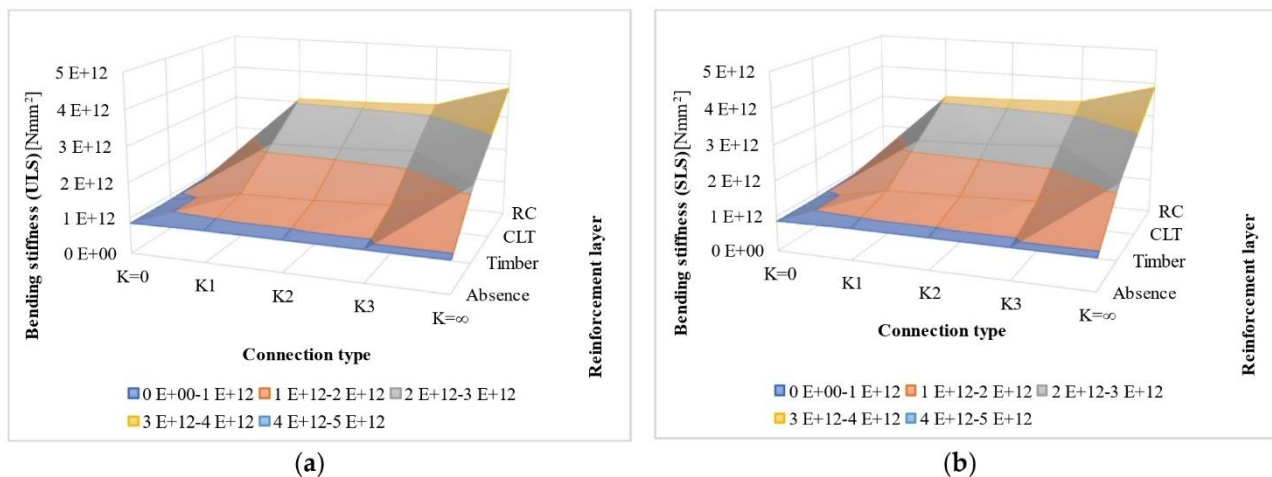


Figure 4. D graphs of bending stiffness variation (10 mm diameter screws): ULS (a); SLS (b).

The SLS bending stiffness in Figure 4b shows a greater increment, with a range from 69% (K_1) to 90% (K_3) in case of crossed timber planking, from 149% (K_1) to 172% (K_3) in case of CLT panel, and from 252% (K_1) to 268% (K_3) for of RC slab.

The ULS bending stiffness in Figure 5a for the composite section with 12 mm diameter screws increases from 66% (K_1) to 85% (K_3) with the double-crossed timber planks system, from 145% (K_1) to 165% (K_3) with the homogeneous beech CLT panel, and from 250% (K_1) to 264% (K_3) with the RC slab.

The SLS bending stiffness in Figure 5b shows a greater increment, with a range from 73% (K_1) to 92% (K_3) in the case of crossed timber planking, from 153% (K_1) to 177% (K_3) in case of CLT panel, and from 255% (K_1) to 272% (K_3) for the RC slab.

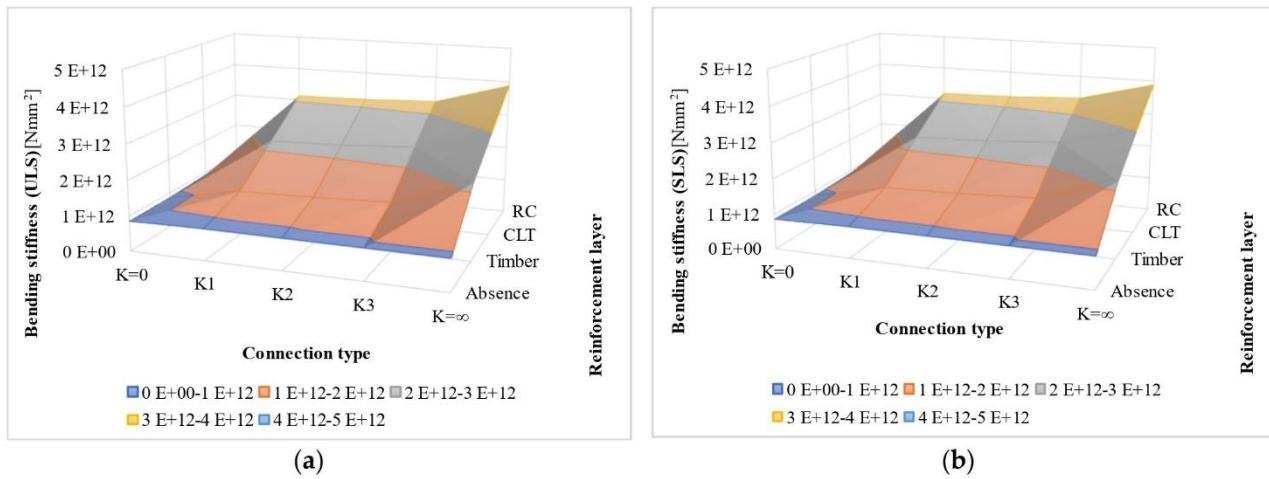


Figure 5. D graphs of bending stiffness variation (12 mm diameter screws): ULS (a); SLS (b).

With respect to the limit cases with $K = 0$ and $K = \infty$, it is also worth to note that the flexible cases K_1 , K_2 and K_3 present bending stiffness values which are necessarily comprised between the above limits, but are rather similar to each other for the same reinforcing system. The typical bending stiffness variation and sensitivity is shown in Figure 6.

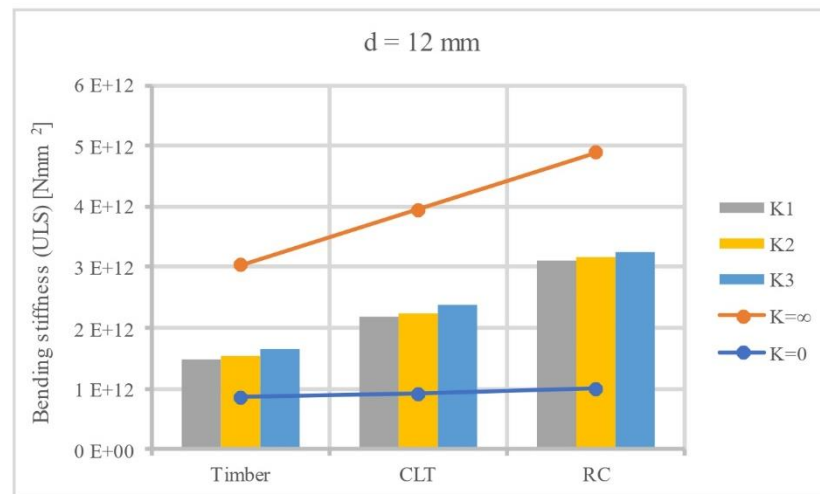


Figure 6. Comparison between limit cases and flexible cases, in terms of ULS bending stiffness for 12 mm diameter screws.

Analysing the results in terms of slip moduli, the values assessed according to EC5 underestimates the experimental values expected from tests in similar timber-to-timber joints [19]. Consequently, even the bending stiffness is underestimated, due to the approximations of the method by [30] and on the presence of the interlayer [31,33], in agreement with other studies [35]. The three flexible cases K_1 , K_2 , K_3 , which represent three possible and realistic choices of screws spacing, were considered to evaluate their influence on the effective bending stiffness. The estimated values in the case of CLT panel as reinforcement, in particular, are greater than those in the case of double-crossed timber planking, although the thickness and density of the material are the same, because of the presence of two layers with the grain direction parallel to the span direction. Considering the RC slab, the Eurocode 5 provides approximated formulas to determine the mean density to be used to evaluate the slip moduli and the consequent bending stiffness. This kind of retrofit technique, although has better mechanical performances, is however not always applicable in historic buildings, where indeed reversible interventions are preferable [3,4,12,13].

A parameter regarding the performance of the flexible connections, indicated as η , can be further analysed, with respect to the two limit cases $K=0$ and $K=\infty$, by calculating it according to Equation (7):

$$\eta = \frac{(EI)_{eff} - (EI)_0}{(EI)_{\infty} - (EI)_0} \quad (7)$$

The so obtained η values, calculated for the K_2 case, are presented in Table 6 and Figure 7.

Table 6. Values for different reinforcement (K_2).

Reinforcing System	$d = 8 \text{ mm}$		$d = 10 \text{ mm}$		$d = 12 \text{ mm}$	
	η (SLS) [-]	η (ULS) [-]	η (SLS) [-]	η (ULS) [-]	η (SLS) [-]	η (ULS) [-]
(i) Timber	0.39	0.35	0.41	0.37	0.43	0.39
(ii) CLT	0.63	0.60	0.65	0.61	0.67	0.63
(iii) RC	0.75	0.74	0.76	0.74	0.77	0.75

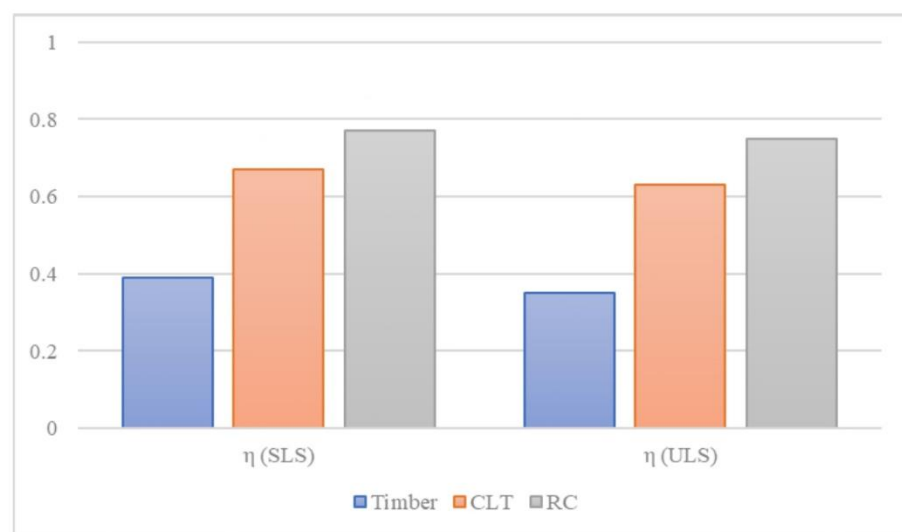


Figure 7. Typical trend of η parameter for 12 mm diameter screws K_2 case.

The η parameter, which usually does not exceed the unit, increases with increasing density of the reinforcing system and with decreasing screws spacing and, consequently, with increasing of the slip modulus.

Therefore, assuming constant effective screws spacing (K_2 case), it increases both going from the timber planks reinforcement to the RC slab and going from ULS to SLS.

3.4. Weight

The considered reinforcing material densities were set in 756 kg/m^3 for double-crossed timber planking and novel beech CLT panel and 2500 kg/m^3 for RC slab.

Regarding the composite system, the additional reinforcing element constitutes about the 40% of the structural permanent loads in the two timber-based solutions, and about the 69% in the case of the RC slab, see Figure 8.

Considering the flexible cases with 12 mm diameter screws, both the weight and bending stiffness increases are noteworthy to be highlighted, so as to identify a suitable compromise between the most efficient mechanical strengthening technique for the existing floor and the corresponding increase of permanent loads.

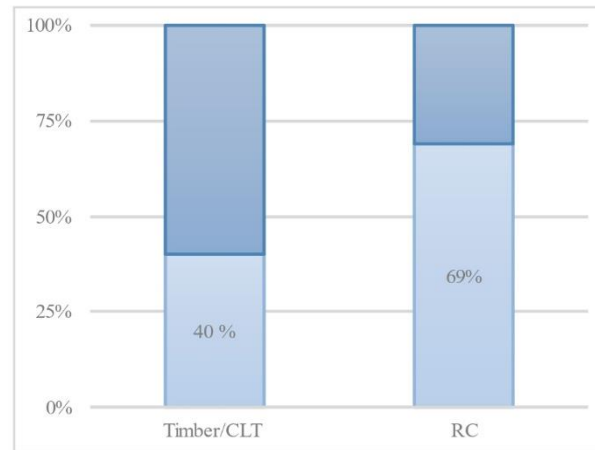


Figure 8. Percentage weight variation of reinforcement, compared to the total permanent weight of timber floor with reinforcing intervention.

In the K_1 case, the ULS bending stiffness increases of 66%, 145% and 250% for double-crossed timber planks, novel CLT panel, and RC slab, respectively. In the K_2 case, the ULS bending stiffness increases of 73%, 152% and 254% for double-crossed timber planks, novel CLT panel, and RC slab, respectively. In the K_3 case, the ULS bending stiffness increases of 85%, 165% and 264% for double-crossed timber planks, novel CLT panel, and RC slab, respectively.

To sum up, see Figure 9, the use of timber planks as reinforcing element determines a ULS bending stiffness equal to $(EI)_{eff} = 1.65 \times 10^{12} \text{ Nmm}^2$ in the stiffer case (K_3), which is about 33% lower than the CLT panel with K_1 value ($(EI)_{eff} = 2.19 \times 10^{12} \text{ Nmm}^2$).

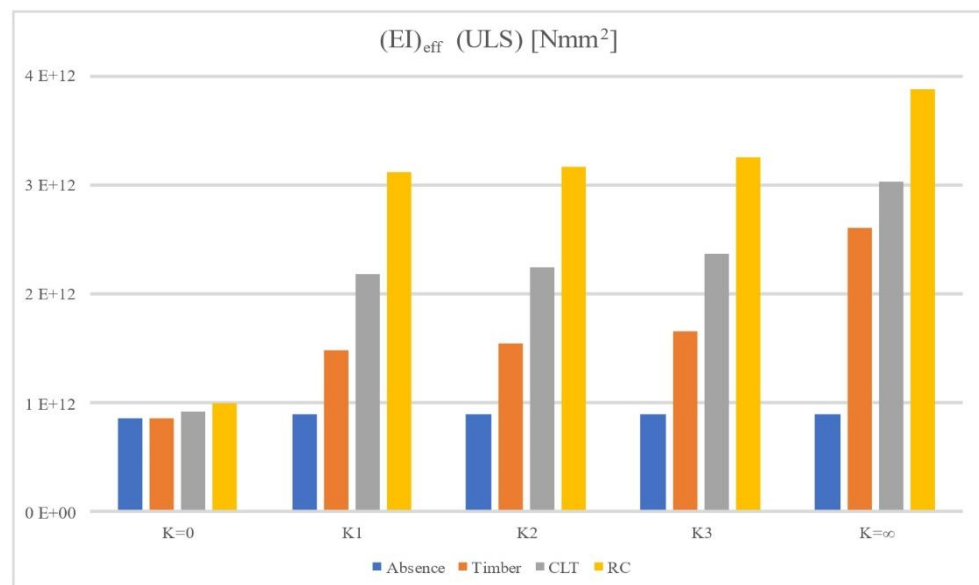


Figure 9. Quantitative comparison of selected reinforcement techniques in terms of $(EI)_{eff}$ at ULS.

On the other hand, the CLT panel in stiffer case (K_3) leads to a ULS value of $(EI)_{eff} = 2.37 \times 10^{12} \text{ Nmm}^2$, which is lower down to about 32% than the RC slab in K_1 case, with $(EI)_{eff} = 3.12 \times 10^{12} \text{ Nmm}^2$.

Similarly, the SLS bending stiffness of the CLT panel in K_1 case is larger of about 31% than timber planks with K_3 value, and the stiffer CLT panel case (K_3) value is lower of about 28% than the RC slab in K_1 case.

Considering the stiffer case K_3 with 12 mm diameter screws, the ULS bending stiffness is $(EI)_{eff} = 2.37 \times 10^{12} \text{ Nmm}^2$ for CLT panel as reinforcement, against $(EI)_{eff} = 1.65 \times 10^{12} \text{ Nmm}^2$ for timber planks and $(EI)_{eff} = 3.25 \times 10^{12} \text{ Nmm}^2$ for RC slab.

In this regard, from the comparison in terms of bending stiffness and weight percentage increase, shown in Figure 10, it is clear that the CLT panel allows to obtain a significant increase of ULS bending stiffness, and also efficiently limit the increase of structural permanent loads on single joists, at around 40%.

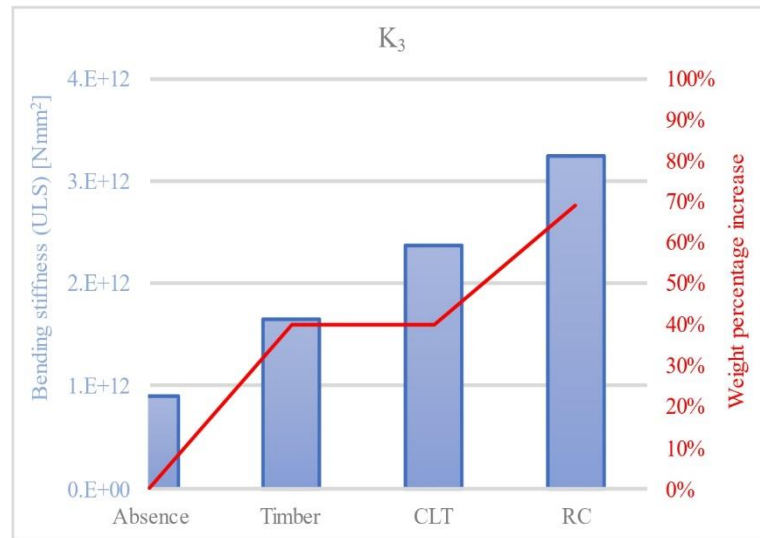


Figure 10. ULS bending stiffness-to-weight increase for K_3 case.

4. Bending Moment and Normal Stresses

Considering the K_2 flexible case with 12 mm diameter screws, it can be important to show how the chosen reinforcing system affects the moment distribution between the joist and the reinforcement itself along the span of the single joist. Alongside the structural permanent loads due to the joists, the existing floor and the reinforcing system, non-structural permanent loads and accidental loads are considered. The design distributed load per single joist considered is equal to 1.90 kN/m, and, for a span of 5 m, it produces a reaction at the supports equal to 4.75 kN for a simply supported beam. Analysing the bending moment distribution $M_n(x)$ along the 5 m span, it can be divided between the elements (reinforcement and joist) of the composite section. Using subscript $n = 1$ for the reinforcing element and subscript $n = 2$ for the joist, moments and axial forces can be determined according to the following Equations (8)–(11):

$$M_1(x) = \frac{E_1 I_1}{(EI)_{eff}} M(x) \quad (8)$$

$$M_2(x) = \frac{E_2 I_2}{(EI)_{eff}} M(x) \quad (9)$$

$$N_1(x) = \frac{\gamma_1 E_1 A_1 a_1}{(EI)_{eff}} M(x) \quad (10)$$

$$N_2(x) = \frac{\gamma_2 E_2 A_2 a_2}{(EI)_{eff}} M(x) \quad (11)$$

In order to respect the condition expressed by Equation (12):

$$M(x) = M_1(x) + M_2(x) + N_1(x) \cdot a_1 + N_2(x) \cdot a_2 \quad (12)$$

Considering the bending moment distributions (Figure 11 left graphs), M_1 for the $K = 0$, K_2 , and $K = \infty$ cases increases when the reinforcement stiffness increases, and M_2 decreases progressively. Consequently, normal stresses can be evaluated according to Annex B of Eurocode 5 [11], Equations (13) and (14):

$$\sigma_i = \frac{\gamma_i E_i a_i M}{(EI)_{eff}} \quad (13)$$

$$\sigma_{m,i} = \frac{0.5 E_i h_i M}{(EI)_{eff}} \quad (14)$$

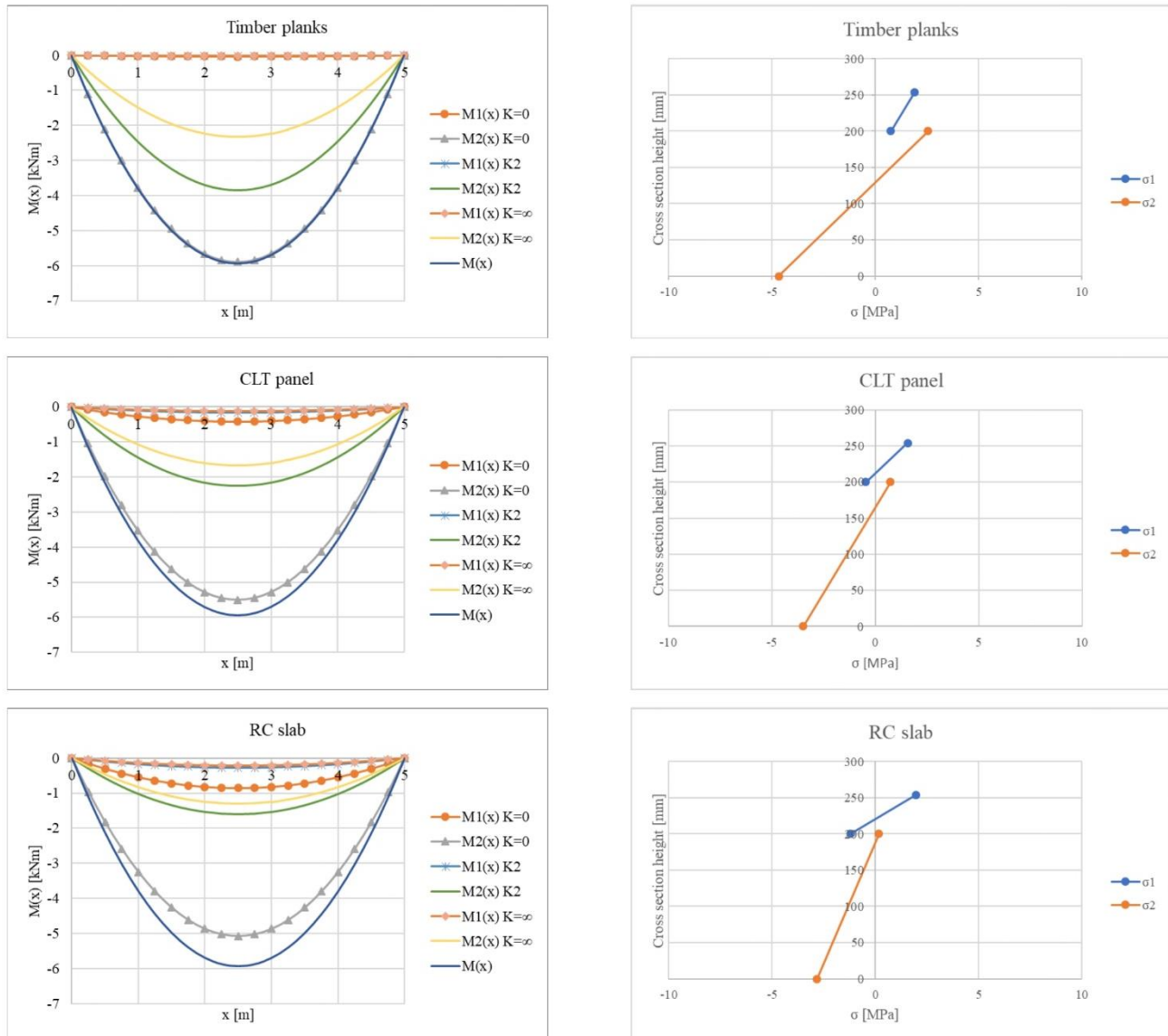


Figure 11. Bending moment distributions along the span for the $K = 0$, K_2 , and $K = \infty$ cases, and maximum normal stress distributions along the cross-section height for each reinforcement.

Considering the most stressed cross section in terms of bending moment, i.e., the one in the middle of the span, the variation of the normal stresses can be analysed along the height of the cross section, Figure 11 right graphs. Comparing the different reinforcements, the normal stresses in the joist, σ_2 , decreases as the stiffness of the reinforcing system increases, and even in this comparison CLT panel determines an intermediate behaviour between timber planks and RC slab.

5. Conclusions

The sustainable exploitation of wood resource for products other than firewood, where the latter currently represent its main use in Italy, can increase the interest in the management of rural areas, which are usually underdeveloped and abandoned. The use of short supply chain wood-based products for the restoration of historical and ancient buildings can be a significant practice and it could lead to several benefits over time such as the economic enhancement of local forests, the preservation of the architectural heritage with minimally invasive interventions, and sustainability advantages due to the use of wood in the construction sector.

To promote this kind of applications, comparative analysis regarding the out-of-plane strengthening of existing one-way floor were performed. Three different retrofit interventions were considered: double-crossed timber planks, CLT panels and reinforced concrete slab. The first and the third are two of the most commonly used techniques; the second one considers thin homogeneous beech cross-laminated timber panels recently mechanically characterized. In order to focus the comparison on the nature of the reinforcing elements, the thickness of the reinforcements was assumed equal to that of the CLT panels. The comparison in terms of out-of-plane bending stiffness was conducted by evaluating slip moduli and effective bending stiffness according to the mechanically jointed beam theory, Annex B of Eurocode 5, both at ULS and at SLS.

A total of three flexible cases, i.e., K_1 , K_2 and K_3 slip moduli for screwed connections characterized by different spacing along the span of the member, and three screw diameters, were considered. In addition, the performance of the flexible connections was assessed with respect to the two limit cases corresponding to the absence of any connection ($K = 0$) and to the presence of a fully rigid connection ($K = \infty$). From the comparisons proposed in this work, it was shown that the choice of CLT panels leads to a range of SLS bending stiffness increase from 145% (K_1 and $d = 8$ mm) to 177% (K_3 and $d = 12$ mm), against the ranges from 66% (K_1 and $d = 8$ mm) to 92% (K_3 and $d = 12$ mm) for double-crossed timber planks and from 246% (K_1 and $d = 8$ mm) to 272% (K_3 and $d = 12$ mm) for the RC slab solution. Although based on the use of hardwood, this solution can also minimize the weight increase for the examined geometry, in about the 40% part of the structural permanent loads, against the 69% term determined for the RC slab, and it allows to realize a fully reversible intervention.

Even though the RC slab leads to the greatest bending stiffness values, this solution is in fact not always applicable to existing buildings, especially when subjected to superintendence of architectural heritage restrictions. In addition, concrete and steel are considered less environmentally friendly than wood, and for this reason are often less preferable in the construction sector, in order to pursue sustainability goals.

Due to the growing interest in retrofitting solutions based on engineered wood products, the application of novel Italian beech CLT panels proved to represent a significant alternative for the retrofitting of existing timber floors, especially when belonging to the built cultural heritage. In this way, even further innovative structural applications could be detected and optimised for local species, specifically to beech and in general to hardwood, which both represent a consistent percentage of the Italian wooden areas.

Author Contributions: Conceptualization, M.F.; methodology, L.S., M.S., C.B. and M.F.; software, L.S. and M.S.; validation, L.S. and M.S.; formal analysis, L.S.; investigation, L.S., M.S. and C.B.; resources, M.S. and M.F.; data curation, L.S.; writing—original draft preparation, L.S., M.S., C.B. and M.F. All authors have read and agreed to the published version of the manuscript.

Funding: This research received no external funding.

Data Availability Statement: Data will be shared upon request.

Conflicts of Interest: The authors declare no conflict of interest.

References

- Branco, J.M.; Kekeliak, M.; Lourenço, P.B. In-plane stiffness of timber floors strengthened with CLT. *Eur. J. Wood Wood Prod.* **2015**, *73*, 313–323. [[CrossRef](#)]
- Gubana, A.; Melotto, M. Efficacy Assessment of Timber Based In-Plane Strengthening of Wooden Floors on the Seismic Response of Masonry Structures by means of DEM Analyses. *Procedia Struct. Integr.* **2023**, *44*, 1885–1892. [[CrossRef](#)]
- Gubana, A. State-of-the-Art Report on high reversible timber to timber strengthening interventions on wooden floors. *Constr. Build. Mater.* **2015**, *97*, 25–33. [[CrossRef](#)]
- Riggio, M.; Tomasi, R.; Piazza, M. Refurbishment of a Traditional Timber Floor with a Reversible Technique: Importance of the Investigation Campaign for Design and Control of the Intervention. *Int. J. Arch. Herit.* **2014**, *8*, 74–93. [[CrossRef](#)]
- Shan, B.; Xiao, Y.; Zhang, W.; Liu, B. Mechanical behavior of connections for glulam-concrete composite beams. *Constr. Build. Mater.* **2017**, *143*, 158–168. [[CrossRef](#)]
- Bedon, C.; Fragiaco, M. Three-Dimensional Modelling of Notched Connections for Timber–Concrete Composite Beams. *Struct. Eng. Int.* **2017**, *27*, 184–196. [[CrossRef](#)]
- Frangiaco, M.; Amadio, C.; Macorini, L. Short- and long-term performance of the “Tecnaria” stud connector for timber-concrete composite beams. *Mater. Struct.* **2007**, *40*, 1013–1026. [[CrossRef](#)]
- Bedon, C.; Rajcic, V.; Barbalic, J.; Perkovic, N. CZM-based FE numerical study on pull-out performance of adhesive bonded-in-rod (BiR) joints for timber structures. *Structures* **2022**, *46*, 471–491. [[CrossRef](#)]
- Miotto, J.L.; Dias, A.A. Evaluation of perforated steel plates as connection in glulam–concrete composite structures. *Constr. Build. Mater.* **2012**, *28*, 216–223. [[CrossRef](#)]
- Dias, A.M.P.G.; Kuhlmann, U.; Kudla, K.; Mönch, S.; Dias, A.M.A. Performance of dowel-type fasteners and notches for hybrid timber structures. *Eng. Struct.* **2018**, *171*, 40–46. [[CrossRef](#)]
- Dias, A.; Schänzlin, J.; Dietsch, P. *A State-of-the-Art Report by COST Action FP1402/WG 4 Design of Timber–Concrete Composite Structures*; Shaker: Maastricht, Germany, 2018.
- Angeli, A.; Piazza, M.; Riggio, M.P.; Tomasi, R. Refurbishment of traditional timber floors by means of wood-wood composite structures assembled with inclined screw connectors. In Proceedings of the World Conference on Timber Engineering, Trentino, Italy, 20–24 June 2010.
- Corradi, M.; Mustafaraj, E.; Speranzini, E. Sustainability considerations in remediation, retrofit, and seismic upgrading of historic masonry structures. *Environ. Sci. Pollut. Res.* **2023**, *30*, 25274–25286. [[CrossRef](#)]
- Borri, A.; Corradi, M. Architectural Heritage: A Discussion on Conservation and Safety. *Heritage* **2019**, *2*, 631–647. [[CrossRef](#)]
- Lagomarsino, S.; Cattari, S. Seismic Performance of Historical Masonry Structures Through Pushover and Nonlinear Dynamic Analyses. In *Perspectives on European Earthquake Engineering and Seismology*; Springer: Berlin/Heidelberg, Germany, 2015. [[CrossRef](#)]
- Anzani, A.; Cardani, G.; Condoleo, P.; Garavaglia, E.; Saisi, A.; Tedeschi, C.; Tiraboschi, C.; Valluzzi, M.R. Understanding of historical masonry for conservation approaches: The contribution of Prof. Luigia Binda to research advancement. *Mater. Struct.* **2018**, *51*, 140. [[CrossRef](#)]
- Unuk, Ž.; Premrov, M.; Leskovic, V. Development of an Innovative Approach for the Renovation of Timber Floors with the Application of CLT Panels and Structural Glass Strips. *Int. J. Arch. Herit.* **2021**, *15*, 627–643. [[CrossRef](#)]
- Tomasi, R.; Crosatti, A.; Piazza, M. Theoretical and experimental analysis of timber-to-timber joints connected with inclined screws. *Constr. Build. Mater.* **2010**, *24*, 1560–1571. [[CrossRef](#)]
- Schiro, G.; Giongo, I.; Sebastian, W.; Riccadonna, D.; Piazza, M. Testing of timber-to-timber screw-connections in hybrid configurations. *Constr. Build. Mater.* **2018**, *171*, 170–186. [[CrossRef](#)]
- De Santis, Y.; Sciomenta, M.; Spera, L.; Rinaldi, V.; Fragiaco, M.; Bedon, C. Effect of Interlayer and Inclined Screw Arrangements on the Load-Bearing Capacity of Timber–Concrete Composite Connections. *Buildings* **2022**, *12*, 2076. [[CrossRef](#)]
- Nie, Y.; Valipour, H.R. Experimental and analytical study of timber-timber composite (TTC) beams subjected to long-term loads. *Constr. Build. Mater.* **2022**, *342*, 128079. [[CrossRef](#)]
- Chiniforush, A.; Valipour, H.; Ataei, A. Timber-timber composite (TTC) connections and beams: An experimental and numerical study. *Constr. Build. Mater.* **2021**, *303*, 124493. [[CrossRef](#)]
- Aicher, S.; Hirsch, M.; Christian, Z. Hybrid cross-laminated timber plates with beech wood cross-layers. *Constr. Build. Mater.* **2016**, *124*, 1007–1018. [[CrossRef](#)]
- Franke, S. Mechanical properties of beech CLT. In Proceedings of the World Conference on Timber Engineering, Vienna, Austria, 22–25 August 2016.
- Crovella, P.; Kurzinski, S. Predicting the Strength and Serviceability Performance of Cross-laminated Timber (CLT) Panels Fabricated with High-Density Hardwood. In Proceedings of the World Conference on Timber Engineering, Santiago, Chile, 9–12 August 2021.
- Sciomenta, M.; Spera, L.; Bedon, C.; Rinaldi, V.; Fragiaco, M.; Romagnoli, M. Mechanical characterization of novel Homogeneous Beech and hybrid Beech-Corsican Pine thin Cross-Laminated timber panels. *Constr. Build. Mater.* **2021**, *271*, 121589. [[CrossRef](#)]
- Li, H.; Wang, L.; Wang, B.J.; Wei, Y. Study on in-plane compressive performance of cross-laminated bamboo and timber (CLBT) wall elements. *Eur. J. Wood Wood Prod.* **2022**, *81*, 343–355. [[CrossRef](#)]

28. Concu, G.; De Nicolo, B.; Fragiaco, M.; Trulli, N.; Valdes, M.; Dupray, S.; Simm, J.; Williams, J.; Kuna, K.; Airey, G.; et al. Grading of maritime pine from Sardinia (Italy) for use in cross-laminated timber. *Proc. Inst. Civ. Eng.-Constr. Mater.* **2018**, *171*, 11–21. [[CrossRef](#)]
29. Wang, T.; Wang, Y.; Crocetti, R.; Wälinder, M.; Bredesen, R.; Blomqvist, L. Adhesively bonded joints between spruce glulam and birch plywood for structural applications: Experimental studies by using different adhesives and pressing methods. *Wood Mater. Sci. Eng.* **2023**, *18*, 1141–1150. [[CrossRef](#)]
30. *EN 1995-1-1; Eurocode 5: Design of Timber Structures—Part 1-1: General—Common Rules and Rules for Buildings*. European Committee for Standardization: Brussels, Belgium, 2004.
31. Bedon, C.; Sciomenta, M.; Fragiaco, M. Correlation approach for the Push-Out and full-size bending short-term performances of timber-to-timber slabs with Self-Tapping Screws. *Eng. Struct.* **2021**, *238*, 112232. [[CrossRef](#)]
32. Jeong, G.Y.; Pham, V.S.; Tran, D.K. Development of predicting equations for slip modulus and shear capacity of CLT–concrete composite with screw connections. *J. Build. Eng.* **2023**, *71*, 106468. [[CrossRef](#)]
33. Denouwé, D.D.; Messan, A.; Fournely, E.; Bouchair, A. Influence of Interlayer in Timber–Concrete Composite Structures with Threaded Rebar as Shear Connector–Experimental Study. *Am. J. Civ. Eng. Arch.* **2018**, *6*, 38–45. [[CrossRef](#)]
34. *DRAFT prEN 1995-1-1; Eurocode 5—Design of Timber Structures—Part 1-1: General Rules and Rules for Buildings*. European Committee for Standardization: Brussels, Belgium, 2023.
35. Unuk, Ž.; Leskovar, V.Ž.; Premrov, M. Timber Floors and Strengthening Techniques (Illustrated with a Numerical Example). *Tek. Dergi* **2019**, *30*, 9261–9288. [[CrossRef](#)]

Disclaimer/Publisher’s Note: The statements, opinions and data contained in all publications are solely those of the individual author(s) and contributor(s) and not of MDPI and/or the editor(s). MDPI and/or the editor(s) disclaim responsibility for any injury to people or property resulting from any ideas, methods, instructions or products referred to in the content.

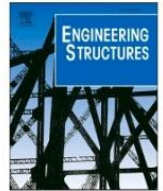
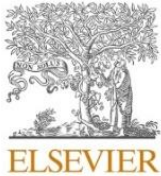
4. Glue-laminated timber beams

Glue-laminated timber (glulam) is an engineered wood product composed of wood laminations with the grain parallel to each other and to the main dimension of the member. The final product has a one-dimensional behaviour, and it can be customized straight, curved, arched, and tapered depending on the purposes. Therefore, glulam is preferable to sawn timber to produce larger dimensions and spans, for the freedom in the choice of geometrical shape and aesthetic appearance, for the improved strength and stiffness properties (because of the controlled manufacturing process and the lower influence of defects which are smaller and spread throughout the member volume), for the stability of shape during exposure to moisture, and for the dimensional accuracy. It was one of the oldest wood composites for structural purposes and thanks to its versatility it can be used in many structure types, such as buildings, bridges, malls, sporting centres, and pavilions. The production process consists in cutting some planks, usually 40-50 mm thick and 1500 to 5000 mm long, in joining them lengthwise, and in glueing the laminations together. The planks are usually kiln dried, because the adhesives used require a maximum moisture content of wood of about 15%, and they are then pre-planned and strength graded. In Italy, glulam must be manufactured according to EN 14080 (UNI Ente nazionale italiano di unificazione, 2013), which specifies the performance requirements for the use in buildings and bridges, the minimum production requirements, and the provisions for the assessment and certification of conformity of glue-laminated wood products.

4.1. Homogeneous beech and hybrid beech-Corsican pine glue-laminated timber beams

As further experimental investigation about the application of local wood in engineered wood products, the mechanical characterization of novel glue-laminated timber beams, made of the same local wood species previously mentioned and, in particular, of the same batch of boards described in the paper published in Construction and Building Materials journal, was carried out. A total of 28 eight-layered glue-laminated timber beams were manufactured, half in homogeneous beech (*Fagus sylvatica*) configuration and half in hybrid beech (*Fagus sylvatica*) - Corsican pine (*Pinus nigra subsp. Laricio (Poir.) Maire*) configuration. This latter one was characterized by two outer layers per each edge made of beech wood and four inner layers made of Corsican pine wood.

Four-point bending tests were performed according to EN 408 (UNI Ente nazionale italiano di unificazione, 2012a) with a span length of 18 times the height in the case of bending tests and of 9 times the height in the case of shear tests. During the tests, a loading cell and inductive displacement transducers were respectively used to measure load values and beams displacements. Regarding the homogeneous beech beams, a comparison between the mechanical properties experimentally obtained and those predicted by the DT resistance classes (recently formulated for medium density hardwood as described in the following) was conducted. The average load-displacement curve of the tested specimens resulted closer to the class DT 46 in terms of stiffness, but it does not reach the bending strength expected from that class. With regard to the hybrid beams, a comparison between the experimental values and those obtained considering the γ Method of Eurocode 5 and the GL44hyb class of the German standard Z-9.1-679:2019 was exposed. For the γ Method: in the first case (γ -Method (Exper.)), the elastic modulus values deriving from linear regressions of the dynamic elastic modulus obtained during the table classification phase were assigned; in the second case (γ -Method (EN 338)), the elastic modulus values provided by the EN 338:2016 standard for the strength classes D40 and C20 were assigned. The GL44hyb class curve resulted closer to the average experimental stiffness, and the γ -Method (Exper.) curve was closer to the experimental behaviour than the γ -Method (EN 338). A comparison with a commercial product, made of GL24h, was performed by means of finite element numerical simulations and the principal experimental and numerical results denoted the suitability of hardwood for the manufacturing of glulam beams, and the good performance of the hybrid configuration, as detailed in the following work by (Sciomenta et al., 2022).



Mechanical characterization of homogeneous and hybrid beech-Corsican pine glue-laminated timber beams

Martina Sciomenta^{a,*}, Luca Spera^b, Alfredo Peditto^c, Edoardo Ciuffetelli^d, Francesco Savini^e, Chiara Bedon^f, Manuela Romagnoli^g, Michela Nocetti^h, Michele Brunettiⁱ, Massimo Fragiaco^j

^a Department of Civil, Architecture and Building and Environmental Engineering, University of L'Aquila, Via Giovanni Gronchi 18, 67100 L'Aquila, Italy

^b Department of Civil, Architecture and Building and Environmental Engineering, University of L'Aquila, Via Giovanni Gronchi 18, 67100 L'Aquila, Italy

^c Department of Civil, Architecture and Building and Environmental Engineering, University of L'Aquila, Via Giovanni Gronchi 18, 67100 L'Aquila, Italy

^d Department of Civil, Architecture and Building and Environmental Engineering, University of L'Aquila, Via Giovanni Gronchi 18, 67100 L'Aquila, Italy

^e Department of Civil, Architecture and Building and Environmental Engineering, University of L'Aquila, Via Giovanni Gronchi 18, 67100 L'Aquila, Italy

^f Department of Engineering and Architecture, University of Trieste, Via Alfonso Valerio, 6/1, 34127 Trieste, Italy

^g Department of Innovation of Biological, Food and Forestry Systems (DIBAF), University of Tuscia, Via S. Camillo de Lellis, 01100 Viterbo, Italy

^h CNR-IBE, Institute of BioEconomy, Via Madonna del Piano 10, 50019 Sesto Fiorentino, FI, Italy

ⁱ CNR-IBE, Institute of BioEconomy, Via Madonna del Piano 10, 50019 Sesto Fiorentino, FI, Italy

^j Department of Civil, Architecture and Building and Environmental Engineering, University of L'Aquila, Via Giovanni Gronchi 18, 67100 L'Aquila, Italy

ARTICLE INFO

Keywords:

Glue-laminated timber (glulam)
Beech wood (*Fagus sylvatica* L.)
Corsican pine wood (*Pinus nigra* subsp. *laricio* (Poir.) Maire)
Mechanical characterization
Four-point bending tests
Finite Element
Short Chain Timber

ABSTRACT

This paper describes the results of an experimental investigation on novel homogeneous and hybrid beech-Corsican pine glue-laminated timber (glulam) beams made of short supply chain timber boards and melamine-based adhesive. The aim is to carry out the mechanical characterization of these glulam beams both in the homogeneous and in the hybrid configuration by four-point bending tests with different span to depth ratios of the specimens in order to differentiate bending and shear tests. The experimental results were fitted analytically as well as by means of Finite Element (FE) numerical simulations. Moreover, the stiffness of these novel beams is further evaluated, with respect to a comparison with a commercial product made of GL24h glulam. The experimental and numerical analysis point out the goodness of hardwood for the manufacturing of glulam beams, even in hybrid configuration in which the inner layers are made of low graded timber boards, with a great opportunity to optimize the raw material.

1. Introduction

In recent times timber has been more and more used in building construction, thanks to its advantages both as sawn timber and as engineered wood products. Among the latter ones, glue-laminated timber (glulam) and cross-laminated timber (CLT) proved to be competitive with other traditional construction materials, such as reinforced concrete, as studied by Baharami et al. [1] with regard to load-bearing capacities of CLT panels and by Li et al. [2] about innovative configuration of bamboo-wood composite CLT. Furthermore, an interest in wood-based products is developing with respect to the use of thin wood veneers as investigated by Chybiński et al. [3]. Glue-laminated timber was one of the first wood composite employed for structural purposes. The

first application of glulam timber, in Europe, was in the early 1890s and, in 1901, a patent from Switzerland signalled the true beginning of glue-laminated timber constructions. Notwithstanding the long-lasting production in time, glulam must be still considered as an actual composite product, due to the chance to get long sized beams and adopting low quality logs compared to solid beams. Conifers have been by far the most preferred tree species for glulam production due to the lower density compared to hardwoods and a better shape of the logs. The greatest value of conifers was to increase trusting in the glulam composite, giving life to a well-defined product in terms of mechanical performances by varying the environmental conditions in which it could be used; due to such reasons, glulam manufactured from conifers is still much used by building designers. Despite the fact that the employment of timber as

* Corresponding author.

E-mail address: martina.sciomenta@univaq.it (M. Sciomenta).

<https://doi.org/10.1016/j.engstruct.2022.114450>

Received 29 December 2021; Received in revised form 10 April 2022; Accepted 21 May 2022

Available online 2 June 2022

0141-0296/© 2022 Elsevier Ltd. All rights reserved.

construction material is beneficial, a more conscious choice of wood origin and application could be more advisable since conifers products are even too much widespread in territories where their presence must be considered historically unsustainable looking to the history and the landscape [4]. From the technological point of view, because of lower density, glulam made of coniferous species is characterized by good workability (sawing, drying, grading, gluing), but also by a reduction in the strength parameters and lower Young's and shear moduli compared to hardwood [5]. In the recent years the use of hardwoods in wooden construction has become a very important topic in Central Europe [6,7], this is because hardwoods have proven to cope better climatic changes and environmental stresses such as they are more soil and climate apt to face strong wind falls, the interest in them is more and more increasing [8]. In the last time the consumer is more accustomed to the use of hardwoods [9] and many attempts of glulam based on hardwood have been made [10]. Among hardwoods, beech is considered one of the most promising species because of its diffusion at European level but currently the use of beech and other species find in energy its preeminent competitive use [11], an intermediate step, e.g. as building material, could add value to this resource [12] and promote the principle of cascade use in wood. Indeed, beech composite products for structural purposes well fit the concept of short supply chain [4], which is one of the pillars of the bioeconomy strategy which has been launched at European and Italian level, sustaining the low carbon economy [13]. The idea of using beech for structural products and glulam is not new, with important researches by Egner and Kolb [14] and later by Gehri [15], Ehrhart et al. [16] and Frese and Blass [17]. Recent studies have demonstrated the high strength of beech engineered wood products such as glulam beams and cross-laminated timber panels [18]. So far beech glulam beams use was restricted by the lack of standards for grading beech lamellae strength, and the absence of design values needed in construction design. Some technical hurdles have now been solved in beech wood grading for structural purposes [19,20] and also bonding has provided fine results [12,21], enabling the exploitation of mechanical properties of the species.

The object of the paper is to present the results of an experimental investigation, concerning the mechanical characterization of glulam beams made of beech (*Fagus sylvatica*) and Corsican pine (*Pinus nigra* subsp. *Laricio*). Two main configurations are studied, the first one consisting in homogeneous beech glulam beams and the second one in hybrid glulam beams with the outer layers of beech and the inner layers of Corsican pine. A total of 28 four-point bending tests was carried out, with different span length to height ratios for the bending and shear tests, according to EN 408 [22].

Moreover, Finite Element (FE) numerical simulations were performed in order to analyse the differences between the experimental configurations and commercial products and to point out the advantages in using hardwood for the manufacturing of glulam beams.

2. Materials & methods

2.1. Characterization of the raw material

The raw material used to manufacture the glulam beams was made of Corsican pine (*Pinus nigra* subsp. *laricio*) and beech (*Fagus sylvatica* L.) boards originated from South Italy (Calabria). The boards had a nominal cross-section of 120 mm width and 20 mm thick, and an average length of 3.10 m (beech) and 4.00 m (pine). The batch of boards was kiln-dried in order to reach the suitable moisture content for the manufacturing gluing process, fixed at 10%.

Before further processing, the dynamic modulus of elasticity of each board was determined by the grading machine ViSCAN-Portable (MICROTEC). Each board was firstly weighed and measured to determine its density ρ . Then, the natural frequency of vibration f induced by a percussion was measured by using a laser interferometer. The dynamic modulus of elasticity E_{dyn} was thus calculated as:

$$E_{dyn} = \rho (2lf)^2 \quad (1)$$

Where ρ is the density of the board, l is the length and f is the frequency.

The machine settings for the strength grading of beech and pine were developed according to the technical standardization EN 14081-2 [23] in previous studies by Nocetti et al. [24] and Brunetti et al. [25]. The dynamic modulus of elasticity was the main parameter used during the strength grading and the raw material was qualified as D40 and rejects for beech and C20 and rejects for pine according to EN 338 [26].

The 95% of beech boards was graded as D40, while the remaining 5% was discarded mostly because of defects (presence of fiber deviations and not uniform planing). The yields for Corsican pine boards were: 73% graded as C20 and 27% rejected. Totally 210 beech boards and 74 Corsican pine boards were hence used for the production of two series of glue-laminated beams.

Besides, the dynamic modulus of elasticity measured during the strength grading procedure was used to estimate the modulus of rupture (f_m) and the global and local static modulus of elasticity (E_{gl} and E_l respectively) of the raw material. Regression analysis was performed based on destructive tests carried out on beech and pine during the machine setting development. Linear regression expressions were defined by using the E_{dyn} as explanatory variable. The results of the measurements carried out during grading (density and E_{dyn}), and the following estimation of the static properties are summarized in Table 1 with the relative standard deviations s_y and standard errors of estimation $s.e$.

2.2. Glue-laminated beam specimens

Two different series of eight-layered glue-laminated timber beams, made respectively of beech and beech and Corsican pine, were realized to carry out an extended experimental campaign to assess their mechanical properties prior to the industrial production. The hybrid configuration is composed by two beech outer layers and six Corsican pine inner layers. A total of 28, eight-layered glue-laminated timber beams were manufactured at the Pagano S.r.L factory (Oricola – AQ – Italy).

In order to guarantee the suitable planar surface, preferred for the face gluing, boards were cut to the required length and planed to a thickness of 18 mm. This resulted in a cross-sectional depth of 144 mm for all the specimens. The layering of the boards and the gluing process were performed by machine (Fig. 1 left).

Timber boards were overlapped and glued together by a Melamine Urea Formaldehyde (MUF) adhesive (GripPro™ Design – AkzoNobel, that was obtained by mixing a two component hardener (H002) and a liquid flexible resin (A002)). The choice of employing the melamine adhesive was due to the usage of beech hardwood boards in both homogeneous and hybrid beam's configurations with Corsican pine's boards [27]. In particular, the GripPro™ adhesive is specifically designed for softwood as well as for hardwood timber, such as beech,

Table 1

Mean values of the density (ρ), dynamic modulus of elasticity (E_{dyn}), measured during strength grading and mean values of bending strength (f_m) and local and global modulus of elasticity (E_l , E_{gl}), derived by regression analysis based on E_{dyn} . Standard deviation s_y and the standard errors of estimation $s.e$ are also reported.

Timber species	ρ [kg/m ³]	E_{dyn} [N/mm ²]	f_m [N/mm ²]	E_l [N/mm ²]	E_{gl} [N/mm ²]
Beech	753	16,506	83.1	16,640	15,977
s_y	40	1597	–	–	–
$s.e$	–	–	± 6.1	± 1321	± 1407
Corsican pine	497	9501	37.6	9588	8359
s_y	43	2348	–	–	–
$s.e$	–	–	± 7.1	± 2072	± 1949

Table 2

Size (B = base; L = length; H = height), configuration and test type of the examined glue-laminated timber specimens.

Beam series	Configuration / Timber	Specimen				Test type
		n°	B [mm]	L [mm]	H [mm]	
HB	Homogeneous beech	7	120	2800	144	Bending
		7	120	1500	144	Shear
BP	Hybrid beech/ Corsican pine	7	120	2800	144	Bending
		7	120	1500	144	Shear

birch, oak and chestnut. The adhesive was distributed by means of extrusion systems in which the adhesive mixture flows in the form of thin, very fluid and suitably spaced lines, through the orifices of special ducts in which the adhesive is under pressure and is mixed with hardener (in our case in the ratio 2 to 1) (Fig. 1 right). The average of glue grammage was 600 g/m². The adhesive was applied in a factory condition of 25° C, with an environmental moisture of 65%. Formed beams were then cold-pressed for 12 h, with a pressure of 11 bar. No finger joints were forecasted in glue-laminated beams of this experimental campaign.

3. Test methods

In accordance with EN 408 [22], the bending and shear stiffness parameters were evaluated from a four-point bending test setup (Fig. 2).

3.1. Bending and shear tests

The bending test is a four-point bending test over a span length of 18 times the depth (H). The shear test is a four-point bending test over a span length of 9 times the depth (H). In both cases, the specimen is simply supported and loaded symmetrically in bending at two points.

3.2. Test methods and instruments

The experimental setup is composed by an hydraulic jack which spreads the load via a rigid beam fixed under the piston, on two symmetric loading heads (Fig. 3 right). The loading rate was kept fix that was set in 0.003H mm/s, so as to reach the failure configuration after 300 ± 120 s. All the specimens were simply supported at the ends. In order to minimize the risk of possible local indentations, reaction bearing plates (no larger than one-half the tested piece thickness) were interposed between the supports and the bottom surface of the specimens. Similarly, additional steel load bearing supports were placed also between the loading heads and the top face of the specimens (Fig. 3 left). The deformations w were taken as the average of measurements detected by inductive displacement transducers (LVDT) that were placed on both the faces of each specimen. The experimental campaign was performed in a heated and air-conditioned environment, with about 20 °C.

In accordance with EN 408 [22], local and global stiffness parameters were evaluated from the experimental measurement of force and deflections:

$$E_{m,gl} = \frac{F^2(F_2 - F_1)}{bh^3(w_2 - w_1)} \left[\left(\frac{3a}{4l} \right) - \left(\frac{a}{l} \right)^3 \right] \tag{2}$$



Fig. 1. Glue-laminated timber beams: left) Gluing phase; right) Assembly prior to pressing.

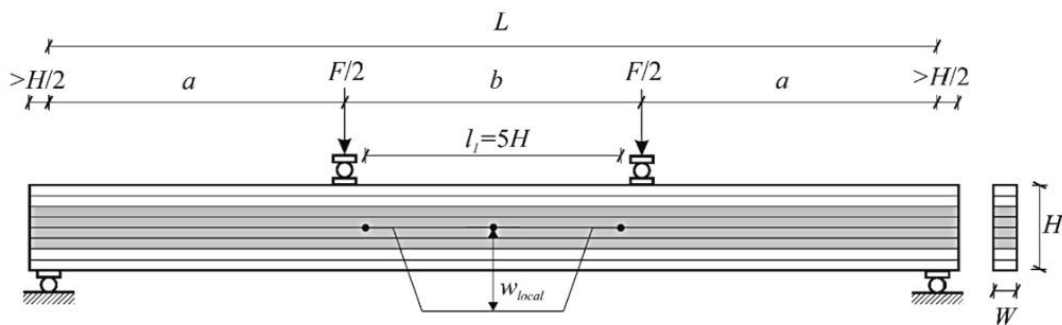


Fig. 2. Test set-up for bending perpendicular to the plane (a = b = 6H) and rolling shear test (a = b = 3H) [adapted from [22]].



Fig. 3. Set-up left) Equipment details; right) Front view.

$$E_{m,l} = \frac{a l^2 (F_2 - F_1)}{16 I (w_2 - w_1)} \quad (3)$$

with l the length of span in bending, a the distance between the loading heads and the nearest support, b and h are respectively the width and depth of specimen cross section in bending test, I the second moment of area, F_1 and F_2 the 10% and 40% of the ultimate force F_{max} respectively, and w_1 and w_2 the related recorded deflections.

Based on the theory of elasticity, the flexural (f_m) and the shear (f_v) stresses evaluated at the time of specimen failure is evaluated using the equation:

$$f_m = \frac{a F_{max}}{2 W} \quad (4)$$

$$f_v = \frac{3 F_{max}}{4 A} \quad (5)$$

where W is the section modulus and A is the area of rectangular-shaped sections.

4. Test results

4.1. Bending

The results of bending tests are summarized in Table 3.

For each specimen, the flexural stiffness, the bending strength and the failure mode are proposed. Moreover, for both series of beams, the average values, the standard deviation s_y and the characteristic values (5th-percentile) m_k are also estimated according to EN 14,358 [28].

As shown, the most prevalent failure pattern for homogeneous beech beams HB was bending while for hybrid beech/ Corsican pine beams BP was shear failure (Fig. 4).

The load–displacement curves of all specimens, except for HB-4, until the value of load equal to the 40% of the ultimate force F_{max} are presented both for the homogeneous configuration and for the hybrid one (Fig. 5). The displacement considered is the vertical one at the midspan of the beam. These curves represent the elastic region of the overall behaviour and show how also the hybrid configuration offers good performances in term of stiffness with respect to the homogeneous one.

4.2. Shear

The results of shear tests are summarized in Table 4.

For each specimen, the flexural stiffness, the shear strength and the failure mode are proposed. Moreover, for both series of beams, the

Table 3
Bending test results.

Beam-Specimen n°	$E_{m,gl}$ [N/mm ²]	$E_{m,l}$ [N/mm ²]	$E_{m,gl} I$ [kNm ²]	F_{max} [kN]	f_m [N/mm ²]	Failure mode
HB -1	14,202	16,672	424	81	42.0	b
HB -2	17,737	20,822	530	106	55.4	b
HB -3	16,852	19,783	503	116	60.2	b
HB -4*	–	–	–	–	–	–
HB -5	16,886	19,822	504	99	51.4	b
HB -6	17,290	20,296	516	107	55.5	b
HB -7	15,954	18,729	476	99	51.7	d
Average	16,487	19,354	492	100	52.7	
s_y	1265	1485	38	12	6.1	
m_k	–	–	–	74	39.3	
BP -1	15,160	17,796	453	93	48.3	s
BP -2	14,304	16,792	427	91	47.2	s
BP -3	15,029	17,643	449	93	48.5	b
BP -4	13,317	15,633	398	89	46.3	s + k
BP -5	14,354	16,850	429	90	46.7	b
BP -6	14,881	17,469	444	90	46.9	s
BP -7	14,757	17,324	441	104	54.5	s
Average	14,543	17,072	434	93	48.3	
s_y	727	854	22	5	2.8	
m_k	–	–	–	81	42.5	

b: bending failure, d: delamination, k: knots influence, s: shear. * omitted due to test instrumental issues.

Where $E_{m,l}$ is the local and $E_{m,gl}$ is the global stiffness parameter, $E_{m,gl} I$ is the flexural stiffness, F_{max} is the ultimate force and f_m is the flexural stress, s_y is the standard deviation and m_k the 5th percentile.

average values, the standard deviation s_y and the characteristic values (5-percentile) m_k are also estimated according to EN 14,358 [28]. As shown in Fig. 4, the most prevalent failure pattern for homogeneous beech beams HB was shear, in some cases delamination occurred, while for hybrid beech/ Corsican pine beams BP was shear failure.

As for the bending tests, the load–displacement curves of all specimens, except for HB-6, until the value of load equal to the 40% of the ultimate force F_{max} are presented both for the homogeneous configuration and for the hybrid one (Fig. 6). Even in these tests the hybrid configuration presents similar performances in term of stiffness with respect to the homogeneous one.

5. Standard comparison

According to § 5.1.3 of EN 14,080 [29], the characteristic strength, stiffness and density properties of glue-laminated timber shall be verified either i) from classifications from layups and lamination properties

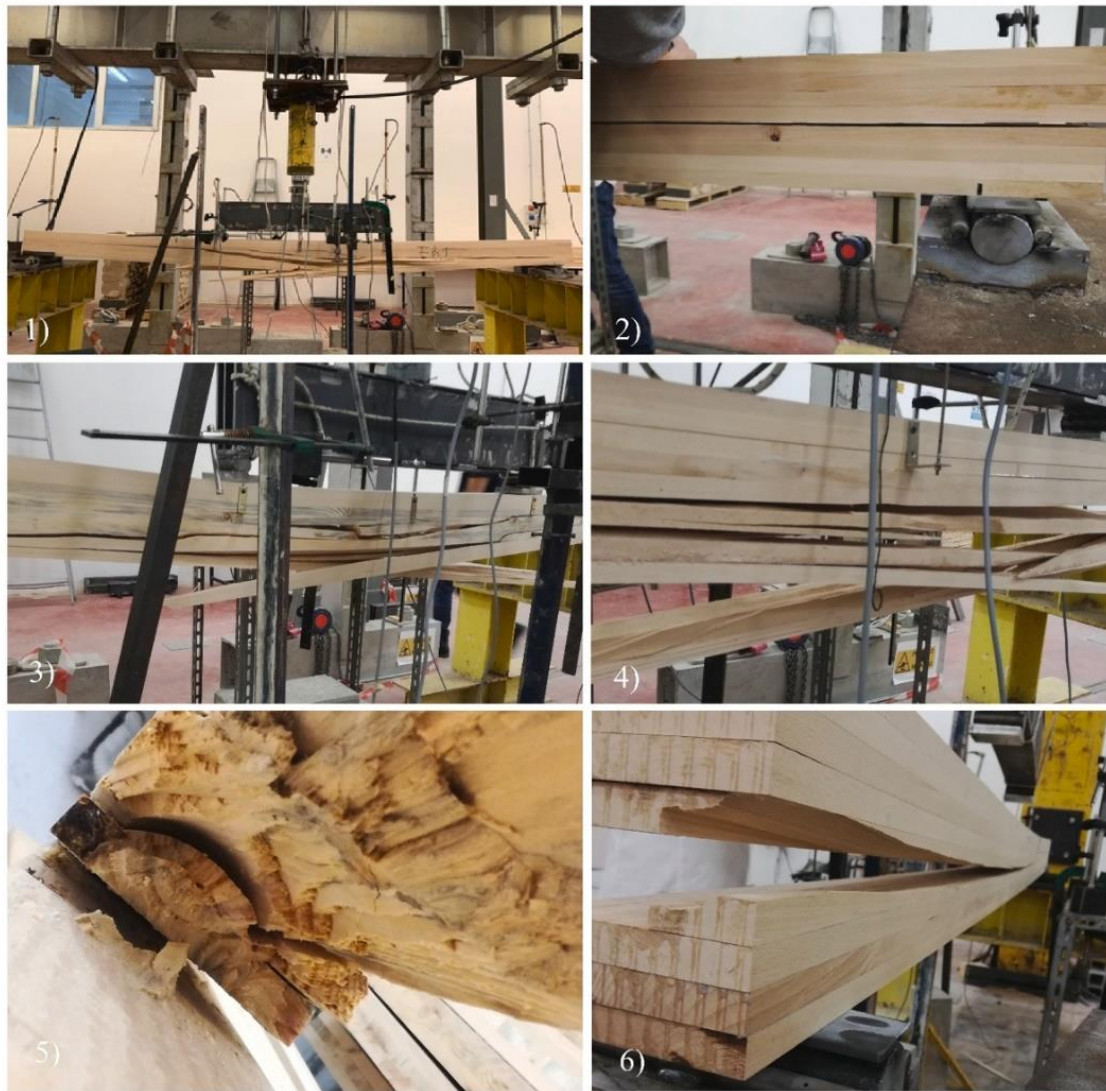


Fig. 4. Details of failure modes of the bending tests: 1), 2), and 3) bending failure modes; 2) and 6) delamination failure modes; 3) and 5) influence of defects.

ii) from calculations taking into account the cross sectional layup and documented properties of boards and finger joints or iii) from full scale tests.

In our case, the characterization and grading of laminations and glulam beams were performed as summarized in Fig. 7.

The Z-9.1-679 is a German provision specifically formulated for beech glulam beams.

5.1. Beam grading

5.1.1. Homogeneous beams

Some novel tensile DT-classes for medium-density European hardwoods (mainly beech and ash) proposed by Kovryga et al. [6], are adopted to define the strength class of homogeneous GLT beams; the mechanical features are evaluated in accordance with the formulations of EN 14,080 [29].

Some of the most influencing parameters on GLT bending strength concerns the material modulus of elasticity and type of lamellas in the tension zone, in particular, on the high-stressed lamellas in the outer tension zone of GLT, while the probability of failure in compression zone can be neglected. So instead of using D-classes, defined for bending applications and developed in relation to bending MOE and strength, these novel DT-classes are formulated with regards to tensile MOE and

are characterized by a higher tensile MOE values parallel to the grain, it would make possible a better exploitation of the hardwood GLT beams behaviour.

Different approaches have been adopted in order to define the strength class, based on the most influential parameters:

1. Based on the machine grading procedure, the beech board class was D40 ($f_{m,k} = 40$ MPa, $f_{t,0,k} = 24$ MPa), as summarized in the previous paragraph; assuming the bending and tensile strength as main parameters (consistently with the previous considerations) a DT24 class was attributed to boards based on the Kovryga et al.'s proposal. Adopting the formulations of EN 14,080 Table 6, the evaluation of the beam class is summarized in Table 5. The formulation for the bending strength was applied by considering the case of board without finger joints and taking, in accordance with the EN 14,080 a characteristic flat wise bending strength of the finger joint as: $f_{m,j,k} = 1,4f_{t,0,k} + 12$.
2. Based on the local elastic modulus calculated from the experimental E_{dyn} by linear regressions and density, a DT 46 class was attributed to beech boards ($\rho_m = 750$ kg/m³, $E_{0,mean} = 16500$ MPa). The expressions of EN 14,080 Table 6 were adopted for the evaluation of the beam class. The main mechanical properties of the beams are summarized in Table 6.

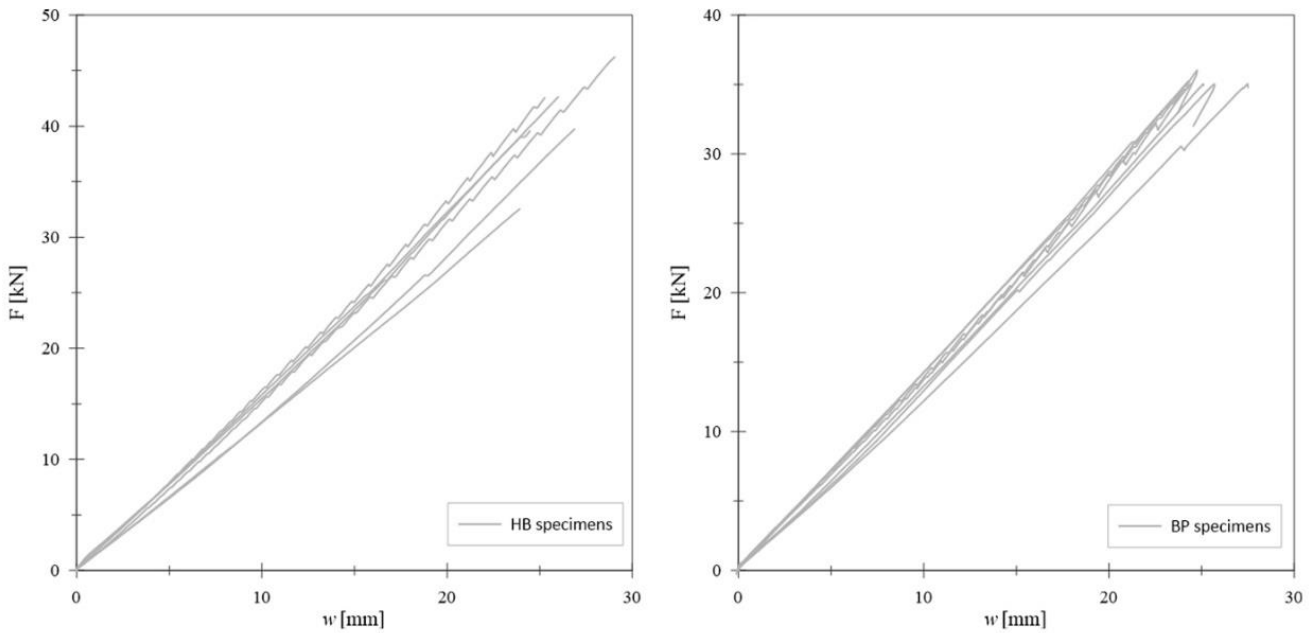


Fig. 5. Load-displacement curves: left) homogeneous beech specimens; right) beech/Corsican pine specimens.

Table 4
Shear test results.

Beam-Specimen n°	$E_{m,gl}$ [N/mm ²]	$E_{m,l}$ [N/mm ²]	$E_{m,gl}I$ [kNm ²]	F_{max} [kN]	f_v [N/mm ²]	Failure mode
HB -1	14,263	16,744	426	156	3.4	s
HB -2	13,808	16,210	412	147	3.2	s
HB -3	16,128	18,934	482	186	4.0	s
HB -4	18,472	21,685	552	225	4.9	s
HB -5	15,272	17,928	456	193	4.2	d
HB -6*	-	-	-	-	-	-
HB -7	13,176	15,467	393	147	3.2	d
Average	15,187	17,828	454	176	3.8	
s_y	1923	2257	58	31	0.68	
m_k	-	-	-	103	2.5	
BP -1	12,299	14,438	367	111	2.4	s
BP -2	12,309	14,449	368	109	2.4	s
BP -3	12,624	14,819	377	116	2.5	s
BP -4	13,803	16,203	412	121	2.6	s
BP -5	13,503	15,852	403	118	2.6	s
BP -6	12,671	14,874	378	125	2.7	s
BP -7	13,463	15,805	402	139	3.0	s
Average	12,953	15,206	387	120	2.6	
s_y	648	760	19	10	0.21	
m_k	-	-	-	97	2.2	

b: bending failure, d: delamination, k: knots influence, s: shear. * omitted due to test instrumental issues.

Where $E_{m,l}$ is the local and $E_{m,gl}$ is the global stiffness parameter, $E_{m,gl}I$ is the flexural stiffness, F_{max} is the ultimate force and f_v is the shear stress, s_y is the standard deviation and m_k the 5th percentile.

3. Based on the f_m value calculated from the experimental E_{dyn} by linear regressions, the characteristic value was evaluated ($f_{m,k} = 63.2$ MPa $s_y = 11.2$) a DT 38 class was attributed to beech boards ($f_{m,k} = 61$ MPa) and the expressions of EN 14080 Table 6 were adopted for the evaluation of the beam class. The main mechanical properties of beams are summarized in Table 7.

In Fig. 8 is clearly visible how the adoption of DT 46 class is suitable to fit some of the experimental curves, the main difference in term of stiffness (evaluated considering the curve slope between 0.1 F_{max} and 0.4 F_{max}) is 4%. But it overestimates the characteristic bending strength

of the glulam beam. Experimentally we obtained a 5th percentile of bending strength of 39.3 MPa and a minimum value of 42 MPa (Table 2). In this sense, the values calculated using the strength class of the lamellas (D40 corresponding to a DT24) resulted in a better fit with the experimental achievements, but conservative.

Most likely, the best fitting profile would be the one calculated by the mechanical properties of the lamellas (DT38), assuming that the value of the glulam characteristic strength was penalized by the limited number of tests.

The shear strength tabled and verified experimentally were in line (3.5 MPa vs 3.8 MPa).

5.1.2. Hybrid beams

In accordance with EN 14,080 [29], the evaluation of mechanical features such as characteristic bending, the mean modulus of elasticity and the characteristic density of a combined glue-laminated timber shall be determined from the respective values of the different lamination zones considered as homogeneous glue-laminated timber by means of the elastic composite beam theory.

The γ -method proposed in Eurocode 5 is adopted to evaluate the effective bending stiffness of hybrid beams; those latter can be represented as elements made up of different parts mutually connected (Fig. 9). The degree of connection between each part is accounted by the coefficients γ_i which can be equal to 1 for rigid connection or 0 in case of disconnected parts.

The effective bending stiffness is evaluated in Table 8 and 9 as:

$$(EI)_{ef} = \sum_{i=1}^3 E_i I_i + \gamma_i E_i A_i a_i^2 \tag{6}$$

As elastic modulus were assumed as: i) the local modulus of elasticity obtained by using linear regressions from the experimental modulus of elasticity as well as ii) the nominal modulus of elasticity for D40 and C20 class.

In the last decades, many studies have been carried out in order to establish the structural performances of glulam beech beams in combined as well as in the hybrid configuration. The main works were developed by Frese and Blaß [17] and in Z-9.1-679 [30] German provision some class specifically formulated are available for beech glulam beams. In Table 3 of Z-9.1-679 are summarized the six classes developed

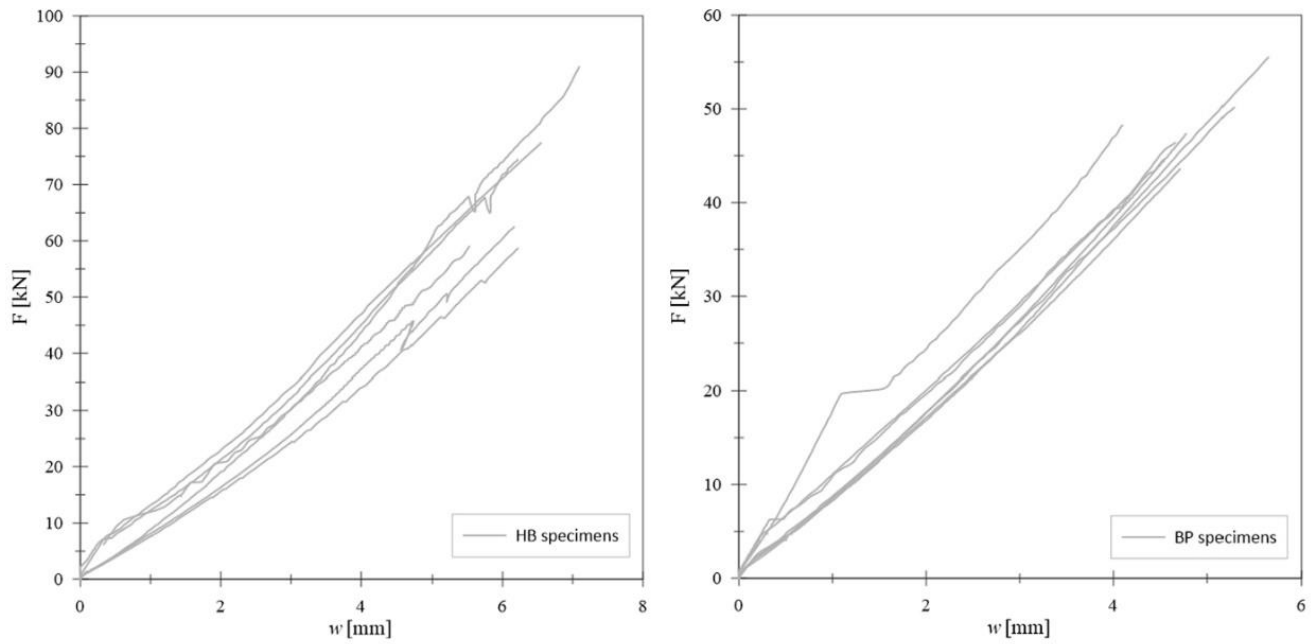


Fig. 6. Load-displacement curves: left) homogeneous beech specimens; right) beech/Corsican pine specimens.

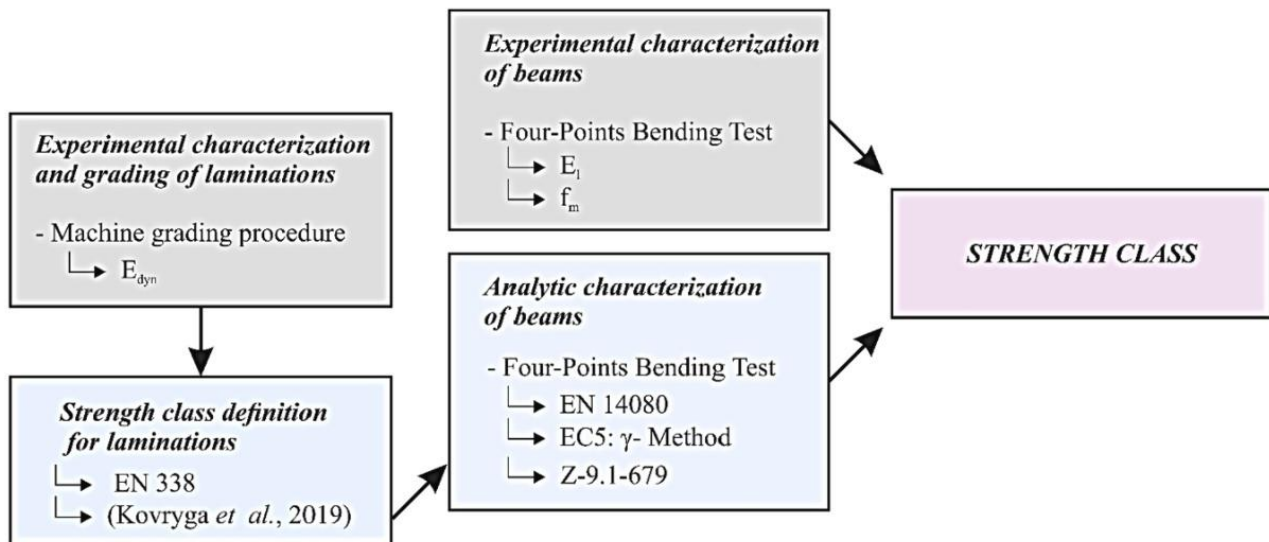


Fig. 7. Chart of characterization and grading procedure of laminations and beams.

Table 5
Homogeneous beech beam features evaluated assuming a board class DT 24.

Homogeneous beech beams		
	Property	
$f_{m,g,k}$	33.5	MPa
$f_{t,0,g,k}$	26.8	MPa
$f_{t,90,g,k}$	0.5	MPa
$f_{c,0,g,k}$	33.5	MPa
$f_{c,90,g,k}$	2.5	MPa
$f_{v,g,k}$	3.5	MPa
$f_{r,g,k}$	1.2	MPa
$E_{0,g,mean}$	14,175	MPa
$E_{90,g,mean}$	300	MPa
$G_{g,mean}$	650	MPa
$G_{r,g,mean}$	65	MPa

Table 6
Homogeneous beech beam features evaluated assuming a board class DT 46.

Homogeneous beech beams		
	Property	
$f_{m,g,k}$	50.5	MPa
$f_{t,0,g,k}$	40.4	MPa
$f_{t,90,g,k}$	0.5	MPa
$f_{c,0,g,k}$	50.5	MPa
$f_{c,90,g,k}$	2.5	MPa
$f_{v,g,k}$	3.5	MPa
$f_{r,g,k}$	1.2	MPa
$E_{0,g,mean}$	17,325	MPa
$E_{90,g,mean}$	300	MPa
$G_{g,mean}$	650	MPa
$G_{r,g,mean}$	65	MPa

Table 7
Homogeneous beech beam features evaluated assuming a board class DT 38.

Homogeneous beech beams		
	Property	
$f_{m,g,k}$	44.6	MPa
$f_{t,0,g,k}$	35.7	MPa
$f_{t,90,g,k}$	0.5	MPa
$f_{c,0,g,k}$	44.6	MPa
$f_{c,90,g,k}$	2.5	MPa
$f_{v,g,k}$	3.5	MPa
$f_{r,g,k}$	1.2	MPa
$E_{0,g,mean}$	16,275	MPa
$E_{90,g,mean}$	300	MPa
$G_{g,mean}$	650	MPa
$G_{r,g,mean}$	65	MPa

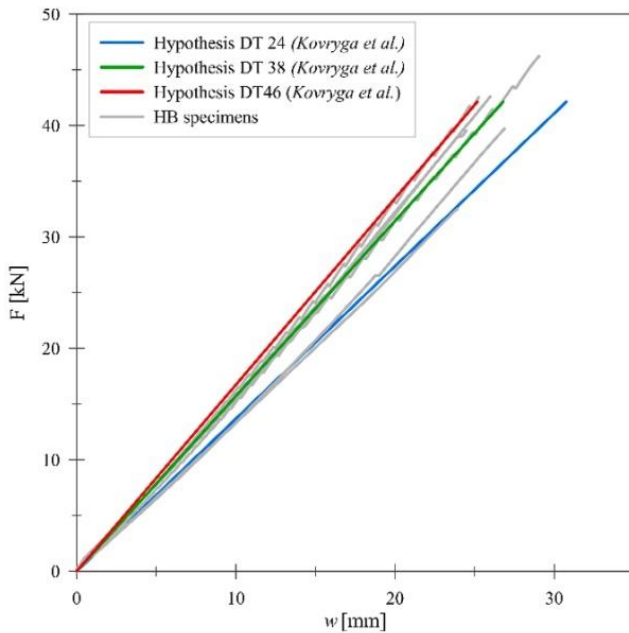


Fig. 8. Comparison of load–deflection curve from experimental tests vs hypothetical beam classified as DT24 DT38 and DT46.

for hybrid configuration; the main hypothesis is that *i*) inner layers of softwood must be visually classified as S10 in accordance with DIN 4074-1 [31] or C24 in accordance with EN14080-1 [29] and DIN 20000-5 [32] and *ii*) the bending stiffness of softwood finger joints must be $\geq 32 \text{ N/mm}^2$. Satisfying this conditions, the glulam class was defined by knowing the visual classification class (LS13 + E15) and the value of E_{dyn} .

A GL 44 hyb class was assessed and mechanical characteristics defined in Table 5 of Z-9.1-679 [30] are herein summarized ($f_{m,y,k} = 44 \text{ N/mm}^2$, $f_{m,z,k} = 32 \text{ N/mm}^2$, $f_{v,k} = 2.5 \text{ N/mm}^2$, $E_{0,mean} = 14700 \text{ MPa}$).

In both cases, the flexural stiffness was adopted to evaluate the deflection, assuming as load values the experimental one. In Fig. 10 the result of comparisons is graphically represented.

As a result, the comparison with the experimental envelope curve is perfectly fitting with both analytical curves. From the comparison with the curve obtained by applying the γ -method, the scatter in term of stiffness (evaluated considering the curve slope between $0.1 F_{max}$ and $0.4 F_{max}$) is -3.4% , while comparing the curve of GL44hyb class with the experimental one, the stiffness difference is 2% .

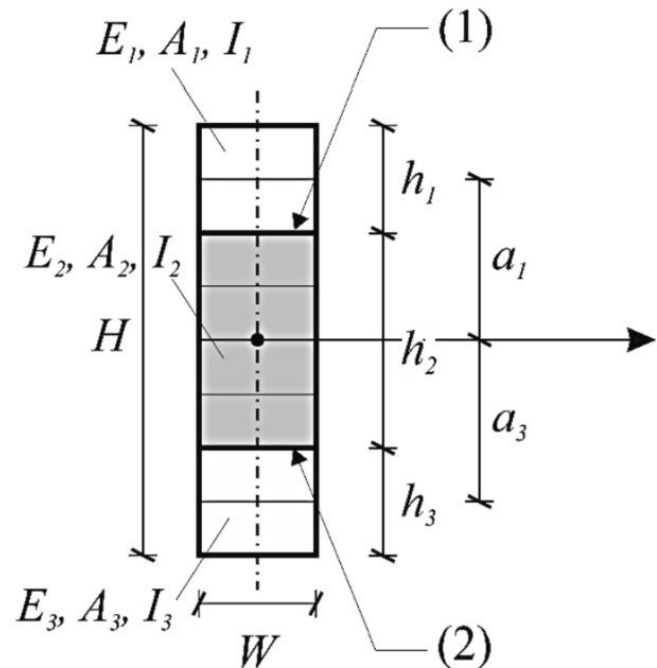


Fig. 9. Beam cross section for γ -method calculations.

6. Finite elements modelling

6.1. Main purpose

The main aims of the following FE models are: *i*) defining how a different material's assignment to the model could affect the accuracy of numeric analysis as well as, *ii*) compare the mechanical performances of the two beam 'series with those of commercial beams made of conifer timber; the hypothesis are to model these latter products assigning the same class of our Corsican pine boards and same geometrical features of our beams and carry on a four-point bending simulation using the software Abaqus/Explicit [33].

6.2. Model description

A comparison in terms of deflection and stiffness of the experimental results with numerical Finite Element (FE) simulations was carried out. Both the homogeneous and the hybrid configurations were reproduced in order to define a well-fitting finite brick-element model. The model reproduces with good accuracy the experimental four-point bending tests setup Fig. 11; in addition to the beam, also the steel ending supports and load plates were introduced in order to simulate the real BCs (hinge and carriage respectively) and the friction conditions between the support surfaces and the bottom of the beam.

An amount of 4655 C3D8R mesh elements, size 22, were used with the structured meshing technique to describe the geometry of the specimens. In the 'property' module timber was modelled as orthotropic elastic material with the definition of different engineering constants and steel as isotropic elastic material. In the hybrid beam model, Corsican pine and beech timber have been assigned after partitioning suitably the beam. Interactions between steel and timber elements were accounted as frictional surface-to-surface contacts with the tangential and normal behaviors described by 'penalty' and 'hard contact' formulations respectively. A static friction coefficient set in 0.3 for steel-to-timber contact and in 0.15 for steel-to-steel contact was applied.

At first, two fitting models were carried on by accounting as beech and Corsican pine elastic and shear modulus those summarized in Table 2. Deflections were compared taking as reference point the beam

Table 8
Bending stiffness evaluation applying γ -method formulation and EN 338 modulus of elasticity.

Layer n°	h_i [mm]	E_i [MPa]	I_i [mm ⁴]	A_i [mm ²]	γ_i	$a_{1,3}$	a_2	$E_i I_{i,ef}$ [Nmm ²]
1	36	13,000	466,560	4320	1	54	0	1,70E + 11
2	72	9500	3,732,480	8640	1	0	0	3,55E + 10
3	36	13,000	466,560	4320	1	54	0	1,70E + 11
Σ								3,75E + 11

Table 9
Bending stiffness evaluation applying γ -method formulation and experimental modulus of elasticity.

Layer n°	h_i [mm]	E_i [MPa]	I_i [mm ⁴]	A_i [mm ²]	γ_i	$a_{1,3}$	a_2	$E_i I_{i,ef}$ [Nmm ²]
1	36	16,440	466,560	4320	1	54	0	2,17E + 11
2	72	9588	3,732,480	8640	1	0	0	3,58E + 10
3	36	16,640	466,560	4320	1	54	0	2,17E + 11
Σ								4,68E + 11

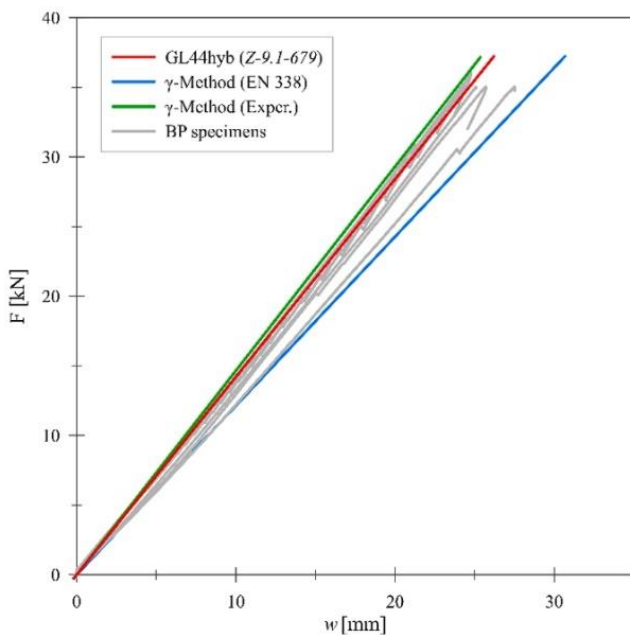


Fig. 10. Comparison of load–deflection curves from experimental tests vs hypothetical beam classified as GL44hyb and analytical evidences from γ -method calculations.

center-line (Fig. 12). The FE model fits with great approximation the experimental values leading to an overestimation of the deflection of 7 % for the homogeneous configuration and of 5 % for the hybrid one (Table 10 and 11).

Then, other models for the homogeneous and hybrid configuration respectively were developed with the aim to evaluate how a different material assignment (beams mechanical features instead to laminations features) affects the goodness of FE modelling.

- The model called “*Glulam Beam DT38*” was carried on by assigning to the beam the mechanical properties of a glulam beam (Table 6) evaluated in accordance with EN 14,080 with laminations classified ad DT38;
- The model called “*Glulam Beam GL 44 hyb*” was carried on by assigning to the beam the mechanical properties of GL 44 hyb class defined by Allgemeine bauaufsichtliche Zulassung Z-9.1–679.
- The model “*Glulam Beam DT38*” overestimates the experimental deflection of 10.5% and overestimates the deflection obtained by assigning the proper material to each beam partition (outer and inner beech lamellas) of 4.3%.

- The model “*Glulam Beam GL 44 hyb*” overestimates the experimental deflection of 15.2% and overestimates the deflection obtained by assigning the proper material to each beam partition (outer beech and inner Corsican pine lamellas) of 14.2%.
- Moreover, a comparison between the experimental homogeneous and hybrid specimens and commercial beam was numerically simulated. This commercial product was classified supposing C24 lamellas in accordance with EN 338, in order to have the same class of inner hybrid layers and stress out the advantages of having outer beech layers in hybrid configuration. Due to the lamellas classification, the properties of a homogeneous GL 24 h beam were calculated in accordance with EN 14080.

From the comparison in Table 12 both hybrid and homogeneous beams show a stiffer behavior, leading to a smaller deflection with respect to GL 24 h beams thanks to the contribution of the more performing beech layers. Therefore, this hybrid configuration represents a good example of timber boards optimization and the highlight the excellent performances of beech timber.

7. Conclusions

This paper describes the results, based on experimental tests, analytical analyses and FE modelling, on novel homogeneous and hybrid beech-Corsican pine glue-laminated timber (glulam) beams made of short supply chain timber boards and melamine-based adhesive.

1. The experimental campaign highlights the excellent mechanical performance of the panels, both homogeneous and hybrid. In particular, by analysing the results obtained by the four points bending tests, it emerges that the two configurations have almost comparable performances; the homogeneous beams have reached a maximum force, F_{max} which is 7% higher than the hybrid ones and a flexural stress f_m greater than 8.3 %. Analyzing the failure mechanisms occurred during the bending tests, a greater variability is observed for the hybrid beams rather than for the homogeneous ones, with particular reference to delaminations. Significant differences are observed by comparing the shear performance of the two beams configurations, the homogeneous beams have reached a maximum force, F_{max} which is 31.5% higher than the hybrid ones and a shear stress f_v greater than 31.8 %. Analyzing the shear failure mechanisms, less variability is observed as for homogeneous as for hybrid configuration.
2. In the second part of this work, the goal was to understand whether the EN 14,080 formulations valid for attributing a strength class to beams made with coniferous lamellas can be extended to homogeneous broad-leaved and hybrid products, under which hypotheses and with what results. For homogeneous beams, the tensile DT-



Fig. 11. a) Four-point bending experimental setup, b) FE model beam with ending support and load plates details c) Setup carriage, d) Setup hinge.

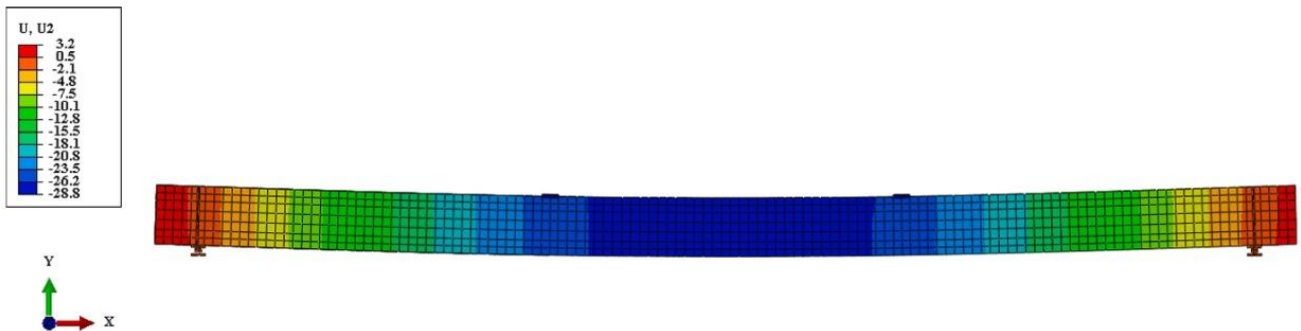


Fig. 12. Vertical deflection (w) for glulam beam GL 44 hyb.

Table 10

Numerical evidences and comparison for homogeneous beams.

HOMOGENEOUS CONFIG.	Test type	E_1 [N/mm ²]	$E_2 = E_3$ [N/mm ²]	$G_{12} = G_{23} = G_{13}$ [N/mm ²]	$0.4 F_{max}$ [kN]	w [mm]	Δf [%]
	Experimental envelope	–	–	–	39.8	25.5	–
	FE Boards classif. Prop. (beech)	16,440	1165	1040		26.6	–4.3
	Glulam Beam DT38	16,275	300	650		28.2	–10.5

Table 11

Numerical evidences and comparison for hybrid beams.

HYBRID CONFIG.	Test type	E_1 [N/mm ²]	$E_2 = E_3$ [N/mm ²]	$G_{12} = G_{23} = G_{13}$ [N/mm ²]	$0.4 F_{max}$ [kN]	w [mm]	Δf [%]
	Experimental envelope	–	–	–		25.0	–
	FE Boards classif. Prop. (beech-pine)	16640–9588	1065–639	998–599	34.7	25.2	–0.8
	Glulam Beam GL 44 hyb	14,700	300	650		28.8	–15.2

Table 12

Numerical evidences and comparison with commercial GL 24 h beam.

Material & Configuration Description	Class	E_1 [N/mm ²]	$E_2 = E_3$ [N/mm ²]	$G_{12} = G_{23} - G_{13}$ [N/mm ²]	0.4 F_{max} [kN]	w [mm]	Δf [%]
Homogeneous Commercial Conifer	GL 24 h	11,500	300	650	34.7	33.4	
Tested Hybrid beech/Pine	GL 44 hyb	14,700	300	650		30.7	-8.7
Tested Homogeneous beech	-	16,275	300	650		28.2	-18.4

classes for medium-density European hardwoods (mainly beech and ash) proposed by Kovryga et al. [6] were adopted. In order to define what parameters are more suitable to attribute the glulam class, three different hypothesis have been carried out choosing the bending and tensile strength, the bending stress and the dynamic modulus of elasticity respectively. By comparing the experimental evidences with the analytical ones that the DT38 class (based on the closer dynamic modulus of elasticity) was the best choice. For the hybrid beam, the γ -method and the Z-9.1-679 [30] German provision were adopted. This latter choice allowed attributing a GL44h class to our hybrid beam which fitted with great accuracy the experimental test.

- At last, a FE modelling was provided in order to compare our products with the commercial one (classified supposing C24 lamellas in accordance with EN 338, in order to have the same class of inner hybrid layer). The strength classes previously attributed were reproduced in the FE models as assigning to each lamellas the right material features, as well as by modelling the whole beam with its own class. From the comparison in terms of deflections it was evident that the hybrid and homogeneous beams could experience a smaller deflection for the same amount of load rather than the conifer beam.

From the results of this work is possible conclude that:

- The classification of the lamellas and the accuracy of this procedure is fundamental for the right attribution of strength class of the beams. The setting up of classification rules for species that are still little used should be preferred in order to broaden them knowledge and possibilities of use.
- Experimental tests clarified that hybrid and homogeneous hardwood glulam beams have high mechanical performances, so, further investigations could be useful to have a wider comprehension of other species of hardwood timber as well as to fix some points in the open field of adhesives and gluing methods involving hardwood lamellas.
- It has been demonstrated that, under the previous hypothesis, is still possible to adopt the EN 14,080 formulations valid for conifer glulam beams also for the definition of the features of hardwood beams. However, adopting the mechanical parameters suggested by EN 338 leads to a considerable underestimation of the beam stiffness. For hybrid products, the strength classes proposed in the German provision Z-9.1-679 [30] as well as the γ -method with the experimental values of timber coming from the board classification allow to fit with good accuracy of the specimens experimental stiffness.

Funding

This work was funded by Italian Ministry of University and Research - PRIN 2015, grant number 2015YW8JWA_002.

The development of machine setting for black pine was performed in the frame of the A.Pro.Fo.Mo.project, financed by GALStart, (Leader m. 124, PSR 2007-2013 Toscana Region). The financial support is gratefully acknowledged.

Credit authorship contribution statement

Martina Sciomenta: Conceptualization, Methodology, Formal

analysis, Formal analysis, Supervision, Investigation, Writing – review & editing. **Luca Spera:** Formal analysis, Writing – review & editing. **Alfredo Peditto:** Investigation. **Edoardo Ciuffetelli:** Investigation. **Francesco Savini:** Investigation, Formal analysis. **Chiara Bedon:** Methodology. **Manuela Romagnoli:** Supervision, Funding acquisition, Writing. **Michela Nocetti:** Timber Characterization, Supervision, Conceptualization, Funding acquisition. **Michele Brunetti:** Timber Characterization, Funding acquisition. **Massimo Fragiaco:** Supervision, Funding acquisition.

Declaration of Competing Interest

The authors declare that they have no known competing financial interests or personal relationships that could have appeared to influence the work reported in this paper.

Acknowledgements

The authors would like to thank the Pagano Srl and Xlam Dolomiti Srl for the manufacturing of CLT panel and Glulam Beams, Enzo Mattaini from AkzoNobel Coatings Spa for the valuable help and advices.

References

- Bahrami A, Vall A, Khalaf A. Comparison of Cross-Laminated Timber and Reinforced Concrete Floors with Regard to Load-Bearing Properties. *Civ Eng Archit* 2021;9(5):1395–408.
- Li H, Wang BJ, Wang L, Wei P, Wei Y, Wang P. Characterizing engineering performance of bamboo-wood composite cross-laminated timber made from bamboo mat-curtain panel and hem-fir lumber. *Compos Struct* 2021;266:113785. <https://doi.org/10.1016/j.compstruct.2021.113785>.
- M. Chybiński and Ł. Polus, "Experimental and numerical investigations of laminated veneer lumber panels," *Arch. Civ. Eng.*, vol. LXVII, no. 3, pp. 351–372, 2021.
- Romagnoli M, Fragiaco M, Brunori A, Follesa M, Mugnozza G. Solid Wood and Wood Based Composites: The Challenge of Sustainability Looking for a Short and Smart Supply Chain: Innovative Techniques of Representation in Architectural Design. *Lecture Notes Civ Eng* 2019:783–807.
- S. Aicher, Z. Christian, and G. Dill-Langer, "HARDWOOD GLULAMS – EMERGING TIMBER PRODUCTS OF SUPERIOR MECHANICAL PROPERTIES," Sep. 2014, doi: 10.13140/2.1.5170.1120.
- A. Kovryga, S. Peter, and Jan Willem G van de Kuilen, "Mechanical properties and their interrelationships for medium-density European hardwoods, focusing on ash and beech," *Wood Mater. Sci. Eng.*, pp. 289–302, 2019, doi: <https://doi.org/10.1080/17480272.2019.1596158>.
- Aicher S, Ohnesorge D. Shear strength of glued laminated timber made from European beech timberSchubfestigkeit von Brettschichtholz aus europäischem Buchenholz. *Eur J Wood Wood Prod* 2011;69(1):143–54. <https://doi.org/10.1007/s00107-009-0399-9>.
- J. Van Acker, X. Jiang, and J. Van den Bulcke, *Innovative Approaches to Increase Service Life of Poplar Lightweight Hardwood Construction Products*. 2020.
- P. Schlotzhauer, A. Kovryga, L. Emmerich, Bollmus, V. Kuilen, and H. Miltz, "Analysis of Economic Feasibility of Ash and Maple Lamella Production for Glued Laminated Timber," *Forests*, vol. 10, p. 529, Jun. 2019, doi: 10.3390/f10070529.
- F. Carbone, S. Moroni, W. Mattioli, F. Mazzocchi, M. Romagnoli, and L. Portoghesi, "Competitiveness and competitive advantages of chestnut timber laminated products," *Ann. For. Sci.*, vol. 77, Jun. 2020, doi: 10.1007/s13595-020-00950-4.
- Paletto A, Biancolillo I, Bersier J, Keller M, Romagnoli M. A literature review on forest bioeconomy with a bibliometric network analysis. *J For Sci* 2020;66(N0. 7): 265–79. <https://doi.org/10.17221/75/2020-JFS>.
- Sciomenta M, Spera L, Bedon C, Rinaldi V, Fragiaco M, Romagnoli M. Corrigendum to "Mechanical characterization of novel Homogeneous Beech and hybrid Beech-Corsican Pine thin Cross-Laminated timber panels" [*Constr. Build. Mater.* 271 (2021) 121589]. *Constr Build Mater* 2021;288:123495.

- [13] Commissione europea, "Bioeconomy policy." <https://ec.europa.eu/research/bioeconomy/index.cf>, 2017.
- [14] Egner K, Kolb H. Geleimte Träger und Binder aus Buchenholz. *Bau mit Holz* 1966; 68(4):147–54.
- [15] Gehri E. Möglichkeiten des Einsatzes von Buchenholz für Tragkonstruktionen. *Schweizer Bauwirtschaft* 1980;79(56):14–8.
- [16] Ehrhart T, Steiger R, Lehmann M, Frangi A. European beech (*Fagus sylvatica* L.) glued laminated timber: lamination strength grading, production and mechanical properties. *Eur J Wood Wood Prod* 2020;78(5):971–84. <https://doi.org/10.1007/s00107-020-01545-6>.
- [17] Frese M, Blaß HJ. Characteristic bending strength of beech glulam. *Mater Struct* 2007;40(1):3–13. <https://doi.org/10.1617/s11527-006-9117-9>.
- [18] Aicher S, Hirsch M, Christian Z. Hybrid cross-laminated timber plates with beech wood cross-layers. *Constr Build Mater* 2016;124:1007–18. <https://doi.org/10.1016/j.conbuildmat.2016.08.051>.
- [19] M. Brunetti, G. Aminti, M. Nocetti, and G. Russo, "Validation of visual and machine strength grading for Italian beech with additional sampling," *iForest - Biogeosciences For.*, vol. 14, no. 3, pp. 260–267, 2021, doi: <https://doi.org/10.3832/ifer3649-014>.
- [20] M. Brunetti et al., "Structural products made of beech wood: quality assessment of the raw material," *Eur. J. Wood Wood Prod.*, vol. 78, no. 5, pp. 961–970, 2020, doi: [10.1007/s00107-020-01542-9](https://doi.org/10.1007/s00107-020-01542-9).
- [21] Y. Jiang, J. Schaffrath, M. Knorz, S. Winter, and J.-W. van de Kuilen, "Applicability of various wood species in glued laminated timber-parameter study on delamination resistance and shear strength," *WCTE 2014 - World Conf. Timber Eng. Proc.*, Jan. 2014.
- [22] UNI (Ente nazionale italiano di unificazione), "EN 408:2012 - Timber structures - Structural timber and glued laminated timber: Determination of some physical and mechanical properties," 2012.
- [23] UNI (Ente nazionale italiano di unificazione), "EN 14081-2:2018 - Timber structures - Strength graded structural timber with rectangular cross section - Part 2: Machine grading; additional requirements for type testing." 2018.
- [24] M. Nocetti, M. Bacher, M. Brunetti, A. Crivellaro, and J. W. G. van de Kuilen, "Machine grading of Italian structural timber: preliminary results on different wood species," in *World Conference on Timber Engineering*, 2010, pp. 285–292.
- [25] Brunetti M, Aminti G, Nocetti M, Russo G. Validation of visual and machine strength grading for Italian beech with additional sampling. *IForest* 2021;14(3): 260–7. <https://doi.org/10.3832/ifer3649-014>.
- [26] UNI (Ente nazionale italiano di unificazione), "EN 338:2016 - Structural timber - Strength classes." 2016.
- [27] Brunetti M, Nocetti M, Pizzo B, Negro F, Aminti G, Burato P, et al. Comparison of different bonding parameters in the production of beech and combined beech-spruce CLT by standard and optimized tests methods. *Constr Build Mater* 2020; 265:120168. <https://doi.org/10.1016/j.conbuildmat.2020.120168>.
- [28] UNI (Ente nazionale italiano di unificazione), *UNI EN 14358:2016 - Timber structures - Calculation and verification of characteristic values*. 2016.
- [29] Uni. (Ente nazionale italiano di unificazione), "EN 14080:2013 - Timber structures - Glued laminated timber and glued solid timber -. Requirements" 2013.
- [30] Allgemeine bauaufsichtliche Zulassung des DIBt, "Allgemeine bauaufsichtliche Zulassung Z-9.1-679 BS-Holz aus Buche und BS-Holz Buche-Hybridträger." 2019.
- [31] Önorm. "DIN 4074-1: Sortierung von Holz nach der Tragfähigkeit - Teil 1. Nadel-schnittholz" 2012.
- [32] "DIN 20000-5: Anwendung von Bauprodukten in Bauwerken - Teil 5: Nach Festigkeit sortiertes Bauholz für tragende Zwecke mit rechteckigem Querschnitt." 2016.
- [33] Dassault Systèmes Simulia, "Abaqus F.E.A. v. 6.12 computer software." Provid. RI, USA, 2015.

4.2. Timber-timber composite (TTC) joints made of short-supply chain beech: Push-out tests of inclined screw connectors

Following the mechanical characterization of short-supply timber prototypes, it is significant to study possible connection systems to be used in the local building context, both experimentally and in terms of limits required by Italian legislation.

In this paragraph, the ongoing work about experimental tests on timber-to-timber specimens jointed by means of flexible connections is presented.

After a bibliographic study and a general framework about beech forests in Italy and in the Abruzzo Region, the production process of the specimens is described, and the main results are exposed.

Short-term and long-term deflections for different floor spans and joists spacing, with reference to the gamma method and the slip moduli of the connections experimentally tested for determining the bending stiffness of the timber-to-timber composite sections, are evaluated according to the Italian technical standards.

Furthermore, the main ultimate limit states are taken into account to examine their influence in the design process.

Authors: Martina Sciomenta¹, Pasqualino Gualtieri¹, Luca Spera¹, Francesco Contu², Massimo Fragiaco¹

¹ University of L'Aquila, Department of Civil, Construction-Architecture & Environmental Engineering, L'Aquila, Italy.

² Coordination and Planning Office in the Forestry Sector of the Abruzzo Region, L'Aquila, Italy.

4.2.1. Introduction

In the future decades, the climate changes and global warming will harshly affect the natural ecosystems. For coniferous forests, the higher temperatures and drier conditions will make them hard to survive at the current altitudes.

As a consequence, the distribution of conifers will shift at higher altitudes [1], and conifers may be overtaken by deciduous trees which are more adapted to warmer temperatures. The current timber market is bind tightly to the use of conifers and this scenario highlights its vulnerability to the impacts of climate change. Right away, it is necessary to explore alternative timber supply sources and species to preserve the biodiversity, to assure a sustainable and fair supply chain and to avoid prohibitive costs in the future decades.

The 35% of the total land area of Europe is covered by forests; the 46% of European forests are predominantly coniferous, 37% are predominantly broadleaved, and the rest are mixed [2]. By grouping the European countries into six groups with more homogeneous climate features, the latter rates change; in particular the South-West (Italy, Spain and Portugal) regions have predominantly broadleaved stands (61.4%), being beech oak and birch the most widespread species [2].

From the data of the third National Forest Inventory of 2015 (INFC, 2015) it appears that pure broad-leaved forests occupy over 6.220.000 ha in Italy. The beech forests (*Fagus sylvatica L.*) are largely ascribed to this category, occupying a total of 1.053.183 ha and characterizing the mountain landscape of the entire Apennine range, including Sicily.

In the Abruzzo Region these populations present an extension of 124.468 ha, resulting the most widespread forest type in the regional territory [3].

In the central Apennines, the beech forest dominates the mountain horizon at altitudes between 900 and 1900 m above sea level; due to the different climatic conditions (rainfall in particular), it is characterized by peculiar aspects that make it partly different from the Alpine beech forest. Furthermore, the subdivision of the Abruzzo beech forests, as regards the phytosociological aspect, into two large groups can be attributed to climatic factors: thermophilic (low-mountain beech forests) and microthermal beech forests, which occupy the highest mountain range [4]. The first group includes forest populations in which beech mixes with mesophilous broad-leaved trees typical of hilly forests (*Acer sp.*, *Sorbus aucuparia L.*, *Quercus cerris L.*, *Carpinus betulus L.*, *Fraxinus ornus L.*, etc.). Sometimes *Taxus baccata L.*, *Abies alba L.*, *Fraxinus excelsior L.*, *Tilia platyphyllos L.*, *Ulmus glabra L.* become part of the arboreal layer of these woods. These formations, which occupy the altitude range between 900 and 1400 m above sea level, often appear as aged coppices, woods usually cultivated in the past for the production of firewood. In the 1960s extensive interventions were carried out regarding these populations, so that today we often find them in the form of transitional high forests, which, despite having a high forest structure, are mainly made up from individuals of agamic origin.

In microthermal beech forests, the beech grows almost in purity and high forest management is more frequent. These formations are located on the highest mountain massifs of Abruzzo (northern side of the “Gran Sasso”, “Sirente-Velino”, mountains of the Abruzzo National Park, etc.) in the altitude range between 1.400 and 1.900 m above sea level, mainly on north-facing slopes characterized by high atmospheric humidity and fresh, deep soils. In some cases, silver fir is found together with beech,

more frequently in acidophilic formations that grow on alternating sandaceous and sandstone-marly substrates in the “Monti della Laga” and on the north-western slopes of Gran Sasso between 900 and 1.800 m above sea level altitude.

In the Map of Forest Types of Abruzzo (2010) [5], three forest types are identified: (i) the rocky high-mountain beech forest, with an extension calculated at 11.642,58 hectares, which represents the predominantly beech forests located at the limits of the tree vegetation, on very steep slopes, along the ridges and along the warm slopes with rocky outcrops, which are of no interest as regards wood production; (ii) the thermophilic and low-mountain beech forest, whose extension is calculated as 29.960,67 hectares, in which the beech mixes with other broad-leaved trees, in the past intensively used as coppice to obtain firewood and today the subject of extensive conversion interventions trunk, which are of interest for the production of wood for work in the medium-long term; and (iii) the mountain beech forest (eutrophic-mesoneutrophilic-acidophilic), made up of almost pure beech, in excellent growing conditions, located above 1.000 m above sea level. on fertile and deep calcareous or arenaceous soils. The latter type of forest, which occupies 93.732,85 hectares, is the one that presents the greatest interest to produce timber for construction purposes.

4.2.2. State of the art

In the last two decades, the interest in hardwood species for construction purposes has grown fast and, among all species, beech (*Fagus sylvatica L.*) is one with the greatest potential due to its wide diffusion [6], its excellent strength and stiffness properties compared to the well-known softwood species [7] and its relatively ease glueability [8,9]. The most challenging aspects are the high moisture sorptivity and low dimensional stability, leading to high swelling and shrinkage, with the resulting stresses [10] as well as the reduced durability, which allows just its use in service class 1, according to Eurocode 5 [11].

The possibility to use beech timber for load-bearing applications has been investigated since the last decade both in Europe and in Italy [12]. Important studies have been conducted to determine the main mechanical properties of beech sawn timber [13–16], laminated veneer lumber (LVL) [17], cross laminated timber (CLT) panels [18–22] and glued laminated timber (glulam) [23–25] beams. Focusing on these latter load-bearing components, important research was carried out on the assessment of the raw material [26], the lamination strength grading [27,28], the

production [29,30] and the mechanical characterization of glulam [31–33] including the introduction of suitable strength classes [33,34]. The suitability of beech for glulam was recently confirmed by technical approvals in Europe and, in particular, in Germany for load bearing structures [35].

In timber engineering, connections play a fundamental role and due to the influence of wood density to the stiffness of the joints, it was necessary to settle suitable connectors for applications involving hardwoods. For instance, the potential for efficient dowel-type connections with LVL made of beech, in truss structures, was deepened in [36], while the withdrawal and lateral resistance of screw connections for three hardwood species as beech, hornbeam and poplar was studied in [37].

The connectors 'characteristic features are provided by the manufacturers in the product standard (i.e. European Technical Assessment, ETA) for different type of engineered wood products and configurations. It is evident that when such connectors are used in configurations that are not specifically described by the product standards, their performance needs to be evaluated experimentally [38,39]. Push-out tests are usually performed to determine strength and deformation characteristics of joints made with mechanical fasteners and the reference standard is EN 26891 [40].

Several studies were carried out to investigate mechanical performances of connections involving hardwood components, with special focus on beech wood. An extensive experimental programme including fifty-eight push-out tests on a total of fourteen different arrangements of the specimens, varying the species, from softwood to hardwood, the connected timber products, the type and the inclination of the screws, was performed by Schiro et al. [38]. The main results in terms of stiffness, strength, static ductility, residual strength and failure mode were presented and some practical remarks were also highlighted, including the following: (i) double threaded screws despite having a smaller diameter than the single threaded screws, highlighted a greater stiffness; (ii) specimens with hardwood-hardwood or hardwood-softwood configurations, especially when hardwood was employed for the central element, showed higher stiffness and maximum capacity; and (iii) the alternative use of impact driver and grease to realize screws connections in hardwood products.

The influence of the load-to-grain angle and of the fastener diameter on the embedment behaviour of beech wood was investigated through experimental tests and comparison with standards by Franke and Magnière [41]. Also, the withdrawal and lateral resistance of wood screw in three hardwood species, among which beech wood, was studied and a comparison between experimental and predicted values

with theoretical formulations was performed in [37]. The withdrawal strength of laminated veneer lumber made of poplar and beech wood was assessed in transverse, radial and tangential directions, analysing the influence of the veneers thickness, as shown in [42]. Moreover, double-shear steel to timber joints of beech laminated veneer lumber with slotted-in steel plates and high strength steel fasteners were analysed to optimize the connection when considering high mechanical properties wood species and engineered wood products, as described in [43].

In this paper, the mechanical behaviour of timber-to-timber connections (VGZ fully threaded screws produced by Rothoblaas) loaded in shear was investigated for the use on glulam beech, according to the aforementioned standard EN 26891 [40]. In fact, up to now, these screws were tested, certified and calculated only for CLT and high-density woods such as beech LVL but not for glulam. Furthermore, the beech glulam was itself a novel product, which is currently not available on the market. In particular, the glulam employed in this research derives from a short supply chain production aiming to establish the usability of local beech wood for structural purposes and to enhance the use of natural resources in the Abruzzo Region (in central Italy).

4.2.3. Materials and methods

The procurement and selection of raw materials is integral part of the present research since one of its objectives was to realize EWPs in accordance with the principles of short supply chain. First, a survey was carried out jointly with the Coordination and Planning Office in the Forestry Sector of Abruzzo Region aimed at selecting the most suitable native species as well as the best area where to carry out the forest harvesting, since the Abruzzo Region has the highest percentage of protected area of Italy (37%).

The raw material used to manufacture the specimens, including boards and lamellas for glulam beams was local beech (*Fagus sylvatica L.*) originated from the Municipality of Cappadocia, a mountainous territory in the province of L'Aquila (Abruzzo) - Central Italy. To that place, the most extensive forest formation is certainly the beech forest, which originated through both natural and agamic dissemination made up of similar groups more or less uniformly handled with subsequent cuts. The beech high forest is growing extensively from 900 to 1900 meters altitude together with other common species such as: the mountain ash (*Sorbus aucuparia L.*), the whitebeam (*Sorbus aria L.*), the mountain elm (*Ulmus*

glabra L.), the mountain maple (*Acer pseudoplatanus L.*), the Norway maple (*Acer platanoides L.*), the local lime tree (*Tilia platyphyllos Scop*) and, more seldom, the yew (*Taxus baccata L.*).

The forest harvesting for this research's procurement was performed in the framework of a wider silvicultural intervention aiming at carefully handling the forest by thinning it out. More specifically, the scope of this activity was to improve the current conditions of the forest, by respecting the principles of naturalistic silviculture, which supports, without enforcing, the natural evolutionary processes. Therefore, the thinning interventions favours the perpetuation of the forest, protects the biodiversity of the forest heritage and improve the quality of wood enabling the production of timber.

4.2.3.1. Glulam production

The sawn logs were carried from the harvesting site to the sawmill in L'Aquila and properly cut into boards. The boards had a nominal cross-section of 130 mm width and 45 mm thickness, and an average length of 4 m. The board's batch was moved to Lamel Legno S.r.l factory (Montefalcone nel Sannio – CB – Italy) where it was kiln-dried in order to reach the suitable moisture content for the manufacturing gluing process, fixed at 12%. Before further processing, boards were visual graded in accordance with EN 11035-2 as LS2; additionally, the WoodEye system owned by the enterprise was suitably calibrated based on the aforementioned Standard's limit and employed as a support tool for the grading optimization.

Through the use of special automated lines (cross cutting saw line, finger jointing and planer line) the boards were multi-bladed, end-jointed (Fig. 1a) and planed to a thickness of 40 mm to guarantee the suitable planar surface, preferred for the face gluing. The layering of the boards and the face gluing process were mechanically performed (Fig. 1b).

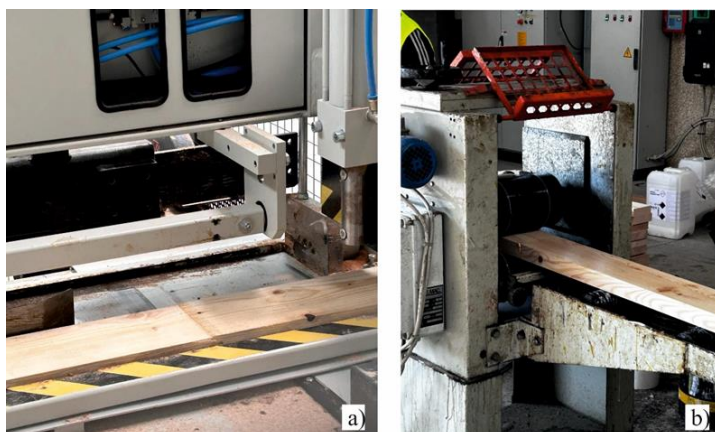


Fig. 1 Glue-laminated timber beams: a) Manufacturing of finger joints and bonding; b) Face gluing.

Timber boards were overlapped and glued together using a Melamine Urea Formaldehyde (MUF) adhesive (GripPro™ Design – AkzoNobel), that was obtained by mixing a two component hardener (H021) and a liquid flexible resin (A002). The choice of employing the melamine adhesive was due to the valuable bonding features recorded in previous experimental programmes which involved the use of beech boards [20,44]. In particular, the GripPro™ adhesive is specifically designed for softwood as well as for hardwood timber, such as beech, birch, oak and chestnut. The adhesive was smeared by means of extrusion systems where the adhesive mixture flows in the form of thin, very fluid and suitably spaced lines, through the orifices of special ducts in which the adhesive is under pressure and is mixed with the hardener (in our case in the ratio 2 to 1) (Fig. 1 right). The average of glue grammage was 180 g/m² for single face and 350 g/m² for double face application, respectively. The adhesive was applied in a factory condition of 23° C, with an environmental relative humidity of 65%. The formed beams were then cold-pressed for 2 hours, with a pressure of 10 bar. As a result, seven six-layered glue-laminated timber beams (B x H x L / 130 x 240 x 4000 mm) were produced in accordance with EN 14080.

4.2.3.2. Timber characterization

Since the visual classification of the timber planks resulted in the LS2 class, the strength class was assumed as D24 according to UNI EN 338:2016 [48].

The mechanical properties of the glulam beams were assessed by testing four beech beams by four-point bending tests in accordance with the EN 408 [49]. The outcomes from this experimental programme are summarized in Table 1.

Table 1 Mechanical properties of planks and glulam beams.

Strength class	$f_{m,k}$ [N/mm ²]	$E_{0,mean}$ [kN/mm ²]	ρ_m [kg/m ³]
D24 (EN 338:2016 [48])	24.00	10.00	580
Experimental glulam	40.00	14.36	695

4.2.3.3. Specimens description

To carry out the push out tests, the common double-shear specimen layout was adopted. It consists of a central timber element flanked by two side elements symmetrically arranged and connected. In this research, the central timber elements were obtained by cutting three glulam beech beams into seven parts with a length of 560 mm. The side elements consisted of beech boards, which were put on stage as a single layer of planking (Series #1) and as a double-crossed planking (Series #2).

In both series, the fully threaded VGZ screws supplied by Rothoblaas were used. Due to the different thickness of the side elements, the fastener length varies from 160 mm for Series #1 to 180 mm for Series #2. Additionally, two different screw diameters were tested, in accordance with the configurations described in Table 2. The fastener spacing was maintained fixed at 200 mm and two screws per side were installed (Fig. 2).

The two series were investigated with the aim to characterize the mechanical behaviour, in terms of stiffness and strength, of the screws designed for the construction of low-engineered timber-to-timber composite (TTC) floors.

Table 2 Test configurations.

Series #	Configuration	Repetitions	Planking		Screw		
			Type	Thickness [mm]	D [mm]	L [mm]	α [°]
1	a	5	single	40	9	160	+45°
	b	5		40	7	160	
2	a	5	double-crossed	30 + 30	9	180	
	b	5		30 + 30	7	180	

Note: α is the screw's angle of inclination with respect to the grain direction

The full-scale construction schemes of the two floors associated with the push outs of Series #1 and Series #2 are represented in Fig. 2.

In particular, the first scheme refers to TTC floor with glulam joists, secondary joists, and single planking; the second scheme regards TTC floor with the same glulam joists and a double-crossed planking. The aim is to propose technical solutions that can be fully developed in the local context of reference, where the wood supply chain is not yet fully developed.

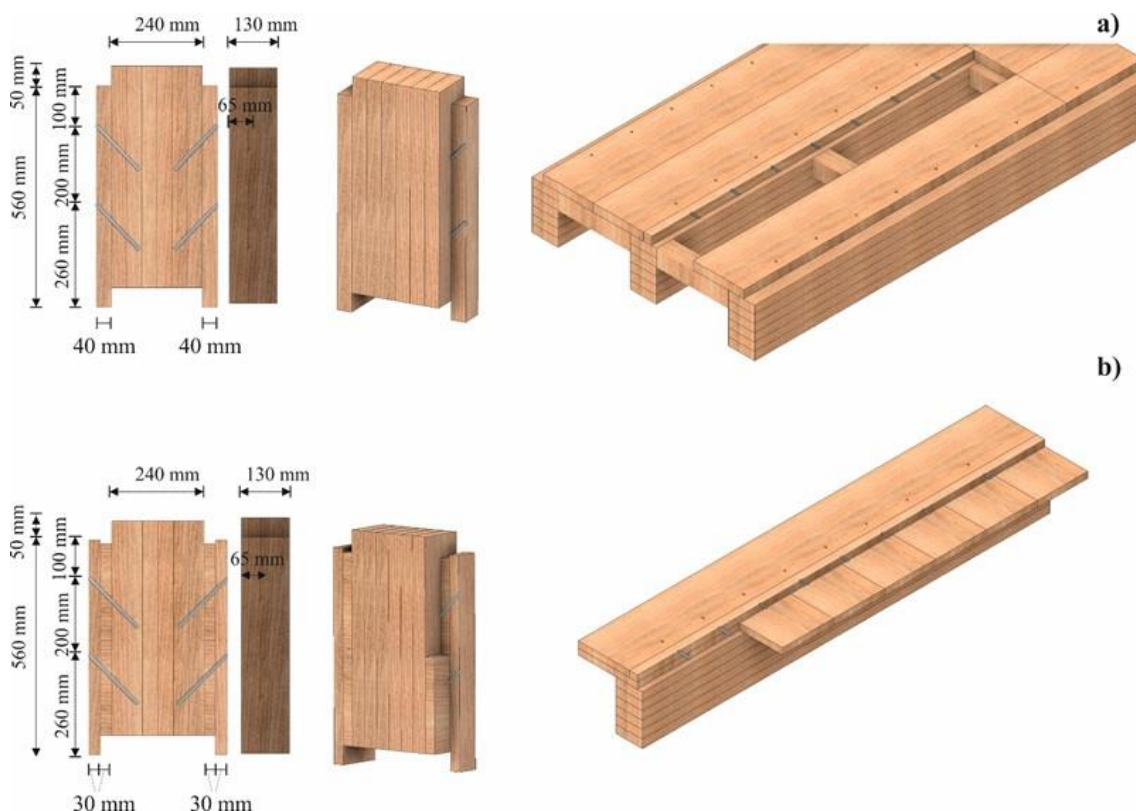


Fig. 2 Push-out specimens and related floor scheme: a) Series 1: single layer of planking with floor joists; b) Series 2: double layer of cross planking.

4.2.3.4. Test setup and instrumentations

The experimental programme was carried out at the laboratory of the Department of Civil, Construction-Architectural and Environmental Engineering (DICEAA) of the University of L'Aquila. It consisted of push-out tests carried out by applying the loading procedure of EN 26891 [40] on each specimen. Firstly, according to the Standard, an estimated maximum load was determined for each of the four configurations (1a, 1b, 2a, 2b). Then, the load was applied up to and maintained for 30 s. The load was then reduced to and maintained for 30 s. Thereafter the load was increased until the slip of 30 mm was reached in accordance with the EN 12512 [46] but the setup was designed to reach a maximum displacement of 50 mm.

The load, introduced by a Zwick Roell universal testing machine (Fig. 3a) through a hydraulic actuator, was monitored with a 300 kN load cell. A constant slip rate of 0,06 mm/s was adopted (it was kept in the range between 0.02 mm/s and 0.2 mm/s recommended by the Eurocode 5 [45]). Two Micro-Epsilon OptoNCDT 1320 | 100 mm laser displacement transducers (LVDTs) were employed (Repeatability of 10 μ m) to measure: i) for the configuration with single planking, the slip between the central and side planking elements (Fig. 3b) and, ii) for the configuration with

double crossed planking, the slip between the central and the inner layer as well as the slip between the central and the outer planking layer (Fig. 3c). Furthermore, the crosshead displacement was recorded. The recording was done continuously with a frequency rate of 2 Hz via a multi-channel data recording device.

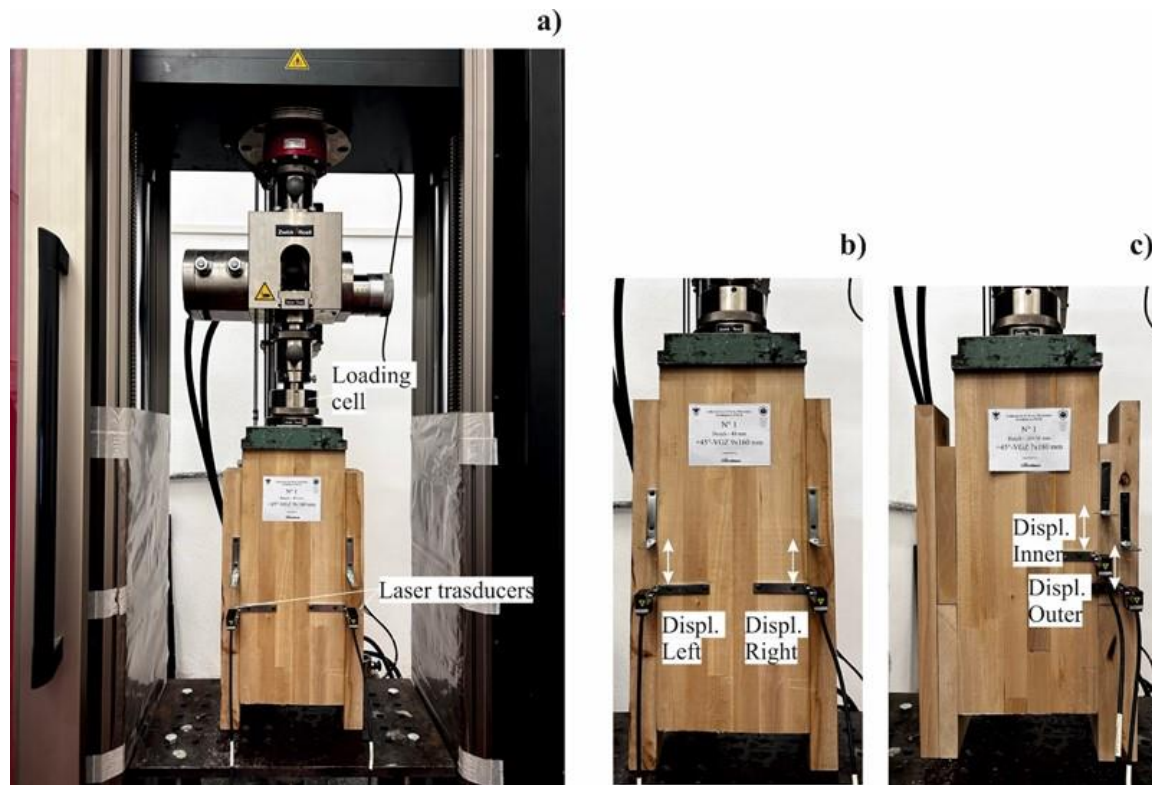


Fig. 3 Tests: a) Testing instruments and loading machine; b) Single-layer planking: laser transducers position; c) Double-layer crossed planking: laser transducers position.

4.2.3.5. Calculation methods of the mechanical parameters of connections

The standards adopted as reference for the evaluation of the connection performance parameters (yield point, secant stiffness, ultimate conditions and static ductility) were EN 12512 [46] and EN 26891 [40]. The slip modulus of the connections (corresponding to the slip modulus provided by EN 1995-1-1 [45]) was calculated by means of the following equation:

$$K_s = \frac{0.4 F_{est}}{\frac{4}{3}(v_{04} - v_{01})} \quad (1)$$

Where v_{01} and v_{04} are the connection slips (evaluated for each specimen) corresponding to the load levels of $0.1F_{est}$ and $0.4F_{est}$ respectively; F_{est} is the estimated maximum load for each configuration based on preliminary tests

(consistently with EN 26891 [40] excluding values that deviated by more than 20% from the mean). For each test, $F'_{\max,i}$ is equal to the actual maximum load $F'_{\max,R}$ when the corresponding slip value was less than 15 mm, otherwise the load corresponding to a 15 mm slip F_{15} was used [40]. According to EN 12512 [46], the yield point (F_y, v_y) was determined, taking into account the pronounced non-linear behaviour of the load-slip curves. The ultimate slip v_u corresponds to the attainment of the first of the following conditions: i) failure of the specimen, ii) slip at 0.8 times $F'_{\max,R}$ on the descending branch, and iii) a slip value of 30 mm [46]. The ductility D is calculated as the ratio between ultimate slip and yield slip according to [46].

4.2.4. Results

The force-displacements curves in terms of shear force versus slip of the entire specimen for all the configurations and screwed connections are plotted in Fig. 4.

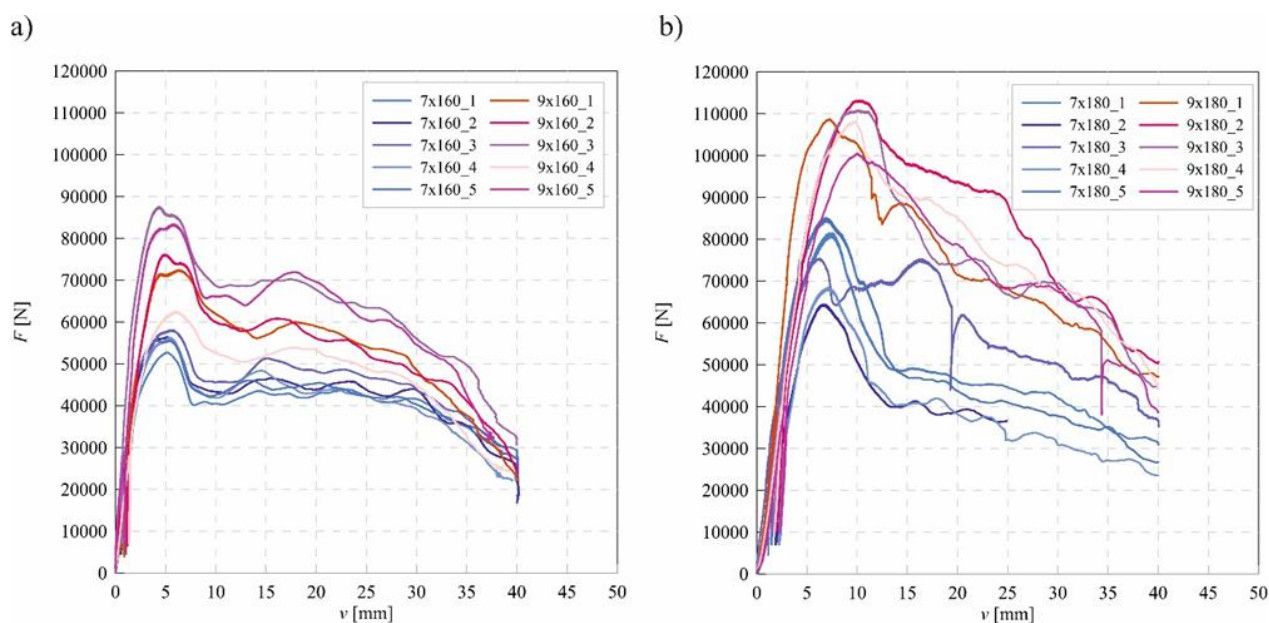


Fig. 4 Test results: a) single planking; b) double-crossed planking.

The experimental results in terms of ultimate force F'_{\max} , slip modulus K_s (assessed according to EN 1995-1-1 [45]), yielding force F_y (evaluated according to EN 12512 case B [46]), yielding displacement v_y , ultimate displacement v_u and ductility D (calculated according to EN 12512 [46]) of the entire connection system for each specimen are given in Tables 3-6.

Table 3 Screw configuration 1a ($F_{est} = 60$ kN).

Specimens	F'_{max}	K_s	F_y	v_y	v_u	D
	[kN]	[kN/mm]	[kN]	[mm]	[mm]	[-]
9x160_1	72,43	20,24	70,73	3,61	30,00	8,31
9x160_2	76,13	17,69	73,47	3,94	30,00	7,61
9x160_3	87,56	27,49	80,09	2,79	30,00	10,74
9x160_4	62,47	20,86	53,60	2,40	30,00	12,50
9x160_5	83,38	23,89	77,05	3,06	30,00	9,81
Mean	76,39	22,03	70,99	3,16	30,00	9,80
St. dev	8,75	3,37	9,25	0,55		1,74
CoV	11,5%	15,3%	13,0%	17,5%		17,8%

Table 4 Screw configuration 2a ($F_{est} = 100$ kN).

Specimens	F'_{max}	K_s	F_y	v_y	v_u	D
	[kN]	[kN/mm]	[kN]	[mm]	[mm]	[-]
9x180_1	108,63	19,50	101,38	5,01	30,00	5,99
9x180_2	113,14	19,32	100,27	5,76	30,00	5,21
9x180_3	110,87	20,45	96,91	5,08	30,00	5,91
9x180_4	108,13	18,33	95,92	5,53	30,00	5,43
9x180_5	100,51	17,49	88,79	5,63	30,00	5,33
Mean	108,25	19,02	96,65	5,40	30,00	5,57
St. dev	4,26	1,02	4,42	0,30		0,31
CoV	3,9%	5,4%	4,6%	5,5%		5,6%

Regarding the 9 mm diameter screws, in the single planking configuration a lower mean ultimate force and a greater mean slip modulus were measured and assessed with respect to the double planking configuration. In addition, the presented standard deviation and the coefficient of variation values show less scatter for the case with double planking. The mean ductility value is greater for the single planking case which presents also a greater scatter of the ductility values.

Table 5 Screw configuration 1b ($F_{est} = 45$ kN).

Specimens	F'_{max}	K_s	F_y	v_y	v_u	D
	[kN]	[kN/mm]	[kN]	[mm]	[mm]	[-]
7x160_1	52,70	28,01	38,01	1,28	30,00	23,41
7x160_2	56,39	24,67	47,12	2,28	30,00	13,17
7x160_3	58,06	16,83	53,41	3,14	30,00	9,56
7x160_4	56,26	17,61	50,36	2,72	30,00	11,05
7x160_5	55,67	32,24	43,22	1,25	30,00	24,00
Mean	55,81	23,87	46,42	2,13	30,00	16,24
St. dev	1,75	5,94	5,40	0,76		6,21
CoV	3,1%	24,9%	11,6%	35,6%		38,2%

Table 6 Screw configuration 2b ($F_{est} = 60$ kN).

Specimens	F'_{max}	K_s	F_y	v_y	v_u	D
	[kN]	[kN/mm]	[kN]	[mm]	[mm]	[-]
7x180_1	81,49	20,40	68,98	3,70	9,83	2,66
7x180_2	64,43	11,70	61,47	5,24	9,83	1,88
7x180_3	75,37	19,18	66,40	3,21	21,24	6,62
7x180_4	68,48	10,68	66,54	6,02	30,00	4,98
7x180_5	85,10	22,89	74,13	3,67	30,00	8,18
Mean	74,97	16,97	67,50	4,37	20,18	4,86
St. dev	7,73	4,88	4,11	1,07		2,36
CoV	10,3%	28,7%	6,1%	24,6%		48,5%

Even for the 7 mm diameter screws, the single planking configuration leads to a lower mean ultimate force and a greater mean slip modulus with respect to the double planking configuration. On the contrary, the standard deviation and the coefficient of variation values show less scatter for the single planking case with the exception of the standard deviation of the slip modulus. The mean ductility value is

greater for the single planking case which presents also a greater standard deviation and a lower coefficient of variation of the ductility values.

4.2.5. Deflection limits

Italian technical standard for buildings [47] does not provide deflection limits for timber floors. On the other hand, deflection limits are given for steel floors and roofs, so they can be taken as a reference for floors and roofs in general.

Considering the two cases of timber floors previously described (i.e. glulam joists connected by screws with single planking and glulam joists connected by screws with double-crossed planking), the short-term and long-term deflection limits can be assumed as 1/300 and 1/250 of the floor span, respectively.

To determine the geometrical limits of the aforementioned timber floors in terms of floor span and joists spacing, calculations of the short-term and long-term deflections under structural permanent, non-structural permanent and variable load were performed. The bending stiffness of the TTC section was evaluated according to the γ -method, i.e. the mechanically jointed beam theory provided by Annex B of Eurocode 5 [45] for composite beams with flexible shear connections, assuming as the slip modulus the mean experimental value for each configuration for the single fastener as given in Table 7.

Table 7 Experimental slip moduli for the single fastener.

Configurations	K_s [kN/mm]
7x160	5.97
7x180	4.24
9x160	5.51
9x180	4.76

4.2.5.1. Short-term deflection

The short-term deflection is usually assessed according to the so-called characteristic (or rare) load combination [47] without the permanent loads. For floors under a unique variable load, the combination load is equal to the variable

load itself. Considering the TTC section composed by a single glulam joist screwed to the upper planking, the deflections for different floor spans, joists spacings, and variable load (Q_k) values were evaluated so as to compare them to the standard limits (Tables 8, 9).

Table 8 Short-term deflections values [mm] varying geometry for $Q_k = 2 \text{ kN/m}^2$.

j.s.	Connection	Span [m]			
		4.5	5.0	5.5	6.0
0.50 m	7x160	1.55	2.31	3.31	4.59
	7x180	1.77	2.64	3.80	5.28
	9x160	1.56	2.33	3.34	4.64
	9x180	1.75	2.61	3.75	5.21
0.55 m	7x160	1.65	2.47	3.54	4.92
	7x180	1.90	2.84	4.08	5.68
	9x160	1.66	2.49	3.57	4.96
	9x180	1.88	2.81	4.04	5.61
0.60 m	7x160	1.75	2.62	3.76	5.23
	7x180	2.03	3.03	4.36	6.07
	9x160	1.76	2.64	3.79	5.27
	9x180	2.01	3.00	4.31	6.00
Short-term deflection limits [mm]		15.00	16.70	18.30	20.00

Legend: j.s. = joints spacing

Table 9 Short-term deflections values [mm] varying geometry for $Q_k = 4 \text{ kN/m}^2$.

j.s.	Connection	Span [m]			
		4.5	5.0	5.5	6.0
0.50 m	7x160	3.09	4.61	6.62	9.19
	7x180	3.54	5.28	7.59	10.55
	9x160	3.12	4.65	6.68	9.27
	9x180	3.50	5.22	7.50	10.42
0.55 m	7x160	3.30	4.93	7.08	9.84
	7x180	3.80	5.69	8.17	11.36
	9x160	3.33	4.97	7.14	9.93
	9x180	3.76	5.62	8.07	11.22
0.60 m	7x160	3.50	5.24	7.52	10.46
	7x180	4.06	6.07	8.72	12.14
	9x160	3.53	5.28	7.59	10.55
	9x180	4.02	6.00	8.62	11.99
Short-term deflection limits [mm]		15.00	16.70	18.30	20.00

Legend: j.s. = joints spacing

With regard to the considered geometries, the short-term deflections are lower than the standard limits of 1/300 of the floor span, even in the case of the maximum span and maximum joists spacing under the variable load of 4 kN/m².

4.2.5.2. Long-term deflection

The long-term deflection is usually assessed by adding two contributions: the instantaneous deflection due to the so-called characteristic (or rare) load combination, and the creep deflection due to the so-called quasi-permanent load combination [47]. Similarly to the previous paragraph, the long-term deflections were estimated considering in this case two different values of non-structural permanent load G_{k2} as shown in Tables 10-13. The long-term deflection is assessed according to EN 1995-1-1:2004 [45], namely by multiplying the elastic deflection assessed with the γ -method by the creep coefficient of the shear connection (the deformation coefficient k_{def} according to EN 1995-1-1:2004 [45] for which the value 0.6 has been assumed).

Table 10 Long-term deflections values [mm] ($G_{k2} = 1\text{kN/m}^2$ and $Q_k = 2\text{kN/m}^2$).

j.s.	Connection	Span [m]			
		4.5	5.0	5.5	6.0
0.50 m	7x160	3.93	5.86	8.40	11.66
	7x180	4.61	6.88	9.89	13.75
	9x160	3.96	5.91	8.47	11.77
	9x180	4.56	6.81	9.77	13.58
0.55 m	7x160	4.20	6.27	9.00	12.50
	7x180	4.95	7.41	10.64	14.80
	9x160	4.23	6.32	9.08	12.61
	9x180	4.90	7.33	10.52	14.62
0.60 m	7x160	4.46	6.67	9.57	13.31
	7x180	5.28	7.90	11.36	15.81
	9x160	4.49	6.72	9.65	13.42
	9x180	5.23	7.82	11.23	15.62
Long-term deflection limits [mm]		18.00	20.00	22.00	24.00

Legend: j.s. = joints spacing

Table 11 Long-term deflections values [mm] ($G_{k2} = 2\text{kN/m}^2$ and $Q_k = 2\text{kN/m}^2$).

j.s.	Connection	Span [m]			
		4.5	5.0	5.5	6.0
0.50 m	7x160	5.16	7.70	11.04	15.33
	7x180	6.02	9.00	12.92	17.97
	9x160	5.20	7.77	11.14	15.48
	9x180	5.96	8.90	12.77	17.75

0.55 m	7x160	5.52	8.25	11.83	16.44
	7x180	6.47	9.68	13.91	19.35
	9x160	5.56	8.31	11.93	16.58
	9x180	6.41	9.57	13.75	19.11
0.60 m	7x160	5.86	8.76	12.58	17.49
	7x180	6.90	10.33	14.85	20.67
	9x160	5.91	8.83	12.69	17.64
	9x180	6.84	10.22	14.68	20.42

Long-term deflection limits [mm] 18.00 20.00 22.00 24.00

Legend: j.s. = joints spacing

Table 12 Long-term deflections values [mm] ($G_{k2} = 1\text{kN/m}^2$ and $Q_k = 4\text{kN/m}^2$).

j.s.	Connection	Span [m]			
		4.5	5.0	5.5	6.0
0.50 m	7x160	6.31	9.41	13.49	18.73
	7x180	7.33	10.95	15.73	21.88
	9x160	6.36	9.49	13.61	18.91
	9x180	7.25	10.83	15.55	21.61
0.55 m	7x160	6.75	10.07	14.45	20.07
	7x180	7.88	11.78	16.93	23.55
	9x160	6.80	10.15	14.58	20.26
	9x180	7.80	11.65	16.74	23.26
0.60 m	7x160	7.16	10.70	15.37	21.36
	7x180	8.41	12.58	18.08	25.16
	9x160	7.21	10.78	15.49	21.55
	9x180	8.32	12.44	17.87	24.85

Long-term deflection limits [mm] 18.00 20.00 22.00 24.00

Legend: j.s. = joints spacing

Table 13 Long-term deflections values [mm] ($G_{k2} = 2\text{kN/m}^2$ and $Q_k = 4\text{kN/m}^2$).

j.s.	Connection	Span [m]			
		4.5	5.0	5.5	6.0
0.50 m	7x160	7.55	11.26	16.14	22.41
	7x180	8.74	13.07	18.77	26.10
	9x160	7.60	11.35	16.28	22.61
	9x180	8.65	12.92	18.55	25.78
0.55 m	7x160	8.07	12.05	17.29	24.01
	7x180	9.40	14.06	20.20	28.10
	9x160	8.13	12.14	17.43	24.23
	9x180	9.31	13.90	19.96	27.75
0.60 m	7x160	8.56	12.80	18.38	25.54
	7x180	10.03	15.00	21.57	30.01
	9x160	8.62	12.90	18.53	25.76

	9x180	9.93	14.84	21.32	29.65
Long-term deflection limits [mm]		18.00	20.00	22.00	24.00

Legend: j.s. = joists spacing

Regarding the studied geometries, the long-term deflections are lower than the standard limits of 1/250 of the floor span under the variable load of 2 kN/m²; instead for Q_k = 4 kN/m² the deflections exceed the standard limits: i) in the case of G_{k2} = 1 kN/m² for a 6.0 m span and joists spacing of 0.6m; ii) in the case of G_{k2} = 2 kN/m² for a 6 m span whatever the joists spacing.

4.2.6. Ultimate limit states

The ultimate limit states (ULS) verifications according to the Italian technical standard for buildings [47] are described in this section. The slip moduli at ULS of the composite section for the four deformable cases were assessed as 2/3 of the slip modulus at serviceability limit states (SLS) and are given in Table 14.

Table 14 Slip moduli at ULS for the single fastener.

Configurations	K_u
	[kN/mm]
7x160	3.98
7x180	2.83
9x160	3.67
9x180	3.17

Considering the same geometrical properties, mechanical properties and loads of the previous section, the design bending moments and axial forces were divided between joist and upper planking according to the equations (2 to 5) from the mechanically jointed beam theory [45], using subscript n= 1 for the planking and subscript n= 2 for the joist.

$$M_1(x) = \frac{E_1 I_1}{(EI)_{eff}} \cdot M(x) \quad (2)$$

$$M_2(x) = \frac{E_2 I_2}{(EI)_{eff}} \cdot M(x) \quad (3)$$

$$N_1(x) = \frac{\gamma_1 E_1 A_1 a_1}{(EI)_{eff}} \cdot M(x) \quad (4)$$

$$N_2(x) = \frac{\gamma_2 E_2 A_2 a_2}{(EI)_{eff}} \cdot M(x) \quad (5)$$

The ultimate limit state for coupled tension and bending of the joist was examined. The design tensile $f_{t,o,d}$ (parallel to the grain) and bending $f_{m,d}$ strengths were estimated equal to 12.05 N/mm² and 20.09 N/mm², respectively, according to [47] (assuming $k_{mod} = 0.8$ and $\gamma_M = 1.45$).

The design tensile $\sigma_{t,o,d}$ and bending $\sigma_{m,d}$ stresses due to the fundamental load combination [47], along with the verification ratios which must be lower than or equal to the unit according to the design inequalities (6-7), for each geometry and load condition, are reported in Tables 15-18.

$$\frac{\sigma_{t,o,d}}{f_{t,o,d}} + \frac{\sigma_{m,y,d}}{f_{m,y,d}} + k_m \cdot \frac{\sigma_{m,z,d}}{f_{m,z,d}} \leq 1 \quad (6)$$

$$\frac{\sigma_{t,o,d}}{f_{t,o,d}} + k_m \cdot \frac{\sigma_{m,y,d}}{f_{m,y,d}} + \frac{\sigma_{m,z,d}}{f_{m,z,d}} \leq 1 \quad (7)$$

Table 15 ULS for coupled tensile-bending ($G_{k2} = 1$ kN/m² and $Q_k = 2$ kN/m²).

j.s.	Connection	Span [m]											
		4.5			5.0			5.5			6.0		
		$\sigma_{t,o,d}$ [N/mm ²]	$\sigma_{m,d}$ [N/mm ²]	v.r. [-]	$\sigma_{t,o,d}$ [N/mm ²]	$\sigma_{m,d}$ [N/mm ²]	v.r. [-]	$\sigma_{t,o,d}$ [N/mm ²]	$\sigma_{m,d}$ [N/mm ²]	v.r. [-]	$\sigma_{t,o,d}$ [N/mm ²]	$\sigma_{m,d}$ [N/mm ²]	v.r. [-]
0.50 m	7x160	1.13	3.15	0.25	1.49	4.13	0.33	1.82	5.07	0.40	2.15	5.97	0.48
	7x180	1.01	3.59	0.26	1.33	4.71	0.34	1.63	5.79	0.42	1.93	6.84	0.50
	9x160	1.14	3.17	0.25	1.50	4.16	0.33	1.84	5.11	0.41	2.17	6.02	0.48
	9x180	1.00	3.56	0.26	1.32	4.67	0.34	1.62	5.73	0.42	1.91	6.76	0.50
0.55 m	7x160	1.28	3.33	0.27	1.68	4.36	0.36	2.06	5.36	0.44	2.43	6.32	0.52
	7x180	1.16	3.82	0.29	1.52	5.01	0.38	1.87	6.17	0.46	2.21	7.28	0.55
	9x160	1.29	3.35	0.27	1.69	4.39	0.36	2.07	5.40	0.44	2.45	6.37	0.52
	9x180	1.15	3.79	0.28	1.50	4.96	0.37	1.85	6.10	0.46	2.18	7.20	0.54
0.60	7x160	1.42	3.49	0.29	1.86	4.58	0.38	2.29	5.63	0.47	2.71	6.65	0.56

7x180	1.30	4.03	0.31	1.71	5.29	0.41	2.10	6.52	0.50	2.48	7.71	0.59
9x160	1.43	3.51	0.29	1.88	4.61	0.39	2.31	5.67	0.47	2.73	6.70	0.56
9x180	1.29	4.00	0.31	1.69	5.25	0.40	2.08	6.46	0.49	2.46	7.62	0.58

Legend: j.s. = joints spacing; v.r. = verification ratio.

Table 16 ULS for coupled tensile-bending ($G_{k2} = 2 \text{ kN/m}^2$ and $Q_k = 2 \text{ kN/m}^2$).

j.s.	Connection	Span [m]											
		4.5			5.0			5.5			6.0		
		$\sigma_{t,0,d}$ [N/mm ²]	$\sigma_{m,d}$ [N/mm ²]	v.r. [-]	$\sigma_{t,0,d}$ [N/mm ²]	$\sigma_{m,d}$ [N/mm ²]	v.r. [-]	$\sigma_{t,0,d}$ [N/mm ²]	$\sigma_{m,d}$ [N/mm ²]	v.r. [-]	$\sigma_{t,0,d}$ [N/mm ²]	$\sigma_{m,d}$ [N/mm ²]	v.r. [-]
0.50 m	7x160	1.45	4.02	0.32	1.90	5.27	0.42	2.33	6.47	0.52	2.75	7.63	0.61
	7x180	1.29	4.58	0.34	1.70	6.01	0.44	2.09	7.40	0.54	2.46	8.74	0.64
	9x160	1.46	4.05	0.32	1.91	5.31	0.42	2.35	6.52	0.52	2.77	7.69	0.61
	9x180	1.28	4.55	0.33	1.68	5.96	0.44	2.07	7.32	0.54	2.44	8.64	0.63
0.55 m	7x160	1.64	4.26	0.35	2.14	5.58	0.46	2.64	6.86	0.56	3.11	8.09	0.66
	7x180	1.48	4.88	0.37	1.94	6.41	0.48	2.39	7.89	0.59	2.82	9.32	0.70
	9x160	1.65	4.28	0.35	2.16	5.62	0.46	2.65	6.91	0.56	3.13	8.16	0.67
	9x180	1.47	4.85	0.36	1.92	6.35	0.48	2.37	7.81	0.59	2.79	9.22	0.69
0.60 m	7x160	1.82	4.48	0.37	2.39	5.87	0.49	2.94	7.23	0.60	3.47	8.53	0.71
	7x180	1.67	5.17	0.40	2.19	6.79	0.52	2.70	8.36	0.64	3.19	9.88	0.76
	9x160	1.83	4.50	0.38	2.41	5.91	0.49	2.96	7.28	0.61	3.50	8.60	0.72
	9x180	1.65	5.13	0.39	2.17	6.73	0.52	2.67	8.28	0.63	3.15	9.78	0.75

Legend: j.s. = joints spacing; v.r. = verification ratio.

Table 17 ULS for coupled tensile-bending ($G_{k2} = 1 \text{ kN/m}^2$ and $Q_k = 4 \text{ kN/m}^2$).

j.s.	Connection	Span [m]											
		4.5			5.0			5.5			6.0		
		$\sigma_{t,0,d}$ [N/mm ²]	$\sigma_{m,d}$ [N/mm ²]	v.r. [-]	$\sigma_{t,0,d}$ [N/mm ²]	$\sigma_{m,d}$ [N/mm ²]	v.r. [-]	$\sigma_{t,0,d}$ [N/mm ²]	$\sigma_{m,d}$ [N/mm ²]	v.r. [-]	$\sigma_{t,0,d}$ [N/mm ²]	$\sigma_{m,d}$ [N/mm ²]	v.r. [-]
0.50 m	7x160	1.76	4.90	0.39	2.31	6.41	0.51	2.84	7.88	0.63	3.34	9.29	0.74
	7x180	1.57	5.58	0.41	2.07	7.32	0.54	2.54	9.00	0.66	3.00	10.63	0.78
	9x160	1.77	4.93	0.39	2.33	6.46	0.51	2.86	7.94	0.63	3.37	9.36	0.75
	9x180	1.56	5.53	0.40	2.05	7.25	0.53	2.51	8.91	0.65	2.97	10.51	0.77
0.55 m	7x160	1.99	5.19	0.42	2.61	6.80	0.56	3.21	8.36	0.68	3.79	9.86	0.81
	7x180	1.80	5.95	0.45	2.37	7.81	0.59	2.91	9.62	0.72	3.44	11.36	0.85
	9x160	2.01	5.22	0.43	2.63	6.85	0.56	3.24	8.42	0.69	3.82	9.94	0.81
	9x180	1.79	5.90	0.44	2.34	7.74	0.58	2.88	9.52	0.71	3.40	11.24	0.84
0.60 m	7x160	2.22	5.46	0.46	2.92	7.17	0.60	3.59	8.82	0.74	4.24	10.41	0.87
	7x180	2.03	6.31	0.48	2.67	8.28	0.63	3.29	10.20	0.78	3.89	12.06	0.92
	9x160	2.23	5.49	0.46	2.94	7.21	0.60	3.61	8.88	0.74	4.27	10.49	0.88
	9x180	2.02	6.26	0.48	2.65	8.21	0.63	3.26	10.10	0.77	3.85	11.93	0.91

Legend: j.s. = joints spacing; v.r. = verification ratio.

Table 18 ULS for coupled tensile-bending ($G_{k2}=2 \text{ kN/m}^2$ and $Q_k = 4 \text{ kN/m}^2$).

j.s.	Connection	Span [m]											
		4.5			5.0			5.5			6.0		
		$\sigma_{t,0,d}$ [N/mm ²]	$\sigma_{m,d}$ [N/mm ²]	v.r. [-]	$\sigma_{t,0,d}$ [N/mm ²]	$\sigma_{m,d}$ [N/mm ²]	v.r. [-]	$\sigma_{t,0,d}$ [N/mm ²]	$\sigma_{m,d}$ [N/mm ²]	v.r. [-]	$\sigma_{t,0,d}$ [N/mm ²]	$\sigma_{m,d}$ [N/mm ²]	v.r. [-]
0.50 m	7x160	2.08	5.77	0.46	2.72	7.56	0.60	3.34	9.28	0.74	3.94	10.94	0.87
	7x180	1.85	6.57	0.48	2.43	8.62	0.63	2.99	10.61	0.78	3.53	12.53	0.92
	9x160	2.09	5.81	0.46	2.74	7.61	0.61	3.37	9.35	0.74	3.97	11.03	0.88
	9x180	1.84	6.52	0.48	2.41	8.54	0.63	2.96	10.50	0.77	3.50	12.39	0.91
0.55 m	7x160	2.35	6.12	0.50	3.08	8.02	0.66	3.79	9.86	0.81	4.47	11.63	0.95
	7x180	2.13	7.02	0.53	2.79	9.22	0.69	3.43	11.34	0.85	4.06	13.40	1.00
	9x160	2.36	6.15	0.50	3.10	8.08	0.66	3.82	9.93	0.81	4.51	11.73	0.96
	9x180	2.11	6.96	0.52	2.77	9.13	0.68	3.40	11.23	0.84	4.01	13.26	0.99
0.60 m	7x160	2.62	6.45	0.54	3.44	8.46	0.71	4.24	10.41	0.87	5.00	12.29	1.03
	7x180	2.40	7.44	0.57	3.15	9.78	0.75	3.88	12.04	0.92	4.59	14.23	1.09
	9x160	2.64	6.48	0.54	3.46	8.51	0.71	4.26	10.48	0.88	5.04	12.38	1.03
	9x180	2.38	7.39	0.57	3.13	9.69	0.74	3.85	11.93	0.91	4.54	14.09	1.08

Legend: j.s. = joints spacing; v.r. = verification ratio.

Only with $G_{k2} = 2 \text{ kN/m}^2$ and $Q_k = 4 \text{ kN/m}^2$ for 6 m span and 0.60 m joist spacing, the design inequalities are not satisfied for each connection type. With regard to the case of 6 m span and 0.55 m joist spacing, the verification ratio overcomes the unit only for the 7x180 connection.

Even for the loads of Table 18, the joist spacing equal to 0.60 m and the floor span equal to 6.0 m, the design compression stresses $\sigma_{c,0,d}$ are lower than both the design compression strength parallel to the grain $f_{c,0,d}$ (estimated of 15.06 N/mm^2 from a characteristic value of 21.00 N/mm^2) and the design compression strength perpendicular to the grain $f_{c,90,d}$ (estimated of 3.51 N/mm^2 from a characteristic value of 4.90 N/mm^2) of the upper planking (D24 strength class), as shown in Table 19.

Table 19 Design compression stresses $\sigma_{c,0,d}$ for the planking.

Configurations	$\sigma_{c,0,d}$
	[N/mm ²]
7x160	1.51
7x180	1.77
9x160	1.43
9x180	1.91

In addition, the design loads on a fastener, assessed according to equation (8) of Annex B of Eurocode 5 [45] and using subscript $i=1$ for the planking and subscript $i=2$ for the joist, are reported in Tables 20 to 23.

$$F_i = \frac{\gamma_i E_i A_i a_i s_i}{(EI)_{ef}} V \quad (8)$$

For each connection case, the design load values of the fastener were compared to the design shear strengths of the connection according to [47], assuming $k_{mod} = 0.8$ and $\gamma_M = 1.25$, marking in bold the values exceeding the corresponding strengths.

The characteristic strengths of the single screw were assessed from the experimental ultimate force F_{max} values (Tables 2 to 5) divided by 4 to obtain the value for the single fastener. Considering in the design two screws spaced at 200 mm centre to centre along the joist span, the following design strengths were evaluated: 15.64 kN for 7x160; 17.13 kN for 7x180; 16.67 kN for 9x160; 30.34 kN for 9x180.

Table 20 Load on a fastener $F_{i,d}$ ($G_{k2} = 1 \text{ kN/m}^2$ and $Q_k = 2 \text{ kN/m}^2$).

j.s.	Connection	Span [m]							
		4.5		5.0		5.5		6.0	
		$F_{1,d}$ [kN]	$F_{2,d}$ [kN]	$F_{1,d}$ [kN]	$F_{2,d}$ [kN]	$F_{1,d}$ [kN]	$F_{2,d}$ [kN]	$F_{1,d}$ [kN]	$F_{2,d}$ [kN]
0.50 m	7x160	1.20	7.08	1.56	7.73	1.95	8.35	2.38	8.95
	7x180	1.02	6.32	1.33	6.91	1.68	7.48	2.05	8.03
	9x160	1.13	7.12	1.47	7.78	1.85	8.41	2.26	9.02
	9x180	1.12	6.27	1.45	6.85	1.81	7.40	2.21	7.94
0.55 m	7x160	1.25	7.97	1.62	8.71	2.04	9.42	2.51	10.11
	7x180	1.08	7.21	1.41	7.89	1.78	8.54	2.19	9.17
	9x160	1.17	8.02	1.53	8.77	1.93	9.49	2.38	10.19
	9x180	1.18	7.15	1.53	7.82	1.92	8.46	2.35	9.08
0.60 m	7x160	1.29	8.86	1.68	9.69	2.13	10.49	2.61	11.26
	7x180	1.13	8.11	1.47	8.88	1.87	9.62	2.30	10.34
	9x160	1.21	8.91	1.58	9.75	2.01	10.56	2.48	11.35
	9x180	1.23	8.05	1.60	8.80	2.02	9.53	2.49	10.23

Legend: j.s. = joists spacing

Table 21 Load on a fastener $F_{i,d}$ ($G_{k2} = 2 \text{ kN/m}^2$ and $Q_k = 2 \text{ kN/m}^2$).

j.s.	Connection	Span [m]							
		4.5		5.0		5.5		6.0	
		$F_{1,d}$ [kN]	$F_{2,d}$ [kN]	$F_{1,d}$ [kN]	$F_{2,d}$ [kN]	$F_{1,d}$ [kN]	$F_{2,d}$ [kN]	$F_{1,d}$ [kN]	$F_{2,d}$ [kN]
0.50 m	7x160	1.53	9.04	1.99	9.87	2.49	10.66	3.04	11.43
	7x180	1.31	8.07	1.70	8.83	2.14	9.55	2.62	10.25

	9x160	1.44	9.10	1.87	9.94	2.36	10.75	2.89	11.52
	9x180	1.43	8.00	1.85	8.74	2.31	9.45	2.82	10.14
0.55 m	7x160	1.60	10.21	2.08	11.15	2.62	12.06	3.21	12.94
	7x180	1.38	9.23	1.80	10.10	2.27	10.93	2.80	11.74
	9x160	1.50	10.27	1.96	11.23	2.47	12.15	3.04	13.04
	9x180	1.51	9.15	1.96	10.01	2.46	10.82	3.01	11.62
0.60 m	7x160	1.65	11.37	2.16	12.43	2.73	13.46	3.35	14.44
	7x180	1.44	10.40	1.89	11.38	2.39	12.34	2.95	13.26
	9x160	1.55	11.43	2.03	12.51	2.57	13.55	3.17	14.55
	9x180	1.58	10.32	2.06	11.28	2.60	12.22	3.19	13.12

Legend: j.s. = joists spacing

Table 22 Load on a fastener $F_{i,d}$ ($G_{k2} = 1 \text{ kN/m}^2$ and $Q_k = 4 \text{ kN/m}^2$).

j.s.	Connection	Span [m]							
		4.5		5.0		5.5		6.0	
		$F_{1,d}$ [kN]	$F_{2,d}$ [kN]	$F_{1,d}$ [kN]	$F_{2,d}$ [kN]	$F_{1,d}$ [kN]	$F_{2,d}$ [kN]	$F_{1,d}$ [kN]	$F_{2,d}$ [kN]
0.50 m	7x160	1.86	11.00	2.42	12.01	3.03	12.98	3.70	13.91
	7x180	1.59	9.82	2.07	10.74	2.61	11.62	3.19	12.48
	9x160	1.75	11.07	2.28	12.09	2.87	13.08	3.52	14.02
	9x180	1.74	9.74	2.25	10.64	2.81	11.50	3.43	12.34
0.55 m	7x160	1.95	12.44	2.53	13.59	3.19	14.70	3.91	15.77
	7x180	1.68	11.25	2.19	12.31	2.77	13.33	3.41	14.31
	9x160	1.83	12.51	2.39	13.68	3.02	14.81	3.71	15.89
	9x180	1.84	11.16	2.39	12.19	3.00	13.19	3.67	14.16
0.60 m	7x160	2.02	13.87	2.63	15.17	3.33	16.42	4.09	17.63
	7x180	1.76	12.69	2.31	13.89	2.92	15.05	3.60	16.17
	9x160	1.89	13.94	2.48	15.26	3.14	16.53	3.87	17.76
	9x180	1.93	12.59	2.51	13.77	3.17	14.91	3.89	16.00

Legend: j.s. = joists spacing

Table 23 Load on a fastener $F_{i,d}$ ($G_{k2} = 2 \text{ kN/m}^2$ and $Q_k = 4 \text{ kN/m}^2$).

j.s.	Connection	Span [m]							
		4.5		5.0		5.5		6.0	
		$F_{1,d}$ [kN]	$F_{2,d}$ [kN]	$F_{1,d}$ [kN]	$F_{2,d}$ [kN]	$F_{1,d}$ [kN]	$F_{2,d}$ [kN]	$F_{1,d}$ [kN]	$F_{2,d}$ [kN]
0.50 m	7x160	2.20	12.96	2.85	14.15	3.57	15.29	4.36	16.39
	7x180	1.88	11.57	2.44	12.65	3.07	13.70	3.76	14.70
	9x160	2.07	13.04	2.69	14.25	3.38	15.41	4.15	16.53
	9x180	2.04	11.48	2.65	12.54	3.32	13.56	4.05	14.54
0.55 m	7x160	2.30	14.67	2.99	16.03	3.76	17.34	4.61	18.60
	7x180	1.98	13.27	2.59	14.51	3.27	15.72	4.02	16.88
	9x160	2.16	14.76	2.82	16.14	3.56	17.46	4.37	18.74
	9x180	2.17	13.16	2.81	14.38	3.54	15.56	4.33	16.70
0.60	7x160	2.38	16.37	3.11	17.90	3.93	19.38	4.83	20.81

7x180	2.08	14.98	2.72	16.40	3.45	17.77	4.25	19.09
9x160	2.23	16.46	2.92	18.02	3.71	19.52	4.57	20.96
9x180	2.27	14.86	2.96	16.25	3.74	17.60	4.59	18.89

Legend: j.s. = joists spacing

For variable load usually considered for residential use ($Q_k = 2 \text{ kN/m}^2$), only for the 7x160 connection (considering the maximum values of floor span and joists spacing and non-structural permanent load G_{k2} equal to 2 kN/m^2) the design load on a fastener overcomes the corresponding design strength.

For variable load greater than the residential value ($Q_k = 4 \text{ kN/m}^2$), for the 7x160, 7x180 and 9x160 connection cases (considering the maximum values of floor span and joists spacing and non-structural permanent load G_{k2} equal to 2 kN/m^2) the design load on a fastener overcomes the corresponding design strength.

4.2.7. Conclusions

The experimental investigation consisted of 20 push-out tests and was divided into four main groups (7x160, 7x180, 9x160, 9x180).

The VGZ fully threaded screws produced by Rothoblaas resulted to be suitable for glulam and sawn timber made of beech wood in both the configurations (single and double-crossed planking). With the 7 mm fastener diameter, the double-crossed planking configuration showed a mean ultimate force F'_{\max} greater than single planking one by about 34% and a mean slip modulus K_s lower than single planking one by about 29%.

With the 9 mm fastener diameter, the double-crossed planking configuration showed a mean ultimate force F'_{\max} greater than the single planking one by about 42% and a mean slip modulus K_s lower than the single planking one by about 14%.

The lower values of the slip modulus in the case of double-crossed planking can be justified by the presence of the orthogonal planking which acts as an interlayer. The scatter of the experimental data leads to similar values in terms of slip modulus in the two single planking cases, with a mean value of 22.03 kN/mm for the 9x160 group and of 23.87 kN/mm for the 7x160 group.

The experimental slip moduli of all the groups were used for calculations of short and long-term deflections (according to the Italian technical standards NTC2018) of some design cases of timber floors varying the floor span, the joists spacing, and the load values.

The long-term deflections were found to govern the design for spans greater than 5 m under significant variable loads ($Q_k = 4 \text{ kN/m}^2$ for uses other than residential),

especially for the more deformable configuration, i.e. the one with double-crossed planking. Moreover, the ultimate limit states for coupled tension and bending of the joists, compression of the planking and shear of the fasteners were considered.

The slip moduli values at ULS resulted limiting especially in the 7x160 connection case. For maximum values of floor span and joists spacing, both the ULS for coupled tension and bending of the joists and the ULS for shear of the fasteners resulted difficult to be satisfied increasing the values of non-structural permanent and accidental loads, limiting the design process as the long-term deflections.

In the end, the proposed low-engineered floor configuration based on the use of locally sourced beech planks connected with inclined screws to a glulam beam made of locally supplied beech planks can be considered as a suitable solution for low to medium residential composite floors when a short-supply chain of locally-grown hardwood is to be used.

4.2.8. References

- [1] R. Malla, P.R. Neupane, M. Köhl, Climate change impacts: Vegetation shift of broad-leaved and coniferous forests, *Trees, For. People.* 14 (2023) 100457. <https://doi.org/https://doi.org/10.1016/j.tfp.2023.100457>.
- [2] Forest Europe, UNECE, FAO, FOREST EUROPE 2020: State of Europe's Forests 2020, Liaison Unit Bratislava, 2020. www.foresteuropa.org.
- [3] P., Gasparini, L., Di Cosmo, A. Floris, (2022). "Area and Characteristics of Italian Forests. In: Gasparini, P., Di Cosmo, L., Floris, A., De Laurentis, D. (eds) Italian National Forest Inventory—Methods and Results of the Third Survey." Springer Tracts in Civil Engineering. Springer, Cham. https://doi.org/10.1007/978-3-030-98678-0_7.
- [4] G., Pirone, G., Ciaschetti, A., Frattaroli, "La caratterizzazione fitosociologica dei boschi in Abruzzo, in La Carta Tipologico-Forestale della Regione Abruzzo", Volume Generale, 49-60.
- [5] <http://geoportale.regione.abruzzo.it/Cartanet/viewer>
- [6] A. Merino, C. Real, J.G. Álvarez-González, M.A. Rodríguez-Gutián, Forest structure and C stocks in natural *Fagus sylvatica* forest in southern Europe: The effects of past management, *For. Ecol. Manage.* 250 (2007) 206–214. <https://doi.org/https://doi.org/10.1016/j.foreco.2007.05.016>.
- [7] T. Ehrhart, R. Steiger, A. Frangi, European beech glued laminated timber, 2021. <https://doi.org/10.3929/ethz-b-000402805>.
- [8] S. Aicher, D. Ohnesorge, Shear strength of glued laminated timber made from European beech timber, *Eur. J. Wood Wood Prod.* 69 (2011) 143–154. <https://doi.org/10.1007/s00107-009-0399-9>.
- [9] H. Stolze, M. Schuh, S. Kegel, C. Fürkötter-Ziegenbein, C. Brischke, H. Militz, Monitoring of Beech Glued Laminated Timber and Delamination

- Resistance of Beech Finger-Joints in Varying Ambient Climates, Forests. 12 (2021) 14. <https://doi.org/10.3390/f12121672>.
- [10] P. Niemz, Physik des Holzes und der Holzwerkstoffe, 1° edizione, 2017.
- [11] E.C. for S. (CEN), Eurocode 5 – Design of timber structures, Part 1–1 General – Common rules and rules for buildings, Eurocode 5. Brussels, (2004).
- [12] S. Aicher, Z. Christian, G. Dill-Langer, Hardwood glulams - Emerging timber products of superior mechanical properties, WCTE 2014 - World Conf. Timber Eng. Proc. (2014).
- [13] K. Frühwald, G. Schickhofer, Strength grading of hardwoods, Proc. 14th Int. Symp. Nondestruct. Test. Wood. (2005) 198–208.
- [14] K. Frühwald, Procedure for determination of characteristic values of hardwood, (2008). <http://www.coste53.net/downloads/Oslo/Oslo-WG3/COSTE53-MeetingOslo-WG3-Fruehwald.pdf>.
- [15] R. Lagača, A. Rohanová, Characteristics values of beech timber for potential construction applications, Ann. Warsaw Univ. Life Sci. – SGGW For. Wood Technol. For. Wood Technol. 75 (2011) 26–29.
- [16] R. Widmann, J.L. Fernandez-Cabo, R. Steiger, Mechanical properties of thermally modified beech timber for structural purposes, Eur. J. Wood Wood Prod. 70 (2012) 775–784. <https://doi.org/10.1007/s00107-012-0615-x>.
- [17] G. Dill-Langer, S. Aicher, Glulam Composed of Glued Laminated Veneer Lumber Made of Beech Wood: Superior Performance in Compression Loading, RILEM Bookseries. 9 (2014) 603–613. https://doi.org/10.1007/978-94-007-7811-5_55.
- [18] T. Ehrhart, R. Steiger, M. Lehmann, A. Frangi, European beech (*Fagus sylvatica* L.) glued laminated timber: lamination strength grading, production and mechanical properties, Eur. J. Wood Wood Prod. 78 (2020) 971–984. <https://doi.org/10.1007/s00107-020-01545-6>.
- [19] M. Brunetti, M. Nocetti, B. Pizzo, G. Aminti, C. Cremonini, F. Negro, R. Zanuttini, M. Romagnoli, G. Scarascia Mugnozza, Structural products made of beech wood: quality assessment of the raw material, Eur. J. Wood Wood Prod. 78 (2020) 961–970. <https://doi.org/10.1007/s00107-020-01542-9>.
- [20] M. Sciomenta, L. Spera, A. Peditto, E. Ciuffetelli, F. Savini, C. Bedon, M. Romagnoli, M. Nocetti, M. Brunetti, M. Fragiaco, Mechanical characterization of homogeneous and hybrid beech-Corsican pine glue-laminated timber beams, Eng. Struct. 264 (2022). <https://doi.org/10.1016/j.engstruct.2022.114450>.
- [21] M. Sciomenta, L. Spera, C. Bedon, V. Rinaldi, M. Fragiaco, M. Romagnoli, Mechanical characterization of novel Homogeneous Beech and hybrid Beech-Corsican Pine thin Cross-Laminated timber panels, Constr. Build. Mater. 271 (2021). <https://doi.org/10.1016/j.conbuildmat.2020.121589>.
- [22] C. Fabrizio, M. Sciomenta, L. Spera, Y. De Santis, S. Pagliaro, A. Di Egidio, M. Fragiaco, Experimental investigation and beam-theory-based analytical model of cross-laminated timber panels buckling behavior, Arch. Civ. Mech. Eng. 23 (2023). <https://doi.org/10.1007/s43452-023-00713-8>.

- [23] M. Frese, H.J. Blaß, Beech glulam strength classes; Paper 38-6-2, CIB W18 - Meet. Thirty-Eight. (2005).
- [24] D. Ohnesorge, K. Richter, G. Becker, Influence of wood properties and bonding parameters on bond durability of European Beech (*Fagus sylvatica* L.) glulams, *Ann. For. Sci.* 67 (2010). <https://doi.org/10.1051/forest/2010002>.
- [25] A. Frühwald, J.B. Ressel, A. Bernasconi, P. Becker, B. Pitzner, R. Wonnemann, U. Mantau, C. Sörgel, C. Thoroe, M. Dieter, H. Englert, Hochwertiges Brettschichtholz aus Buchenholz, Bundesforschungsanstalt Für Forst - Und Holzwirtschaft, Abschlussbericht BMBF-Vorhaben, Förderkennzeichen 0339827. (2003) 186.
- [26] M. Nocetti, M. Brunetti, M. Bacher, Efficiency of the machine grading of chestnut structural timber: prediction of strength classes by dry and wet measurements, *Mater. Struct. Constr.* 49 (2016) 4439–4450. <https://doi.org/10.1617/s11527-016-0799-3>.
- [27] M. Brunetti, G. Aminti, M. Nocetti, G. Russo, Validation of visual and machine strength grading for italian beech with additional sampling, *IForest.* 14 (2021) 260–267. <https://doi.org/10.3832/ifor3649-014>.
- [28] M. Brunetti, M. Nocetti, B. Pizzo, G. Aminti, C. Cremonini, F. Negro, R. Zanuttini, M. Romagnoli, G. Scarascia Mugnozza, Structural products made of beech wood: quality assessment of the raw material, *Eur. J. Wood Wood Prod.* 78 (2020) 961–970. <https://doi.org/10.1007/s00107-020-01542-9>.
- [29] M. Dugmore, M. Nocetti, M. Brunetti, Z. Naghizadeh, C.B. Wessels, Bonding quality of cross-laminated timber: Evaluation of test methods on *Eucalyptus grandis* panels, *Constr. Build. Mater.* 211 (2019) 217–227. <https://doi.org/10.1016/j.conbuildmat.2019.03.240>.
- [30] M. Betti, M. Brunetti, M.P. Lauriola, M. Nocetti, F. Ravalli, B. Pizzo, Comparison of newly proposed test methods to evaluate the bonding quality of Cross-Laminated Timber (CLT) panels by means of experimental data and finite element (FE) analysis, *Constr. Build. Mater.* 125 (2016) 952–963. <https://doi.org/10.1016/j.conbuildmat.2016.08.113>.
- [31] B. Franke, A. Schusser, A. Müller, Analysis of finger joints from beech wood, in: *WCTE 2014 - World Conf. Timber Eng. Proc.*, 2014.
- [32] T. Ehrhart, R. Steiger, P. Palma, A. Frangi, Estimation of the tensile strength of European beech timber boards based on density, dynamic modulus of elasticity and local fibre orientation, in: *WCTE 2018 - World Conf. Timber Eng.*, Seoul, 2018.
- [33] M. Frese, H.J. Blaß, Characteristic bending strength of beech glulam, *Mater. Struct. Constr.* 40 (2007) 3–13. <https://doi.org/10.1617/s11527-006-9117-9>.
- [34] M. Frese, H.J. Blaß, Beech glulam strength classes; Paper 38-6-2, in: *CIB W18 - Meet. Thirty-Eight*, 2005.
- [35] S. Aicher, Z. Christian, G. Dill-Langer, Hardwood glulams - Emerging timber products of superior mechanical properties, in: *WCTE 2014 - World Conf. Timber Eng. Proc.*, 2014.
- [36] P. Kobel, R. Steiger, A. Frangi, Experimental Analysis on the Structural Behaviour of Connections with LVL Made of Beech Wood, *RILEM*

- Bookseries. 9 (2014) 211–220. https://doi.org/10.1007/978-94-007-7811-5_20.
- [37] M.A. Taj, S. Kazemi Najafi, G. Ebrahimi, Withdrawal and lateral resistance of wood screw in beech, hornbeam and poplar, *Eur. J. Wood Wood Prod.* 67 (2009) 135–140. <https://doi.org/10.1007/s00107-008-0294-9>.
- [38] G. Schiro, I. Giongo, W. Sebastian, D. Riccadonna, M. Piazza, Testing of timber-to-timber screw-connections in hybrid configurations, *Constr. Build. Mater.* 171 (2018) 170–186. <https://doi.org/10.1016/j.conbuildmat.2018.03.078>.
- [39] C. Loss, M. Piazza, R. Zandonini, Connections for steel–timber hybrid prefabricated buildings. Part I: Experimental tests, *Constr. Build. Mater.* 122 (2016) 781–795. <https://doi.org/10.1016/j.conbuildmat.2015.12.002>.
- [40] E.C. for S. (CEN), EN 26891 - Joints made with mechanical fasteners. General principles for the determination of strength and deformation characteristics, European Committee for Standardization (CEN), (1991).
- [41] S. Franke, N. Magnière, The Embedment Failure of European Beech Compared to Spruce Wood and Standards, *RILEM Bookseries.* 9 (2014) 221–229. https://doi.org/10.1007/978-94-007-7811-5_21.
- [42] G. Celebi, M. Kilic, Nail and screw withdrawal strength of laminated veneer lumber made up hardwood and softwood layers, *Constr. Build. Mater.* 21 (2007) 894–900. <https://doi.org/10.1016/j.conbuildmat.2005.12.015>.
- [43] A. Misconel, M. Ballerini, J.W. Van De Kuilen, Steel-to-timber joints of beech-LVL with very high strength steel dowels, in: *WCTE 2016 - World Conf. Timber Eng.*, 2016.
- [44] M. Brunetti, M. Nocetti, B. Pizzo, F. Negro, G. Aminti, P. Burato, C. Cremonini, R. Zanuttini, Comparison of different bonding parameters in the production of beech and combined beech-spruce CLT by standard and optimized tests methods, *Constr. Build. Mater.* 265 (2020). <https://doi.org/10.1016/j.conbuildmat.2020.120168>.
- [45] European Committee for Standardization, “EN 1995-1-1, Eurocode 5: Design of timber structures - Part 1-1: General - Common rules and rules for buildings.” 2004.
- [46] UNI Ente nazionale italiano di unificazione. (2006). UNI EN 12512:2006 - Strutture di legno - Metodi di prova - Prove cicliche di giunti realizzati con elementi meccanici di collegamento.
- [47] Ministero delle Infrastrutture e dei Trasporti, “Aggiornamento delle «Norme tecniche per le costruzioni».”, D.M. 17 gennaio 2018.
- [48] UNI Ente nazionale italiano di unificazione. (2016). UNI EN 338:2016 - Legno strutturale - Classi di resistenza.
- [49] British Standard Institution, EN 408:2010+A1:2012: Timber structures - Structural timber and glued laminated timber - Determination of some physical and mechanical properties, *BSI Stand. Publ.* (2012) Brussels.

Concluding remarks

The research reported in the present thesis has investigated the mechanical properties of novel engineered wood products, made from Italian hardwood and softwood species (i.e. beech and pine), also following the preliminary phases of procurement, classification, and production. Both cross-laminated timber (CLT) panels and glue-laminated timber (glulam) beams, manufactured in homogeneous beech and in hybrid beech-Corsican pine configurations, have been mechanically characterized by means of four-point bending tests and they have been compared with commercial products made of softwood through numerical simulations to assess their performances. From the bending test in the direction perpendicular-to-plane on the CLT panels, rolling shear collapse modes were prevalent due to the reduced panel length. Homogeneous Corsican Pine panels were affected by knot influence in the definition of mechanical performances and collapse mode. Hybrid and homogeneous beech configurations under in-plane shear tests were analysed in terms of size effect and it was observed, by changing the panel dimensions, that the scatter of elastic stiffness between hybrid and homogeneous specimens was mostly constant, while the scatter of ultimate force increases from 4% to 15%.

By means of numerical simulation, the experimental outcomes were further assessed and compared with a widely used market product, i.e. traditional C24 spruce CLT panels. Hybrid panels showed good performances giving evidence of a less pronounced deformability than the C24 Spruce panels, in both the bending and shear loading conditions. The mechanical behaviour of these novel products has been

acceptable both in homogeneous beech and in hybrid configuration, demonstrating the great potential of beech and, in the second configuration, the possibility to optimize the raw material wood.

The experimental campaign on glulam beams highlighted good mechanical performance of the prototypes, both homogeneous and hybrid. By analysing the results from the four points bending tests, the two configurations have almost comparable performances: the homogeneous beams showed maximum force, F_{max} , and flexural strength, f_m , values greater than the values of the hybrid ones of about 7% and 8.3 %, respectively. Analysing the failure mechanisms occurred during the bending tests, a greater variability was observed for the hybrid beams, with particular reference to delamination. Significant differences are observed by comparing the shear performance of the two configurations: the homogeneous beams have reached a maximum force, F_{max} , higher of about 31.5% and a shear strength, f_v , greater of about 31.8 % than the hybrid ones. Analysing the shear failure mechanisms, less variability is observed as for homogeneous as for hybrid configuration.

In addition, the possible adoption of the EN 14080 formulations, valid for attributing a strength class to beams made with coniferous lamellas, to homogeneous broad-leaved and hybrid products was considered. For homogeneous beams, the tensile DT Table classes for medium-density European hardwoods (mainly beech and ash) proposed by Kovryga et al. were adopted. In order to define what parameters are more suitable to attribute the glulam class, three different hypotheses have been carried out choosing the bending and tensile strength, the bending stress and the dynamic modulus of elasticity respectively. By comparing the experimental evidences with the analytical ones, the DT38 class (based on the closer dynamic modulus of elasticity) resulted the best choice. For the hybrid beam, the γ -method and the Z-9.1–679 German provision were adopted. This latter choice allowed to attribute a GL44h class to our hybrid beam which fitted with great accuracy the experimental results.

Lastly, a FE modelling was provided in order to compare the prototypes with commercial product (graded supposing C24 lamellas in accordance with EN 338, in order to have the same class of inner hybrid layer). From the comparison in terms of deflections, the prototypes in both hybrid and homogeneous configuration resulted stiffer than the conifer beam.

It has been demonstrated, under the previous hypotheses, the possibility to adopt the EN 14.080 formulations valid for conifer glulam beams also for the definition of the features of hardwood beams. However, adopting the mechanical parameters

suggested by EN 338 leads to a considerable underestimation of the stiffness.

For hybrid products, the strength classes proposed in the German provision Z-9.1-679 as well as the γ -method with the experimental values of timber coming from the board classification allow to fit with good accuracy of the experimental stiffness.

These results could be a reference to incentivize the production of timber components for structural purposes, overcoming the current predominant usage as firewood in the Italian context.

Furthermore, interesting topics regarding the aforementioned thin CLT panels have been explored like the buckling and the reinforcement of existing timber floors.

The first subject has been deepened both experimentally, through central axial compressive tests, and analytically, through the formulation of a model to predict the limit load with relative differences with experimental values lower than 20%.

In particular, the buckling behaviour of three-layered CLT panels was investigated, first by means of 14 experimental tests and then by developing an analytical formulation calibrated on the specific test setup. The experimental campaign was conducted on two different groups of seven specimens, each one related to a specific configuration characterized by the panels cross-section's arrangement.

The first configuration (homogeneous, labelled HO) presented three layers made of the same timber specie (beech), whereas, in the second one (hybrid, labelled HB), the inner layer was made of a different timber specie (Corsican pine).

The experimental tests aimed to evaluate the failure limit loads of the specimens, under an increasing tip compression force. The homogeneous panels showed almost exclusively a mid-span bending failure mode while for the hybrid panels, different failure mechanisms, such as rolling shear failure, as well as delamination failure, were observed at the ends, singularly or in conjunction. Such a circumstance is likely to follow from the lower rolling shear strength of the inner layer in the hybrid panels. Nevertheless, the two groups showed quite similar average limit loads; however, the hybrid specimens presented results with a higher standard deviation with respect to those related to the homogeneous ones.

An analytical model was then developed in the attempt to describe theoretically the system object of the experimentation.

The moderately high length to width ratio of the specimens, the absence of side restraints in the test setup and, above all, the intent to develop a simplified approach to the problem at hand, led straight to a beam-based theoretical formulation.

Starting from a model for a panel with a generic number of layers, modelled as a stack of planar Timoshenko beams connected each other by continuous distributions of normal and tangential elastic springs representing the glue lines, the general

model was then adapted to a three-layer system, similar to the panels of the experimental campaign, by means of some internal constraints, and considering a side displacement field in the form of a sine, as a result of an initial sine shape for the imperfect panel's longitudinal axis line. From such a model, a closed-form solution for the elastic problem, together with the related Eulerian critical load, was determined. In the model, two non-dimensional parameters were introduced to express the interaction among the wooden layers due to the tangential stiffness of the glue and the rolling shear tangential stiffness of the inner layer. The proposed model includes the influence of the elastic response of the glue lines, which represents the novelty of the presented theoretical approach with respect to others which generally overlook the presence of the adhesive layers. However, although it was recognized that the influence of the glue stiffness on the critical load is negligible, it should be highlighted that the modelling of the adhesive layers, beyond allowing a richer description of the response of the three-layer CLT panel, permitted the investigation of the delamination failure mode observed during the laboratory tests. Such a delamination mode enlarges the range of possible failure modes for a CLT panel, which includes the classical bending mode and the shear mode.

On the basis of the achieved closed-form solution and recalling the different failure mechanisms detected during the experimental campaign, three different failure criteria were introduced, leading to a unique theoretic compression limit load.

The first one accounts for the bending–buckling failure, the second refers to the rolling shear failure mechanism of the inner layer, and finally the last takes into account the delamination phenomena. A comparison among the experimental and the theoretic limit loads was performed after the calibration of the analytical model on the basis of some of the experimental results as well as on some parameters derived from the literature. The comparison showed that the analytical formulation describes sufficiently well the real behaviour of the CLT panels, both with a homogeneous or hybrid configuration, with relative differences on the limit loads lower than 20%. As a beam-based formulation, the proposed model, besides being adopted for a comparison with the specific test described above, seems to configure a potential preliminary design tool for stability verification, since it considers one of the most demanding configurations for a three-layer panel wall, though substantially unusual in the construction practice, with no vertical sides' restraints and hinges on both the horizontal ends. However, it should be recognized that the model is clearly unable to describe the two-dimensional buckling behaviour of a panel wall in the presence of restraints along its vertical border and/or of a width to height ratio higher than unity.

The second subject has been analysed theoretically, adopting the mechanically jointed beam theory to compare common reinforcing techniques with the application of the considered CLT panels as reinforcement of hypothetical existing one-way timber floors. Three different retrofit interventions were considered: double-crossed timber planks, CLT panels and reinforced concrete slab. The first and the third are two of the most used techniques; the second one considers the homogeneous beech CLT panels mechanically characterized in the first paper. In order to focus the comparison on the nature of the reinforcing elements, the thickness of the reinforcements was assumed equal to that of the CLT panels. The comparison in terms of out-of-plane bending stiffness was conducted by evaluating slip moduli and effective bending stiffness according to the mechanically jointed beam theory, Annex B of Eurocode 5, both at ULS and at SLS. A total of three flexible cases, i.e., K1, K2 and K3 slip moduli for screwed connections characterized by different spacing along the span of the member, and three screw diameters, were considered. In addition, the performance of the flexible connections was assessed with respect to the two limit cases corresponding to the absence of any connection ($K = 0$) and to the presence of a fully rigid connection ($K = \infty$). It was shown that the choice of CLT panels leads to a range of SLS bending stiffness increase from 145% (K1 and $d = 8$ mm) to 177% (K3 and $d = 12$ mm), against the ranges from 66% (K1 and $d = 8$ mm) to 92% (K3 and $d = 12$ mm) for double-crossed timber planks and from 246% (K1 and $d = 8$ mm) to 272% (K3 and $d = 12$ mm) for the RC slab solution.

Although based on the use of hardwood, this solution can also minimize the weight increase for the examined geometry, in about the 40% parts of the structural permanent loads, against the 69% term determined for the RC slab, and it allows to realize a fully reversible intervention.

Even though the RC slab leads to the greatest bending stiffness values, this solution is in fact not always applicable to existing buildings, especially when subjected to superintendence of architectural heritage restrictions. In addition, concrete and steel are considered less environmentally friendly than wood, and for this reason are often less preferable in the construction sector, in order to pursue sustainability goals.

Due to the growing interest in retrofitting solutions based on engineered wood products, the application of novel Italian beech CLT panels proved to represent a significant alternative for the retrofitting of existing timber floors, especially when belonging to the built cultural heritage. In this way, even further innovative structural applications could be detected and optimised for local species, specifically to beech and in general to hardwood, which both represent a consistent percentage of the Italian wooden areas.

Lastly, timber-to-timber screwed connections have been experimentally studied through push-out tests performed on symmetric specimens with the central element made of homogeneous beech glulam and the lateral element made of beech planking. The experimental investigation, divided into four main groups (7x160, 7x180, 9x160, 9x180), consisted in a total of 20 push-out tests.

The VGZ fully threaded screws produced by Rothoblaas resulted to be suitable for glulam and sawn timber made of beech wood in both the configurations (single and double-crossed planking).

With the 7 mm fastener diameter, the double-crossed planking configuration showed a mean ultimate force F'_{max} greater than single planking one by about 34% and a mean slip modulus K_s lower than single planking one by about 29%.

With the 9 mm fastener diameter, the double-crossed planking configuration showed a mean ultimate force F'_{max} greater than the single planking one by about 42% and a mean slip modulus K_s lower than the single planking one by about 14%.

The lower values of the slip modulus in the case of double-crossed planking can be justified by the presence of the orthogonal planking which acts as an interlayer.

The scatter of the experimental data leads to similar values in terms of slip modulus in the two single planking cases, with a mean value of 22.03 kN/mm for the 9x160 group and of 23.87 kN/mm for the 7x160 group.

The experimental slip moduli of all the groups were used for calculations of short and long-term deflections (according to the Italian technical standards NTC2018) of some design cases of timber floors varying the floor span, the joists spacing, and the load values.

The long-term deflections were found to govern the design for spans greater than 5 m under significant variable loads ($Q_k = 4\text{kN/m}^2$ for uses other than residential), especially for the more deformable configuration, i.e. the one with double-crossed planking. Moreover, the ultimate limit states for coupled tension and bending of the joists, compression of the planking and shear of the fasteners were considered.

The slip moduli values at ULS resulted limiting especially in the 7x160 connection case. For maximum values of floor span and joists spacing, both the ULS for coupled tension and bending of the joists and the ULS for shear of the fasteners resulted difficult to be satisfied increasing the values of non-structural permanent and accidental loads, limiting the design process as the long-term deflections.

In the end, the proposed low-engineered floor configuration based on the use of locally sourced beech planks connected with inclined fully threaded screws to a glulam beam made of locally supplied beech planks can be considered as a suitable solution for low to medium residential composite floors when a short-supply chain

of locally-grown hardwood is to be used.

In reference to the pre-established research objectives, the first one was achieved by means of bibliographic studies and by collaboration with municipalities and the Coordination and Planning Office in the Dept. of Agriculture (Forests and Parks) of the Abruzzo Region offices in L'Aquila (AQ – Italy).

It resulted that one of the most interesting locally grown wood species in Abruzzo Region, and in general in Italy, is a hardwood, i.e. beech (*Fagus Sylvatica L.*), both for its mechanical properties and for abundance and future climate changing issues. For this reason, the developed works were mainly focused on this wood species.

Regarding the second and third research objectives, two published papers are dedicated to the classification, production, and characterization of CLT panels and glulam beams manufactured from Italian beech and Corsican pine wood.

The classification was carried out by National Council for Research - Institute for Bio-Economy of Sesto Fiorentino (CNR-IBE) by using a laser interferometer MICROTEC Viscan-FMMF. The CLT panels were manufactured out of the Abruzzo Region at the XLam Dolomiti factory (Castelnuovo – TN – Italy), while the glulam beams were produced at the Pagano S.r.l factory (Oricola – AQ – Italy). The four-point bending tests to characterize the specimens were performed at the laboratory of tests, materials and structures (L.P.M.S.) of the University of L'Aquila (L'Aquila– AQ – Italy). Concerning the fourth research objective, the application of thin homogeneous beech CLT panels as reinforcement of existing timber floors and the use of homogeneous beech glulam beams as joists of new timber floors, with focus to the flexible timber-to-timber connections, were addressed. The glulam beams were manufactured at Lamel Legno S.r.l factory (Montefalcone nel Sannio – CB – Italy). The push-out tests to characterize the TTC joints were carried out at the laboratory of tests, materials and structures (L.P.M.S.) of the University of L'Aquila (L'Aquila– AQ – Italy).

To conclude, despite the great abundance of forested areas, the current Abruzzo Region background seems to be immature to exploit wood resource to its full potential in the building sector, due to the lack of sawmills, production factories, construction companies and workmen specialized in timber structures.

However, the outcomes of this research clearly show the potential of local wood species and their possible applications in laminated wood products and more.

Especially beech, which is the most abundant hardwood species in the Abruzzo Region, results the specie to be valorised and on which research must be focused, due to the current interest in its use as construction material both in Italy and in Europe. The existing sawmills and production factories, although they are small in

number, represent a reality of great importance and possess the fundamental know-how to produce high technological content wood products.

Therefore, this study should be considered as a motivation to invest more in the production process and in the sustainable management of the forests so as to increase the usage of native species for building purposes and to promote short supply chain wood as a renewable and sustainable material.

The development of a short supply timber chain can offer numerous benefits of environmental, economic, and social nature, both in the application of local wood as construction material and in the reduction of importation and its consequent CO₂ emissions. Only a cultural change of the local mindset can truly produce positive effects, and the main purpose of this research is to provide a contribution to this cause.

Subjects for further research

Additional tests should be performed on polyurethane bonded CLT panels, to deepen the finding about increasing deformability and ultimate force related to the same panels bonded with melamine adhesive.

Further investigations could be useful to have a wider comprehension of other species of hardwood timber as well as to fix some points in the open field of adhesives and gluing methods involving hardwood lamellas.

Since the last topic presented in this thesis has regarded timber-to-timber joints, it would be relevant to perform full-scale tests of floors specimens with a realistic span, at least 4 or 5 meters, both for the configuration with single planking and for the one with double-crossed planking.

Through four-point bending tests it would be possible to determine the mechanical properties of the composite section, also varying the spacing of the fasteners.

Moreover, due to the fact that timber floors are particularly susceptible to human-induced vibrations, it could be important to explore the vibrational response of this timber-to-timber systems.

Another issue to be faced in the future regards the durability of engineered wood products made of local species, especially hardwood as beech or others, with a special focus on the identification of suitable service classes.

Appendix

To extend the written description of the FE model reported in section 3.1, the images of the Abaqus model are shown in the following figures.

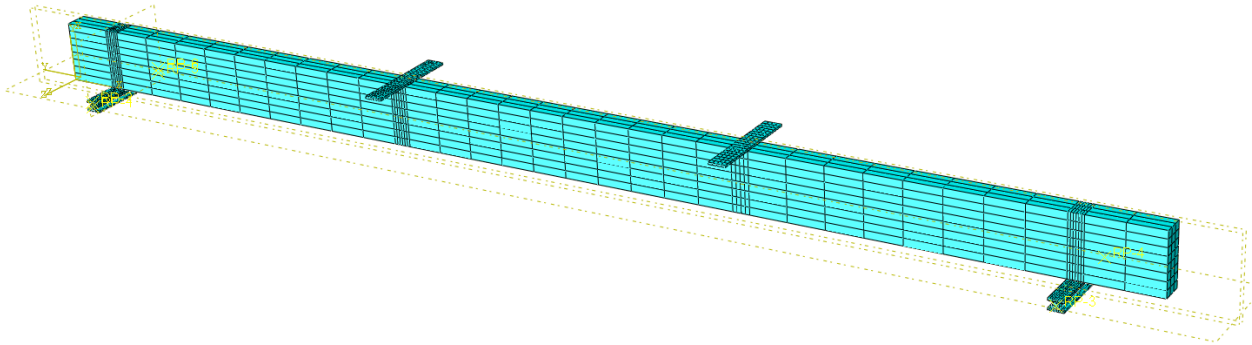


Fig. 1 Example of 3D FE model.

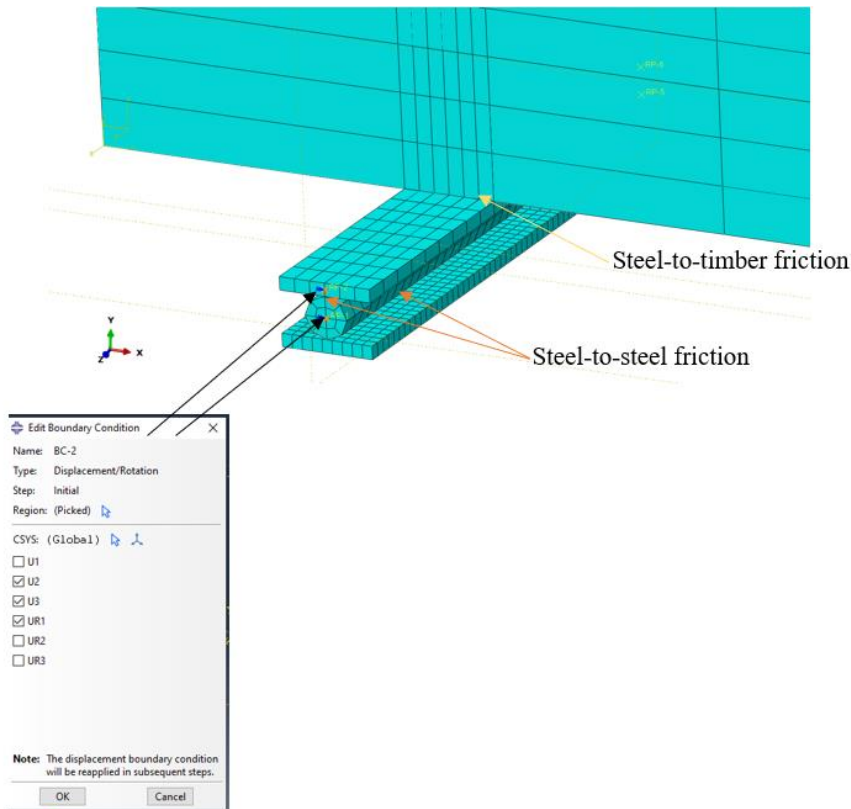


Fig. 2 Boundary conditions named BC-2.

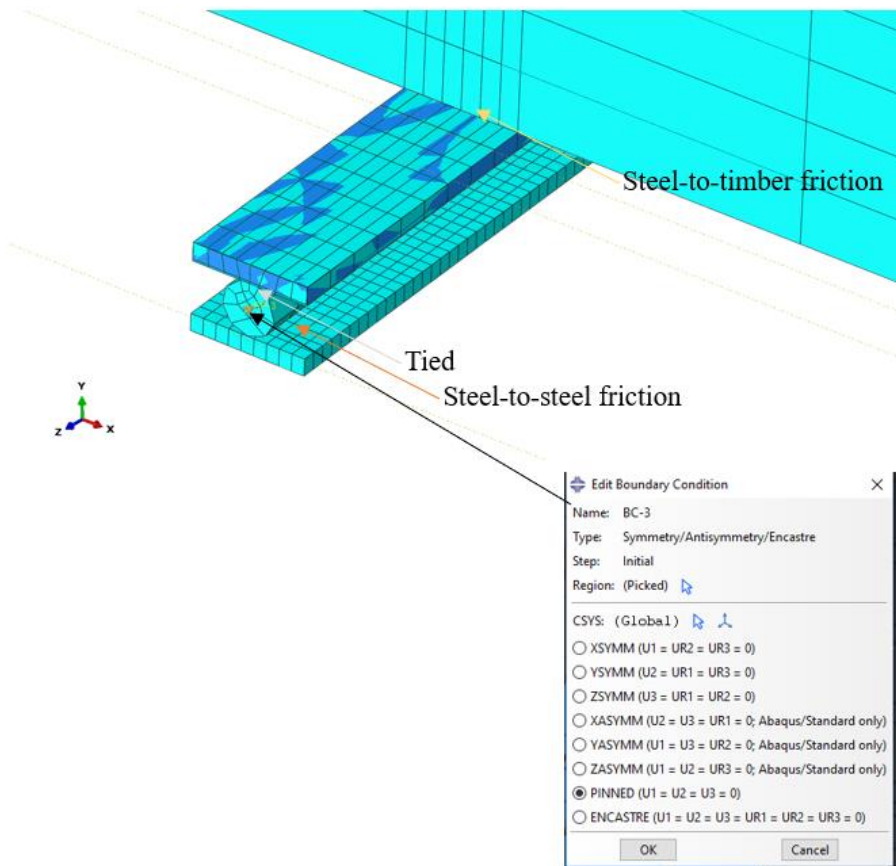


Fig. 3 Boundary conditions named BC-3.

In addition, a flow chart similar to Fig. 7 in section 4.1 is provided for the procedure followed for CLT panels in section 3.1.

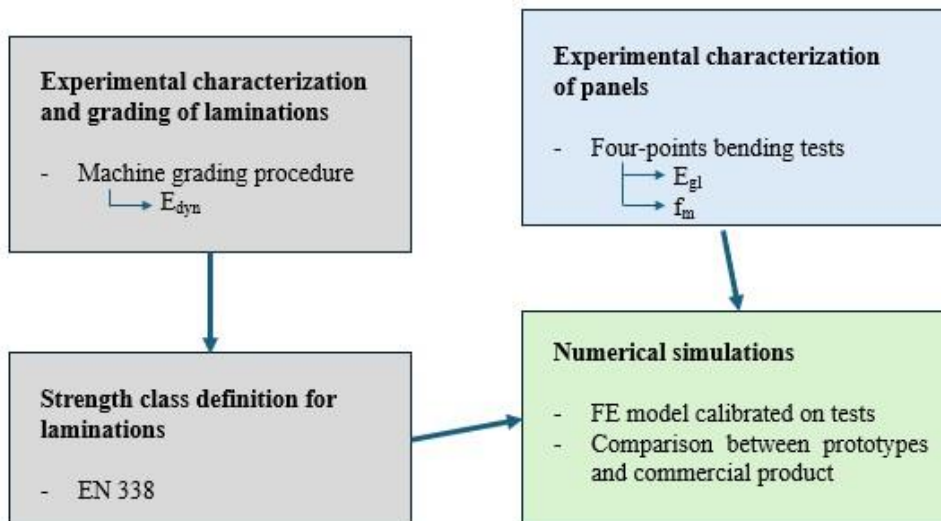


Fig. 4 Flow chart for the procedure followed for CLT panels.

Regarding the FE model reported in section 4.1, the assumption of the steel-steel contact friction coefficient equal to 0.15 derives from the following reference considering the steel-to-steel lubricated case: <https://www.tribology-abc.com/abc/cof.htm>.

References

- Aicher, S., Christian, Z., & Dill-Langer, G. (2014, September). Hardwood glulams – emerging timber products of superior mechanical properties. World Conference on Timber Engineering.
- Bacher, M. (2008, October 29). Comparison of different machine strength grading principles. Conference COST E53.
- Brunetti, M., Nocetti, M., Pizzo, B., Aminti, G., Cremonini, C., Negro, F., Zanuttini, R., Romagnoli, M., & Mugnozza, G. S. (2020). Structural products made of beech wood: quality assessment of the raw material. *European Journal of Wood and Wood Products* Volume, 78, 961–970.
- Brunetti, M., Nocetti, M., Pizzo, B., Negro, F., Aminti, G., Burato, P., Cremonini, C., & Zanuttini, R. (2020). Comparison of different bonding parameters in the production of beech and combined beech-spruce CLT by standard and optimized tests methods. *Construction and Building Materials*, 265, 120168. <https://doi.org/10.1016/J.CONBUILDMAT.2020.120168>
- Ceccotti, A., Sandhaas, C., Okabe, M., Yasumura, M., Motoi, Minowa, C., & Kawai, N. (2013). SOFIE project – 3D shaking table test on a seven-storey full-scale cross-laminated timber building. *Earthquake Engineering & Structural Dynamics*, 42(13), 2003–2021.
- Centro Studi FederlegnoArredo. (2021, December 3). 6° Rapporto Edilizia in legno. <https://www.federlegnoarredo.it/it/associazioni/assolegno/attivita-e-servizi-per-i-soci/analisi-di-mercato/6-rapporto-edilizia-in-legno>
- Concu, G., de Nicolo, B., Fragiaco, M., Trulli, N., & Valdes, M. (2018). Grading of maritime pine from Sardinia (Italy) for use in cross-laminated timber. *Proceedings of the Institution of Civil Engineers - Construction Materials*, 171(1), 11–21.
- Egner, K., & Kolb, H. (1966). Geleimte Träger und Binder aus Buchenholz. *Bau. Mit Holz*, 68(4), 147–154.
- Ehrhart, T., Steiger, R., Lehmann, M., & Frangi, A. (2020). European beech (*Fagus sylvatica* L.) glued laminated timber: lamination strength grading, production and mechanical properties. *European Journal of Wood and Wood Products*, 78, 971–984.
- European Commission. (2018). Knowledge Centre for Bioeconomy. https://knowledge4policy.ec.europa.eu/bioeconomy_en
- Fabrizio, C., Sciomenta, M., Spera, L., Santis, Y. De, Pagliaro, S., Egidio, A. Di, & Massimo, F. (2023). Experimental investigation and beam-theory-based analytical model of cross-laminated timber panels buckling behavior. *Archives of Civil and Mechanical Engineering*, 23. <https://doi.org/https://doi.org/10.1007/s43452-023-00713-8>
- Fragiaco, M., Riu, R., & Scotti, R. (2015). Can Structural Timber Foster Short Procurement Chains within Mediterranean Forests? A Research Case in Sardinia. *South-East European Forestry*, 6(1), 107–117.

- Frese, M., & Blaß, H. J. (2007). Characteristic bending strength of beech glulam. *Materials and Structures*, 40, 3–13.
- Fridley, K. J. (2002). Wood and Wood-Based Materials: Current Status and Future of a Structural Material. *Journal of Materials in Civil Engineering*, 14(2).
- Gehri, E. (1980). Möglichkeiten des Einsatzes von Buchenholz für Tragkonstruktionen. *Schweizer Bauwirtschaft*, 79(56), 14–18.
- Hossain, A., Popovski, M., & Tannert, T. (2018). Cross-laminated timber connections assembled with a combination of screws in withdrawal and screws in shear. *Engineering Structures*, 168, 1–11. <https://doi.org/10.1016/J.ENGSTRUCT.2018.04.052>
- Izzi, M., Polastri, A., & Fragiaco, M. (2018). Modelling the mechanical behaviour of typical wall-to-floor connection systems for cross-laminated timber structures. *Engineering Structures*, 162, 270–282. <https://doi.org/10.1016/J.ENGSTRUCT.2018.02.045>
- Lam, F. (2001). Modern structural wood products. *Progress in Structural Engineering and Materials*, 3(3), 238–245.
- Mallo, M. F. L., & Espinoza, O. (2016, August). Cross-laminated timber vs. Concrete/steel: cost comparison using a case study. *World Conference on Timber Engineering*.
- Ministero delle infrastrutture e dei trasporti. (2018). D.M. 17 gennaio 2018 “Aggiornamento delle «Norme tecniche per le costruzioni».”
- Nocetti, M., Bacher, M., Brunetti, M., Crivellaro, A., & van de Kuilen, J.-W. G. (2010, June). Machine grading of italian structural timber: Preliminary results on different wood species. *World Conference on Timber Engineering*.
- Parisi, M., & Piazza, M. (2000). Mechanics of plain and retrofitted traditional timber connections. *Journal of Structural Engineering*, 126(12).
- Pedrotti, F. (1996). Suddivisioni botaniche dell’Italia. *Giorn. Bot. Ital.*, 130(1), 214–225.
- Ramage, M. H., BurrIDGE, H., Busse-Wicher, M., Fereday, G., Reynolds, T., Shah, D. U., Wu, G., Yu, L., Fleming, P., Densley-Tingley, D., Allwood, J., Dupree, P., Linden, P. F., & Scherman, O. (2017). The wood from the trees: The use of timber in construction. *Renewable and Sustainable Energy Reviews*, 68, 333–359. <https://doi.org/10.1016/J.RSER.2016.09.107>
- Reynolds, T., Casagrande, D., & Tomasi, R. (2016). Comparison of multi-storey cross-laminated timber and timber frame buildings by in situ modal analysis. *Construction and Building Materials*, 102, 1009–1017. <https://doi.org/10.1016/J.CONBUILDMAT.2015.09.056>
- Romagnoli, M., Fragiaco, M., Brunori, A., Follesa, M., & Mugnozza, G. (2019). Solid Wood and Wood Based Composites: The Challenge of Sustainability Looking for a Short and Smart Supply Chain: Innovative Techniques of Representation in Architectural Design. In *Lecture Notes in Civil Engineering* (pp. 783–807). https://doi.org/10.1007/978-3-030-03676-8_31

Sciomenta, M., Spera, L., Bedon, C., Rinaldi, V., Fragiaco, M., & Romagnoli, M. (2021). Mechanical characterization of novel Homogeneous Beech and hybrid Beech-Corsican Pine thin Cross-Laminated timber panels. *Construction and Building Materials*, 271, 121589. <https://doi.org/10.1016/J.CONBUILDMAT.2020.121589>

Sciomenta, M., Spera, L., Peditto, A., Ciuffetelli, E., Savini, F., Bedon, C., Romagnoli, M., Nocetti, M., Brunetti, M., & Fragiaco, M. (2022). Mechanical characterization of homogeneous and hybrid beech-Corsican pine glue-laminated timber beams. *Engineering Structures*, 264(114450). <https://doi.org/https://doi.org/10.1016/j.engstruct.2022.114450>

Tampone, G. (1996). *Il restauro delle strutture di legno: il legname da costruzione, le strutture lignee e il loro studio, restauro, tecniche di esecuzione del restauro.* (Hoepli Editore, Ed.).

UNI Ente nazionale italiano di unificazione. (2010). UNI 11035-3:2010 - Legno strutturale - Classificazione a vista dei legnami secondo la resistenza meccanica - Parte 3: Travi Uso Fiume e Uso Trieste.

UNI Ente nazionale italiano di unificazione. (2012a). UNI EN 408:2012 - Strutture di legno - Legno strutturale e legno lamellare incollato - Determinazione di alcune proprietà fisiche e meccaniche.

UNI Ente nazionale italiano di unificazione. (2012b). UNI EN 1912:2012 - Legno strutturale - Classi di resistenza - Assegnazione delle categorie visuali e delle specie.

UNI Ente nazionale italiano di unificazione. (2013). UNI EN 14080:2013 - Strutture di legno - Legno lamellare incollato e legno massiccio incollato - Requisiti.

UNI Ente nazionale italiano di unificazione. (2016). UNI EN 338:2016 - Legno strutturale - Classi di resistenza.

UNI Ente nazionale italiano di unificazione. (2022a). UNI 11035-1:2022 - Legno strutturale - Classificazione a vista dei legnami secondo la resistenza meccanica - Parte 1: Conifere a sezione rettangolare.

UNI Ente nazionale italiano di unificazione. (2022b). UNI 11035-2:2022 - Legno strutturale - Classificazione a vista dei legnami secondo la resistenza meccanica - Parte 2: Latifoglie e sezione rettangolare.

United Nations General Assembly. (2015). Sustainable Development Goals. https://ec.europa.eu/info/strategy/international-strategies/sustainable-development-goals_en

van der Linden, M. L. R., & Blass, H. J. (1996). Timber-concrete composite floor systems. *International Wood Engineering Conference*.

List of publications

Publications part of the Doctoral Thesis

- Sciomenta, M., Spera, L., Bedon, C., Rinaldi, V., Nocetti, M., Brunetti, M., Fragiaco, M., Romagnoli, M., “Corrigendum to ‘Mechanical characterization of novel Homogeneous Beech and hybrid Beech-Corsican Pine thin Cross-Laminated timber panels’ [Constr. Build. Mater. 271 (2021) 121589]”, *Construction and Building Materials*, vol. 288, p. 123495, Jun. 2021, <https://doi.org/10.1016/j.conbuildmat.2021.123495>.
- Sciomenta, M., Spera, L., Peditto, A., Ciuffetelli, E., Savini, F., Bedon, C., Romagnoli, M., Nocetti, M., Brunetti, M., Fragiaco, M., “Mechanical characterization of homogeneous and hybrid beech-Corsican pine glue-laminated timber beams”, *Engineering Structures*, vol. 264, p. 114450, Aug. 2022, <https://doi.org/10.1016/j.engstruct.2022.114450>.
- Fabrizio, C., Sciomenta, M., Spera, L., De Santis, Y., Pagliaro, S., Di Egidio, A., Fragiaco, M., “Experimental investigation and beam theory based analytical model of cross laminated timber panels buckling behavior”, *Archives of Civil and Mechanical Engineering*, vol. 23, Jun. 2023, <https://doi.org/10.1007/s43452-023-00713-8>.
- Spera, L., Sciomenta, M., Bedon, C., Fragiaco, M., “Out-of-Plane Strengthening of Existing Timber Floors with Cross Laminated Timber Panels Made of Short Supply Chain Beech”, *Buildings*, vol. 14, Mar. 2024, <https://doi.org/10.3390/buildings14030749>.

Other publications

- De Santis, Y., Sciomenta, M., Spera, L., Rinaldi, V., Fragiaco, M., Bedon, C., “Effect of Interlayer and Inclined Screw Arrangements on the Load-Bearing Capacity of Timber-Concrete Composite Connections.”, *Buildings*, 12(12), Nov. 2022, <https://doi.org/10.3390/buildings12122076>.

- Fragiaco, M., De Berardinis, P., Sciomenta, M., Spera, L., Rinaldi, V., De Santis, Y., Marchionni, C., D'Alessandro, G, "Timber structure inclusions in historical masonry heritage: intervention techniques and durability details", World Conference on Timber Engineering, Santiago, Chile, 9-12 August 2021.
- Sciomenta, M., De Santis, Y., Castoro, C., Spera, L., Rinaldi, V., Bedon, C., Fragiaco, M., Gregori, A., "Finite elements analyses of timber-concrete and timber- rubberised concrete specimens with inclined screws", World Conference on Timber Engineering, Santiago, Chile, 9-12 August 2021.
- Rinaldi, V., Casagrande, D., Cimini, C., Follesa, M., Sciomenta, M., Spera, L. , Fragiaco, M., "Simplified strategies for the numerical modelling of CLT buildings subjected to lateral loads", World Conference on Timber Engineering, Santiago, Chile, 9-12 August 2021.

